Clinical Pharmacokinetics of Anticancer Drugs:
focus on E7070, methotrexate and paclitaxel

Clinical Pharmacokinetics of Anticancer Drugs:
focus on E7070, methotrexate and paclitaxel

Klinische Farmacokinetiek van Geneesmiddelen tegen kanker:
E7070, methotrexaat en paclitaxel

(met een samenvatting in het Nederlands)

PROEFSCHRIFT

ter verkrijging van de graad van doctor
aan de Universiteit Utrecht
op gezag van Rector Magnificus, Prof. dr. W.H. Gispen,
ingevolge het besluit van het College van Promoties
in het openbaar te verdedigen
op donderdag 14 november 2002 des namiddags te 14.30 uur

Door

Hubertina Johanna Gemma Desirée van den Bongard

geboren op 12 juli 1972 te Sittard

Promotores

Prof. dr. J.H.M. Schellens   The Netherlands Cancer Institute / Antoni van Leeuwenhoek Hospital, Amsterdam; Faculty of Pharmaceutical Sciences, Utrecht University, Utrecht, The Netherlands.

Prof. dr. J.H. Beijnen   The Netherlands Cancer Institute / Slotervaart Hospital, Amsterdam; Faculty of Pharmaceutical Sciences, Utrecht University, Utrecht, The Netherlands.

Thesis committee

Prof. dr. G.H. Blijham

Prof. dr. A. de Boer

Prof. dr. J. Verweij

Dr. P. Baas

Dr. J.H. Schornagel

Ter nagedachtenis aan mijn moeder

Contents

4   Paclitaxel

Preface

Despite significant improvement in the treatment of cancer over the past decades, tumour response rates and survival in patients with advanced cancer are still poor. Therefore, it is important to find anticancer agents with a novel mechanism of action and to further optimise existing treatment. Anticancer agents have a very narrow therapeutic window. In clinical practice, anticancer agents are administered at the maximum dose tolerated by the patient. Therapeutic drug monitoring (TDM) and, consequently, the assessment of pharmacokinetic parameters, allows the characterisation of relationships between pharmacokinetic parameters and therapeutic efficacy and toxicity [1]. The determination of pharmacokinetic parameters of anticancer agents can help to facilitate optimal dosing of these agents in the clinic in order to improve therapeutic efficacy and to decrease toxicity. The objective of this thesis is to study the pharmacokinetics of anticancer agents, with an emphasis on E7070, methotrexate and paclitaxel.

The thesis consists of four chapters. The aim of the first chapter is to review the current insights into pharmacokinetically guided administration of anticancer agents. In cancer treatment, the dose calculation of most anticancer agents is based on body surface area (BSA). The interpatient pharmacokinetic variability of anticancer agents can be attributed to variable drug absorption, distribution and elimination processes [1]. TDM and pharmacokinetically guided dosing are not routinely used clinically, except for methotrexate and carboplatin. In current practice, TDM is routinely used in the clinic for treatment with moderate to high-dose methotrexate to guide supportive measures in patients at high risk for developing significant toxicity. For carboplatin, the Calvert formula is clinically used to calculate the individualised dose [2]. In this chapter, clinical studies of pharmacokinetically guided administration of anticancer agents have been evaluated.

The second chapter consists of pharmacokinetic studies of E7070, a novel sulphonamide agent that is currently in phase II of clinical development for the treatment of cancer. Sulphonamide agents are well known to have a variety of pharmacological activities including antibacterial, carbonic anhydrase-inhibitory, antidiabetic, diuretic, and antithyroid activity [3,4]. E7070 arrests the tumour cells at the transition of the G1- into the S-phase of the cell cycle by inhibiting the phosphorylation step of cyclin E and activation of cyclin dependent kinase 2. An excretion balance and pharmacokinetic study was performed following the intravenous infusion of E7070 radiolabelled with carbon-14, in patients with solid tumours (Chapter 2.1.1). Phase I trials of E7070 revealed non-linear pharmacokinetics (saturable distribution and elimination) after intravenous administration of the drug [5]. We studied the *in vitro* distribution of E7070 in human whole blood whether non-linear binding either to red blood cells or to plasma proteins (Chapter 2.1.2) can cause the non-linear distribution of E7070. Moreover, an *in vitro* and *in vivo* pharmacokinetic study was performed to investigate whether there is a drug-drug interaction between E7070 and acenocoumarol. Since three patients in the phase I trials, treated with prophylactic daily oral

maintenance therapy with acenocoumarol (Sintrom®), developed a haemorrhagic tendency and/or a prolonged prothrombin time following the intravenous administration of E7070. The influence of E7070 on the pharmacokinetics of acenocoumarol was studied in vivo, and the potential of E7070 to displace acenocoumarol from its plasma protein binding sites and/or to inhibit its hepatic metabolism was studied in vitro (Chapter 2.2).

The third chapter consists of pharmacokinetic studies of methotrexate after high-dose administration. The pharmacokinetics of methotrexate, an antimetabolite, vary considerably among patients mainly due to high interindividual variation in renal excretion of the drug and its major metabolite 7-hydroxy-methotrexate [6]. The successful rescue of a patient with severe methotrexate induced renal toxicity is presented (Chapter 3.1). An integrated population pharmacokinetic model for methotrexate and 7-hydroxy-methotrexate was developed to describe the pharmacokinetics of both compounds, and to study the influence of patient characteristics on the pharmacokinetic parameters (Chapter 3.2).
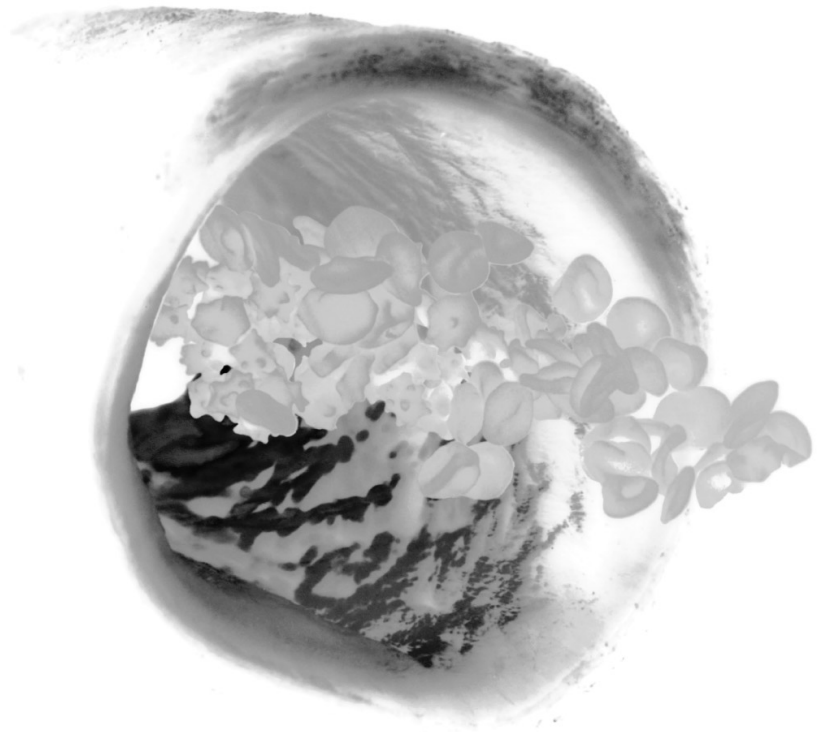
Chapter four describes the pharmacokinetics of paclitaxel and Cremophor EL. Cremophor EL is a polyethoxylated castor oil that is used for the formulation of vitamin preparations and a variety of poorly water-soluble drugs including teniposide and cyclosporin A. Cremophor EL can form micelles in blood in vitro, acting as a high-affinity drug-transporting site for paclitaxel that results in a decreased unbound paclitaxel fraction in plasma. Cremophor EL can decrease the blood-plasma ratio of paclitaxel at higher dose-levels by reducing the uptake in red blood cells [7,8]. A population pharmacokinetic model of Cremophor EL, used as a formulation vehicle for paclitaxel, was developed (Chapter 4.1). Since the unbound paclitaxel concentration in blood is the pharmacologically active fraction, we developed a method for the quantification of the unbound paclitaxel fraction in human plasma (Chapter 4.3).

The relationships between plasma pharmacokinetics and pharmacodynamics of paclitaxel have been reported in patients with ovarian cancer and non-small cell lung cancer (NSCLC), whereby the drug's efficacy and toxicity were related to the time above a threshold concentration of paclitaxel in plasma [9-11]. A population model of paclitaxel was developed and used to evaluate the feasibility of Bayesian dose individualisation in patients with NSCLC (Chapters 4.2.1 and 4.2.2).

References

1. Grochow LB. Individualized dosing of anticancer drugs and the role of therapeutic monitoring. In: Gochow LB, Ames MM, editors. A clinician's guide to chemotherapy pharmacokinetics and pharmacodynamics. Baltimore: Williams & Wilkins, 1998:3-16.
2. Calvert AH, Newell DR, Gumbrell LA, et al. Carboplatin dosage: prospective evaluation of a simple formula based on renal function. J Clin Oncol 1989;7:1748-1756.
3. Owa T, Okauchi T, Yoshimatsu K, et al. A focused compound library of novel N-(7-indolyl)benzenesulfonamides for the discovery of potent cell cycle inhibitors. Bioorg Med Chem Letters 2000;10:1223-1226.
4. Owa T, Yoshino H, Okauchi T, et al. Discovery of novel antitumor sulfonamides targeting G1 phase of the cell cycle. J Med Chem 1999;42:3789-3799.
5. Van Kesteren C, Mathôt R, Raymond E, et al. Population pharmacokinetic analysis of the novel anti-cancer agent E7070 during phase I studies: model building and validation. J Clin Oncol *in press*.
6. Treon SP, Chabner BA. Concepts in use of high-dose methotrexate therapy. Clin Chemistry 1996;42:1322-1329.
7. van Tellingen O, Huizing MT, Nannan Panday VR, et al. Cremophor EL causes (pseudo-) non-linear pharmacokinetics of paclitaxel in patients. Br J Cancer 1999;81:330-335.
8. van Zuylen L, Verweij J, Sparreboom A. Role of formulation vehicles in taxane pharmacology. Invest New Drugs 2001;19:125-141.
9. Huizing MT, Keung ACF, Rosing H, et al. Pharmacokinetics of paclitaxel and metabolites in a randomised comparative study in platinum-pre-treated ovarian cancer patients. J Clin Oncol 1995;11:2127-2135.
10. Gianni L, Kearns CM, Gianni A, et al. Nonlinear pharmacokinetics and metabolism of paclitaxel and its pharmacokinetic/pharmacodynamic relationships in humans. J Clin Oncol 1995;13:180-190.
11. Huizing MT, Giaccone G, van Warmerdam LJC, et al. Pharmacokinetics of paclitaxel and carboplatin in a dose-escalating and sequencing study in patients with non-small cell lung cancer. J Clin Oncol 1997;15:317-329.

Introduction 1

Chapter 1

Pharmacokinetically Guided Dosing of Chemotherapeutic Agents

HJG Desirée van den Bongard, Ron AA Mathôt, Jos H Beijnen and Jan HM Schellens

Summary

The current practice for dose calculation of most anticancer agents is based on body surface area (BSA [in m²]), although lower interpatient variation in pharmacokinetic (PK) parameters has been reported with pharmacokinetically guided administration. As chemotherapeutic agents have a narrow therapeutic window, pharmacokinetically-guided dosing may lead to less toxicity and higher efficacy than administration on the basis of BSA. Pharmacokinetically guided administration, using parameters such as area under the plasma concentration-time curve (AUC), steady state plasma drug concentration and drug exposure time above a certain plasma concentration, has been studied for many antineoplastic agents. Assessment of pharmacokinetic profiles allows the characterisation of relationships between pharmacokinetic parameters and efficacy and toxicity. AUC appears to be more closely correlated with the pharmacodynamics than does the dose per unit of BSA. In particular, the AUC-guided administration of carboplatin has been extensively studied, based on the close relationship between the renal clearance and glomerular filtration rate (GFR). Several formulae and limited sampling models have been derived to predict the AUC of carboplatin. The relationship between AUC and pharmacodynamics has also been studied for other anticancer agents, for example fluourouracil, topotecan, etoposide, cisplatin, and busulfan but all less extensively than for carboplatin. The pharmacokinetically guided administration of these agents needs to be investigated further before the use of alternative administration formulae can become standard clinical practice.

Prospective studies of pharmacokinetically guided dosing versus surface area-based administration should be performed to validate pharmacokinetic-pharmacodynamic relationships and to facilitate optimal dosage of anticancer agents in the clinic.

1. Rationale for individualised dosing of anticancer agents

In clinical practice, anticancer agents are almost invariably dosed per unit of body surface area (BSA [in m²]) and administered at the maximum dose tolerated (MTD) by the patient. Compared with many other drugs, anticancer agents have a very narrow therapeutic window, with delayed therapeutic effects and toxicity. Moreover, interpatient pharmacokinetic variability is generally high because of variable drug absorption, distribution and elimination processes.[1-8] Table 1 lists the major aetiological factors of pharmacokinetic alterations in patients with cancer. In addition, metabolism may vary by genetically determined variation in expression and activity of drug metabolising enzyme systems. These enzymes can be cytochrome P450 (CYP) in cyclophosphamide, ifosfamide, paclitaxel and docetaxel metabolism; dihydropyrimidine dehydrogenase (DPD) in 5-fluorouracil metabolism; and thiopurine methyltransferase (TPMT) activity in the elimination of 6-mercaptopurine (6-MP).[1,2,9]

In patients with significant renal or hepatic dysfunction dosage, reduction of the dosage of drugs eliminated through these organs is recommended to prevent severe toxicity. In general, no dosage reduction is recommended when the contribution of renal clearance to the excretion of the drug is below 33% and/or renal function is 70% or more of normal function.[4,7] It is more complicated to correlate liver enzyme levels with modification of hepatic elimination activity, since there is no reliable biochemical test that adequately quantifies the modified hepatic drug clearance. This has resulted in conflicting recommendations for dosage reduction in patients with a modification of these biochemical tests.[6,7]

For several anticancer drugs, plasma concentration parameters (area under the plasma concentration-time curve (AUC), steady-state plasma concentration (Css) and peak plasma concentration (Cmax)) and drug exposure time above a certain threshold concentration have been reported to correlate with toxicity and therapeutic effect.[1,3,5,9-13] Consequently, individualised dosing may result in less undertreatment or severe toxicity compared with administration based on the BSA. To understand and predict normal tissue toxicity and tumour response, it is necessary to explore dose- or concentration-effect relationships. In several randomised prospective studies, AUC-guided administration has been compared with conventional dosing based on BSA. Adaptive administration of methotrexate, etoposide and fluourouracil using pharmacokinetic parameters to reach a predefined efficacy target AUC has been shown to result in a narrower and more accurate exposure range compared with administration based on unit of BSA alone.[14-18]

In this review, we focus on the methods for pharmacokinetically guided dosing (emphasising AUC-guided administration) of anticancer agents that have been developed to decrease pharmacokinetic and pharmacodynamic variability. Clinical studies of pharmacokinetically guided administration correlated with therapeutic efficacy and toxicity will be presented and discussed. Futhermore, we discuss the requirements for, and feasibility of, the wider applications of individualised administration in clinical practice.

Table 1. Etiology of altered absorption, distribution and elimination of anticancer agents in patients with cancer

	Alteration	Aetiological factor	References
Absorption[a]	↓	Nausea/vomiting	2,8
	↓	Prior surgery, radiotherapy or chemotherapy affecting the g.i. tract	
	↓/⇑	Drug-drug interaction	
	⇑/↓	↓/⇑ g.i. peristalsis (e.g. antiemetics/laxatives/tumour)	
Distribution	↓	Bodyweight loss	2,8
	↓	Decreased body fat (less distribution of lipophilic drugs)	
	←	Hypoalbuminaemia (higher amount of free drug in plasma)	
		↓ Protein binding (drug-drug interactions)	
	←	Peritoneal or pleural effusions (e.g. methotrexate which necessitates prolonged administration of folinic acid rescue therapy)	
	←	Elevated AAG (e.g. docetaxel)	
Elimination	↓	Renal dysfunction due to dehydration, tumour infiltration, tumour lysis syndrome, (previous) renal toxic drugs and surgery	2,4,6,8
	↓	Hepatic dysfunction due to tumour infiltration, biliary obstruction, (previous) hepatotoxic drugs, surgery, inhibition of metabolism (cimetidine) and polymorphic drug metabolism	2,4,6,8
	←	Induction of metabolism (barbiturates, rifampicin)	2

a   Oral drugs only.
AAG = α₁-acid glycoprotein; GI = gastro-intestinal.

2. Area under the plasma concentration-time curve (AUC)-guided dosing

The systemic exposure of a drug is most often defined as the AUC. The AUC is the relevant pharmacokinetic parameter when toxicity and therapeutic effect of anticancer drugs are studied. An increased AUC in patients with a low elimination rate may result in more severe toxicity whereas a decreased AUC may result in a lower efficacy. Therapeutic drug monitoring (TDM) can be used to determine the AUC during the first course of chemotherapy and to adjust the dose to achieve the target AUC in subsequent courses.[3,11]

2.1 Carboplatin

AUC-guided administration has been investigated extensively for carboplatin. This method has resulted in more precise prediction of the effect of carboplatin in terms of dose-limiting toxicity (mainly thrombocytopenia). The drug differs from many antineoplastic drugs in that its total body clearance (CL) is predominantly determined by glomerular filtration.[19-21] Consequently, the AUC of carboplatin is better correlated with the creatinine clearance (CL_{cr}) than with the dose per unit of BSA.

Determination of the AUC requires frequent blood sampling and is inconvenient for the patient. This has resulted in the development of more simple methods to calculate the AUC of carboplatin. *A priori* prediction of the desired AUC results in dose calculation based on the target AUC and glomerular filtration rate (GFR).[22-24] This method is based on the correlation of the AUC with pharmacodynamics during prior cycles. As frequent blood sampling may be inconvenient for the patient, limited sampling models (LSMs) have been developed. The equation is derived to predict one single variable, usually the AUC, based on plasma concentrations measured at several time-points. The doses for the following courses can be adapted to achieve an exposure at the target AUC.[12,25-27]

2.1.1 A priori prediction of AUC

Egorin and co-workers demonstrated a significant correlation between CL_{cr} and platelets nadir (PN).[22] They developed a formula in which the calculated dose was based on CL_{cr} determined by 24-hour urine collection (CL_{CR-24h}) and the target platelet nadir in pretreated and in non-pretreated patients (males and females).

For non-pretreated patients:

$$\text{Dose} = (0.091) \times \left(\frac{CL_{CR}}{BSA} \right) \cdot \left[\frac{(\text{pretreatment PC - desired PN})}{\text{pretreatment PC}} \cdot 100 \right] + 86 \qquad \text{equation 1}$$

For pretreated patients:

$$\text{Dose} = (0.091) \times \left(\frac{CL_{CR}}{BSA} \right) \cdot \left[\left(\frac{(\text{pretreatment PC - desired PN})}{\text{pretreatment PC}} \cdot 100 \right) - 17 \right] + 86 \qquad \text{equation 2}$$

where the BSA is measured in m²; CL_{CR} in ml/min; dose in mg/m² and platelet count (PC) in cells/µl).

These equations have been validated prospectively in studies of single-agent and combination chemotherapy, which demonstrated their usefulness.[28,29]

Calvert and co-workers[23] developed a dosage formula by retrospective analysis of carboplatin administration in 18 patients with a GFR range of 33 to 136 ml/min (determined by the ⁵¹chromium-ethylenediaminetetra-acetic acid excretion (⁵¹Cr-EDTA) method):

$$\text{Dose} = \text{target AUC}_{\text{free}} \cdot (\text{GFR} + 25) \qquad\qquad \text{equation 3}$$

where the dose is measured in mg, AUC_{free} is the area under the free carboplatin plasma concentration-time curve in mg/ml*min and GFR is in ml/min.

As the clearance of carboplatin is mainly determined by CL_{cr}, GFR can be replaced by CL_{cr}.[30] The value '25' accounts for carboplatin clearance by non-GFR routes. Calvert et al validated this formula in a prospective study of 31 patients with solid tumours with a target

Table 2. Studies of carboplatin (single agent) showing a correlation between area under the concentration-time curve (AUC) and pharmacodynamics

Carboplatin dose determined by	Effect	Comments	References
Patients with lung cancer			
BSA	WBC↓, PLT↓	Low correlation AUC-myelotoxicity	31
BSA	PLT↓	In combination with thoracic irradiation, prospective evaluation of the correlation AUC-response is warranted	32
Patients with solid tumours			
Calvert formula	PLT↓	⁵¹Cr-EDTA clearance to measure GFR is also more accurate than calculated CL_{CR} in patients pretreated with nephrotoxic chemotherapy	23
Patients with ovarian cancer			
Calvert formula	WBC↓, PLT↓, response	AUC ≥5 mg/ml does not increase response	33
Calvert formula	PLT↓	Further elevation of AUC with stem-cell transplantation	34
Calvert formula	WBC↓, ANC↓, PLT↓, response	Survival rates may be increased by a target AUC >12 mg/ml*min (with haematological support)	35

ANC↓ = neutropenia; BSA = body surface area; CL_{CR} = creatinine clearance; ⁵¹CrEDTA = determination of clearance of ⁵¹Cr-labelled EDTA; GFR = glomerular filtration rate; PLT↓ = thrombocytopenia; WBC↓ = leucopenia.

AUC escalating from 3 to 8 mg/ml*min and concluded that this formula predicted the AUC accurately.[23] On the basis of the observed toxicities, they recommended a target AUC of 7 mg/ml*min for non-pretreated patients and 5 mg/ml*min for pretreated patients.[23]

Table 2 lists the pharmacokinetic studies of carboplatin infusion in which a correlation between AUC and toxicity has been observed.[23,31-35] In 4 of these studies the Calvert formula has been applied to achieve a target AUC.[23,33-35] In 2 other studies the AUC of ultrafiltrable carboplatin was calculated by the trapezoidal rule.[32,33] In a retrospective study of 1028 patients with ovarian cancer, Jodrell and co-workers reported that tumour response, in contrast with myelotoxicity, does not increase above a carboplatin AUC of 5 to 7 mg/ml*min.[33] Two studies in patients with ovarian cancer have demonstrated that an increase of the target AUC from 4 to 8[36] or 6 to 12[35] mg/ml*min resulted in enhanced myelotoxicity, whereas the observed response remained constant. In a study by Lind and colleagues further escalation of the target AUC above 9 mg/ml*min with granulocyte colony-stimulating factor (G-CSF) was impossible because of haematological toxicity.[34] The authors concluded that an AUC of 7 mg/ml*min every 14 days for 4 cycles is the maximum tolerated AUC that can be achieved with G-CSF. They suggested that a further increase in the AUC may be possible using a combination of cytokines or haematological support by peripheral stem-cell transplantations.[34] Shea and co-workers demonstrated that non-haematological toxicities are dose-limiting at a target AUC of 25 mg/ml*min with autologous bone marrow transplantation.[37] AUC-based administration of high-dose carboplatin in combination with haematological support should be further investigated to establish a relationship between a high target AUC and therapeutic efficacy.

In a prospective study, Ghazal-Aswad et al. have demonstrated that carboplatin dose calculated by the Calvert formula (GFR calculated by the ^{51}Cr-EDTA method) predicts the dose required to achieve the target AUC of the free carboplatin concentration (AUC of 5,7 and 9 mg/ml*min).[38]

In conclusion, the Calvert formula can be applied in exploring the relationship between target AUCs of 5 to 25 mg/ml*min and pharmacodynamics, and is instrumental in AUC-guided carboplatin administration.

2.1.2 Calculation of carboplatin clearance

The application of the Calvert formula results in dose reduction in patients with low renal clearance and dose increase in patients with higher than average renal clearance.[23]

Accurate AUC-guided carboplatin administration is dependent on precise measurement of the GFR. The reference standard for GFR is the renal clearance of inulin at steady-state concentration during a continuous inulin intravenous infusion.[36] However, this method is rarely used in clinical practice since it is very inconvenient and time-consuming. Kinowski et al. have reported a simplified method in which the number of blood samples was reduced to only one at 2 hours after infusion.[39] A Bayesian estimate of the CL_{CR} was obtained after a 10-minute intravenous

infusion of inulin. This approach resulted in a less inconvenient 1-sample strategy with a good precision and low bias [CL_{CR} 7.85 ± 1.96 L/h, bias 0.397, 95% confidence interval (CI): -0.414, 1.21; precision 1.97, 95% CI: -0.59, 4.53]. Nevertheless, it is not a standard method in clinical practice, probably since it is still time-consuming in comparison with other methods.[39]

The determination of CL_{CR} by ^{51}Cr-EDTA is accurate but is an invasive method, and therefore of limited use in clinical practice.[40-42] In comparison, 24-hour urine collection to measure CL_{CR-24h} may result in inaccurate estimation of the GFR. Hence, over- or under-exposure to carboplatin can occur when this method is applied, which may be because of an incomplete 24-hour urine collection and/or fluctuation in the endogenous creatinine production.[43-45] Alternatively, CL_{CR} can be calculated by the Cockcroft-Gault (CG) or Jelliffe (J) formulae based on patient characteristics, including serum creatinine level (S_{CR}), age, gender and bodyweight (BW):[46,47]

$$CL_{CR-CG} = \frac{1.23 \cdot (140 - age) \cdot BW}{S_{CR}} \left(\cdot\, 0.85 \text{ if female} \right) \qquad \text{equation 4}$$

$$CL_{CR-J} = \frac{98 - 16 \cdot \left(\dfrac{age - 20}{20} \right)}{S_{CR}} \left(\cdot\, 0.9 \text{ if female} \right) \qquad \text{equation 5}$$

where CL_{CR} is measured in ml/min, age in years, S_{CR} in µmol/L and bodyweight in kg.

In a similar manner, Chatelut and co-workers[24] included these patient characteristics in a formula to predict carboplatin clearance ($CL_{carboplatin}$) that was developed from a population pharmacokinetic analysis in 70 patients:

$$CL_{Carboplatin} = 0.134 \cdot BW + \frac{218 \cdot BW \cdot (1 - 0.00457 \cdot age) \cdot (1 - 0.314 \cdot gender)}{S_{CR}} \qquad \text{equation 6}$$

where $CL_{carboplatin}$ is measured in ml/min, age in years, Scr in µmol/L, bodyweight in kg and gender has the value 0 if male and 1 if female.

Consequently, the dose to be administered can be calculated using:

$$Dose = CL_{carboplatin} \cdot AUC \qquad \text{equation 7}$$

where dose is in mg; $CL_{carboplatin}$ in ml/min and AUC in mg/ml*min.

Chatelut and co-workers concluded that $CL_{carboplatin}$ calculated by their method was almost as accurate as that calculated by the Calvert method when the ^{51}Cr-EDTA clearance measurement of clearance was used.[24] However, both Calvert et al. and Chatelut et al.

reported that the CL_{CR-CG} and CL_{CR-J} both underestimate the GFR determined by the ^{51}Cr-EDTA method.[24,42] Van Warmerdam et al. reported that the AUC calculated by using the Calvert formula with a GFR based on CL_{CR-CG} (S_{CR} determined by the Jaffé method) or CL_{CR-24h} resulted in an overprediction of 10% and an underprediction of 10%, respectively, compared with the observed AUC.[48] The AUC calculated by the Chatelut formula showed an accurate prediction of the AUC.[48] However, Okamoto et al. reported in a comparable study that the Calvert formula based on CL_{CR-CG} or CL_{CR-24h} predicted the observed carboplatin clearance better than the Chatelut formula.[30] These discrepant results may be attributed to the application of different assays for the measurement of serum creatinine, the determination of a non-steady-state concentration of serum creatinine, pretreatment with nephrotoxic drugs, and the different patient populations.[23,30,36,46,49-51] Currently, the Jaffé method (alkaline picrate) and the enzymatic method (e.g. EKTACHEM Clinical Chemistry Slides) are applied in clinical practice for the measurement of S_{CR}. The Jaffé method overestimates the S_{CR} because of interference by non-creatinine chromogens whereas the enzymatic method is more accurate.[51,52] The Calvert formula was originally based on the GFR measured by the ^{51}Cr-EDTA method, whereas CL_{CR-CG} is based on the Jaffé method and the Chatelut formula for $CL_{carboplatin}$ is based on the enzymatic method.[23,24,46]

In two recent studies, new formulae were developed and validated to calculate the GFR derived from the ^{51}Cr-EDTA plasma concentration-time curves. Data were analysed according to a population pharmacokinetic analysis by using the nonlinear mixed effects modelling approach (NONMEM).[53,54] The formula derived by Martin et al.[53] is:

$$GFR = \frac{163 \cdot ABW \cdot (1 - 0.00496 \cdot age) \cdot (1 - 0.252 \cdot gender)}{S_{CR}}$$
equation 8

where GFR is in ml/min, ABW is the actual bodyweight in kg, age is in years, gender has the value 0 if male and 1 if female and S_{CR} is in µmol/L.

The formula derived by Wright et al.[54] is:

$$GFR = \frac{(6600 - 40 \cdot age) \cdot (1 - 0.17 \cdot gender) \cdot BSA}{S_{CR}}$$
equation 9

where GFR is in ml/min, age is in years, gender has the value 0 if male and 1 if female, BSA is in m² and S_{CR} is in µmol/L.

The formula derived by Martin et al. (NONMEM formula) resulted in a more accurate prediction of the individual GFR than did CL_{CR-CG}. The ratio between the GFR predicted by the NONMEM formula and observed GFR in the validation group was 0.95 ± 0.23 (mean ± SD), whereas the ratio with CL_{CR-CG} was 0.86 ± 0.21. The Wright et al. formula was more accurate than CL_{CR-J} and CL_{CR-CG} (bias -3% *vs* -18% and -11%, precision 20% *vs* 24% and 25%,

Table 3. Studies of carboplatin (combination therapy) showing a correlation between area under the concentration-time curve (AUC) and pharmacodynamics

Coadministered agents	Effect	Comments	References
Patients with ovarian cancer			
Cyclophosphamide or ifosfamide	PLT↓	Prospective evaluation of the correlation AUC-pharmadynamics is warranted	60
Cyclophosphamide	PLT↓	Increased myelotoxicity during following courses (similar AUC)	20
	WBC↓, PLT↓, response	AUC ≥8 mg/ml*min does not increase response	37
	WBC↓, PLT↓	Prospective evaluation of relationship AUC-response is warranted	56
Paclitaxel	PLT↓	Less PLT↓ at dose level 175 mg/m^2 compared with 150 mg/m^2	42
Patients with testicular cancer			
Etoposide, bleomycin	PLT↓	High variation in platelet nadir after the first course	57
	WBC↓, PLT↓, response	AUC shows a significant correlation with BSA-based dose	58
	PLT↓	Only poor correlation AUC-PLT↓, no correlation AUC-response	63
Etoposide	WBC↓, ANC↓, PLT↓, Hgb↓	Pharmacokinetic-pharmacodynamic correlation only during first course	70
Patients with solid tumour and lymphoma			
Ifosfamide, etoposide + G-CSF	PLT↓	No correlation AUC-response	59
Patients with urothelial cancer			
Methotrexate, vinblastine	ANC↓	Optimal AUC needs to be determined for each carboplatin combination chemo-therapy	71
Patients with lung cancer			
Paclitaxel	PLT↓, ANC↓, vomiting	Further evaluation of AUC with haematological support	68
Cisplatin +/- G-CSF	PLT↓	No pharmacokinetic interaction between paclitaxel and carboplatin	62
Cisplatin +/- ifosfamide	PLT↓, ANC↓	No correlation AUC-response	72

ANC↓ = neutropenia; BSA = body surface area; G-CSF = granulocyte colony-stimulating factor; Hb↓ = anaemia; PLT↓ = thrombocytopenia; WBC↓ = leucopenia.

respectively).[54] Thus, the formulae derived by Martin et al. and Wright et al. predicted the individual patients' GFR more accurately than did CL_{CR-CG} in their study populations.[53,54]

2.1.3 Application of AUC based carboplatin administration formulae in combination chemotherapy

The Calvert formula has been applied by other investigators and appears accurate if carboplatin is infused in combination chemotherapy.[20,34,36,43,55-73] In Table 3, studies are listed in which a significant correlation between the AUC and the severity of bone marrow toxicity and/or therapeutic efficacy was demonstrated.[20,37,42,56-60,62,63,68,70-72] These are mainly retrospective studies in which the dose was based on BSA, and the AUC was calculated after administration by inverting the Calvert formula [AUC = Dose/(GFR + 25)]. However, retrospective analysis may result in overlooking confounding factors in the relationship between AUC and therapeutic effect. These factors may be the observed variation in the methods applied to determine the GFR and the S_{CR} values. Also, a high retrospectively calculated AUC may be attributed to a poor renal function, which can be caused by pretreatment with cisplatin. Pretreated patients may not respond to carboplatin chemotherapy because of cross-resistance between carboplatin and cisplatin.[74]

In conclusion, the Calvert and Cockcroft-Gault formulae are widely used to calculate the carboplatin dose based on a target AUC and the GFR, respectively. The application of the Cockcroft-Gault formula in combination with the Calvert formula also results in less variability in AUC of carboplatin in single-drug and combination chemotherapy than does administration per unit of BSA, despite the outlined limitations.[43] Preferably, the formulae for carboplatin administration and the S_{CR} assays should be standardised to prevent variations in dose calculations and to facilitate the comparison of the dose and GFR of patients treated in different centres.

2.1.4 Limited sampling models in AUC-guided dosing

LSMs have been developed to limit the frequency of blood sampling needed for the quantification of AUC. After blood sampling the concentrations at each individual sample time are correlated to the AUC value by multivariate analysis. The sample times that show the highest correlation with the AUC can be included in a corresponding regression line. Consequently, the LSMs enable the prediction of AUC based on a single or multiple time-point(s). After blood sampling at specific time-points during the first course, the AUC can be calculated and dose can be adjusted during the following courses to reach the target AUC. However, a limitation of the LSMs is that they need to be applied and prospectively validated in treatments using the same anticancer agents, doses, administration schedules and duration of infusion as the original study from which the LSM was established.[11,12,75-77] Several LSMs for carboplatin have been developed. These models are listed in Table 4, and have also been validated by other investigators.[25-27,78] Sørensen 's single sample model was validated by van Warmerdam et al. in 9 patients treated with high dose chemotherapy

Table 4. Limited sampling models for the estimation of the AUC of carboplatin

Administration schedule	Dose (mg/m²)	Limited sampling models	Validation results	References
1-hour infusion (following cyclophosphamide)	250/375/ 500	$AUC^a = 0.52 \times C_{2.75h}{}^b + 0.92$ $AUC^a = 0.053 \times C_{0.25h}{}^b + 0.401 \times C_{2.75h}{}^b + 0.628$	Bias -4.4%; precision 13.9% Bias -2.2%; precision 9.4%	25
60-100 min infusion	20-1600 or target AUC 2-8 mg/ml*min	$AUC_{free}{}^a = (C_{24h}{}^c + 0.3)/0.82$	Bias -4.2%; precision 11.5%	26
90 min infusion (following irinotecan)	300	$AUC_{free}{}^a = 0.784 \times C_{free,4h}{}^b + 1.30$ $AUC_{free}{}^a = 0.100 \times C_{free,0.25h}{}^b + 0.597 \times C_{free,4h}{}^b + 0.140$	Bias 2.41%; precision 9.42% Bias 1.22%; precision 5.49%	27
30 min infusion (in combination with paclitaxel)	300-550	$AUC_{free}{}^a = 418 \times C_{free,2.5h}{}^d + 0.43$	Bias 3.4%; precision 10.1%	78

[a] mg/ml*min.
[b] µg/ml.
[c] µmol/L.
[d] mg/ml.

AUC_{free} = area under the free carboplatin plasma concentration-time curve; C = total plasma carboplatin concentration; C_{free} = free carboplatin plasma concentration.

(carboplatin, cyclophosphamide and thiothepa).[76] The model proved to be accurate despite a different administration schedule and carboplatin dose.

The single sample model of Ghazal-Aswad et al. was validated by Nannan Panday et al., who proved the inability of this model to predict the AUC of carboplatin in combination with paclitaxel and in high dose chemotherapy (cyclophosphamide and thiothepa).[26,79] They developed a new LSM in order to refine the carboplatin dose when given in combination with paclitaxel. This validated single-sample model appeared to be precise and showed low bias (bias 3.4%, precision 10.1%).[78]

A Bayesian approach may allow optimal interpretation of limited sample information, since it combines pharmacokinetic information from an individual patient with that of the population. During the following courses, dose adjustment can be carried out with the intention of achieving a target AUC. Guillet et al. demonstrated the feasibility of the Bayesian approach in carboplatin combination chemotherapy (120-hour infusion).[80] Bayesian estimation of the individual pharmacokinetic parameters based on 2 individual drug plasma concentrations (1 and 12 hours after the start of the 120-hour carboplatin infusion) enabled estimation of the plasma carboplatin concentration at the end of the infusion. In 36 patients, dose adjustment was performed to achieve concentrations of 1.0, 1.5 or 1.8 mg/L at 24 hours after the start of the infusion. This method showed good precision and acceptable bias for the 3 target concentrations. Thrombocytopenia was most frequently observed in the group with the highest concentration at the end of the infusion.[80]

Duffull et al. have developed a sequential Bayesian algorithm to estimate the carboplatin dose (single agent, target AUC 5 to 7 mg/ml*min, 30-minute infusion) in 12 patients.[81] Recent total carboplatin concentrations weighted more than earlier concentrations in the dose adjustment of individual patients.

Very recently, a Bayesian approach was developed and validated by our group for the estimation of carboplatin AUC in high dose chemotherapy.[82] This method was compared with the LSM developed by Sørensen et al. and the Chatelut and Calvert formulae (using CL_{CR-CG}, CL_{CR-J} and the Wright formula to calculate CL_{CR}) for the prediction of the AUC.[23-25,46,47,54]. The Bayesian analysis (bias <4%, precision <18%) and the Sørensen LSM (bias -13.7%, precision 17.8%) predicted the AUC better than the Chatelut and Calvert formulae (bias <12%, precision >22%). As a result, the Calvert or Chatelut formulae may be used for calculation of the first dose of carboplatin. For subsequent courses the Bayesian approach or the Sørensen model can be applied to estimate the AUC.

In general, the Bayesian approach may be recommended, as it is more flexible in infusion duration and sampling times than LSMs such as the Sørensen model.[12,82,83]

2.2 Other anticancer agents

The relationships between the AUC and pharmacodynamics of other anticancer agents are listed in Table 5.

Table 5. Anticancer agents (except carboplatin) for which a relationship between area under the concentration-time curve (AUC) and pharmacodynamics has been demonstrated

Anticancer agent (combination)	Pharmacodynamic parameter	Results	References
Oral administration			
Busulfan (high dose chemotherapy and BMT)	VOD	High correlation between AUC and VOD	85
	VOD	Relationship lower dose of cyclophosphamide and less risk of VOD needs further evaluation	86
	VOD	AUC tends to be higher in patients with VOD, relationship lower dose cyclophophamide, less risk VOD?	87
Etoposide	Myelotoxicity	No correlation AUC-response	88
Idarubicin	WBC↓, response	No correlation AUC-time to final progression, unknown cytotoxic effect of idarubicinol	89
Menogaril	WBC↓	Prospective investigation of dosage adjustment is warranted	90
Topotecan	ANC↓, PLT↓, diarrhoea	Merits prospective evaluation of pharmacokinetics and therapeutic effect	91
Fluouracil + etoposide	ANC↓	No correlation AUC-response	92
Intravenous administration			
Cisplatin (bleomycin, vincristine, methotrexate and/or etoposide)	Nephrotoxicity	Pharmacokinetic-pharmacodynamic relationship needs further evaluation	93
Cisplatin	Response	Correlation AUA-response	94
Cyclophosphamide	Cardiac dysfunction	Median duration of response longer in patients with lower AUCs	95
Docetaxel	Time to progression	Population pharmacokinetic-pharmacodynamic analysis	96
Epirubicin	WBC↓	No correlation AUC-response	97

Drug	Endpoint	Conclusion	Ref
Etoposide (+/- cisplatin)	WBC↓, PLT↓	No correlation AUC-response	98
Etoposide (cisplatin or cyclophosphamide)	Response	Probable contribution of cisplatin and cyclophosphamide to pharmacodynamics	99
Etoposide (cisplatin)	Neutropenia	Prospective validation of the LSM and the pharmacodynamic model is warranted	100
Etoposide	WBC↓, PLT↓	No correlation AUC-response	101
Fluorouracil	WBC↓, PLT↓	No correlation AUC-response	102
	Toxicity	Only qualitative analysis of toxicity (present/not present)	103
Fluorouracil (cisplatin)	Toxicity[a]	No correlation AUC-response	104
	Toxicity[a], response	Prospective randomised study to evaluate pharmacokinetic-pharmacodynamic administration is warranted	105
	Survival	Prospective randomised study to evaluate pharmacokinetic-pharmacodynamic administration is warranted	106
	Toxicity[b], response	Prospective randomised study to evaluate pharmacokinetic-pharmacodynamic administration is warranted	107
	Toxicity[c], response	Evaluation of larger patient populations is needed	16
Fluorouracil (leucovorin)	Hand-foot syndrome, diarrhoea	Dose optimisation by inflexible nomograms	108,109
Hexamethylene bisacetamide	PLT↓	No correlation AUC-response	110
	PLT↓	No correlation AUC-response	111
	PLT↓	In only 6 of 10 patients toxicity was correlated with AUC, no correlation AUC-response	112
4'-Iodo-4'-deoxydoxorubicin	ANC↓	Unclear role of the metabolite IDOXOL in pharmacodynamics	113
	ANC↓ PLT↓	Metabolite IDOXOL is probably a better predictor of pharmacodynamics	114
Menogaril	WBC↓, ANC↓	To predict the individual pharmacokinetic parameters further	115

	Toxicity		Reference
	WBC↓, ANC↓	Prospective evaluation of patients with hepatic dysfunction is warranted	116
Paclitaxel	WBC↓	Prospective investigation of dosage adjustment is warranted	117
	Musculoskeletal toxicity, neurotoxicity	No correlation AUC-ANC↓	118
Teniposide (cytarabine)	WBC↓	Correlation AUC-free topotecan	119
	WBC↓	Further evaluation in routine clinical setting is warranted	120
Topotecan	ANC↓, PLT↓	Merits prospective evaluation of pharmacokinetic and therapeutic effect	121
	ANC↓	Merits prospective evaluation of pharmacokinetic and therapeutic effect	122
	ANC↓	Further study of pharmacokinetic-pharmacodynamic relation is warranted	123
	ANC↓	Only a poor correlation AUC-ANC↓, no correlation AUC-response	124
	ANC↓	No correlation AUC-response, low pharmacodynamic variability in this administration schedule. Is TDM needed?	125
Topotecan (etoposide)	WBC↓ ANC↓	Same degree of neutropenia observed in topotecan monotherapy	126
Intravenous and intra-arterial administration			
Fluorouracil	Toxicity[a]	No correlation AUC-response	127

[a] Myelosuppression, gastrointestinal toxicity, stomatitis.
[b] Neutropenia and stomatitis.
[c] Neutropenia, thrombocytopenia, mucositis.

ANC↓ = neutropenia; AUC = area under the plasma concentration-time curve; AUA = area under the DNA-adduct time curve; BMT = bone marrow transplantation; LSM = limited sampling model; PLT↓ = thrombocytopenia; TDM = therapeutic drug monitoring; VOD = veno-occlusive disease; WBC↓ = leucopenia.

2.2.1 Busulfan

Busulfan is an alkylating agent orally administered in patients as part of preparative regimens for patients undergoing bone marrow transplantation. The dose-limiting toxicity is hepatic veno-occlusive disease (VOD), which is experienced in 20% of the patients and results in a mortality of 40%.[128] The absorption and clearance of busulfan show a high interindividual variability. The therapeutic efficacy and toxicity of the agent has been correlated with the AUC of busulfan in patients with cancer.[128-130] Grochow and associates reported a high correlation between the AUC of busulfan and the occurrence of dose-limiting VOD in 15 patients.[85] Several investigators have observed the same phenomenon. However, they also reported a higher incidence of VOD in patients treated with higher doses of cyclophosphamide in combination with busulfan (without an increased AUC of busulfan).[86,87]

2.2.2 Cisplatin

Cisplatin, a platinum compound, is primarily eliminated by renal clearance. The drug has dose-limiting toxicities including nephrotoxicity, ototoxicity, and peripheral neuropathy. Elevated plasma concentrations of ultrafilterable platinum (Pt_U) may result in decreased renal clearance.[131,132] Reece and colleagues reported a significant correlation between the C_{max} and the AUC of Pt_U in 12 of 22 patients treated with cisplatin in a 2- hour infusion.[93] This may demonstrate that this single plasma sample may predict the nephrotoxicity in this small group of patients. They proposed increasing the AUC of Pt_U and decreasing the Cmax of Pt_U by increasing the dose in combination with a longer duration of infusion.

Cisplatin can bind covalently to DNA bases, so-called intra- and interstand cross-links or platinum-DNA (Pt-DNA) adducts. Several clinical studies revealed a significant correlation between white blood cells (WBC) and buccal cells Pt-DNA adduct concentration and response.[94,133-137] Moreover, Schellens et al. reported a significant correlation between the AUC of free cisplatin, area under the DNA-adduct time curve (AUA) in WBC and response.[94]

2.2.3 Cyclophosphamide

Cyclophosphamide is an alkylating drug that requires bioactivation before exerting its cytotoxic effects.[95,138,139] An LSM has been developed to define the AUC without frequent blood sampling. Validation of the LSM resulted in an accurate prediction of the AUC (bias 3.3 ± 3.6%, precision 9.3 ± 2.7) despite different dose levels in the 2 groups (1000 mg/m² as a 1-hour intravenous infusion *vs* 300, 600 or 1200 mg/m² as 1-hour intravenous infusions).[138] This LSM has been applied in a study of high dose cyclophosphamide (1.5, 3.0, 4.5 and 6.0 g/m²) in combination with granulocyte-macrophage colony-stimulating factor (2.5, 5 and 10 μg/kg). No relationship between the AUC of cyclophosphamide and degree of myelosuppression could be established.[139] Ayash et al. have demonstrate a negative correlation between the plasma concentrations of total cyclophosphamide and

the development of cardiac dysfunction in 19 patients with breast cancer (with no signs of cardiotoxicity before treatment) treated with high dose combination chemotherapy (cyclophosphamide 6000 mg/m^2 as a 96-hour infusion) and autologous bone marrow transplant.[95] They also observed a longer median duration of response of 22 months in patients with lower AUC values (<5000 µmol/L*h) compared with 5 months in patients with higher AUC values (>5000 µmol/L*h). These data support that a higher concentration of active cyclophosphamide metabolite contributes to more cytotoxicity and cardiotoxicity.

2.2.4 Docetaxel

Docetaxel is a semisynthetic taxoid drug. The precursor is extracted from the needles of the western yew, *Taxus baccata*. The drug enhances microtubule assembly and inhibits the depolymerisation of tubulin. Docetaxel is active in patients with solid tumours, including non-small-cell lung cancer (NSCLC), breast cancer, and head and neck cancers.[140-142]

Hudis et al. performed a pharmacokinetic-pharmacodynamic analysis of docetaxel after infusion (1-hour intravenous infusion, 100 mg/m^2) in 35 patients with breast cancer during the first cycle of a phase II study.[143] Although no overall correlation was observed between AUC and toxicity, a high AUC was observed in 1 patient (with hepatic metastases) who experienced severe toxicity (neutropenia and mucositis) and died.

Bruno et al. performed a population pharmacokinetic-pharmacodynamic analysis of docetaxel during the first course of phase II studies.[96] They used a Bayesian approach to estimate individual pharmacokinetic parameters in patients with breast cancer (n=231) and NSCLC (n=189) who received docetaxel at doses of 75 or 100 mg/m^2 (1-hour infusion). They demonstrated that the AUC was a significant predictor of the time to progression in patients with NSCLC (using Cox and logistic regression analysis). This study proved the feasibility of population pharmacokinetic-pharmacodynamic evaluation based on LSMs.

2.2.5 Epirubicin

Epirubicin is an anthracycline that shows an antitumour activity analogous to doxorubicin but has less cardiotoxicity. Jakobsen and colleagues have demonstrated a significant correlation between the AUC of epirubicin and its metabolite epirubicinol and the decrease in WBC count.[97] They used a previously validated single sample model for 2- or 4-hour infusions, and single-sample or 2-sample models for 10-minute infusions to calculate the AUC. The calculated AUC was retrospectively correlated with the WBC decrease and resulted in 2 models to predict the WBC decrease based on 1 or 2 plasma concentrations. These models enable prediction of myelotoxicity from 1 or 2 samples and allow adjustment of the dosage, which may result in a safer therapeutic regimen:

$$\log \text{WBC}_{nadir} = \log \text{WBC}_{initial} - 0.0073 \cdot C_6 - 0.14 \qquad \text{equation 10}$$

where C_6 is the plasma concentration at 6 hours after administration in µg/L.

Future studies should be directed to validate the correlation between the severity of toxicity and the therapeutic effect of epirubicin.

2.2.6 Etoposide

Etoposide is a topoisomerase II inhibitor that belongs to the epipodophyllotoxins. It is used for treatment of patients with solid tumours and as a part of preparative regimens for bone marrow transplantation. Previous studies have demonstrated a significant relationship between the AUC of etoposide and its myelotoxicity or therapeutic efficacy in patients treated with doses based on the BSA.[88,98,99,101] Miller and colleagues have confirmed the relationship between AUC and toxicity by an LSM and a pharmacodynamic model, which enables the estimation of the clearance and the neutrophil nadir.[100]

Lowis and colleagues have validated an LSM based on one plasma concentration in 13 children.[144] They concluded that administration based on estimation of the AUC guided by a single blood sample resulted in a significant reduction in the variation of AUC seen with administration based on BSA.[144] Two studies have proven the feasibility of adaptive dosing of etoposide, which resulted in less pharmacokinetic variability.[145,146] Lowis and co-workers studied adaptive dosing in 9 children using their LSM and a predefined target AUC.[145] The AUC of the first etoposide dose was estimated using the LSM. Subsequent doses were calculated according to the equation:

$$\text{Dose on day 2} = \frac{(\text{dose on day 1})}{\text{AUC on day 1}} \cdot \text{target AUC on day 2} \qquad \qquad \text{equation 11}$$

where dose is in mg and AUC is in mg/ml*min.

As the interpatient variability in pharmacokinetic parameters was already low after administration of the first dose, they concluded that future pharmacokinetic studies should be performed in patients who may benefit from pharmacokinetically guided dosing, for example patients with renal dysfunction.[145]

2.2.7 Fluorouracil

Fluorouracil, an antimetabolite, is applied in the treatment of primarily gastrointestinal, breast, and head and neck carcinomas. The drug shows a high interpatient variability in metabolism which is related to the genetic polymorphism of dihydropyrimidine dehydrogenase. This is the key enzyme of endogenous pyrijmidine metabolism; deficiencies of this enzyme result in high concentrations of fluorouracil with severe toxicity. Moreover, toxicity is dependent on the duration of infusion. Myelosuppression is dose-limiting after bolus intravenous injection, and diarrhoea and oral ulceration are mainly dose-limiting after continuous infusion.[109,147]

A significant correlation between the AUC of fluorouracil and the drug-induced toxicity after intravenous and hepatic intra-arterial administration has been demonstrated.[102-104,127] In these studies, the AUC-guided dose was based on retrospective calculation of pharmacokinetic parameters after conventional administration. Further research revealed higher complete response rates and longer survival in patients after adaptive administration guided by the AUC of fluorouracil.[105-107] Fety and colleagues have compared prospectively AUC-guided dosing (pharmacokinetic arm) with conventional administration (standard arm, 4 g/m²) of fluorouracil in 122 patients with head and neck carcinomas.[16] In the first course there was no difference in AUC between the pharmacokinetic and standard arms. During the following courses (2 and 3), the AUC values were significantly lower in the pharmacokinetic arm with less interpatient variability for AUC values. More frequent toxicity and a larger variety of symptoms of severe toxicity [thrombocytopenia, neutropenia, and mucositis grade 3-4 according to common toxicity criteria (CTC)] were seen in the standard arm. The objective response rate was comparable in both arms.[16]

Gamelin et al. reported that acute toxicity (hand-foot syndrome and diarrhoea) was correlated with plasma fluorouracil concentrations >3000 µg/L during a weekly 8-hour infusion of the drug at different dose levels in combination with high dose leucovorin.[108] The quality of response was better in 40 patients with higher than mean plasma concentrations at the different dose levels. Consequently, they defined an optimal therapeutic and nontoxic range of 2000 to 3000 µg/L, which equates to an AUC of 16 to 24 mg/L*h. They then modified the fluorouracil dose according to previous plasma concentrations and doses using dosage normograms, and observed the resulting toxicity in 152 patients with colorectal cancer. The correlation between plasma fluorouracil concentration and acute toxicity was confirmed, and a high response rate and overall survival was reported.[108,109] In these studies, pharmacokinetically guided administration of fluouroucil resulted in less toxicity than did conventional administration.[16,108,109] Moreover, Ychou et al. showed that individual fluorouracil dose adjustment guided by AUC using normograms was feasible in patients with colorectal cancer treated with fluorouracil and leucovorin with a 14-day interval.[148]

Recently, a population pharmacokinetic model has been developed in 65 patients with colorectal cancer treated with the same dosage schedule.[149] Bayesian estimation (based on 2 individual samples) has been performed to estimate the individual pharmacokinetic parameters in 20 patients. The Bayesian approach was reported to be a more flexible method than the normogram method since it could optimise the fluorouracil dose in every treatment schedule.[149] Nevertheless, randomised studies should be performed to validate the efficacy of this approach.

2.2.8 Hexamethylene bisacetamide

Hexamethylene bisacetamide belongs to the hybrid polar compounds, which are potent inducer of differentiation in cell lines *in vitro*.[150] Several phase I studies have shown that

the dose-limiting thrombocytopenia is correlated with the C_{ss} and AUC.[110-112] Conley and associates combined these features in an individualised administration study of the drug in the presence of concurrent alkalinisation with sodium bicarbonate.[150] The dose-limiting toxicity was neurotoxicity at a C_{ss} of >2 mmol/L. Consequently, the C_{ss} was set at 1.5 to 2 mmol/L in combination with an increased duration of infusion to maximise the exposure in relation to the observed thrombocytopenia. The target AUC was set at 7.5 mmol/L*day because of dose-limiting neurotoxicity.[150]

2.2.9 Idarubicin

Idarubicin is an anthracycline derivative that can be administered orally, mainly for the treatment of breast cancer and leukaemia. Elbæk and associates demonstrated a positive correlation between the cumulative AUC of idarubicin and its metabolite idarubicinol and the effect (leucopenia and response).[89,151] More recently, Schleyer and colleagues showed a significant correlation between plasma concentration at 24 hours after oral administration of idarubicin and the AUC, which may result in a potent prediction parameter of toxicity and therapeutic effect.[152]

2.2.10 4'-Iodo-4'-deoxydoxorubicin

The relationship between the AUC and effect for 4'-Iodo-4'-deoxydoxorubicin (IDOX), a less toxic analogue of doxorubicin, has also been studied.[113,114] The dose-limiting toxicities thrombocytopenia and, mainly, granulocytopenia are correlated with the AUC of IDOX and probably the AUC of its metabolite 4'-iodo-4'-deoxy-doxorubicinol (IDOXOL). However, phase II studies have shown a low therapeutic effect in combination with severe toxicities which prohibits further escalation of the dose intensity.[153,154]

2.2.11 Menogaril

Menogaril is a derivative of the antibiotic anthracycline nogalamycin and is less cardiotoxic compared with the other antibiotic anthracyclines doxorubicin and daunorubicin. The pharmacokinetic parameters of menogaril have been investigated in relation to its dose-limiting toxicity leukocytopenia after intravenous and oral administration.[90,115,116] Egorin and colleagues reported a positive correlation between the AUC of menogaril and toxicity (leckopenia and neutropenia) in cancer patients with and without hepatic dysfunction.[115,116] Patients with liver dysfunction showed more leukocytopenia than those with normal liver function. As no difference was observed in the relationship between leukocytopenia and AUC, they concluded that a dosage reduction might not be necessary in patients with hepatic dysfunction (elevated concentrations of bilirubin, ALT, AST and/or alkaline phosphatase).[115,116]

2.2.12 Paclitaxel

Paclitaxel is a taxane antimicrotubule agent that is used in the treatment of ovarian, breast, and lung cancers. Several studies have explored the relationship between the AUC and toxicity. Non-hematological toxicities including musculoskeletal and neurotoxicity have been correlated with AUC in children.[117] A significant correlation between the exposure and hematological toxicity or response has not yet been reported.[69,73,118,155] However, Huizing et al. and later Gianni et al. reported a relationship between the duration of the plasma concentration above a defined threshold and pharmacodynamics, which will be discussed further in section 3.2.[69,73,155]

2.2.13 Teniposide

Teniposide, which belongs to the group of the epipodophyllotoxins, is highly bound to plasma proteins (>95%). The unbound concentration exerts the cytotoxic activity. A correlation between the exposure and pharmacodynamics has been reported in patients with leukaemia.[119,156,157] In a subsequent trial, pharmacokinetic analysis by TDM was conducted daily during the first administration of teniposide (200 mg/m^2 as a 4-hour infusion for 3 consecutive days). The aim of the study was to decrease the interpatient variability, resulting in a higher dose intensity without increased toxicity. The second and third doses were adapted to yield a target AUC of 1060 µmol/L*h. In subsequent patient cohorts the target AUC was increased to 1656 µmol/L*h which was not accompanied with an observed increase in toxicity.[120]

2.2.14 Topotecan

Topotecan is a semisynthetic camptothecin analogue that inhibits the DNA-topoisomerase I enzyme causing persistent DNA strand breaks. The dose limiting toxicities (leucopenia, neutropenia, thromboctyopenia and diarrhoea) were shown to be closely correlated with the AUC of topotecan or the cytotoxic lactone form (T_m), and also with the dose in some schedules.[91,92,121-126] This relationship has resulted in the development and validation of an optimal sample strategy utilising one plasma concentration. A plasma concentration determined at 2 hours after the end of a 30-minute infusion of topotecan (dose 0.5 to 1.5 mg/m^2/day) was used to estimate the sum AUC of (total) topotecan and Tm on 5 consecutive days.[158] In a phase II study (36 patients) using LSM, the mean AUC of topotecan was 8.71 µmol/min*day and the mean AUC of Tm was 11.49 µmol/min*day when topotecan 1.5 mg/m^2/day was given as 30-minute infusions on 5 consecutive days. As large interpatient pharmacokinetic variability was observed, but only small pharmacodynamic variability, the authors concluded that TDM of topotecan may not be very valuable in this treatment schedule.[125]

2.3 Practical considerations

Systemic exposure to several anticancer agents has been studied in relation to pharmacodynamics, but AUC-guided administration has been limited to clinical trials except for carboplatin. The investigated relationships between the systemic exposure, toxicity and clinical response need to be validated in prospective studies in a sufficient number of patients. In these studies, it is important to consider that the correlation between AUC and effect may be dependent on the treatment schedule. Consequently, this correlation should be validated in various treatment schedules. We conclude that LSMs and Bayesian analysis are pharmacokinetic strategies well suited for AUC-guided dosing in the clinical experimental setting. Further studies are warranted to determine the potential therapeutic benefit of use of these strategies under conditions more reflective of routine clinical practice.

3. Other targets for pharmacokinetically guided dosing

AUC has been extensively studied as the pharmacokinetic parameter that correlates with the pharmacodynamics. However, relationships between effect and other pharmacokinetic parameters have been reported as well. For some anticancer agents more than one pharmacokinetic parameter can be correlated with pharmacodynamics.

3.1 Steady-state plasma drug concentration

The therapeutic window may be used as a target for adaptive administration. The response can be increased by keeping the plasma concentration or C_{ss} above a certain value, whereas toxicity can be avoided by keeping the C_{ss} below the plasma level where unacceptable toxicity develops. Methotrexate is a drug for which TDM is routinely used clinically to identify patients at high risk for developing significant toxicity. In general, serum drug concentrations above 0.1 µmol/L at 48 hours after administration, and/or any serum concentrations above 10 µmol/L require intensified standard leucovorin rescue.[159-163] Furthermore, several investigators have studied adaptive administration based on a target C_{ss} of high-dose methotrexate compared with fixed-dose administration of the drug. The individualised treatment group showed less variation in the serum methotrexate concentrations with a marked reduction in the severity of toxicity and/or a lower risk of relapse compared to the standard treated group (Table 6).[14,15]

C_{ss} has been related to the pharmacodynamics of other anticancer agents. A significant correlation has been demonstrated when the dose was guided by the target C_{ss} in relation to toxicity and, to a minor extent, response.[17,18,89,110-113,118,131,147,150-152,156,164-168,170-172] These anticancer agents , including etoposide, doxorubicin, cisplatin, fluorouracil, teniposide, vinblastine, thymidine, and hexamethylene bisacetamide are also listed in Table 6.[14,15,108-112,131,156,157,159,160,164-168,170,172] However, these drugs need to be investigated in prospective randomized studies

Table 6. Anticancer agents for which a relationship between steady-state and defined plasma concentration and pharmacodynamics has been demonstrated

Anticancer agent	Indication	PK parameter	Effect	References
Cisplatin	Solid tumour	C_{ss}	Nephrotoxicity	81
	Neuroblastoma	C_{48h}	Ototoxicity	164
Doxorubicin	Solid tumour	C_{ss}	WBC nadir	165
Etoposide	Solid tumour	C_{ss}	WBC↓, PLT↓	166
Fluorouracil	Colorectal carcinoma	C_{ss}	WBC↓	167
	Colorectal carcinoma	C_{ss}	WBC↓, stomatitis	147
Hexamethylene bisacetamide	Solid tumour	C_{ss}	PLT↓	110
	Solid tumour	C_{ss}	PLT↓, neurotoxicity, nephrotoxicity	111
	Solid tumour	C_{ss}	PLT↓, neurotoxicity, nephrotoxicity	112
	Solid tumour	C_{ss}	Neurotoxicity, nephrotoxicity	168
Methotrexate	Solid tumour	C_{48h}	WBC↓, PLT↓, nephrotoxicity, mucositis	159
	ALL	C_{ss}	Period of remission	14
	ALL	C_{ss}	Period of remission	15
	Head and neck carcinoma	C_{36h}	Mucositis, nephrotoxicity	160
Teniposide	Leukaemia	C_{ss}	Mucositis	157
	Leukaemia	C_{ss}	WBC↓, peripheral neuropathy	156
Thymidine	Solid tumour, lymphoma	C_{ss}	Response	169
Vinblastine	Solid tumour, melanoma, lymphoma	C_{ss}	PLT↓	170

ALL = acute lymphocytic leukemia; C_x = plasma concentration at x hours after administration; C_{ss} = steady state concentration; 5FU = fluorouracil; PD = pharmacodynamics; PK = pharmacokinetic; PLT↓ = thrombocytopenia; WBC↓ = leucopenia.

to confirm these pharmacokinetic-pharmacodynamic correlations before implementation of adaptive control algorithms in clinical practice.

3.2 Drug exposure time above a defined threshold concentration

As previously mentioned in section 2.2.12, the toxicity and therapeutic effect of paclitaxel are correlated with the duration of the drug concentration above a certain level (Table 7). Huizing et al. reported a correlation between median survival and duration of the serum paclitaxel concentration above a threshold value of 0.1 µmol/L that was proven to be pharmacologically active *in vitro* and related with bone marrow toxicity.[69,169] This relationship could be described mathematically by a sigmoidal E_{max} model, and a duration of 15 hours or more above 0.1 µmol/L resulted in a lower leukocyte nadir and potentially higher response rates.[69,73] Other investigators demonstrated a correlation between myelosuppression, especially neutropenia, and the duration of plasma levels above 0.05 µmol/L.[117] Furthermore, van Warmerdam and colleagues reported a significant correlation between duration of topotecan concentration above 10 nmol/L and neutropenia.[123] Further investigation to confirm these pharmacokinetic-pharmacodynamic correlations is warranted.

4. Conclusions

Standardised administration of anticancer agents is complicated by pharmacokinetic variability and the small therapeutic window. It is common practice to calculate doses of chemotherapeutic agents guided on the basis of BSA and to reduce the dose if significant toxicity occurs. This may result in inappropriate dosage and suboptimal treatment in some patients or exposure resulting in unacceptable toxicity in others. The therapeutic efficacy and toxicity of many anticancer agents may be more closely related to the exposure than to the dose adjusted on the basis of BSA.[3,12] As a result of extensive pharmacological research of antineoplastic agents, our knowledge of pharmacokinetic parameters and clinical effects has increased markedly in recent years. An impressive number of reports has been published on the pharmacokinetic-pharmacodynamic relationships of anticancer drugs, and in particular the relationship between pharmacokinetic parameters and toxicity has been extensively studied. AUC-guided administration has a prominent role in these studies, as AUC and effect (mainly toxicity) are closely related for many anticancer agents. *A priori* prediction of AUC, LSMs and Bayesian analysis based on population pharmacokinetic parameters and resulting adaptive administration have been investigated widely. Carboplatin has been extensively studied, since carboplatin clearance is highly correlated with the GFR which can be determined relatively easily. Formulae have been derived for individualised dose calculation according to renal function, resulting in AUC-guided administration. Methotrexate is another anticancer agent for which TDM is clinical routine. For other antineoplastic agents, such

Table 7. Anticancer agents for which a relationship between drug exposure time above a defined threshold concentration and pharmacodynamics has been demonstrated

Anticancer agent	Type of cancer	Treshold plasma concentration	Effect	References
Paclitaxel	Ovarian	0.1 µmol/L	WBC↓, ANC↓	74
Paclitaxel	Lung	0.1 µmol/L	Response rate, survival	70
Paclitaxel	Ovarian and breast	0.05 µmol/L	ANC↓	145
Topotecan	Solid tumours	10 nmol/L	ANC↓	155

ANC↓ = neutropenia; WBC↓ = leucopenia.

as fluorouracil, cisplatin, topotecan, etoposide and teniposide, AUC has been correlated with toxicity in clinical trials. Application of administration algorithms for these agents is not current clinical practice, since the more complex elimination of these anticancer agents complicates the derivation of a simple formula.

Prospective randomised pharmacodynamic studies of individualised administration of these other anticancer agents should be performed to demonstrate whether individualised administration results in a clinical benefit. The validation of the correlation between pharmacokinetic parameters and the clinical effect should be performed in various populations and treatment schedules. Future studies should also focus on the development of population pharmacokinetic models and Bayesian analysis for adaptive control. Bayesian analysis is recommended for pharmacokinetic-pharmacodynamic studies because of its flexibility, whereas LSMs may be more convenient for TDM in clinical practice. Moreover, mathematical formulations to calculate the individualised dosage of anticancer agents should be made accessible to practicing clinicians.[12,173,174] Pharmacokinetic-pharmacodynamic research to improve and refine administration procedures should be extended to demonstrate whether adaptive dosing has therapeutic benefit and whether individual administration algorithms can be implemented in daily clinical practice.

References

1. Grochow LB. Individualized dosing of anticancer drugs and the role of therapeutic monitoring. In: Grochow LB, Ames MM, editors. A clinician's guide to chemotherapy pharmacokinetics and pharmacodynamics. Baltimore: Williams & Willkins, 1998:3-16.

2. Gibaldi M. Revisiting some factors contributing to variability. Ann Pharmacother 1992;26:1002-1007.

3. Canal P, Chatelut E, Guichard S. Practical treatment guide for dose individualisation in cancer chemotherapy. Drugs 1998;56:1019-1038.

4. Powis G. Effect of human renal and hepatic disease on the pharmacokinetics of anticancer drugs. Cancer Treat Rev 1982;9:85-124.

5. Gurney H. Dose calculation of anticancer drugs:a review of the current practice and introduction of an alternative. J Clin Oncol 1996;14:2590-2611.

6. Donelli MG; Zucchetti M, Munzone E, et al. Pharmacokinetics of anticancer agents in patients with impaired liver function. Eur J Cancer 1997;34:33-46.

7. Kintzel PE, Dorr RT. Anticancer drug renal toxicity and elimination: dosing guidelines for altered renal function. Cancer Treat Rev 1995;21:33-64.

8. Ratain MJ, Schilsky RL, Conley BA, et al. Pharmacodynamics in cancer therapy. J Clin Oncol 1990;8:1739-1753.

9. Workman P, Graham MA. Pharmacokinetics and chemotherapy. Eur J Cancer 1994;30A:706-710.

10. Judson IR. Pharmacokinetic modelling-a prelude to therapeutic drug monitoring for all cancer patients? Eur J Cancer 1995;31A:1733-1735.

11. Desoize B, Robert J. Individual dose adaptation of anticancer drugs. Eur J Cancer 1994;30A:844-851.

12. Kobayashi K, Jodrell DI, Ratain MJ. Pharmacodynamic-pharmacokinetic relationships and therapeutic drug monitoring. In: Workman P, Graham MA, editors. Pharmacokinetics and cancer chemotherapy. Cold Spring Harbor: Cold Spring Harbor Laboratory Press, 1993:51-87.

13. Egorin MJ. Overview of recent topics in clinical pharmacology of anticancer agents. Cancer Chemother Pharmacol 1998;42 Suppl.:S22-S30.

14. Evans WE, Relling MV, Rodman JH, et al. Conventional compared with individualized chemotherapy for childhood acute lymphoblastic leukemia. N Engl J Med 1998;338:499-505.

15. Evans WE, Crom WR, Abromowitch M, et al. Clinical pharmacodynamics of high-dose methotrexate in acute lymphocytic leukaemia. N Engl J Med 1986;314:471-477.

16. Fety R, Rolland F, Barberi-Heyob M, et al. Clinical impact of pharmacokinetically-guided dose adaptation of 5-fluorouracil: results from a multicentric randomized trial in patients with locally advanced head and neck carcinomas. Clin Cancer Res 1998;4:2039-2045.

17. Ratain MJ, Schilsky RL, Choi KE, et al. Adaptive control of etoposide dosing: impact of interpatient pharmacodynamic variability. Clin Pharmacol Ther 1989;45:226-233.

18. Ratain MJ, Mick R, Schilsky RL, et al. Pharmacologically based dosing of etoposide: a means of safely increasing dose intensity. J Clin Oncol 1991;9:1480-1486.

19. Sørensen BT, Strömgren A, Jakobsen P, et al. Renal handling of carboplatin. Cancer Chemother Pharmacol 1992;30:317-320.

20. Sørensen BT, Strömgren A, Jakobsen P, et al. Dose-toxicity relationship of carboplatin in combination with cyclophosphamide in ovarian cancer patients. Cancer Chemother Pharmacol 1991;28:397-401.

21. Van der Vijgh WJF. Clinical pharmacokinetics of carboplatin. Clin Pharmacokinet 1991;21:242-261.

22. Egorin MJ, Van Echo DA, Tipping SJ, et al. Pharmacokinetics and dosage reduction of cis-diammine (1,1-cyclobutanedicarboxylato)platinum in patients with impaired renal function. Cancer Res 1984;44:5432-5438.

23. Calvert AH, Newell DR, Gumbrell LA, et al. Carboplatin dosage: prospective evaluation of a simple formula based on renal function. J Clin Oncol 1989;7:1748-1756.

24. Chatelut E, Canal P, Brunner V, et al. Prediction of carboplatin clearance from standard morphological and biological patient characteristics. J Natl Cancer Inst 1995;87:573-580.

25. Sørensen BT, Strömgren A, Jakobsen P, et al. A limited sampling method for estimation of the carboplatin area under the curve. Cancer Chemother Pharmacol 1993;31:324-327.

26. Ghazal-Aswad S, Calvert AH, Newell DR. A single-sample assay for the estimation of the area under the free carboplatin plasma concentration versus time curve. Cancer Chemother Pharmacol 1996;37:429-434.

27. Asai G, Ando Y, Saka H, et al. Estimation of the area under the concentration-versus-time curve of carboplatin following irinotecan using a limited sampling model. Eur J Clin Pharmacol 1998;54:725-727.

28. Egorin MJ, Van Echo DA, Olman EA, et al. Prospective validation of a pharmacologically based dosing scheme for the cis-diaminedichloroplatinum (II) analogue diamminecyclobutanedicarbo xylatoplatinum. Cancer Res 1985;45:6502-6506.

29. Belani CP, Egorin MJ, Abrams JS, et al. A novel pharmacodynamically based approach to dose optimization of carboplatin when used in combination with etoposide. J Clin Oncol 1989;7:1896-1902.

30. Okamoto H, Nagatomo A, Kunitoh H, et al. Prediction of carboplatin clearance calculated by patient characteristics or 24-hour creatinine clearance: a comparison of the performance of three formulae. Cancer Chemother Pharmacol 1998;42:307-312.

31. Newell DR, Siddik ZH, Gumbrell LA, et al. Plasma free platinum pharmacokinetics in patients treated with high dose carboplatin. Eur J Cancer Clin Oncol 1987;23:1399-1405.

32. Groen HJM, Van der Leest AHD, de Vries EGE, et al. Continuous carboplatin infusion during 6 weeks' radiotherapy in locally inoperable non-small-cell lung cancer: a phase I and pharmacokinetic study. Br J Cancer 1995;72:992-997.

33. Jodrell DI, Egorin MJ, Canetta RM, et al. Relationships between carboplatin exposure and tumor response and toxicity in patients with ovarian cancer. J Clin Oncol 1992;10:520-528.

34. Lind MJ, Ghazal-Aswad S, Gumbrell L, et al. Phase I study of pharmacologically based dosing of carboplatin with filgrastim support in women with epithelial ovarian cancer. J Clin Oncol 1996;14:800-805.

35. Gore M, Mainwaring P, A'Hern R, et al. Randomized trial of dose-intensity with single-agent carboplatin in patients with epithelial ovarian cancer. J Clin Oncol 1998;16:2426-2434.

36. Jakobsen A, Bertelsen K, Andersen JE, et al. Dose-effect study of carboplatin in ovarian cancer: a Danish ovarian cancer group study. J Clin Oncol 1997;15:193-198.

37. Shea TC, Flaherty M, Elias A, et al. A phase I and pharmacokinetic study of carboplatin and autologous bone marrow support. J Clin Oncol 1989;7:651-661.

38. Ghazal-Aswad S, Tilby MJ, Lind M, et al. Pharmacokinetically guided dose escalation of carboplatin in epithelial ovarian cancer: effect on drug-plasma AUC and peripheral blood drug-DNA adduct levels. Ann Oncol 1999;10:329-334.

39. Kinowki J-M, Bressole F, Rodier M, et al. A limited sampling model with bayesian estimation to determine inulin pharmacokinetics using the population data modelling program P-Pharm. Clin Drug Invest 1995;9:260-269.

40. Daugaard G, Rossing N, Rorth M. Effects of cisplatin on different measures of glomerular function in the human kidney with special emphasis on high-dose. Cancer Chemother Pharmacol 1988;21:163-177.

41. Sørensen BT, Strömgren A, Jakobsen P et al. Is creatinine clearance a sufficient measure for GFR in carboplatin dose calculation [abstract]? Eur J Cancer 1993;29:S110.

42. Calvert AH, Boddy A, Bailey NP, et al. Carboplatin in combination with paclitaxel in advanced ovarian cancer: dose determination and pharmacokinetic and pharmacodynamic interactions. Semin Oncol 1995;22 Suppl. 12:91-100.

43. Van Warmerdam LJC, Rodenhuis S, ten Bokkel Huinink WW, et al. The use of the Calvert formula to determine the optimal carboplatin dosage. J Cancer Res Clin Oncol 1995;121:478-486.

44. Shea T, Graham M, Bernard S, et al. A clinical and pharmacokinetic study of high-dose carboplatin, paclitaxel, granulocyt colony-stimulating factor, and peripheral blood stem cells in patients with uinresectable or metastatic cancer. Semin Oncol 1995;22 Suppl. 12:80-85.

45. Kearns CM, Belani CP, Erkmen K, et al. Pharmacokinetics of paclitaxel and carboplatin in combination. Semin Oncol 1995;22 Suppl. 12:1-7.

46. Cockcroft DW, Gault MH. Prediction of creatinine clearance from serum creatinine. Nephron 1976;16:31-41.
47. Jelliffe RW. Creatinine clearance: bedside estimation. Ann Intern Med 1973;79:604-605.
48. Van Warmerdam LJC, Rodenhuis S, ten Bokkel Huinink WW, et al. Evaluation of formulas using the serum creatinine level to calculate the optimal dosage of carboplatin. Cancer Chemother Pharmacol 1996;37:266-270.
49. Fujiwara Y, Takahashi T, Yamakido M, et al. Prediction of carboplatin clearance from standard morphological and biological patient characteristics [letter]. J Natl Cancer Inst 1997;89:260-261.
50. Perrone RD, Madias NE, Levey AS. Serum creatinine as an index of renal function: new insights into old concepts. Clin Chem 1992;38:1933-1953.
51. Calvert AH. A review of the pharmacokinetics and pharmacodynamics of combination carboplatin/paclitaxel. Semin Oncol 1997;24 Suppl. 2:85-90.
52. Ando Y, Minami H, Saka H, et al. Adjustment of creatinine clearance improves accuracy of Calvert's formula for carboplatin dosing. Br J Cancer 1997;76:1067-1071.
53. Martin L, Chatelut E, Boneu A, et al. Improvement of the Cockcroft-Gault equation for predicting glomerular filtration in cancer patients. Bull Cancer 1998;85:631-636.
54. Wright JG, Calvert AH, Highley MS, et al. Accurate prediction of renal function for carboplatin dosing [abstract]. Proc Am Assoc Cancer Res 1999;40:384.
55. Langer CJ, Leighton JC, Comis RL, et al. Paclitaxel and carboplatin in combination in the treatment of advanced non-small cell lung cancer: a phase II toxicity, response, and survival analysis. J Clin Oncol 1995;13:1860-1870.
56. Reyno LM, Egorin MJ, Canetta RM, et al. Impact of cyclophosphamide on relationships between carboplatin exposure and response or toxicity when used in the treatment of advanced ovarian cancer. J Clin Oncol 1993;11:1156-1164.
57. Harland SJ, Gumbrell LA, Horwich A. Carboplatin dose in combination chemotherapy for testicular cancer. Eur J Cancer 1991;27:691-695.
58. Horwich A, Dearnaley DP, Nicholls J, et al. Effectiveness of carboplatin, etoposide, and bleomycin combination chemotherapy in good-prognosis metastatic testicular nonseminomatous germ cell tumors. J Clin Oncol 1991;9:62-69.
59. Krigel RL, Palackdharry CS, Padavic K, et al. Ifosamide, carboplatin, and etoposide plus granulocyte-macrophage colony-stimulating factor: A phase I study with apparent activity in non-small-cell lung cancer. J Clin Oncol 1994;12:1251-1258.
60. Green JA, Smith K. Dose intensity of carboplatin in combination with cyclophosphamide or ifosfamide. Cancer Chemother Pharmacol 1990;26 Suppl.:22-25.
61. Obasaju CK, Johnson SW, Rogatko A. Evaluation of carboplatin pharmacokinetics in the absence and presence of paclitaxel. Clin Cancer Res 1996;2:549-552.
62. Belani CP, Kearns CM, Zuhowski EG, et al. Phase I trial, including pharmacokinetic and pharmacodynamic correlations, of combination paclitaxel and carboplatin in patients with metastatic non-small-cell lung cancer. J Clin Oncol 1999;17:676-684.
63. Childs WJ, Nicholls EJ, Horwich A. The optimisation of carboplatin dose in carboplatin, etoposide and bleomycin combination chemotherapy for good prognosis metastatic nonseminomatous germ cell tumours of the testis. Ann Oncol 1992;3:291-296.
64. Siddiqui N, Boddy AV, Thomas HD, et al. A clinical and pharmacokinetic study of the combination of carboplatin and paclitaxel for epithelial ovarian cancer. Br J Cancer 1997;75:287-294.
65. Okamoto H, Nagatomo A, Kunitoh H, et al. A phase I clinical and pharmacologic study of a carboplatin and irinotecan regimen combined with recombinant human granulocyte-colony stimulating factor in the treatment of patients with advanced nonsmall cell lung cancer. Cancer 1998;82:2166-2172.
66. Kattan J, Mahjoubi M, Droz JP, et al. High failure rate of carboplatin-etoposide combination in good risk non-seminomatous germ cell tumours. Eur J Cancer 1993;29A:1504-1509.
67. Meerpohl HG, du Bois A, Luck HJ, et al. Paclitaxel combined with carboplatin in the first-line treatment of advanced ovarian cancer: a phase I trial. Semin Oncol 1997;24 Suppl. 2:17-22.

68. Rowinsky EK, Flood WA, Sartorius SE, et al. Phase I study of paclitaxel as a 3-hour infusion followed by carboplatin in untreated patients with stage IV non-small cell lung cancer. Semin Oncol 1995;22 Suppl. 9:48-54.

69. Huizing MT, Giaccone G, Van Warmerdam LJC, et al. Pharmacokinetics of paclitaxel and carboplatin in a dose-escalating and sequencing study in patients with non-small-cell lung cancer. J Clin Oncol 1997;15:317-329.

70. Sadan S, Barjorin DF, Mazumdar M, et al. Correlation of carboplatin (CBDCA) area under the curve (AUC) with myelosuppression and infection in germ cell tumor (GCT) Patients (PTS) [abstract]. Proc Am Soc Clin Oncol 1993;12:159.

71. Chatelut E, Chevreau C, Brunner V, et al. A pharmacologically guided phase I study of carboplatin in combination with methotrexate and vinblastine in advanced urothelial cancer. Cancer Chemother Pharmacol 1995;35:391-396.

72. Sculier JP, Paesmans M, Thiriaux J, et al. A comparison of methods of calculation for estimating carboplatin AUC with a retrospective pharmacokinetic-pharmacodynamic analysis in patients with advanced non-small cell lung cancer. Eur J Cancer 1999;35:1314-1319.

73. Huizing MT, Keung ACF, Rosing H, et al. Pharmacokinetics of paclitaxel and metabolites in a randomized comparative study in platinum-pretreated ovarian cancer patients. J Clin Oncol 1993;11:2127-2135.

74. Calvert AH. Dose optimisation of carboplatin in adults. Anticancer Res 1994;14:2273-2278.

75. D'Argenio DZ. Optimal sampling times for pharmacokinetic experiments. J Pharmacokinet Biopharm 1981;9:739-756.

76. Van Warmerdam LJC, Rodenhuis S, Van Tellingen O, et al. Validation of a limited sampling model for carboplatin in a high dose chemotherapy combination. Cancer Chemother Pharmacol 1994;35:179-81.

77. Van Warmerdam LJC, Ten Bokkel Huinink WW, Maes RAA, et al. Limited sampling models for anticancer agents. J Cancer Res Clin Oncol 1994;120:427-33.

78. Nannan Panday VR, Van Warmerdam LJC, Huizing MT, et al. A single 24-hour plasma sample does not predict the carboplatin AUC from carboplatin-paclitaxel combinations or from a high-dose carboplatin-thiotepa-cyclophosphamide regimen. Cancer Chemother Pharmacol 1999;43: 435-438.

79. Nannan Panday VR, Van Warmerdam LJC, Huizing MT, et al. A single 24-hour plasma sample does not predict the carboplatin AUC from carboplatin-paclitaxel combinations or from a high-dose carboplatin-thiotepa-cyclophosphamide regimen. Cancer Chemother Pharmacol 1999;43: 435-438.

80. Guillet P, Monjanel S, Nicoara A, et al. A bayesian dosing method for carboplatin given by continous infusion for 120 h. Cancer Chemother Pharmacol 1997;40:143-149.

81. Duffull SB, Begg EJ, Robinson BA, et al. A sequential Bayesian algorithm for dose individualisation of carboplatin. Cancer Chemother Pharmacol 1997;39:317-326.

82. Huitema ADR, Mathôt RAA, Tibben MM, et al. Validation of techniques for the prediction of carboplatin exposure: application of Bayesian methods. Clin Pharmacol Ther 2000;67:621-630.

83. Jodrell DI, Murray LS, Hawtof J, et al. A comparison of methods for limited-samling strategy design using data from a phase I trial of the anthrapyrazole DuP-941. Cancer Chemother Pharmacol 1996;37:356-362.

84. Van Warmerdam LJD, Van den Bemt BJF, Ten Bokkel Huinink WW, et al. Dose individualisation in cancer chemotherapy: Pharmacokinetic and pharmacodynamic relationships. Cancer Res Ther Control 1995;4:277-291.

85. Grochow LB, Jones RJ, Brundrett RB, et al. Pharmacokinetics of busulfan: correlation with veno-occlusive disease in patients undergoing bone marrow transplantation. Cancer Chemother Pharmacol 1989;25:55-61.

86. Dix SP, Wingard JR, Mullins RE, et al. Association of busulfan area under the curve with veno-occlusive disease following BMT. Bone Marrow Transplant 1996;17:225-230.

87. Vassal G, Koscielny S, Challine D, et al. Busulfan disposition and hepatic veno-occlusive disease in children undergoing bone marrow transplantation. Cancer Chemother Pharmacol 1996;37: 247-253.
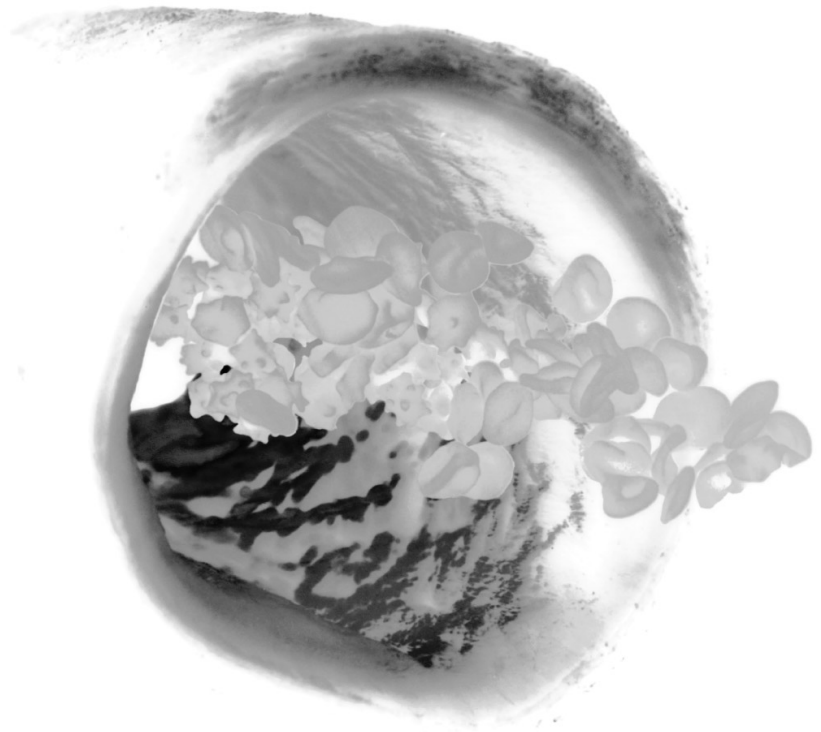
88.   Sonnichsen D, Ribeiro R, Luo X, et al. Pharmacokinetics and pharmacodynamics of 21 day continuous oral etoposide in pediatric patients with solid tumors. Clin Pharmacol Ther 1995;58: 99-107.

89.   Elbæk K, Ebbehoj E, Jakobsen A, et al. Pharmacokinetics of oral idarubicin in breast cancer patients with reference to antitumor activity and side effects. Clin Pharmacol Ther 1989;45:627-34.

90.   Dodion P, De Valeriola D, Crespeigne N, et al. Phase I clinical and pharmacokinetic trial of oral menogaril administered on three consecutive days. Eur J Cancer Clin Oncol 1988;24:1019-1026.

91.   Schellens JHM, Eckardt JR, Creemers GJ, et al. Pharmacokinetics (PK), clinical pharmacodynamics (PD) and safety of chronic oral topotecan (T) in a phase I study [abstract]. Proc Am Soc Clin Oncol 1995;14:457.

92.   Creemers GF, Gerrits CJH, Eckardt JR, et al. Phase I and pharmacologic study of oral topotecan administered twice daily for 21 days to adult patients with solid tumors. J Clin Oncol 1997;15: 1087-1093.

93.   Reece PA, Stafford I, Russell J, et al. Creatinine clearance as a predictor of ultrafilterable platinum disposition in cancer patients treated with cisplatin: relationship between peak ultrafilterable platinum plasma levels and nephrotoxicity. J Clin Oncol 1987;5:304-309.

94.   Schellens JHM, Ma J, Planting ASTh, et al. Relationship between the exposure to cisplatin, DNA-adduct formation in leucocytes and tumour response in patients with solid tumours. Br J Cancer 1996;73:1569-1575.

95.   Ayash LJ, Wright JE, Tretyakov O, et al. Cyclophosphamide pharmacokinetics: correlation with cardiac toxicity and tumor response. J Clin Oncol 1992;10:995-1000.

96.   Bruno R, Hille D, Riva A, et al. Population pharmacokinetics/pharmacodynamics of docetaxel in phase II studies in patients with cancer. J Clin Oncol 1998;1:187-196.

97.   Jakobsen P, Bastholt L, Dalmark M, et al. A randomized study of epirubicin at four different dose levels in advanced breast cancer. Feasibility of myelotoxicity prediction through single blood-sample measurement. Cancer Chemother Pharmacol 1991;28:465-469.

98.   Miller AA, Stewart CF, Tolley EA. Clinical pharmacodynamics of continuous-infusion etoposide. Cancer Chemother Pharmacol 1990;25:361-366.

99.   Desoize B, Marechal F, Cattan A. Clinical pharmacokinetics of etoposide during 120 hours continuous infusions in solid tumours. Br J Cancer 1990;62:840-841.

100.   Miller AA, Tolley EA, Niell HB, et al. Pharmacodynamics of three daily infusions of etoposide in patients with extensive-stage small -cell lung cancer. Cancer Chemother Pharmacol 1992;31: 161-166.

101.   Budman DR, Igwemezie L, Kaul S, et al. Pharmacodynamic findings with etoposide phosphate (BMY 4081), a water soluble prodrug [abstract]. Proc Am Soc Clin Oncol 1994;13:146.

102.   Goldberg JA, Kerr DJ, Willmott N, et al. Pharmaokinetics and pharmacodynamics of locoregional 5 fluorouracil (5FU) in advanced colorectal liver metastases. Br J Cancer 1988;57:186-189.

103.   Van Groeningen CJ, Pinedo HM, Heddes J, et al. Pharmacokinetics of 5-Fluorouracil assessed with a sensitive mass spectrometric method in patients on a dose escalation schedule. Cancer Res 1988;48:6956-6961.

104.   Thyss A, Milano G, Renée N, et al. Clinical pharmacokinetic study of 5-FU in continuous 5-day infusions for head and neck cancer. Cancer Chemother Pharmacol 1986;16:64-66.

105.   Santini J, Milano G, Thyss A, et al. 5-FU therapeutic monitoring with dose adjustment leads to an improved therapeutic index in head and neck cancer. Br J Cancer 1989;59:287-290.

106.   Milano G, Etienne MC, Renée N, et al. Relationship between fluorouracil systemic exposure and tumor response and patient survival. J Clin Oncol 1994;12:1291-1295.

107.   Vokes EE, Mick R, Kies MS, et al. Pharmacodynamics of fluorouracil-based induction chemotherapy in advanced head and neck cancer. J Clin Oncol 1996;14:1664-1671.

108.   Gamelin EC, Danquechin-Dorval EM, Dumesnil YF, et al. Relationship between 5 fluorouracil (5-FU) dose intensity and therapeutic resonse in patients with advanced colorectal cancer receiving infusional therapy containing 5-FU. Cancer 1996;77:441-451.

109.   Gamelin E, Boisdron-Celle M, Delva R, et al. Long-term weekly treatment of colorectal metastatic cancer with fluorouracil and leucovorin: results of a multicentric prospective trial of fluorouracil

dosage optimization by pharmacokinetic monitoring in 152 patients. J Clin Oncol 1998;16:1470-1478.

110. Rowinsky EK, Ettinger DS, McGuire WP, et al. Prolonged infusion of hexamethylene bisacetamide (NSC 95580) administered as a five-day continuous infusion. Cancer Res 1987;47:5788-5795.

111. Egorin MJ, Sigman LM, Van Echo DA, et al. Phase I clinical and pharmacokinetic study of hexamethylene bisacetamide (NSC 95580) administered as a five-day continuous infusion. Cancer Res 1987;47:617-623.

112. Conley BA, Forrest A, Egorin MJ, et al. Phase I trial using adaptive control dosing of hexamethylene bisacetamide (NSC 95580). Cancer Res 1989;49:3436-3440.

113. Gianni L, Vigano L, Surbone A, et al. Pharmacology and clinical toxicity of 4'-iodo-4'-deoxydoxorubicin: an example of successful application of pharmacokinetics to dose escalation in phase I trials. J Natl Cancer Inst 1990;82:469-477.

114. Robert J, Armand JP, Huet S, et al. Pharmacokinetics and metabolism of 4'-iodo-4'-deoxy-doxorubicin in humans. J Clin Oncol 1992;10:1183-1190.

115. Egorin MJ, Van Echo DA, Whitacre MY, et al. Human pharmacokinetics, excretion, and metabolism of the anthracycline antibiotic menogaril (7-OMEN, NSC 269148) and their correlation with clinical toxicities. Cancer Res 1986;46:1513-1520.

116. Egorin MJ, Conley BA, Forrest A, et al. Phase I study and pharmacokinetics of menogaril (NSC 269148) in patients with hepatic dysfunction. Cancer Res 1987;47:6104-6110.

117. Longnecker SM; Donehower RC, Cates AE, et al. High-performance liquid chromatographic assay for taxol in human plasma and urine and pharmacokinetics in a phase I trial. Cancer Treat Rep 1987;71:53-59.

118. Sonnichsen DS, Hurwitz CA, Pratt CB, et al. Saturable pharmacokinetics and paclitaxel pharmacodynamics in children with solid tumors. J Clin Oncol 1994;12:532-538.

119. Evans WE, Rodman JH, Relling MV, et al. Differences in teniposide disposition and pharmacodynamics in patients with newly diagnosed and relapsed acute lymphocytic leukemia. J Pharmacol Exp Ther 1992;260:71-77.

120. Rodman JH, Furman WL, Sunderland M, et al. Escalating teniposide systemic exposure to increase dose intensity for pediatric cancer patients. J Clin Oncol 1993;11:287-293.

121. Stewart CF, Baker SD, Heideman RL, et al. Clinical pharmacodynamics of continuous infusion topotecan in children: systemic exposure predicts hematologic toxicity. J Clin Oncol 1994;12:1946-1954.

122. Haas NB, LaCreta FP, Walczak J, et al. Phase I/pharmacokinetic study of topotecan by 24-hour continuous infusion weekly. Cancer Res 1994;54:1220-1226.

123. Van Warmerdam LJC, Verweij J, Schellens JHM, et al. Pharmacokinetics and pharmacodynamics of topotecan administered daily for 5 days every 3 weeks. Cancer Chemother Pharmacol 1995;35:237-245.

124. Schiller JH, Kim K, Hutson P, et al. Phase II study of topotecan in patients with extensive-stage small-cell carcinoma of the lung: an Eastern Cooperative Oncology Group trial. J Clin Oncol 1996;14:2345-2352.

125. Van Warmerdam LJC, Creemers GJ, Rodenhuis S, et al. Pharmacokinetics and pharmacodynamics of topotecan given on a daily-times-five schedule in phase II clinical trials using a limited-sampling procedure. Cancer Chemother Pharmacol 1996;38:254-260.

126. Herben VMM, ten Bokkel Huinink WW, Dubbelman AC, et al. Phase I and pharmacological study of sequential intravenous topotecan and oral etoposide. Br J Cancer 1997;76:1500-1508.

127. Milano G, Roman P, Khater R, et al. Dose versus pharmacokinetics for predicting tolerance to 5-day continuous infusion of 5-FU. Int J Cancer 1988;41:537-541.

128. Grochow LB. Busulfan disposition: the role of therapeutic monitoring in bone marrow transplantation induction regimens. Semin Oncol 1993;4:18-25.

129. Decker J, Lindley C, McCune J, et al. Busulfan test dose area under the curve (AUC) predicts dose required to achieve targeted therapeutic concentration in bone marrow transplant (BMT) patients [abstract]. Proc Am Soc Clin Oncol 1998;17:189.

130. Yeager AM, Wagner JE, Graham ML, et al. Optimization of busulfan dosage in children undergoing bone marrow transplantation: a pharmacokinetic study of dose escalation. Blood 1992;80:2425-2428.

131. Nagai N, Kinoshita M, Ogata H, et al. Relationship between pharmacokinetics of unchanged cisplatin and nephrotoxicity after intravenous infusions of cisplatin to cancer patients. Cancer Chemother Pharmacol 1996;39:131-137.

132. Campbell AB, Kalman SM, Jacobs C. Plasma platinum levels: relationship to cisplatin dose and nephrotoxicity. Cancer Treat Rep 1983;67:169-172.

133. Reed E, Ozols RF, Tarone R et al. Platinum-DNA adducts in leukocyte DNA correlate with disease response in ovarian cancer patients receiving platinum-based chemotherapy. Proc Natl Acad Sci US 1987;84:5024-5028.

134. Reed E, Ostchega Y, Steinberg SM, et al. Evaluation of platinum-DNA adduct levels relative to known prognostic variables in a cohort of ovarian cancer patients. Cancer Res 1990;50:2256-2260.

135. Reed E, Ozols RF, Tarone R, et al. The measurement of cisplatin-DNA adduct levels in testicular cancer patients. Carcinogenesis 1988;9:1909-1911.

136. Fichtinger-Schepman AMJ, Van der Velde SD, Van Dijk-Knijnenburg HCM, et al. Kinetics of the formation and removal of cisplatin-DNA adducts in blood cells and tumor tissue of cancer patients receiving chemotherapy: comparison with in vitro adduct formation. Cancer Res 1990;50:7887-7894.

137. Parker RJ, Gill I, Tarone R, et al. Platinum-DNA damage in leukocyte DNA of patients receiving carboplatin and cisplatin chemotherapy, measured by atomic absorption spectrometry. Carcinogenesis 1991;12:1253-1258.

138. Egorin MJ, Forrest A, Belani CP, et al. A limited sampling strategy for cyclophosphamide pharmacokinetics. Cancer Res 1989;49:3129-3133.

139. Lichtman SM, Ratin MJ, Van Echo DA, et al. Phase I trial of granulocyte-macrophage colony-stimulating factor plus high-dose cyclophosphamide given every 2 weeks: a cancer and leukemia group B study. J Natl Cancer Inst 1993;85:1319-1326.

140. Van Hoesel QGCM, Verweij J, Catimel G, et al. Phase II study with docetaxel (Taxotere®) in advanced soft tissue sarcomas of the adult. Ann Oncol 1994;5:539-542.

141. Ten Bokkel Huinink WW, Prove AM, Piccart M, et al. A phase II trial with docetaxel (Taxotere®) in second line treatment with chemotherapy for advanced breast cancer. Ann Oncol 1994;5:527-532.

142. Catimel G, Verweij J, Matthijssen V, et al. Docetaxel (Taxotere®): an active drug for the treatment of patients with advanced squamous cell carcinoma of the head and neck. Ann Oncol 1994;5:533-537.

143. Hudis CA, Seidman AD, Crown JPA, et al. Phase II and pharmacologic study of docetaxel as initial chemotherapy for metastatic breast cancer. J Clin Oncol 1996;14:58-65.

144. Lowis SP, Pearson ADJ, Newell DR, et al. Etoposide pharmacokinetics in children: the development and prospective validation of a dosing equation. Cancer Res 1993;53:4881-4889.

145. Lowis SP, Price L, Pearson ADJ, et al. A study of the feasibility and accuracy of pharmacokinetically guided etoposide dosing in children. Br J Cancer 1998;77:2318-2323.

146. Joel SP, Ellis P, O'Byrne K, et al. Therapeutic monitoring of continuous infusion etoposide in small-cell lung cancer. J Clin Oncol 1996;14:1903-12.

147. Trump DL, Egorin MJ, Forrest A, et al. Pharmacokinetic and pharmacodynamic analysis of fluorouracil during 72-hour continuous infusion with and without dipyridamole. J Clin Oncol 1991;9:2027-2035.

148. Ychou M, Duffour J, Pinguet F, et al. Individual 5FU-dose adaptation schedule using bimontly pharmacokinetically modulated LV5FU2 regimen: a feasibility study in patients with advanced colorectal cancer. Anticancer Res 1999;19:2229-2236.

149. Bressole F, Joulia JM, Pinguet F, et al. Circadian rhythm of 5-fluorouracil population pharmacokinetics in patients with metastatic colorectal cancer. Cancer Chemother Pharmacol 1999;44:295-302.

150. Conley BA, Egorin MJ, Sinibaldi V, et al. Approaches to optimal dosing of hexamethylene bisacetamide. Cancer Chemother Pharmacol 1992;31:37-45.

151. Smith DB, Margison JM, Lucas SB, et al. Clinical pharmacology of oral and intravenous 4-demethoxydaunorubicin. Cancer Chemother Pharmacol 1987;19:138-142.

152.   Schleyer E, Kuhn S, Ruhrs, et al. Oral idarubicin pharmacokinetics - correlation of trough level with idarubicin area under curve. Leukemia 1996;10:707-712.

153.   Sessa C, Calabresi F, Cavalli F, et al. Phase II studies of 4'-iodo-4'-deoxydoxorubicin in advanced non-small cell lung, colon and breast cancers. Ann Oncol 1991;2:727-731.

154.   Sørensen JB, Stenbygaard L, Drivsholm L, et al. Phase II study of 4'-iodo-4'-deoxydoxorubicin in non-resectable non-small-cell lung cancer. Cancer Chemother Pharmacol 1993;32:399-402.

155.   Gianni L, Kearns CM, Gianni A, et al. Nonlinear pharmacokinetics and metabolism of paclitaxel and its pharmacokinetic/pharmacodynamic relationships in humans. J Clin Oncol 1995;13:180-190.

156.   Petros WP, Rodman JH, Mirro J, et al. Pharmacokinetics of continuous-infusion amsacrine and teniposide for the treatment of relapsed childhood acute nonlymphocytic leukemia. Cancer Chemother Pharmacol 1991;27:397-400.

157.   Rodman JH, Abromowitch M, Sinkule JA, et al. Clinical pharmacodynamics of continuous infusion teniposide: systemic exposure as a determinant of response in a phase I trial. J Clin Oncol 1987;5:1007-1014.

158.   Van Warmerdam LJC, Verweij J, Rosing H, et al. Limited sampling models for topotecan pharmacokinetics. Ann Oncol 1994;5:259-264.

159.   Stoller RG, Hande KR, Jacobs SA, et al. Use of plasma pharmacokinetics to predict and prevent methotrexate toxicity. N Engl J Med 1977;297:630-634.

160.   Favre R, Monjanel S, Alfonsi M, et al. High-dose methotrexate: a clinical and pharmacokinetic evaluation. Cancer Chemother Pharmacol 1982;9:156-160.

161.   Widemann BC, Balis FM, Murphy RF, et al. Carboxypeptidase-G2, thymidine, and leucovorin rescue in cancer patients with methotrexate-induced renal dysfunction. J Clin Oncol 1997;15:2125-34.

162.   Relling MV, Fairclough D, Ayers D, et al. Patient characteristics associated with high-risk methotrexate concentrations and toxicity. J Clin Oncol 1994;12:1667-1672.

163.   Monjanel S, Rigault JP, Cano JP, et al. High-dose methotrexate: preliminary evaluation of a pharmacokinetic approach. Cancer Chemother Pharmacol 1979;3:189-196.

164.   Crom W, Mauer E, Greene W, et al. relation between cisplatin ototoxicity and platinum accumulation in plasma. Proc Am Assoc Cancer Res 1984;3:28.

165.   Schilsky RL, O'Laughlin K, Ratain MJ. Phase I clinical and pharmacology study of thymidine (NSC 21548) and cisdiamminedichloroplatinum(II) in patients with advanced cancer. Cancer Res 1986;46:4184-4188.

166.   Bennett CL, Sinkule JA, Schilsky RL, et al. Phase I clinical and pharmacological study of 72-hour continuous infusion of etoposide in patients with advanced cancer. Cancer Res 1987;47:1952-1956.

167.   Au JLS, Rustum YM, Ledesma EJ, et al. Clinical pharmacological studies of concurrent infusion of 5-fluorouracil and thymidine in the treatment of colorectal carcinomas. Cancer Res 1982;42:2930-2937.

168.   Ackland SP, Ratain MJ, Vogelzang NJ, et al. Pharmacokinetics and pharmacodynamics of long-term continuous-infusion doxorubicin. Clin Pharm Ther 1989;45:340-347.

169.   Wiernik PH, Schwartz EL, Strauman JJ, et al. Phase I clinical and pharmacokinetic study of taxol. Cancer Res 1987;47:2486-2493.

170.   Ratain MJ, Vogelzang NJ. Phase I and pharmacologic study of vinblastine by prolonged continuous infusion. Cancer Res 1986;44:4827-4830.

171.   Mick R, Ratain MJ. Modeling interpatient pharmacodynamic variability of etoposide. J Natl Cancer Inst 1991;83:1560-1564.

172.   Rowinsky EK, Ettinger DS, Grochow LB, et al. Phase I and pharmacologic study of hexamethylene bisacetamide in patients with advanced cancer. J Clin Oncol 1986;4:1835-1844.

173.   Vozeh S, Steimer JL, Rowland M, et al. The use of population pharmacokinetics in drug development. Clin Pharmacokinet 1996;30(2):81-93.

174.   Duffull SB, Robinson BA. Clinical pharmacokinetics and dose optimisation of carboplatin. Clin Pharmacokinet 1997;33:161-183.

E7070

Chapter 2.1.1

An excretion balance and pharmacokinetic study of the novel anticancer agent E7070 in cancer patients

HJG Desirée van den Bongard, Dick Pluim, Hilde Rosing, Lianda Nan-Offeringa, Margaret Schot, Miroslav Ravic, Jan HM Schellens and Jos H Beijnen.

Summary

E7070 is a novel sulphonamide anticancer agent that arrests the G_1-S phase of the cell cycle. Preclinical and phase I studies have demonstrated non-linear pharmacokinetics of the drug. The objective of this study was to quantify the excretion of E7070 and the metabolite 1,4 benzene-sulphonamide (M1) in cancer patients. 1000 mg of E7070 radiolabelled by carbon-14 (^{14}C) in the benzenedisulphonamide moiety (cohort 1, n=6) or in the indole moiety (cohort 2, n=7) was intravenously (iv) infused over 1 hour. The levels of radioactivity (RA) in plasma, red blood cells, urine and faeces were determined by liquid scintillation counting, and the E7070 and M1 concentrations in plasma, urine and faeces were determined by coupled liquid chromatography-tandem mass spectrometry (LC/ESI-MS/MS). In plasma, the mean area under the concentration-time curve (AUC) based on RA measurements (32.5 and 28.9 h*mmol/L in cohort 1 and 2, respectively) was substantially higher than the mean AUC of E7070 (3.8 h*mmol/L) and M1 (0.1 h*mmol/L) in all patients. The excretion of RA (mean±SD%) as a percentage of administered radioactivity was higher in urine (63.7±9.8% (cohort 1) and 61.5±5.5% (cohort 2)) than in faeces (22.7±2.6% (1) and 21.1±3.1% (2)) during a mean collection period of 11 days. In both cohorts, the contribution of urinary and faecal recovery of E7070 (2.3% and 2.7%, respectively) and M1 (5.3% and 5.1%, respectively) was low. Subsequent HPLC analysis with online radioisotope detection of urine showed that the high radioactivity levels are caused by other compounds than E7070 and M1. The major metabolite is formed by glucuronidation of a hydroxylated metabolite of E7070.

In conclusion, the excretion of the benzene-sulphonamide and the indole moieties of E7070 was the same with a higher renal than gastro-intestinal excretion. E7070 is extensively converted into currently unidentified metabolites. Glucuronidation is a major metabolic pathway.

Introduction

Several sulphonamide derivatives have been synthesised to develop novel cytotoxic agents against solid tumours.[1,2] Sulphonamide agents are well known to have a variety of pharmacological activities including antibacterial, carbonic anhydrase-inhibitory, antidiabetic, diuretic, and antithyroid.[3] The first sulphonamide derivative that has been studied for its antitumour activity is E7010 (N-[2-[(4-hydroxyphenyl)amino]-3-pyridinyl]-4-methoxybenz enesulphonamide), an antimitotic agent that inhibits tubulin polymerisation.[4,5] A follow up compound, E7070 (N-(3-chloro-7-indolyl)-1,4-benzenedisulphonamide), is another sulphonamide derivative that has been studied for its antitumour activity. E7070 exhibited a potent antitumour activity in *in vitro* (in murine and human tumour cell lines) and *in vivo* (in human xenografts) studies. Most antitumour activity was observed in colorectal and lung cancer xenografts (HCT116 colorectal cancer and LX-1 lung cancer models). The drug arrests the transition of the G1- to the S-phase of the cell cycle by inhibiting the phosphorylation step of cyclin E and activation of cyclin dependant kinase 2.[6-8]

To determine the toxicity and maximum tolerated dose of E7070 in humans, phase I trials were initiated using four different infusion schedules in 127 patients with solid tumours.[9,10] The dose-limiting toxicity was mainly haematological. Partial and minor responses were observed in patients with breast, endometrial, renal, and ovarian carcinoma. Non-compartmental PK analysis of these phase I trials revealed non-linear pharmacokinetics with a more than dose-proportional increase of the AUC at higher dose-levels.[9,10] A population pharmacokinetic analysis of E7070 in four phase I studies (n=143) revealed that the concentration-time data could be best fitted to a three-compartment model with saturable transport to one compartment and two parallel pathway of elimination from the central compartment: a linear and a saturable pathway.[11] Phase II studies, with the dosing schemes one hour intravenous (iv) infusion every 3 weeks (700 mg/m²) and 5-day continuous iv infusion every 3 weeks (130 mg/m²), are currently ongoing in patients with solid tumours. To provide a better understanding of the excretion pathway of E7070 and its metabolite 1,4 benzene-sulphonamide (M1) in humans, which is pivotal information for the further development of the drug, a mass balance study was performed following a single dose of radiolabelled carbon-14 (^{14}C) E7070 in patients with solid tumours.

## Materials and Methods

Patients

This prospective, non-randomised, single-centre study was performed between November 1999 and August 2000 at the Antoni van Leeuwenhoek hospital/The Netherlands Cancer Institute in Amsterdam, The Netherlands. The institutional Medical Ethics Committee approved the study. All patients were required to give written informed consent prior to participation in the trial.

Patients with a histologically or cytologically confirmed diagnosis of a solid tumour not amenable to established forms of treatment were eligible for the study. Prior chemotherapy other than E7070, immunotherapy or radiotherapy was allowed, provided that the last treatment was at least four weeks prior to study entry (six weeks for nitrosoureas and extensive radiotherapy) and any resulting toxicities were resolved. Patients of child-bearing potential had to use adequate contraceptives and in fertile females a pregnancy test had to be performed within 1 week before study entry. Other eligibility criteria included: age $\geq$ 18 years, life expectancy of $\geq$ 3 months, performance status $\leq$ 2 according to the World Health Organisation (WHO) scale, acceptable bone marrow function (absolute neutrophil count $\geq$ 1,500/mm^3, platelet count $\geq$ 100,000/mm^3), adequate renal function (serum creatinine $\leq$ 120 µmol/L (1.4 mg/dl) or creatinine clearance $\geq$ 50 ml/min), adequate hepatic function (serum bilirubin < 25 µmol/L (1.5 mg/dl), serum alanine-aminotransferase (ALT) and aspartate-aminotransferase (AST) $\leq$ 2.5 times the upper normal limit, or $\leq$ 5 times the upper normal limit in the case of liver metastases). Exclusion criteria included the presence of active infections, the presence of symptomatic brain metastases, or glaucoma, presence of alcoholism, treatment with sulphonylurea agent for diabetes, any anti-arrhythmic agent or cisapride, pregnancy or breast-feeding, clinical signs of urinary and/or faecal incontinence.

Trial treatment

The patient population consisted of two cohorts because E7070 was radiolabelled at two different locations in the molecule. In the first cohort it was radiolabelled at the benzene sulphonamide moiety, and in the second cohort it was radiolabelled at the indole moiety to study the elimination routes of each part of the molecule. In the first cohort each patient received a single dose of 1000 mg E7070 containing 3.7 MBq ^{14}C-labelled E7070 ([benzene sulphonamide-^{14}C]ER-35744) (Figure 1A) in 1 hour infused iv through a central venous catheter. In the second cohort a single dose of 1000 mg E7070 containing 3.7 MBq ^{14}C-labelled E7070 ([indole ring-U-^{14}C]ER-35744) (Figure 1B) was iv administered in one hour through a central venous catheter. Subsequent courses consisted of 700 mg/m^2 E7070 iv in one hour every three weeks. Eligibility criteria with regard to performance status,

Figure 1. Chemical structure of E7070 [benzene sulphonamide-14C]ER-35744 (A) and [indole ring-U-14C]ER-35744 (B)
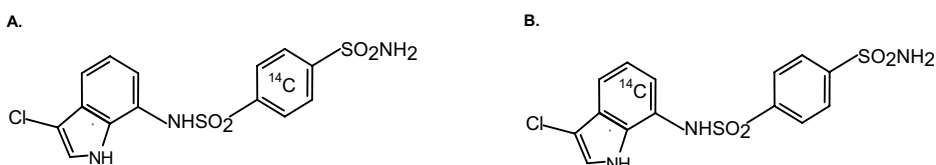
haematological, hepatic, renal functions, intercurrent complications, and medication were checked for re-treatment. Toxicity evaluation was performed every course according to the National Cancer Institute Common Toxicity Criteria (NCI CTC). If toxicity occurred, the patient was retreated upon recovery. Treatment was continued at the same dose provided no serious toxicity and no progressive disease was observed.

E7070 was supplied (Eisai Limited, London, United Kingdom) as a white to pale yellow freeze dried cake, in glass vials containing 100 mg of E7070 with 380 mg of meglumine and 475 mg of mannitol. Vials were stored at 2-8°C in the dark. Ten E7070 vials were reconstituted by adding 5 ml of water to each vial. The E7070 radiolabelled compounds ([benzene sulphonamide-^{14}C]ER-35744 and [indole ring-U-^{14}C]ER-35744) were supplied in glass vials each containing 3.7 Mbq ^{14}C-labelled compound with a specific activity of 2.52 and 2.74 GBq/mmol, respectively (Amersham International Ltd. of Little Chalfont, Amersham, Buckinghamshire, United Kingdom). One vial containing radiolabelled compound and ten reconstituted vials (1000 mg E7070) were added to saline (final volume of 1000 ml) for iv infusion under sterile conditions at the radioisotope laboratory in the Netherlands Cancer Institute. Quality control included endotoxin, sterility testing, and radio-chemical purity testing with HPLC, and was conducted before the administration to the patients.

Sample collection

Blood samples of each 10 ml were collected from a peripheral venous catheter during the first course. Blood samples for E7070 analysis were collected in heparinised tubes immediately pre-dose (0 hours), at 30 minutes after the start of the infusion, at the end of the infusion, at 10, 30 minutes, 1, 2, 4, 6, 8, 12, 24, 36 hours, after the end of the infusion, and at 2, 3, 4, 5, 6,7,8, 13 and 20 days after the day of the infusion. Blood samples were centrifuged (5 minutes, 3,000 rpm), and the plasma layer was separated and immediately stored at -20°C in polypropylene tubes until analysis. The buffy coats with the leukocytes were removed carefully with sufficient margins and discarded, followed by transfer of the red blood cells in polypropylene tubes. After one wash step with ice-cold isotonic phosphate buffered saline (PBS) the red blood cells were centrifuged at 3,000 rpm for 15 minutes and the supernatant was discarded. The washed red blood cells were immediately stored in polypropylene tubes at -20°C until analysis.

Urine was collected pre-dose and in 12-hour intervals between time 0 and 96 hours after the start of the E7070 infusion followed by additional 24 hour cumulative collections. The urine collection was continued until the E7070 concentration in urine and faeces had returned to below 1% in combination with a cumulative excretion percentage higher than 80% of the administered dose (1000 mg). The actual times of the pre-dose urine collection, the times of the urine collection intervals, and the volumes of the urine cumulative collections were recorded. Three aliquots of urine (20 ml) were removed, frozen and stored at -20°C until analysis.

One pre-dose faeces portion and all faeces produced following the administration of E7070 were collected, and the actual time and weight of each collection were recorded. The faecal samples were homogenised in distilled water (1:3, v/v) and stored at -20°C.

Bio-analysis

The detection of beta radiation in plasma, red blood cells, and PBS was performed by a liquid scintillation counter (LSC) (Tri-CARB 2100 CA; Packard Instrument Company, Meriden, USA) with an energy range of 0-2000 keV. Prior to the infusion of E7070 to all patients, a 25 µL aliquot of the infusion solution was removed followed by accurate determination of the radioactivity level by the LSC. Each sample was mixed with 10 ml of Ultima Gold LSC-cocktail (Packard Instrument Company, Meriden, USA) in a plastic vial. The counting-time was 5 minutes per vial. Before the measurement of radioactivity in red blood cells and faeces, red blood cell samples (200 µl) were dissolved and decolourised using 1 ml Solvable™ (Packard Bioscience B.V. Groningen, The Netherlands), 100 µL 0.1 M ethylenediaminetetraaceticacid (EDTA, Titriplex) (Merck, Darmstadt, Germany), and 500 µl hydrogen peroxide (Perhydrol) (Merck KGaA, Darmstadt, Germany). Faecal homogenates were decolourised using 1 ml Solvable™, 1 ml isopropanol (2-propanol) (Biosolve B.V., Valkenswaard, The Netherlands) and 0.4 ml hydrogen peroxide (Perhydrol). The samples were analysed together with calibration standards and QC standards in the LSC. Calibration curves were fitted using least-squares regression analysis. The equation of the calibration curve was used to calculate the radioactivity concentration in all samples in disintegrations per minute (dpm). The lower and upper limits of quantification were 1 and 1,000 µg/ml E7070, respectively.

The concentrations of E7070 and the metabolite 1,4-benzenesulphonamide (M1) in plasma, urine and faecal homogenates were measured using high-performance liquid chromatography coupled to an electrospray ionisation tandem mass spectrometer (LC/ESI-MS/MS).[12] Before shipment from the C laboratory to the non-radioactive laboratory, the plasma, urine and faecal homogenate samples were diluted with blank plasma, blank urine and distilled water, respectively, to a radioactivity concentration of less than 100 Bq/ml. Samples were stored at –20°C until analysis.

Pre-treatment of the plasma and urine samples involved solid-phase extraction (SPE) on 60 mg Oasis cartridges (Waters, Milford, MA, USA). Faecal homogenates were extracted twice with ethylacetate. Reconstituted extracts were injected onto an Apex Octyl column (Jones Chromatography, Hengoed, Mid Glamorgan, UK) and a water/acetonitrile gradient containing 2.5 mM ammonium acetate was used to transfer the analytes to the TurboIonSpray™ sample inlet (Sciex, Thornhill, ON, Canada). Negative ions were created at atmospheric pressure and the parent ions were fragmented in the API 365 triple quadrupole mass spectrometer (Sciex). The transitions for E7070 were selected from m/z 383.9 to 319.8 and for M1 from 235 to 170.5. Deuterated internal standards were used for the quantitation. The lower limits of quantification for E7070 and M1 were 0.10 µg/ml and 0.01 µg/ml in plasma, respectively.

In urine and faeces, the lower limits of quantification for both analytes were 0.05 µg/ml and 0.05 µg/g, respectively. The upper limits of quantification for E7070 and M1 were 10 µg/ml in urine and 10 µg/g in faeces.

Pharmacokinetic analysis

The E7070 and M1 concentrations in plasma were expressed in mmol/L by dividing the concentration in µg/ml by their molecular weights (385.9 and 236.3, respectively). The radioactivity levels in plasma were expressed in mmol/L as the amount of radioactivity expressed in Bq/ml divided by the radioactivity level of the infusion solution in Bq and multiplied by the molarity of the infusion solution (in mmoles).

The pharmacokinetic parameters were calculated by applying a non-compartmental analysis using the pharmacokinetic computer program WINNONLIN™ (Standard Edition version 3.0, 1999, Pharsight Corporation, California, USA). The maximal drug concentration (C_{max}) was derived directly from the experimental data. The first order rate constant λ_z associated with the terminal elimination portion was calculated by log-linear regression analysis of the concentration versus time curve. The area under the plasma concentration-time curve (AUC_{inf}) was calculated by the linear trapezoidal rule up to the last sampling time point with detectable concentration (C_{last}) with extrapolation to infinity of the terminal elimination phase. The terminal half-life ($t_{1/2}$) was calculated by the equation $\ln2/\lambda_z$. The apparent clearance (CL) was calculated by dividing the administered dose by the AUC_{inf}. The apparent volume of distribution at steady state (Vss) by multiplying CL by the mean residence time extrapolated to infinity (MRT_{inf}). MRT_{inf} is determined as $MRT_{inf} = (AUMC_{inf}/AUC_{inf}) - (1/2 \times$ duration of infusion), where $AUMC_{inf}$ is the area under the first moment curve with extrapolation to infinity.

The excretion of total radioactivity in urine and faeces (in mmoles) was calculated as the total amount of excreted radioactivity in Bq divided by the radioactivity of the administered dose in Bq and multiplied by the molarity of the infusion (in mmoles). The excretion of E7070 and M1 in urine and faeces as a percentage of the administered dose was calculated as the total amount of excreted drug (in mmoles) and metabolite (in mmoles) divided by the molarity of the infusion (in mmoles) times 100.

All pharmacokinetic parameters (Cmax, AUC_{inf}, CL, $t_{1/2}$ and Vss) and the excretion of the total radioactivity, E7070 and M1 in urine and faeces are expressed in mean ± standard deviation (SD).

Results

Patients and treatment

Thirteen patients were enrolled in the study. Six patients were included in the first cohort that received 1000 mg of E7070 radiolabelled with [benzene sulphonamide-^{14}C]ER-35744 during the first course. Seven patients were included in the second cohort that received

Table 1. Patient characteristics

Characteristics	Cohort 1[a]	Cohort 2[b]
No. of patients	6	7
Sex		
male	5	4
female	1	3
Age in years		
mean	56	51
SD	8.8	11.3
WHO PS		
0	0	2
1	5	5
2	1	0
Primary tumour		
lung	1	1
gastric	2	1
colorectal	1	1
pancreas	1	0
melanoma	0	1
ovarian	0	1
carcinoid	0	1
hypopharynx	0	1
primary unknown	1	0
Prior treatment		
prior surgery	4	4
prior radiotherapy	2	3
prior chemotherapy	6	7
prior immunotherapy	0	1

[a] The patients in cohort 1 received [benzene sulphonamide-14C]ER-35744.
[b] The patients in cohort 2 received [indole ring-U-14C]ER-35744.
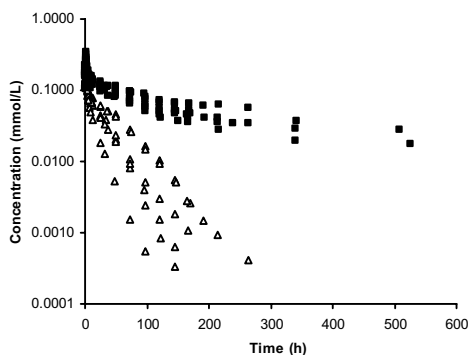PS = Performance status (PS) according to the World Health Organisation (WHO) scale.

1000 mg of E7070 radiolabelled with [indole ring-U-^{14}C]ER-35744 during the first course. The patient characteristics are summarised in Table 1.

Pharmacokinetics

The individual plasma concentrations of total radioactivity in both cohorts (determined by the LSC method) *versus* the mean of the E7070 (determined by the LC/ESI-MS/MS method) as a function of time are depicted in Figure 2A (cohort 1) and in Figure 2B (cohort 2). In both cohorts the radioactivity levels (expressed as E7070 equivalents in mmol/L) in plasma are much higher than can be explained by E7070 (and M1) alone. The E7070 concentrations were substantially higher than the M1 concentrations in plasma in both cohorts of patients. The calculated plasma AUC_{inf} of E7070 (3.75±2.02 h*mmol/L) is higher than the AUC_{inf} of M1 (0.14±0.05 h*mmol/L) (Table 2). The radioactivity levels in plasma and red blood cells (as determined by the LSC method) of all patients (n=13) are outlined in Figure 3. The radioactivity concentration in plasma was higher than in RBC during and shortly after the

Figure 2. Individual plasma concentrations of total radioactivity and the contribution of E7070 as a function of time after the administration of 1000 mg E7070 containing 3.7 MBq of ^{14}C-labelled E7070 in the first cohort (n=6) (A) and in the second cohort (n=7) (B)

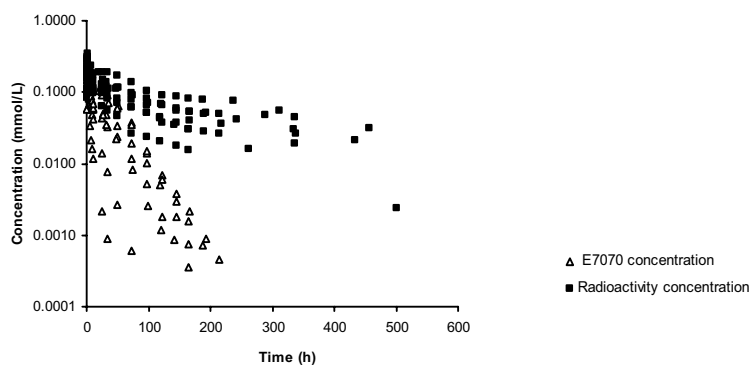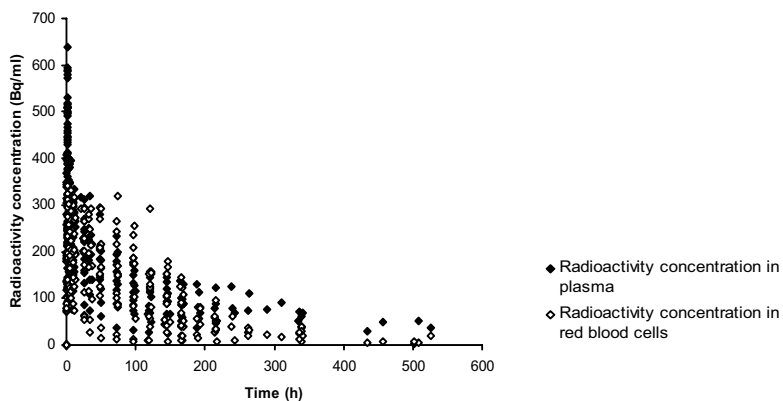**Figure 3.** Red blood cell concentrations and plasma concentrations of radioactivity in all patients (n=13)

Table 2. Pharmacokinetic parameters of E7070 and M1 in plasma after intravenous administration of 1000 mg ^{14}C-labelled E7070 (n=13)

Pharmacokinetic parameter	E7070	M1
Cmax (mmol/L)		
Mean	0.20	0.0026
SD	0.05	0.0008
$t_{1/2}$ (h)		
mean	19.4	117.2
SD	7.7	47.7
AUC_{INF} (h*mmol/L)		
Mean	3.75	0.14
SD	2.02	0.05
CL (ml/min)		
Mean	17.3	NA
SD	15.6	NA
Vss (L)		
Mean	21.5	NA
SD	4.4	NA

AUC_{INF} = area under the concentration-time curve extrapolated to infinity; CL = clearance; Cmax = maximal concentration; NA = not applicable; $t_{1/2}$ = terminal half-life; Vss = distribution volume at steady state.

infusion of ^{14}C-labelled E7070. Later, the radioactivity concentrations in both compartments are in the same range. The courses of the distribution and elimination phases of radioactivity in plasma and red blood cells are synchronic.

The mean urinary and faecal excretion of radioactivity as a percentage of the administered dose in the first and the second cohort is presented in Table 3 (a and b). After the iv infusion of ^{14}C-labelled E7070 the urinary recovery of radioactivity is higher than the faecal recovery in cohort 1 (63.7 ±9.8% and 22.7 ±2.6%, respectively) and in cohort 2 (61.5 ±5.5% and 21.1 ±3.1%, respectively) over a mean collection period of 11 and 10 days, respectively. The total recovery of radioactivity in urine and faeces is 86.4 ±9.0% (cohort 1) and 82.6 ±4.6% (cohort 2) of the administered dose. In the first 48 hours post dosing only 41% (cohort 1) and 43% (cohort 2) of the administered dose was excreted in urine and faeces which illustrates the slow excretion of E7070 and its metabolites. The cumulative urinary and faecal recovery of total radioactivity, E7070 and M1 are shown in Table 4. The total radioactivity levels are much higher (86.4% and 82.6% in cohort 1 and 2, respectively) than the cumulative recovery of E7070 (2.3% and 2.7% in cohort 1 and 2, respectively) and M1 (5.3% and 5.1%, respectively) in urine and faeces. The cumulative recovery of E7070 is almost equal in urine (1.2 ±0.7% and 1.5 ±0.8%) and faeces (1.1 ±0.4% and 1.2 ±0.6%) whereas the cumulative recovery of M1 is higher in faeces (3.7 ±1.6% and 3.5 ±1.1%) than in urine (1.7 ±0.6% and 1.7 ±0.6%) in both cohorts. For the whole patient population (n=13), the cumulative recovery of E7070 and M1 (mean±SD) is 1.4 ±0.8% (E7070) and 1.7 ±0.6% (M1) in urine and 1.1 ±0.5% (E7070) and 3.6 ±1.3% (M1) in faeces. With reference to the high total radioactivity levels that cannot be explained by E7070 and M1, the detection of metabolites other than M1 was

Table 3a. Percentage of the radioactive dose recovered in urine after intravenous administration of 1000 mg ^{14}C-labelled E7070 (cohort 1 and 2)

Time after the E7070 administration (hours)	Cohort 1: n=6 (mean% ± SD)	Cohort 2: n=7 (mean% ± SD)
0-12	14.18 ± 8.2	18.73 ± 12.2
12-24	9.75 ± 4.4	8.97 ± 4.7
24-36	6.89 ± 2.0	6.39 ± 1.5
36-48	4.58 ± 0.8	4.08 ± 0.9
48-60	4.64 ± 0.8	3.65 ± 0.9
60-72	3.73 ± 0.6	2.61 ± 0.9
72-84	3.66 ± 0.9	2.93 ± 1.5
84-96	2.80 ± 1.6	2.04 ± 1.3
96-120	4.25 ± 1.4	3.22 ± 1.8
120-144	3.39 ± 1.2	2.67 ± 1.0
144-168	2.86 ± 1.3	2.08 ± 0.7
168-192	2.00 ± 0.8	1.82 ± 0.9
192-216	1.92 ± 0.9	1.71 ± 0.5
216-240	1.48 ± 0.4	1.33 ± 0.5
240-264	0.80 ± 0.7	1.50 ± 0.9
264-288	1.09 ± 0.2	1.19 ± 0.09
288-312	0.93 ± 0.02	0.98 ± 0.4
312-336	ND	1.05
Total urinary excretion	63.7 ± 9.8	61.5 ± 5.5

ND = not determined.

Table 3b. Percentage of the radioactive dose recovered in faeces after intravenous administration of 1000 mg ^{14}C-labelled E7070 (cohort 1 and 2)

Time after the E7070 administration (hours)	Cohort 1: n=6 (mean% ± SD)	Cohort 2: n=7 (mean% ± SD)
0-48	5.28 ± 3.61	4.46 ± 2.50
48-96	8.94 ± 2.49	6.75 ± 2.33
96-144	5.22 ± 1.54	6.39 ± 2.60
144-192	3.42 ± 2.10	2.72 ± 2.11
192-240	2.23 ± 2.41	0.85 ± 0.51
240-288	0.72 ± 0.61	0.61 ± 0.48
288-336	0.29 ± 0.05	0.34
Total faecal excretion	22.7 ± 2.6	21.1 ± 3.1

Table 4. Urinary and faecal excretion values of total radioactivity, E7070 and M1 following intravenous administration of 1000 mg containing 3.7 MBq ^{14}C-labelled E7070 (cohort 1 and 2)

	Total radioactivity (mean% ± SD)	E7070 (mean% ± SD)	M1 (mean% ± SD)
Cohort 1 (n=6)			
Urine	63.7 ± 9.8	1.2 ± 0.7	1.7 ± 0.6
Faeces	22.7 ± 2.6	1.1 ± 0.4	3.7 ± 1.6
Total	86.4 ± 9.0	2.3 ± 0.9	5.3 ± 1.6
Cohort 2 (n=7)			
Urine	61.5 ± 5.5	1.5 ± 0.8	1.7 ± 0.6
Faeces	21.1 ± 3.1	1.2 ± 0.6	3.5 ± 1.2
Total	82.6 ± 4.6	2.7 ± 1.2	5.1 ± 0.8

performed in urine. Therefore, a mixed urine sample (100 µl) obtained in 6 patients (3 of the first cohort, and 3 of the second cohort) from 0 to 24 hours after the infusion of radiolabelled E7070, was injected on an HPLC system coupled online with a radio-isotope detector. The results are depicted in Figure 4 showing a chromatogram with 15 peaks. E7070 and M1 are represented by the peaks numbered 15 and 3, respectively. The major peak (number 7) represents a metabolite that is formed by glucuronidation after hydroxylation of E7070. This glucuronidated metabolite has a m/z value of 576.3 as identified by mass spectrometry.

In addition, in one patient with malignant ascites an ascites drainage was performed prior to the start of the E7070 infusion, and 7 days after the E7070 administration. The total volume of the evacuated ascites post-dosing was 5.5 L containing a radioactivity level of 3% of the administered dose.

Safety

During this mass balance study the toxicities (related to E7070) observed following the first course of ^{14}C-labelled E7070 were generally mild (maximally CTC grade 1-2). The toxicities included anaemia (n=1), sinus tachycardia (n=1), nausea (n=1), stomatitis (n=1), diarrhoea (n=1), fatigue (n=2), and paresthesias in the face (n=1). All patients continued treatment at a dose of 700 mg/m^2 E7070 infused iv in 1 hour every 3 weeks.

Discussion

The aim of this mass balance study was to determine quantitatively the (metabolic) disposition of E7070 and its metabolite M1 after intravenous administration. Based on the elimination half-life of E7070 as determined in phase I studies, the anticipated collection time

Figure 4. Chromatogram of a urine sample analysed by a HPLC method with online radioisotope detection. 15 = E7070, 3 = M1 metabolite, 7 = metabolite formed by glucuronidation of E7070
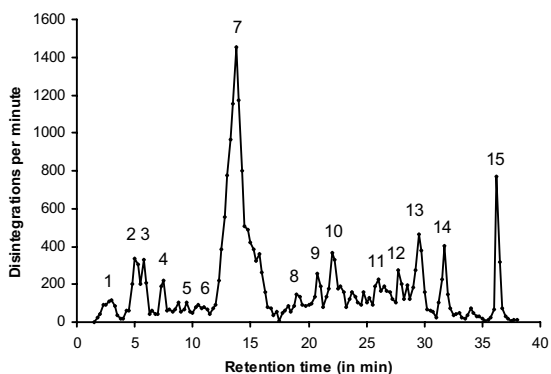
for urine and faeces was 7 days.[9,10] However, due to the prolonged retention of radioactivity in plasma the collection time had to be extended to a maximum of 14 days. The urinary and faecal recovery of total radioactivity (86.4% in cohort 1, 82.6% in cohort 2) indicates that the duration of urinary and faecal collection was sufficiently long to characterise the excretion of E7070 and its metabolite M1 despite the slow rate of elimination of radioactivity from the central compartment. Following the iv administration of ^{14}C-labelled E7070 the major route of elimination of the radioactive tracers is by the kidneys with a mean cumulative urinary recovery of 63.7% (cohort 1) and 61.5% (cohort 2) of the administered dose. We may conclude that the benzene-sulphonamide and indole moieties of E7070 show the same elimination pattern, which probably indicates that the majority of metabolites contain an intact sulphonamide link. E7070 is excreted by the renal and gastro-intestinal routes to the same extent, but its metabolite M1 is primarily excreted by the gut (Table 4). Only a minority of the excreted radioactivity is represented by E7070 and M1. Further detection of metabolites in urine showed that the high total radioactivity levels are caused by 13 other compounds than E7070 and M1. Glucuronidation appears to be an important metabolic route in humans in contrast to preclinical studies in which this metabolite was not identified. Further research is ongoing to elucidate the chemical structures of all metabolites.

From the measured radioactivity level in ascites (3% of the administered dose) at one week post-dosing in one patient, we may conclude that E7070 and/or its metabolites can accumulate in third 'spaces'. However, further clinical studies should demonstrate whether this observation has any therapeutic or toxic consequences.

Preclinical pharmacokinetic studies have been performed to elucidate the disposition of E7070 after a single intravenous administration of ^{14}C-labelled E7070 in mice and rats. In contrast to the observations in humans, the mean cumulative faecal excretion of radioactivity (86% and 67%, respectively) was higher than the urinary excretion (13% and 39%, respectively) calculated as a percentage of the administered dose during a collection period of 7 days in rats and 14 days in mice. In urine, the majority of excreted radioactivity represented polar metabolites and only a minority of radioactivity was excreted as unchanged E7070 and M1. Preliminary indications are that the majority of radioactivity in faeces was associated with E7070 and M1.

In human plasma, the radioactivity levels were substantially higher than can be explained by E7070 (and M1 in the first cohort) which indicates that E7070 is extensively metabolised. The M1 concentration is also very low compared to the E7070 concentrations. In combination with the low recovery of M1 in urine and faeces we may conclude that M1 is only a minor metabolite in man. Based on the higher radioactivity concentrations in plasma compared to red blood cells in humans during and shortly after the infusion, E7070 and its metabolites possessing the benzene-sulphonamide moiety and the indole moiety reached higher initital concentrations in plasma than in red blood cells (Figure 3). In contrast, the pharmacokinetic studies in rodents showed that the radioactivity concentration in red blood cells was higher

than the radioactivity concentration in plasma after administration of ^{14}C-labelled E7070. It remains unclear why the red blood cell-plasma ratio is higher in rodents than in humans.

In conclusion, the results of this mass balance study demonstrate that radiolabelled E7070 given by iv infusion is slowly excreted via urinary and faecal routes. E7070 is excreted by the renal and gastro-intestinal routes but M1 is primarily excreted by the gut. The total radioactivity was primarily excreted by the renal route. A high proportion of the radioactivity in human plasma, urine and faeces is represented by compounds other than E7070 and M1. These high radioactivity levels are caused by the extensive formation of metabolites other than M1. Thus, E7070 is primarily eliminated by metabolism. Glucuronidation appears a major metabolic pathway. Currently, studies are ongoing to identify the chemical structures and pharmacological activities of the other metabolites.

Acknowledgements

References

1. Owa T, Okauchi T, Yoshimatsu K, et al. A focused compound library of novel *N*-(7-indolyl)be nzenesulfonamides for the discovery of potent cell cycle inhibitors. Bioorg Med Chem Letters 2000*;*10:1223-1226.
2. Owa T, Yoshino H, Okauchi T, et al. Discovery of novel antitumor sulfonamides targeting G1 phase of the cell cycle. J Med Chem 1999;42:3789-3799.
3. Maren TH. Relations between structure and biological activity of sulfonamides Annu Rev Pharmacol Toxicol 1976;16:309-327.
4. Yoshimatsu K, Yamaguchi A, Yoshino H, et al. Mechanism of action of E7010, an orally active sulphonamide antitumor agent: inhibition of mitosis by binding to the colchicine site of tubulin. Cancer Res 1997;57:3208-3213.
5. Yoshino H, Ueda N, Niijima J, et al. Novel sulfonamides as potential, systemically active antitumor agents. J Med Chem 1992;35:2496-2497.
6. Sherr JC. Cancer cell cycles. Science 1996;274:1672-1677.
7. Lundberg AS, Weinberg RA. Control of the cell cycle and apoptosis. Eur J Cancer 1999;35:1886-1894.
8. Ozawa Y, Sugi NH, Nagasu T, et al. E7070, a novel sulphonamide agent with potent antitumour activity in vitro and in vivo. Eur J Cancer 2001;37:2275-2282.
9. Raymond E, Fumoleau P, Roche H, et al. Combined results of 4 phase I and pharmacokinetic (PK) studies of E7070, a novel chloroindolyl-sulphonamide inhibiting the activation of cdk2 and cyclin E. Clin Cancer Res 2000;40:384 (abstract).
10. Punt CJA, Fumoleau P, van de Walle B, et al. Phase I and pharmacokinetic study of E7070, a novel sulphonamide, given at a daily times five schedule in patients with solid tumours. A study by the EORTC-early clinical studies group (ECSG). Ann Oncol 2001;12:1289-1293.
11. van Kesteren C, Mathôt R, Raymond E, et al. Population pharmacokinetic analysis of the novel anti-cancer agent E7070 during phase I studies: model building and validation. J Clin Oncol *in press*.
12. Rosing H, Hillebrand MJX, Ravic M, et al. Determination of E7070 and its metabolite M1 in biological matrices using liquid chromatography coupled with electrospray ionization tandem mass spectrometry. In 17th (Montreux) Symposium; Liquid Chromatography (LC/MS;SFC/MS;CE/MS;MS/MS); 2000; 101 (abstract).

Chapter 2.1.2

An *in vitro* pharmacokinetic study of the novel anticancer agent E7070: red blood cell and plasma protein binding in human blood

HJG Desirée van den Bongard, Dick Pluim, Robert CAM van Waardenburg, Miroslav Ravic, Jos H Beijnen and Jan HM Schellens

Summary

E7070 is a novel sulphonamide anticancer agent that arrests the G_1-S phase of the cell cycle. Preclinical and phase I studies have demonstrated non-linear pharmacokinetics of the drug. A population pharmacokinetic (PK) analysis revealed that the human plasma concentration-time data were best described by a 3-compartment model with non-linear distribution. We have studied the *in vitro* interaction of carbon-14 (^{14}C)-radiolabelled E7070 with red blood cells (RBC) and its binding to plasma proteins in the concentration range where non-linearity in disposition was observed in humans to get more insight into the behaviour of the drug. After the addition of E7070 to whole blood at 37°C, the drug is taken up or binds to RBC in a concentration-dependent manner. The addition of sodium azide, however, did not result in a decrease of drug uptake by RBC indicating passive diffusion processes. A non-linear increase in drug uptake was observed at incubation concentrations > 4 µg/ml E7070 in whole blood. This non-linearity was confirmed by lower partition coefficients between RBC and plasma at higher incubation concentrations (from 2.37 at 4 µg/ml to 0.31 at 200 µg/ml). The plasma protein binding of E7070 was high (98-99%) and linear in the concentration range studied (20-200 µg/ml). In conclusion, E7070 in whole blood is preferentially bound to RBC, and exhibits high plasma protein binding. The non-linear distribution of E7070 in humans can be caused, in part at least, by saturable binding of E7070 to RBC.

Introduction

Several sulphonamide derivatives have been synthesised to develop novel cytotoxic agents against solid tumours.[1,2] Sulphonamides are well known to have a variety of pharmacologic activities including antibacterial, carbonic anhydrase-inhibitory, antidiabetic, diuretic, and antithyroid.[3] The novel sulphonamide derivative E7070 (N-(3-chloro-7-indolyl)-1,4-benzenedisulphonamide) arrests the transition of the G1- to S-phase of the cell cycle by inhibiting the phosphorylation of cyclin E and activation of cyclin dependent kinase 2.[1,2,4,5] E7070 exhibited a potent antitumour activity in murine and human tumour cell lines and in human xenograft studies. The highest antitumour activity was observed in colorectal and lung cancer xenografts (HCT116 colorectal cancer and LX-1 lung cancer models).[6]

Phase I trials of E7070 in patients with solid tumours using four different infusion schedules revealed non-linear pharmacokinetics of the drug. There was a pronounced disproportional increase of the area under the concentration-time curve with dose.[7,8] A population pharmacokinetic (PK) analysis of E7070 in phase I studies (n=143) revealed that the concentration-time data could best be described by a three-compartment model with saturable distribution to one compartment and both linear and Michaelis-Menten elimination from the central compartment.[9]

In general, non-linear drug distribution can be caused by saturable plasma protein binding, saturable binding to blood cells or saturation of tissue uptake or binding sites.[10] Sulphonamide agents are well known to bind to carbonic anhydrase, an enzyme abundant in RBC.[11-13] We hypothesised that non-linear binding of E7070 either to RBC or to plasma proteins may explain its PK behaviour. Therefore, we studied the *in vitro* distribution of E7070 in human whole blood and human plasma protein binding within the concentration range observed during the phase I studies.

Materials and methods

Materials

E7070 was supplied by Eisai Limited, London, United Kingdom. The carbon-14 (^{14}C)-radiolabelled E7070 compound ([indole ring-U-^{14}C]ER-35744, Figure 1) was manufactured by Amersham International Ltd. of Little Chalfont, Amersham, Buckinghamshire, United Kingdom. The ^{14}C-radiolabelled compound was dissolved in saline to a final concentration

Figure 1. Chemical structure of ^{14}C-radiolabelled E7070 ([indole ring-U-^{14}C]ER-35744)
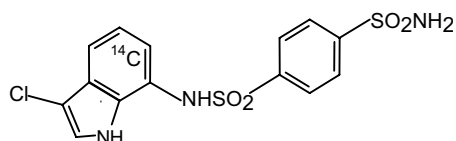
of 1 mg/ml. The radiochemical purity and the chemical purity were at least 98%. The radiolabelled drug was stored at –20°C until use. Isotonic phosphate buffered saline (PBS, pH 7.4) was prepared. Solvable™ was purchased from Packard Bioscience B.V. (Groningen, The Netherlands). Ethylene diamine tetra acetic acid (EDTA, Titriplex®) and hydrogen peroxide (Perhydrol®) were purchased from Merck (Darmstadt, Germany).

Fresh whole blood samples from seven drug-free healthy volunteers were collected from an antecubital vein into heparinized tubes. Additional blood samples were taken from these volunteers to determine the haematological and chemical parameters of the collected blood.

Methods

Uptake of ^{14}C-radiolabelled E7070 in RBC

The uptake of E7070 in RBC was studied at various drug concentrations. Uptake studies were performed *in vitro* by incubation of whole blood with ^{14}C-radiolabelled E7070 in 50 ml falcon tubes in a water bath at 37°C (n=6) and at approximately 0°C (melting ice water, n=6) on a plate with gentle shaking. After pre-incubation of whole blood for 10 minutes, radiolabelled compound was added to yield a final concentration of 200 µg/ml and incubated for 24 hours to determine the time when distribution equilibrium was achieved between plasma and RBC. To determine whether the E7070 uptake in RBC was an adenosine triphosphate (ATP)-dependent transport, the effect of sodium azide on uptake was determined at 37°C (in duplicate). Sodium azide produces a decrease in the intracellular ATP concentration, and was added to give a final concentration of 20 mM which is sufficient to inhibit ATP-dependent systems.[14,15] Whole blood samples (2.5 ml) were taken immediately after the addition of ^{14}C-radiolabelled E7070, at 30, 60 minutes, and at 3, 7 and 24 hours after the addition of ^{14}C-radiolabelled E7070. After the whole blood samples were taken, they were immediately centrifuged at approximately 1600 *g* for 5 minutes (at 4°C). Fifty µl of plasma was transferred to a plastic vial. The rest of the plasma layers and the buffy coats with the leukocytes were carefully removed with sufficient margins, followed by transfer of 200 µl of RBC in 15 ml falcon tubes. After one wash step of the RBC with ice-cold isotonic PBS wash-solvent (1800 µl), the RBC were centrifuged at approximately 1600 *g* for 15 minutes (at 0°C), and the supernatant was discarded. RBC samples (200 µl) were dissolved and decolourised using Solvable™ (1 ml), 0.1 M EDTA (100 µl), and hydrogen peroxide (500 µl).

This experiment was followed by the incubation of 2 ml of whole blood without sodium azide (in triplicate) with ^{14}C-radiolabelled E7070 at concentrations in the range of 0 (blank), 4, 20, 50, 100, 150, 200 µg/ml in 15 ml falcon tubes in a water bath at 37°C, or at approximately 0°C (melting ice water) on a plate with gentle shaking. All whole blood samples were centrifuged (at 1600 *g* for 5 minutes at 4°C) after the equilibrium between plasma and RBC was attained as determined in the previous experiment. After the centrifugation, 100 µl of plasma was transferred from each falcon tube to a plastic vial, and the rest of the plasma layers and buffy coats were carefully removed with sufficient margins. This was followed

by transfer of 500 µl of the RBC samples in 15 ml falcon tubes. After one wash step of the RBC with ice-cold isotonic PBS wash-solvent (4500 µl), the RBC were centrifuged at approximately 1600 *g* for 15 minutes (at 0°C), and the supernatant was discarded. Two hundred µl of the washed RBC samples was dissolved and decolourised using Solvable™ (1 ml), 0.1 M EDTA (100 µl), and hydrogen peroxide (500 µl) in a plastic vial.

Efflux of ^{14}C-radiolabelled E7070 from RBC to plasma

After one wash step of the RBC with ice-cold isotonic PBS, the RBC were incubated (in triplicate) with ^{14}C-radiolabelled E7070 to yield final concentrations of 0 (blank), 6, 50 and 100 µg/ml in 15 ml falcon tubes in a water bath at 37°C with gentle shaking. After 2 hours of incubation, 4 ml of blank plasma was added to each falcon tube with the incubated RBC. At each incubation concentration, 1 sample (2 ml) was taken just before the addition of blank plasma, and samples (2 ml) were taken at 20 minutes, 3 and 24 hours after the addition of blank plasma. Samples were centrifuged at 1600 *g* for 5 minutes (at 4°C). After centrifugation, 100 µl of plasma was transferred from each falcon tube to a plastic vial, and the rest of the plasma layers and buffy coats were carefully removed with sufficient margins. 200 µl of the RBC samples was transferred to 15 ml falcon tubes. After one wash step of the RBC with ice-cold isotonic PBS wash-solvent (1800 µl), the RBC were centrifuged at approximately 1600 *g* for 15 minutes (at 4°C), and the supernatant was discarded. Two hundred µl of the washed RBC samples was dissolved and decolourised using Solvable™ (1 ml), 0.1 M EDTA (100 µl), and hydrogen peroxide (500 µl) in a plastic vial.

Plasma protein binding of ^{14}C-radiolabelled E7070

The binding of E7070 to plasma proteins was determined by the ultrafiltration method after incubation of plasma with ^{14}C-radiolabelled E7070 in a gently shaking water bath. The entire procedure was conducted at 37°C (in triplicate). Amicon micropartition systems (Amicon Corporation, Danvers MA, USA) with membrane discs with a cut off level of 30,000 MW (Millipore Corporation, Amicon, Beverly MA, USA) to separate bound from free E7070 in plasma. Preliminary experiments revealed negligible binding to the ultrafiltration device (3%). After pre-incubation of plasma for 10 minutes, ^{14}C-radiolabelled E7070 was added to plasma to yield a final concentration of 200 µg/ml, and incubated for 24 hours in 50 ml falcon tubes to determine the ratio between the total and free E7070 concentrations in plasma, with time. Plasma samples were taken just before the addition of ^{14}C-radiolabelled E7070, at 5, 10, 20, 30, 45, 60 minutes, and at 2, 3, 4, 5, 6, 7, and 24 hours after the start of the incubation. After the plasma samples (50 and 100 µl) were taken and transferred to a plastic vial, 1 ml plasma samples were immediately transferred into ultrafiltration devices in duplicate. The plasma samples were ultracentrifuged at approximately 1100 *g* for 15 minutes at room temperature, and approximately 200 µl of plasma ultrafiltrate was obtained. 100 µl of plasma ultrafiltrate was transferred to a plastic vial.

After establishing the time when equilibrium is achieved between the total and free drug concentration in plasma in the previous experiment, plasma was incubated (in triplicate) with ^{14}C-radiolabelled E7070 in a concentration range of 20 to 200 µg/ml and at 0 µg/ml. Plasma samples were taken after the time to reach equilibrium between the total and free drug concentration in plasma.

At each incubation concentration, the plasma samples (50 and 100 µl) were taken and transferred to a plastic vial. The rest of the plasma was immediately transferred to 2 ultrafiltration devices and centrifuged at approximately 1100 *g* for 15 minutes at room temperature. Approximately 200 µl of plasma ultrafiltrate was obtained. 100 µl of plasma ultrafiltrate was transferred to a plastic vial.

Bio-analysis

The detection of beta radiation in plasma, RBC and PBS wash solvent was performed by a liquid scintillation counter (LSC) (Tri-CARB 2100 CA; Packard Instrument Company, Meriden, USA) with an energy range of 0-2,000 keV on the same day as the experiments. Each sample was mixed with 10 ml of Ultima Gold cocktail (Packard Instrument Company, Meridine, USA) in a plastic vial. The counting-time was 5 minutes per vial.

The samples were analysed together with calibration standards and quality control (QC) standards in the LSC. Calibration curves were fitted using least-squares regression analysis. According to the disintegration per minute (dpm) level in the *in vitro* samples and the QC control samples as determined by the LSC, the equation of the calibration curve was used to calculate the E7070 concentration in all samples. The calibration standards consisted of 1, 2, 4, 10, 20, 40, 100, 200, 400, 1,000 µg/ml E7070 dissolved in 0.9% NaCl. The QC standards consisted of 20, 100, 500 µg/ml E7070 dissolved in 0.9% NaCl. Results of batches analysed were accepted if at least 2 of the 3 QC standards were within ±20% of their respective nominal values. Sample analysis was performed in duplicate and was repeated if the deviation in measured dpm was more than 10%.

Data analysis

A partition coefficient value between RBC and plasma ($P_{RBC/plasma}$) was defined and used as an indicator for the distribution of E7070 between the RBC and plasma under the various tested conditions. The $P_{RBC/plasma}$ was calculated by the ratio of the E7070 concentration in RBC (C_{RBC}) and plasma (C_p).

$$P_{RBC/plasma} = \frac{C_{RBC}}{C_p} \qquad\qquad \text{equation 1}$$

where C_{RBC} and C_p are expressed in µg/ml.

The uptake of E7070 to RBC was calculated as the E7070 fraction in whole blood bound to RBC (F_{RBC}) taking into account the differences in haematocrit level (Ht) of the blood samples. The following equation was used:

$$F_{RBC} = \frac{C_{RBC} \cdot Ht}{C_{RBC} \cdot Ht + C_P \cdot (1 - Ht)} \qquad\qquad \text{equation 2}$$

where C_{RBC} and C_p are expressed in µg/ml.

The plasma protein binding of E7070 was calculated by dividing the free (Cf) and total (Cp) E7070 concentrations in plasma.

$$\text{Plasma protein binding} = \left(\frac{C_p - C_f}{Cp} \cdot 100 \right) \qquad\qquad \text{equation 3}$$

where plasma protein binding is expressed in %, and C_p and C_f in µg/ml.

Statistical analysis

Statistical analysis was performed with the Statistical Product and Service Solutions (SPSS) for windows, version 10.0.7 (SPSS Inc., Chicago, IL., USA).

Differences between the RBC uptake in different conditions were determined using the Student's t-test with a significance level of < 0.05.

Results

The E7070 concentrations in plasma and RBC were calculated from the radioactivity measurements. No degradation of radioactivity was observed in human RBC and plasma during a 24-hour incubation at 37°C. Validation experiments of the coupled liquid chromatography-tandem mass spectrometry method to determine the E7070 concentrations in human plasma, urine and faeces, showed that E7070 was stable for 24 hours at room temperature.[16] Consequently, we assumed that the radioactivity determinations are an accurate reflection of the E7070 concentrations in human RBC and plasma in this study.

After the addition of E7070 to whole blood *in vitro* at 37°C the drug was taken up by RBC from plasma (Figure 2). The addition of sodium azide to deplete ATP did not result in a significant inhibition of the uptake (data not shown). It was impossible, however, to quantify the ATP-depletion (caused by the addition of sodium azide to whole blood) by a luciferase assay due to interference by haemoglobin. Previous reports indicate that a sodium azide concentration of 20 mM would be sufficient to deplete ATP in RBC.[14] Equilibrium between the E7070 concentration in RBC and plasma was achieved within 2 hours at 37°C. After the incubation of whole blood with various E7070 concentrations for 2 hours at 37°C, the E7070 concentration in RBC achieved a plateau at higher incubation concentrations (Figure 3A). In

Figure 2. E7070 concentration in RBC (A) and in plasma (B) during the incubation with 200 µg/ml E7070 in whole blood at 37°C in vitro. Each value is the mean of 6 experiments
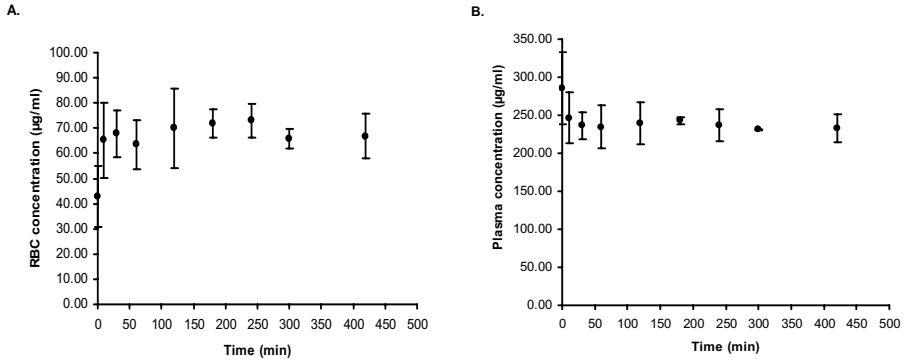

Figure 3. E7070 uptake in RBC (A) and E7070 concentration in plasma (B) following incubation with E7070 in whole blood for 2 hours at 37°C and at approximately 0°C. Each value is the mean ± SD of 3 experiments
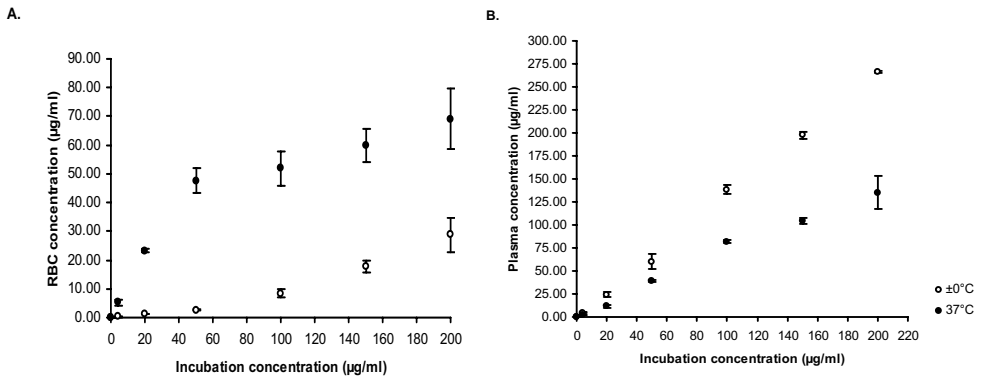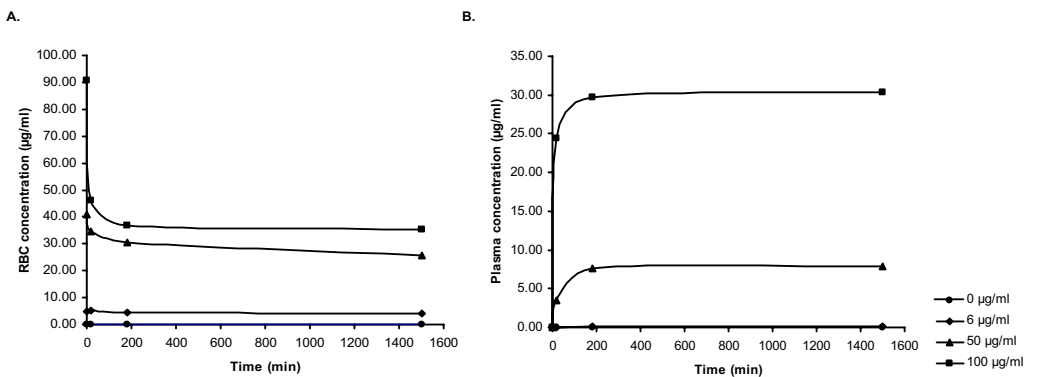

Figure 4. The *in vitro* E7070 efflux from RBC (A) to plasma (B) at various concentrations at 37°C. Each value is the mean of 3 experiments

contrast, the plasma concentration continued to increase at higher incubation concentrations (Figure 3B). Simultaneously, a non-linear increase of the E7070 concentration in PBS (that was used in the washstep of RBC) was observed at higher incubation concentrations in whole blood (data not shown). This indicates that at higher incubation concentrations of E7070 in whole blood, more E7070 was lost in the wash step. This may be explained by non-linear binding of E7070 to other components of whole blood (excluding plasma) at higher incubation concentrations, e.g. leukocytes or platelets.

The drug uptake in RBC was significantly decreased at approximately 0°C compared to 37°C with a corresponding higher E7070 concentration in plasma at 0°C compared to 37°C (Figure 3).

The *in vitro* partition coefficient ($P_{RBC/plasma}$) between RBC and plasma decreased at higher incubation concentrations at 37°C (Table 1). Since the haematocrit of the blood samples ranged from 0.39 to 0.43, the E7070 recovery percentage in whole blood bound to RBC following incubation for 2 hours at 37°C was determined. This percentage decreased from 61.8 ± 6.3% at 4 µg/ml to 17.6 ± 0.5% at 200 µg/ml (Table 1). These data confirm that there is a non-linear increase of the drug uptake into RBC at higher drug concentrations. In Figure 4 the results of the efflux experiments are summarised. The E7070 efflux from RBC to plasma takes place in a concentration- and time-dependent manner.

E7070 showed a high plasma protein binding (98-99%) which was constant over the measured time-period of 24 hours after the addition of 200 µg/ml E7070 to plasma (data not

Table 1. The *in vitro* partition coefficient between RBC and plasma ($P_{RBC/plasma}$) and the fraction of E7070 in RBC following incubation in whole blood for 2 hours at 37°C (n = 3)

Incubation concentration (µg/ml)	$P_{RBC/plasma}$ (mean ± SD)	Recovery in RBC (%) (mean ± SD)
4	2.37 ± 0.42	61.8 ± 6.3
20	2.03 ± 0.28	58.2 ± 5.4
50	1.22 ± 0.10	45.8 ±4.0
100	0.48 ± 0.07	25.0 ± 3.3
150	0.34 ± 0.02	19.1 ± 0.5
200	0.31 ± 0.04	17.6 ± 0.5

Table 2. Plasma protein binding of E7070 after incubation of plasma with E7070 for 30 minutes at 37°C (n = 3)

Incubation concentration (µg/ml)	Mean plasma protein binding (%)	SD (%)
20	98.0	0.66
50	98.8	0.16
100	99.0	0.05
150	99.0	0.16
200	99.0	0.07

shown). The *in vitro* binding was independent of the incubation concentration over a wide range of 20 to 200 µg/ml after 30 minutes of incubation with E7070 (Table 2).

Discussion

The results of these *in vitro* incubation experiments with E7070 in human blood revealed that the equilibrium between RBC and plasma is reached within approximately two hours. The addition of sodium azide caused no significant decrease of the E7070 uptake in RBC. We may thus conclude that the influx of E7070 from plasma into RBC occurs by passive diffusion. The E7070 uptake in RBC occurred in a concentration-dependent manner and RBC became saturated in the concentration range studied (4-200 µg/ml). This non-linearity also appears from the lower mean partition coefficient values between RBC and plasma (2.37 at the 4 µg/ml to 0.31 at the 200 µg/ml concentration), and the lower E7070 fraction in RBC in whole blood (61.8 ± 6.3% at 4 µg/ml to 17.6 ± 0.5% at 200 µg/ml) at higher incubation concentrations. This indicates that E7070 is preferentially bound to RBC when present in whole blood, and that the distribution in the RBC compartment can become saturated. The protein binding of E7070 in plasma was high (98-99%) and showed no signs of non-linearity or saturation in the concentration range of 20 to 200 µg/ml.

From these experiments we can conclude that the non-linear distribution of E7070 in blood is probably, in part at least, caused by a saturable distribution to the RBC compartment. Sulphonamide agents bind to carbonic anhydrase, an intracellular enzyme that is present throughout the body, although RBC account for >90% of this enzyme.[11-13] Recently, several novel sulphonamides with high affinity for the enzyme carbonic anhydrase were synthesised that resemble E7070 and showed antitumour activity.[12] It is possible that E7070 binds to carbonic anhydrase and this binding becomes saturated when blood concentration of drug is higher than the available binding sites of the enzyme in the RBC. This can result in a non-linear distribution of E7070 in the RBC compartment, as has been described for another sulphonamide agent, the carbonic anhydrase inhibitor MK-417.[11]

Recently, a mass balance study of ^{14}C-radiolabelled E7070 in patients with solid tumours has been completed in our institute.[17] The maximal concentration of total radioactivity in plasma was higher compared to that in RBC during and shortly after the infusion of ^{14}C-radiolabelled E7070. At later time-points the radioactivity concentration in both plasma and RBC were in the same range. Consequently, the exposure to radioactivity in plasma was higher than in RBC. We assume that the binding sites of the enzyme carbonic anhydrase in RBC become saturated when relatively high E7070 levels are reached, during and shortly after infusion. Moreover, according to this observation in the mass balance study, and considering the results of the *in vitro* E7070 efflux experiments, we may conclude that E7070 will diffuse from the RBC into plasma during the elimination process in humans. The drug in RBC may not be easily available for extraction by the eliminating organs (i.e. the kidneys and the liver), and the expression

of the pharmacologic activity may be influenced.[18,19] We observed no degradation of radioactivity in RBC during 24 hours of incubation with ^{14}C-radiolabelled E7070. However, we do not know whether E7070 alone or E7070 and its metabolites contribute to this radioactivity. Consequently, we cannot exclude that there might be metabolism of E7070 in the RBC.

In conclusion, E7070 is preferentially bound to RBC in whole blood. This binding is a saturable process at higher concentrations in whole blood. There is no evidence of saturation of protein binding of E7070 in plasma at the concentrations tested. It is postulated that the binding site of E7070 within the RBC is the enzyme carbonic anhydrase.

References

1. Owa T, Yoshino H, Okauchi T, et al. Discovery of novel antitumour sulfonamides targeting G1 phase of the cell cycle. J Med Chem 1999;42:3789-3799.
2. Owa T, Okauchi T, Yoshimatsu K, et al. A focused compound library of novel N-(7-indolyl)benzenesulfonamides for the discovery of potent cell cycle inhibitors. Bioorg Med Chem Letters 2000;10:1223-1226.
3. Maren TH. Relations between structure and biological activity of sulfonamides. Annu Rev Pharmacol Toxicol 1976;16:309-327.
4. Sherr JC. Cancer cell cycles. Science 1996;274:1672-1677.
5. Lundberg AS, Weinberg RA. Control of the cell cycle and apoptosis. Eur J Cancer 1999;35:1886-1894.
6. Ozawa Y, Sugi NH, Nagasu T, et al. E7070, a novel sulphonamide agent with potent antitumour activity in vitro and in vivo. Eur J Cancer 2001;37:2275-2282.
7. Punt CJA, Fumoleau P, Walle B van de, et al. Phase I and pharmacokinetic study of E7070, a novel sulfonamide, given at a daily times five schedule in patients with solid tumours. A study by the EORTC-early clinical studies group (ECSG). Ann Oncol 2001;12:1289-1293.
8. Raymond E, Fumoleau P, Roche H, et al. Combined results of 4 phase I and pharmacokinetic (PK) studies of E7070, a novel chloroindolyl-sulphonamide inhibiting the activation of cdk2 and cyclin E. Clin Cancer Res 2000;40:384 (A2545).
9. van Kesteren Ch, Mathôt RAA, Raymond E, et al. Population pharmacokinetics of the novel anti-cancer agent E7070 during four phase I studies: model building and validation. J Clin Oncol *in press*.
10. Ludden TM. Nonlinear Pharmacokinetics. Clin Pharmacokinet 1991;20:429-446.
11. Lin JH, Lin T, Cheng H. Uptake and stereoselective binding of the enantiomers of MK-927, a potent carbonic anhydrase inhibitor, by human RBC in vitro. Pharm Res 1992;9:339-344.
12. Supuran CT, Briganti F, Tillie S, et al. Carbonic anhydrase inhibitors: Sulfonamides as antitumour agents? Bioorg Med Chem 2001;9:703-714.
13. Edsall JT. Some perspectives on carbonic anhydrase since 1960. Ann N Y Acad Sci 1984;429:18-25.
14. Egorin MJ, Snyder SW, Pan S, et al. Cellular transport and accumulation of thiotepa. Sem Oncol 1991; 17(Suppl 3):7-17.
15. Trapp S, Ashcroft FM. Direct interaction of Na-azide with the K(ATP) channel. Br J Pharmacol 2000;131:1105-12.
16. Rosing H, Hillebrand MJX, Ravic M, et al. Determination of E7070 and its metabolite M1 in biological matrices using liquid chromatography coupled with electrospray ionization tandem mass spectrometry. In 17th (Montreux) Symposium; Liquid Chromatography (LC/MS;SFC/MS;CE/MS;MS/MS);2000;A101.
17. van den Bongard HJGD, Pluim D, Rosing H, et al. An excretion balance and pharmacokinetic study of the novel anticancer agent E7070 in cancer patients. Anti-Cancer Drugs 2002;13:1-8.
18. Lee H-J, Chiou WL. RBC as barriers for drug elimination in the isolated rat liver I. Doxorubicin. Pharm Res 1989;6:833-839.
19. Chen T-M, Abdelhameed MH, Chiou WL. RBC as a total barrier for renal excretion of hydrochlorothiazide: slow influx and efflux across erythrocyte membranes. J Pharm Sci 1993;81:212-218.

Chapter 2.2

Pharmacokinetic drug-drug interaction of the novel anticancer agent E7070 and acenocoumarol

HJG Desirée van den Bongard, Rolf W Sparidans, David JP Critchley, Jos H Beijnen and Jan HM Schellens

Summary

E7070 is a novel sulphonamide anticancer agent that arrests cancer cells at the G1-S boundary of the cell cycle. Three patients who were receiving prophylactic daily oral maintenance therapy with the anticoagulant acenocoumarol experienced bleeding and/or a prolonged prothrombin time after treatment with E7070 at a dose of 700 mg/m² given as a 1-hour infusion. *In vitro* studies have shown that E7070 has the potential to inhibit several cytochrome P450 (CYP)-enzymes, including CYP2C9, CYP2C19, CYP2D6, CYP2E1, and CYP3A4. The major enzyme involved in the metabolism of acenocoumarol in man is CYP2C9. This study was performed to investigate the interaction between E7070 and acenocoumarol. Blood samples were obtained from 2 patients receiving daily oral maintenance treatment with acenocoumarol both prior to and following treatment with E7070. Pharmacokinetic parameters of acenocoumarol were calculated by non-compartmental analysis and revealed that in both patients the area under the concentration-time curve up to 24 hours after the acenocoumarol administration was higher following E7070 (2.56 and 1.58 h*μmol/L) compared to the systemic exposure in the absence of E7070 (1.87 and 1.23 h*μmol/L).

In addition, we incubated acenocoumarol enantiomers with pooled human microsomes with and without E7070 and measured the *in vitro* plasma protein binding of acenocoumarol after incubation with E7070. The formation of acenocoumarol metabolites was retarded by E7070 at already low concentrations (2.1 μM). The plasma protein binding of acenocoumarol was reduced at higher concentrations of E7070 (259 μM).

In conclusion, these results indicate that E7070 may primarily interact with acenocoumarol by reducing its systemic clearance, and by reducing the plasma protein binding to a minor extent. In the absence of careful monitoring this drug-drug interaction may result in hypoprothrombinaemia and a haemorrhagic tendency.

Introduction

E7070 (N-(3-chloro-7-indolyl)-1,4-benzendisulphonamide, GOAL) is a novel sulphonamide anticancer agent (Figure 1) that acts on the G1 phase by inhibiting both the phosphorylation of cyclin E and the activation of cyclin dependent kinase 2 needed for the transition to the S-phase of the cell cycle.[1-3] Phase I trials employing four different infusion schedules in 127 patients with solid tumours showed that the dose-limiting toxicity of E7070 was predominantly haematological. Partial and minor responses were observed in patients with breast, endometrial, renal, and ovarian carcinoma.[4,5] The pharmacokinetics of E7070 are non-linear with a disproportional increase in systemic exposure with increasing administered dose (Figure 2).[4-6] Phase II studies employing two different dosing schedules, a 1-hour administration intravenously (iv) every 3 weeks (700 mg/m^2) and a daily 1-hour iv infusion for 5 consecutive days, repeated every 3 weeks (130 mg/m^2) are currently ongoing in patients with solid tumours.

During the phase I program, three patients who were receiving prophylactic daily oral maintenance therapy with acenocoumarol (Sintrom®) developed a haemorrhagic tendency and/or a prolonged prothrombin time following treatment with 700 mg/m^2 of E7070. Acenocoumarol is frequently involved in drug-drug interactions as a result of its narrow

Figure 1. Molecular structure of E7070 (N-(3-chloro-7-indolyl)-1,4-benzenedisulphonamide)
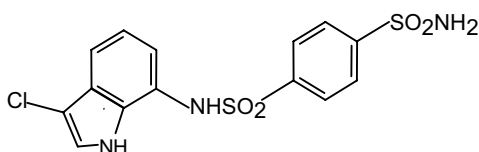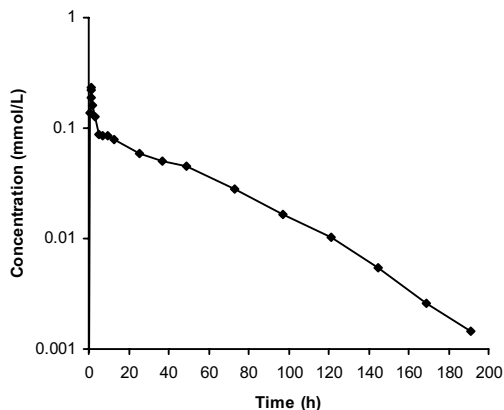

Figure 2. Typical plasma concentration-time curve of E7070 after 1-hour iv infusion of E7070 (1000 mg)

therapeutic index and cytochrome P-450 (CYP)-dependent, hepatic clearance.[7-9] Although, acenocoumarol is administered as a racemic mixture of R(+)- and S(-)-enantiomers, only R(+)-acenocoumarol is active.[7-9] The main metabolic pathways of the enantiomers are 6- and 7-hydroxylation producing 6- and 7-hydroxy-acenocoumarol, respectively. The major enzyme involved in this pathway is CYP2C9.[8-11] Serum protein binding of acenocoumarol (mainly to albumin) is known to be as high as 98.7%.[9,11]

An *in vitro* study performed in our institute indicated that human plasma protein binding for E7070 is also very high (ca. 99%). Moreover, other *in vitro* studies have demonstrated that E7070 may inhibit the activity of several cytochrome P450-related enzymes including CYP2C9, CYP2C19, CYP2D6, CYP2E1 and CYP3A4 (E7070; GOAL, Investigators Brochure). Clinically significant inhibition of CYP2C9 has been reported by existing sulphonamides e.g. sulphaphenazole.[12]

Most pharmacokinetic drug-drug interactions involving oral anticoagulants result from modifications in absorption, protein binding and/or elimination.[9,11] We investigated the potential of E7070 to displace acenocoumarol from its plasma protein binding sites and/or inhibit its hepatic metabolism. To this end, we studied the pharmacokinetics of acenocoumarol with and without E7070 in two patients. In addition, we performed *in vitro* studies to determine whether the plasma protein binding of acenocoumarol and the CYP450 mediated metabolism of acenocoumarol are influenced by the presence of E7070.

Materials and Methods

Drugs and chemicals

Racemic acenocoumarol and 7-hydroxy-acenocoumarol were kindly donated by Novartis Pharma (Basel, Switzerland). E7070 was obtained from Eisai Ltd. (London, UK).

Ethyl acetate and acetonitrile (gradient grade) were obtained from Biosolve (Valkenswaard, The Netherlands) and ammonia (25% (v/v), p.a.), dichloromethane and n-hexane from Merck (Darmstadt, Germany). Further, potassium hydroxide (p.a.) was provided by Lamers & Pleuger ('s Hertogenbosch, The Netherlands) and acetic acid (extra pure) by Riedel-de Haën (Seelze, Germany).

Monosodium D-glucose-6-phosphate, glucose-6-phosphate dehydrogenase, ß-NADP sodium salt and sodium hydrogencarbonate were all purchased from Sigma (St. Louis, MO, USA). Pooled, gender mixed, human liver microsomes (20 mg/ml, lot. 0110032, pooled from 16 donors) were purchased from XenoTech (Cambridge, Kansas City, KS, USA). Blank, drug-free human plasma was obtained from the Blood Transfusion Service (Utrecht, The Netherlands) and water was home-purified by reversed-osmosis on a multi-laboratory scale.

Stock solutions of racemic acenocoumarol were prepared in 10 mM potassium hydroxide and stock solutions of E7070 were prepared in methanol. A 200-µl volume of 15 U/ml glucose-6-phosphate dehydrogenase (Type VII, from bakers yeast), 200 µl of 5 mg/ml ß-NADP sodium

salt and 200 µl of 40 mg/ml monosodium D-glucose-6-phosphate (all in 2% (w/v) sodium hydrogencarbonate) were mixed with 1400 µl water to obtain the NADPH regenerating system (NRS). Human plasma was pooled using equal portions from 4 healthy donors.

Patients

In 3 patients receiving oral maintenance therapy with acenocoumarol, symptoms of hypoprothrombinaemia were observed after treatment with E7070. Bleeding was also observed in other patients treated with E7070 in the phase I programme but this was thought to be related to thrombocytopenia. One patient with advanced rectal cancer (patient #1) was included in a phase I study of E7070 and received a dose of 800 mg/m^2 as a 1-hour administration iv repeated every 3 weeks. The other 2 patients were enrolled in a mass balance study of E7070 and received a dose of 700 mg/m^2 as a 1-hour infusion iv repeated every 3 weeks. Patient #2 had an advanced abdominal gastro-intestinal autonomic nerve cell tumour, and the patient #3 had advanced non-small cell lung cancer. The results of these studies are presented elsewhere.[4-6,13]

Pharmacokinetic sampling

Patients #1 and #2 underwent pharmacokinetic analysis of acenocoumarol with and without E7070. They were maintained on acenocoumarol at an oral dose of 3 mg (#1) and 1 mg (#2) given once daily. Blood samples for acenocoumarol analysis were collected in heparinised tubes just before acenocoumarol administration (0 hours) and at 1, 2, 3, 4, 6, 8, and 11.5 hours after the administration of acenocoumarol with and without E7070. To avoid any effect of E7070 on the absorption of acenocoumarol, the E7070 infusion was started at 3 hours after the administration of acenocoumarol. Blood samples were centrifuged for 5 minutes at approximately 1600 g, and the plasma layer was separated. Plasma was immediately stored at –20°C in polypropylene tubes until analysis.

Microsomal incubation

All incubations were performed in triplicate. Fifty µl of an aqueous dilution of acenocoumarol alone (final concentrations in the incubation mixture were 1.5, 2, 3, 5 and 20 µM) or a combination of acenocoumarol (1.5, 3 and 20 µM) with E7070 (2.1, 5.2 and 20.9 µM) was transferred to a polypropylene micro tube on ice. Twenty-five µl of a 0.5 M potassium phosphate buffer (pH 7.4) and 50 µl of the NRS solution were added. After vortex mixing, the tubes were conditioned at 37°C for 2 min. Next, 5 µl of the microsomal suspension was added, the tube was vortex-mixed and incubated at 37°C for 15 min. The reaction was terminated by adding 125 µl methanol followed by vortex-mixing. Finally, proteins were removed by centrifugation for 1 min at 10^4 g at 4°C. Next, 200 µl of the supernatant was evaporated using nitrogen at 40ºC and the residue was reconstituted in 100 µl of 10 mM potassium hydroxide using vortex-mixing prior to injection onto the analytical column.

Plasma protein binding experiments

Racemic acenocoumarol (13.3, 53.8 and 133 µM) was mixed with pooled blank plasma (obtained from 3 healthy volunteers) and E7070 at incubation concentrations of 0, 2.59, 25.92, 259.2 µM (in triplicate). The mixture was placed at room temperature for at least 15 minutes followed by transfer of 400 µl of plasma before filtration (at 10000 g, 20°C) with Centrisart C4G Centrifugal Concentrators (10 kD MWCO, Supelco, Bellefonte, PA, USA) to separate protein-bound from free drug in plasma.

HPLC analysis

Patient samples

A validated HPLC analysis as described elsewhere was used to determine the acenocoumarol concentrations in patient plasma samples as has been published elsewhere.[14] For plasma samples containing E7070, the internal standard warfarin was replaced by phenprocoumon due to co-elution of E7070 and warfarin.

In vitro samples

For the *in vitro* samples a similar chromatographic assay was employed. Partial-loop injections (50 µl) were made on a Symmetry C_{18} column (100×4.6 mm, d_p = 3.5µm, average pore diameter = 10 nm, Waters) with a Symmetry C_{18} pre-column (20×3.8 mm, d_p = 5 µm, Waters). The column was used at 50°C and the eluent (pumped at 1 ml/min) comprised a mixture of 0.1% (v/v) acetic acid and acetonitrile (pH adjusted to 4.7 using 25% (w/v) ammonia). A model 616 pump with column thermostat (Waters Chromatography, Milford, MA, USA), a Waters in-line degasser, a Waters 717 plus autosampler and a Spectroflow variable wavelength detector (Kratos Analytical, Ramsey, NJ, USA) were used. The micosomal samples were analysed using 25% (v/v) acetonitrile (retention times of 6-hydroxy-acenocoumarol, 7-hydroxy-acenocoumarol, acenocoumarol and E7070 are 6.3, 8.9, 16 and 27 min, respectively) and the ultrafiltrate samples using 30% (v/v) acetonitrile (retention times of acenocoumarol and E7070 are 5.9 and 8.6 min, respectively) in the eluent. The calibration standards of E7070 were prepared in 50 mM phosphate (pH 7.4) and were in the range of 0.1 to 100 µmol/L. Detection was performed using ultraviolet absorption at 305 nm.

Pharmacokinetic analysis

Patient samples

The pharmacokinetic parameters were calculated by applying a non-compartmental analysis using the pharmacokinetic computer program WINNONLIN™ (Standard Edition version 3.0, 1999, Pharsight Corporation, California, USA). The time of the maximum observed concentration (T_{max}) and the concentration corresponding to T_{max}, the maximal drug concentration (C_{max}), were derived directly from the experimental data. The first order rate

constant λ_z associated with the terminal elimination was calculated by log-linear regression analysis of the concentration versus time curve. The terminal half-life ($t_{1/2}$) was calculated by the equation $\ln(2)/\lambda_z$. The area under the plasma concentration versus time curve (AUC) was obtained using the trapezoidal rule from 0 to 24 hours (AUC_{0-24h}). The apparent oral clearance (CL/F) was calculated by dividing the administered dose by the AUC_{INF} where F represents the oral bioavailability. AUC_{INF} is the AUC from the time of dosing to the last sampling point extrapolated to infinity. The apparent volume of distribution (Vz/F) was based on the terminal phase (Vz/F = Dose/λ_z*AUC_{INF}).

In vitro samples

The apparent values of the kinetic parameters Km and Vmax were calculated according to the rate of formation of 7- and 6-hydroxy-acenocoumarol from acenocoumarol at various incubated racemic acenocoumarol concentrations in combination with a range of E7070 concentrations using Lineweaver-Burk plots. Because the 6-hydroxy-acenocoumarol reference compound was not available, the 6-hydroxy-acenocoumarol concentrations were quantified using the 7-hydroxy-acenocoumarol concentrations in the calibration samples as determined by HPLC and the reported ratio of the ultraviolet absorption of 7- and 6-hydroxy-acenocoumarol.[8]

The plasma protein binding of acenocoumarol and E7070 was calculated by dividing the determined free (Cf) and total added (Cp) acenocoumarol and E7070 concentrations in plasma.

$$\text{Plasma protein binding} = \left(\frac{C_p - C_f}{C_p} \cdot 100 \right) \qquad\qquad \text{equation 1}$$

where plasma protein binding is expressed in %, and C_p and C_f in µmol/L.

Results

Patients

In all 3 patients, symptoms of hypoprothrombinaemia were observed (Table 1), with 2 patients (#1 and #2) experiencing bleeding (epistaxis, menorrhagia, bleeding at central venous catheter insertion). A prolonged prothrombin time was observed in patient #1 (>34) and in patient #3 (15.4). The prothrombin time values are expressed in the International Normalised Ratio (INR [0.9-1.15]) according to the equation:

$$\text{INR} = (Pt_{observed}/Pt_{control})^{ISI} \qquad\qquad \text{equation 2}$$

where ISI = international Sensitivity index.[15]

The prolonged prothrombin times were decreased by vitamin K administration and daily frequent measurements of the prothrombin time were performed. Using this approach further bleeding episodes were not observed despite continuing therapy with E7070.

Pharmacokinetic studies in patients

The concentration-time curves of acenocoumarol with and without E7070 are depicted in Figure 3. The pharmacokinetic parameters are summarised in Table 2. After co-administration of E7070, the half-life increased from 18.3 h to 27.5 h in patient #2 and decreased from 17.7 h to 13.6 h in patient #1. After treatment with E7070, the apparent clearance of acenocoumarol decreased in both patients (from 2.26 L/h to 1.77 L/h and from 1.15 L/h to 0.695 L/h),

Table 1. Symptoms of increased hypoprothrombinemia in three patients treated with daily maintenance therapy of acenocoumarol with co-infusion of E7070

| Symptoms	E7070 dose (course number)	Co-medication
Patient #1 Bleeding[a] Prolonged PT-INR (>34)[c]	800 mg/m^2 (3)	methadone clonazepam meloxicam paracetamol
Patient #2 Bleeding[b]	700 mg/m^2 (4)	metoprolol lorazepam triamterene/hydrochlorthiazide microgynon 30
Patient #3 Prolonged PT-INR (15.4)	1000 mg (3)	morphin retard lactulose

[a] epistaxis.
[b] epistaxis, menorrhagia, bleeding from central venous catheter insertion.
PT-INR = prothrombin time value expressed as the International Normalised Ratio.

Table 2. Pharmacokinetic parameters after oral administration of acenocoumarol as a single agent and with E7070 treatment (n=2)

	Pharmacokinetic parameters	
	Patient #1	Patient #2
Dose (mg)	3	1
Single agent		
Cmax (µmol/L)	0.243	0.127
Tmax (h)	3.00	1.02
$t_{1/2}$ (h)	17.7	18.3
AUC_{3-24h} (h*µmol/L)	1.87	1.23
Vz/F (L)	57.9	30.3
CL/F (L/h)	2.26	1.15
Co-infusion of E7070		
Cmax (µmol/L)	0.425	0.105
Tmax (h)	1.05	2.23
$t_{1/2}$ (h)	13.6	27.5
AUC_{3-24h} (h*µmol/L)	2.56	1.58
Vz/F (L)	34.8	27.6
CL/F (L/h)	1.77	0.695

Figure 3. Concentration-time curves of acenocoumarol after administration as a single agent and with co-infusion of E7070 in patient #1 (A) and patient #2 (B)

A.

B.
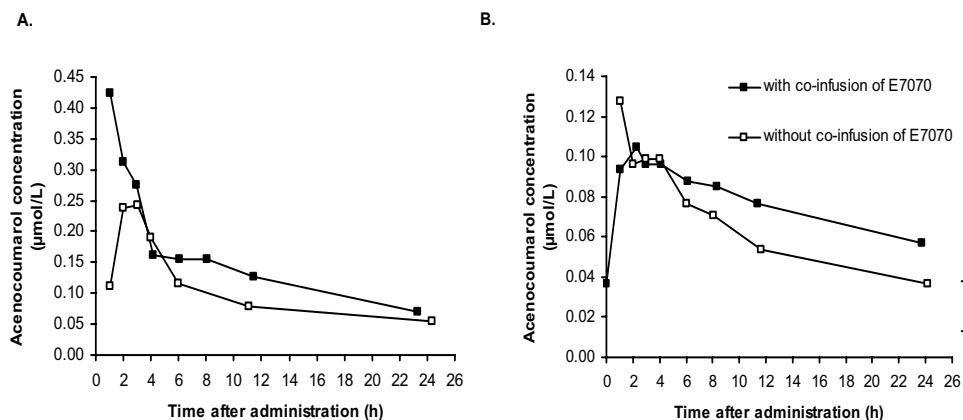
and the apparent volume of distribution (Vz/F) of acenocoumarol showed a decrease in 1 patient (from 57.9 L to 34.8 L). In the other patient, almost no difference in the volume of distribution was observed following E7070 (30.3 L without E7070, and 27.6 L with E7070). In both patients, the AUC_{3-24h} of acenocoumarol was 37% and 28% higher following E7070 (from 1.87 to 2.56 h*μmol/L and from 1.23 to 1.58 h*μmol/L, respectively).

In vitro studies

Km and Vmax were calculated according to Michaelis-Menten enzyme kinetics using least-squares linear regression with the squared concentration (c^2 or X^{-2}) as the weighting factor for the formation of 6- and 7-hydroxy-acenocoumarol at various incubated racemic acenocoumarol concentrations and at various E7070 concentrations. The influence of the presence of E7070 on the apparent Km and Vmax values of 6- and 7-hydroxy-acenocoumarol is depicted in Table 3. The *in vitro* intrinsic clearance of racemic acenocoumarol was 10.0 μl/(min*mg) without E7070, and decreased to 6.0 μl/(min*mg) in the presence of 20.9 μM E7070.

The plasma protein binding of acenocoumarol, both alone and in combination with E7070 are given in Table 4A. Plasma protein binding of E7070 in the presence of acenocoumarol is detailed in Table 4B. The plasma protein binding of acenocoumarol at 133 μM, was 97.3% without and 94.0% in the presence of 259.2 μM E7070 (Table 4A). The binding of E7070 to plasma proteins was not affected by acenocoumarol within the range of acenocoumarol concentrations tested (Table 4B).

Discussion

Oral anticoagulants are widely used in the treatment and prophylaxis of thromboembolic disease.[9,11] Their narrow therapeutic index and extensive plasma protein binding has led to numerous reports of clinically significant drug-drug interactions involving these agents. Interactions between oral anticoagulants and both cardiovascular and cholesterol lowering drugs are well documented.[9,11] These interactions can result in hypoprothrombinaemia, and to a lesser extent hyperprothrombinemia. The purpose of this study was to determine whether a pharmacokinetic interaction occurred between acenocoumarol and E7070. In three patients receiving daily oral maintenance therapy of acenocoumarol, symptoms of hypoprothrombinaemia, bleeding and/or a prolonged prothrombin time were observed following treatment with E7070. No other patients were treated with E7070 and acenocoumarol concomitantly at our institution.

Table 3. The influence of E7070 on the apparent kinetic parameters for the metabolism of racemic acenocoumarol

E7070 concentration[a]	7-hydroxy-acenocoumarol		6-hydroxy-acenocoumarol		Racemic acenocoumarol
	Km^a	$Vmax^b$	Km^a	$Vmax^b$	Cli^c
0	2.0	11.5	2.7	11.4	10.0
2.1	2.9	11.5	3.8	12.0	7.1
5.2	4.0	13.7	5.5	15.2	6.2
20.9	3.4	11.3	5.4	14.4	6.0

[a] in μmol/L
[b] in pmol/(min*mg)
[c] in μl/min*mg
Cli = intrinsic clearance, sum of Vmax/Km values of the 6- and 7-hydroxylations of racemic acenocoumarol.

Table 4A. *In vitro* plasma protein binding (%) of acenocoumarol with and without the presence of E7070. Incubations were performed in triplicate

E7070 concentration (μmol/L)	Acenocoumarol concentration (μmol/L)		
	13.3 mean ± SD	53.8 mean ± SD	133 mean ± SD
0	97.9 ± 0.4	98.1[a]	97.3 ± 0.4
2.59	97.7 ± 0.1	98.0 ± 0.5	97.1 ± 0.4
25.92	97.6 ± 0.1	97.6 ± 0.5	97.2[a]
259.2	96.1 ± 0.6	94.9 ± 0.04	94.0 ± 0.4

[a] in duplicate.

Table 4B. *In vitro* plasma protein binding (%) of E7070 (100 μg/ml) in combination with acenocoumarol. Incubations were performed in triplicate

Acenocoumarol concentration (μmol/L)	E7070 protein binding (%)
13.3	99.9[a]
53.8	99.8 ± 0.04
133	99.8 ± 0.07

[a] in duplicate.

Since E7070 is a sulphonamide derivative, a pharmacokinetic drug-drug interaction was anticipated because several pharmacokinetic interactions between coumarin derivatives and sulphonamides, e.g. co-trimoxazole, have been reported previously.[9,11] These drug-drug interactions include both displacement of acenocoumarol from plasma protein binding sites and inhibition of acenocoumarol metabolism.[9,11]

Acenocoumarol belongs to the group of coumarin derivatives including warfarin and phenprocoumon, which exist as two enantiomers.[7] The elimination half-life of acenocoumarol is 3 to 9 hours and its duration of action following a single oral administration is 48 to 72 hours.[7,16] In our study, the half-lives of acenocoumarol in patients without E7070 were longer than the reported half-life of acenocoumarol in the literature. In both patients the AUC_{3-24h} of acenocoumarol was increased following E7070. This can be attributed to a combined increase of the Cmax and a lower clearance in one patient, and a decreased clearance in the other patient. The results of our experiments indicate the increase in acenocoumarol AUC in both patients following E7070 co-administration is probably caused by a reduction in metabolic clearance specifically the hydroxylation of acenocoumarol to 7- and 6-hydroxy-acenocoumarol by CYP2C9 (Table 3).[17] Previous studies have demonstrated that E7070 is a potential inhibitor of CYP2C9 and our results suggest that this is the most likely explanation for the interaction reported here. A further potentiation of acenocoumarol may also result from a decrease in its plasma protein binding following displacement by E7070 (Table 4A). Our experiments show that the plasma protein binding of acenocoumarol is reduced in plasma spiked with a high concentration E7070 (259 µM), whereas the inhibitory effect of E7070 on the acenocoumarol metabolism is evident at concentrations as low as 2.1 µM. Consequently, the effect of E7070 on the metabolism of acenocoumarol may be of more relevance than the effect of E7070 on the acenocoumarol protein binding in plasma.

In Table 1 the concomitant treatment during the E7070 administration of the patients is detailed. In the literature, no pharmacokinetic interactions between acenocoumarol and any of the listed medications have been reported other than oral contraceptives.[9,11] In twelve women treated with acenocoumarol, withdrawal of oral contraceptives resulted in a reduction in anticoagulant activity.[11] In contrast, it has been reported that oral contraceptives can increase the clearance of phenprocoumon, and may produce hyperprothrombinemia when used simultaneously with warfarin.[9,11] Although none of the concomitant medication is known to interact specifically with acenocoumarol several of the agents listed in Table 1 have been reported to alter the disposition of coumarin anticoagulants. Paracetamol has been shown to prolong the prothrombin time when administered concomitantly with warfarin although the mechanism of this interaction has yet to be defined.[9,11] A pharmacokinetic interaction between phenprocoumon and metoprolol has been reported possibly caused by the displacement of phenprocoumon from its plasma protein binding sites by metoprolol.[11] Nonsteroidal anti-inflammatory drugs including indomethacin,

ketoprofen, piroxicam, sulindac, and topical methylsalicylate ointment, can interact with warfarin causing an increased anticoagulant effect.[9] Consequently, a pharmacodynamic interaction between acenocoumarol and meloxicam may have contributed to the bleeding reported in patient #1. The other drugs listed in Table 1 have not been reported to interact with coumarin anticoagulants. All listed drugs were used prior to the start of the E7070 infusions, and no prior symptoms of hypoprothrombinaemia were observed in the period following the start of the co-medication and before receiving E7070. Thus, it is likely that the increased acenocoumarol-induced anticoagulation is due to E7070 rather than existing medication.

As part of the phase I program a group of patients with advanced cancer received E7070 administered as a continuous infusion for five days at another European institution[18]. Two of these patients were receiving oral maintenance therapy with acenocoumarol. Neither of these patients experienced an increase in prothrombin time or exhibited clinical evidence of a bleeding tendency. No changes in the dose of anticoagulants given to these patients were required. This pattern of administration achieved significantly lower peak concentrations than a single dose given every three weeks. This suggests that any interaction between E7070 and oral acenocoumarin is schedule dependent and may only occur at relatively high concentrations of the drug. Despite protocol warnings a further patient with non-small cell lung cancer who was receiving chronic therapy with phenprocoumon was inappropriately entered into a phase II study of E7070 administered at a dose of 700 mg/m² as a 1-hour iv infusion repeated every 3 weeks. No adverse events were reported nor was the dose of phenprocoumon altered. It is thus possible that the interaction between E7070 and acenocoumarol is more marked than with other anticoagulants of this class.

In conclusion, E7070 appears to increase the anticoagulant effect of acenocoumarol. This effect may be caused by a pharmacokinetic interaction between the two drugs. Limited pharmacokinetic data for acenocoumarol from two patients offer some support for this assertion. Data from *in vitro* investigations presented here suggest that a pharmacokinetic interaction is likely, with the probable primary mechanism for the interaction being an inhibitory effect of E7070 on the hepatic hydroxylation of acenocoumarol. Displacement of acenocoumarol from its plasma protein binding sites might also play a role. For practical purposes, patients who are receiving coumarin anticoagulants should either undergo intense monitoring of their prothrombin time or change to heparin anticoagulants upon starting therapy with E7070.

References

1. Owa T, Okauchi T, Yoshimatsu K, et al. A focused compound library of novel *N*-(7-indolyl)be nzenesulfonamides for the discovery of potent cell cycle inhibitors. Bioorg Med Chem Letters 2000;10:1223-1226.
2. Owa T, Yoshino H, Okauchi T, et al. Discovery of novel antitumor sulfonamides targeting G1 phase of the cell cycle. J Med Chem 1999;42:3789-3799.
3. Lundberg AS, Weinberg RA. Control of the cell cycle and apoptosis. Eur J Cancer 1999;35:1886-1894.
4. Punt CJA, Fumoleau P, van de Walle B, et al. Phase I and pharmacokinetic study of E7070, a novel sulphonamide, given at a daily times five schedule in patients with solid tumours. A study by the EORTC-early clinical studies group (ECSG). Ann Oncol 2001;12:1289-1293.
5. Raymond E, Fumoleau P, Roche H, et al. Combined results of 4 phase I and pharmacokinetic (PK) studies of E7070, a novel chloroindolyl-sulphonamide inhibiting the activation of cdk2 and cyclin E. Clin Cancer Res 2000;40:384 (abstract).
6. van Kesteren Ch, Mathôt R, Raymond E, et al. Population pharmacokinetics of the novel anti-cancer agent E7070 during four phase I studies: model building and validation. J Clin Oncol *in press*.
7. Godbillon J, Richard J, Gerardin A, et al. Pharmacokinetics of the enantiomers of acenocoumarol in man. Br J Clin Pharmacol 1981;12:621-629.
8. Thijssen HH, Flinois J, Beaune PH. Cytochrome P4502C9 is the principal catalyst of racemic acenocoumarol hydroxylation reactions in human liver microsomes. Drug Metab Dispos 2000;28:1284-1290.
9. Freedman MD, Olatidoye AG. Clinically significant drug interactions with the oral anticoagulants. Drug Safety 1994;10:381-394.
10. Hermans JJR, Thijssen HHW. Human liver microsomal metabolism of the enantiomers of warfarin and acenocoumarol: P450 isozyme diversity determines the differences in their pharmacokinetics. Br J Pharmacol. 1993;110:482-490.
11. Harder S, Thürmann. Clinically important drug interactions with anticoagulants. Clin Pharmacokinet 1996;30:417-444.
12. Miners JO, Birkett DJ. Cytochrome P4501C9: an enzyme of major importance in human drug metabolism. Br J Clin Pharmacol 1998;45:525-538.
13. van den Bongard HJGD, Pluim D, Rosing H, et al. An excretion balance and pharmacokinetic study of the novel anticancer agent E7070 in cancer patients. Anti-Cancer Drugs 2002;13:1-8.
14. Thijssen HHW, Baars LG, Reijnders MJ. Analysis of acenocoumarin and its amino and acetamido metabolites in body fluids by high-performance liquid chromatography. J Chrom 1983;274:231-238.
15. Eckman MH, Levine HJ, Pauker SG. Effect of laboratory variation in the prothrombin time ratio on the results of oral anticoagulant therapy. New England J Med 1993;329:696-702.
16. Thijssen HHW, Baars LG. Active metabolites of acenocoumarol: do they contribute to the therapeutic effect? Br J Clin Pharmacol 1983;16:491-496.
17. Kohl C, Steinkellner M. Prediction of pharmacokinetic drug/drug interactions from in vitro data: interactions of the nonsteroidal anti-inflammatory drug lornoxicam with oral anticoagulants. Drug Metab Dispos 2000;28:161-168.
18. Droz J-P, Roche H, Zanetta S, et al. Phase I trial of five-days continuous infusion E7070 [N(3-Chloro 7 indolyl) – 1,4, benzene-disulfonamide] in patients with solid tumours. Proc Am Assoc Cancer Res 2000;41;3876 (abstract).

Methotrexate

3

Chapter 3.1

Successful rescue with leucovorin and thymidine in a patient with high-dose methotrexate induced acute renal failure

HJG Desirée van den Bongard, Ron AA Mathôt, Willem Boogerd, Jan H Schornagel, Marcel Soesan, Jan HM Schellens and Jos H Beijnen

Summary

A 54-year old patient with primary cerebral lymphoma was treated with two 4-weekly cycles of high-dose intravenous cytarabine (12 g/m^2) and methotrexate (3 g/m^2). The administration of the first course proceeded without notable complications. Before the administration of methotrexate in the second cycle blood cell counts and chemistry showed no abnormalities except for slightly increased alkaline phosphatase and gamma-glutamyl-transpeptidase (GGT) levels which was attributed to diphantoin comedication. The patient developed symptoms of acute renal failure 7 hours after methotrexate infusion which resulted in a very high serum methotrexate level (39.8 µmol/L) at 20 hours after infusion. Rescue therapy was intensified: leucovorin dosage was increased (1200 mg continuous iv infusion every 24 hours) and combined with thymidine rescue therapy (8 g/m^2 per day continuous iv infusion every 24 hours). Urine alkalisation was increased and diphantoin therapy was stopped. Leucovorin eye drops and mouth washes were started 5 days after methotrexate administration to prevent conjunctivitis and mucositis as a result of high methotrexate levels (>2.4 µmol/L). In spite of the fact that serum methotrexate levels remained persistently higher than 0.1 µmol/L for 12 days, the patient experienced no further short-term systemic toxicity except for anaemia (grade 3 according to NCI Common Toxicity Criteria). After day 12 intensified rescue therapy and the frequency of alkalisation were decreased to standard procedures and stopped on day 19. It is concluded that iv administration with high-dose methotrexate can result in unpredictable acute toxicity. In our patient, acute methotrexate toxicity was treated successfully by intensification of classical leucovorin rescue therapy in combination with thymidine infusion. In addition, leucovorin mouth washes and eye drops may have prevented mucositis and conjunctivitis, respectively.

Introduction

High-dose methotrexate administered as an intravenous (iv) infusion is used to treat a variety of malignancies in single or combination therapy. Methotrexate belongs to the group of antimetabolites. It binds to and inhibits dihydrofolate reductase (DHFR) in the cytoplasm leading to intracellular depletion of reduced folates. Inhibition of thymidylate and *de novo* purine synthesis occur resulting in decreased RNA and DNA synthesis as a function of both extracellular methotrexate level and the duration of exposure.[1,2] The pharmacokinetics of methotrexate vary considerably among patients mainly due to high interindividual variation in renal excretion of methotrexate and its metabolite 7-hydroxy-methotrexate.[2,3] Administration of high-dose methotrexate may result in acute renal failure possibly due to precipitation of methotrexate and/or 7-hydroxy-methotrexate in the renal tubules, especially when the urinary pH is <7.0. This nephrotoxicity leads to delayed methotrexate elimination, and consequently to toxicities including myelosuppression, gastrointestinal toxicity, dermatitis, hepatitis and/or mucositis.[1,2] In order to prevent (lethal) methotrexate toxicity the patient is vigorously hydrated and alkalinised to enhance the solubility and excretion of the drug in the urine. Standard leucovorin therapy has to be initiated within 24 hours of methotrexate infusion to rescue the systemic organs. Leucovorin (N_5-formyl-FH_4), the biochemical antidote of methotrexate, replenishes tetrahydrofolate (FH_4). Serum methotrexate levels above 0.1 µmol/L at 48 hours after iv drug administration are considered to be toxic and require higher doses and/or a sustained period of leucovorin (D,L diastereomers) rescue therapy due to the short half-life of the L-diastereomers.[4-6] Alternative rescue therapy may comprise thymidine administration which restores the intracellular thymidylate pool, and can be combined with leucovorin in patients with toxic serum methotrexate levels. It must be administered in high doses by continuous infusion due to its rapid clearance.[7-10] Rescue therapy may also comprise carboxypeptidase G (CPDG) which decreases extracellular methotrexate concentrations by cleaving it to the inactive metabolites glutamate and 4-deoxy-4-amino-N_{10}-methylpteroic acid (DAMPA). Extrarenal methods, e.g. haemodialysis, haemoperfusion, and haemodiafiltration have also been investigated.[11-21]

In the current report, we describe a patient who developed unpredictable acute renal failure after iv administration of high-dose methotrexate despite adequate hydration, pre-alkalisation of the urine, and standard leucovorin rescue therapy. Despite high serum methotrexate levels over a long period, the patient experienced no further short-term toxicity as a consequence of intensification of intracellular rescue therapy comprising leucovorin in combination with thymidine infusion.

Patient and methods

Case history

A 54-year-old patient with primary cerebral lymphoma was treated with high-dose chemotherapy. Previously the diagnosis had been confirmed by resection of an occipital

parenchymal lesion. Chemotherapy consisted of two 4-weekly courses of cytarabine given as a 2-hour iv infusion every 12 hours (2 g/m² twice daily, days 1 to 3), and methotrexate as a 1-hour iv infusion (3 g/m², day 21) together with dexamethasone (days 1-15) and leucovorin rescue therapy (first administration 30 mg iv then 30 mg orally every 6 hours) beginning 24 hours after the start of infusion until the serum methotrexate level was below 0.1 µmol/L. Both cycles of methotrexate were preceded by iv fluid hydration, and urine alkalisation with sodium bicarbonate tablets (1 g orally every 6 hours).

Prior to methotrexate infusion, blood cell counts, serum creatinine, and urea nitrogen level were within normal limits. Only hepatic enzymes were elevated before both methotrexate infusions. Serum alanine-amino transferase (ALT) and alkaline phosphatase levels were 45 U/L (upper limit of normal (ULN), 21 U/L) and 130 U/L (ULN 124 U/L), respectively. Before the second infusion, alkaline phosphatase and gamma-glutamyl-transpeptidase (GGT) levels were 149 and 235 U/L (ULN 25 U/L) which was attributed to concomitant diphantoin medication (150 mg orally twice daily). Before and during infusion of methotrexate urinary pH and fluid balance were monitored. After the first administration, the serum methotrexate levels were determined at 24, 48 and 72 hours by fluorescence polarization immunoassay (FPIA). Corresponding values were 0.8, 0.090, and 0.060 µmol/L. Creatinine levels and blood cell counts were monitored during both cycles. The first cycle was complicated by grade 3 (NCI Common Toxicity Criteria) neutropenia (nadir day 11) and grade 4 thrombocytopenia (nadir day 11). Thrombocytopenia was treated with platelet transfusions. On day 15 the patient developed neutropenic fever which was treated with iv antibiotics (Penicillin 1 MU every 4 h). Furthermore, a mild transient dermatitis was noted two days after the first methotrexate infusion.

After the second course of cytarabine the patient developed grade 3 neutropenia (nadir day 10) without fever, grade 2 anaemia (nadirs day 1 and day 12; probably due to the first course) and grade 4 thrombocytopenia (nadir day 12) which were treated with red blood cell and platelet transfusions. During the 7 hours following the second infusion of methotrexate the patient developed abdominal cramps with fever (38.7°C) and later dyspnoea, coughing and a urinary pH of 6.5. Abdominal X-ray and ultrasonography showed no abnormalities, and chest radiography revealed pleural effusion on both sides and signs of interstitial congestion. Treatment with iv antibiotics (imipenem 500 mg every 6 hours) and diuretics (furosemide 80 mg every 24 hours) was started.

The next day (day 1) the serum creatinine level had increased from 87 to 281 µmol/L (Figure 1). The serum methotrexate concentration was 39.8 µmol/L at 20 hours after the start of the infusion. Acute renal failure was diagnosed and treated with increased leucovorin rescue therapy of 1200 mg every 24 hours as a continuous iv administration. Furthermore, alkalisation was intensified (100 ml sodium bicarbonate 8.4% iv every 4 hours), and diphantoin comedication was stopped. Serum methotrexate levels were determined daily (Figure 1). The serum creatinine level was 423 µmol/L (maximum) 3 days after methotrexate

Figure 1. Serum concentration-time profiles obtained during two 4-week courses of methotrexate
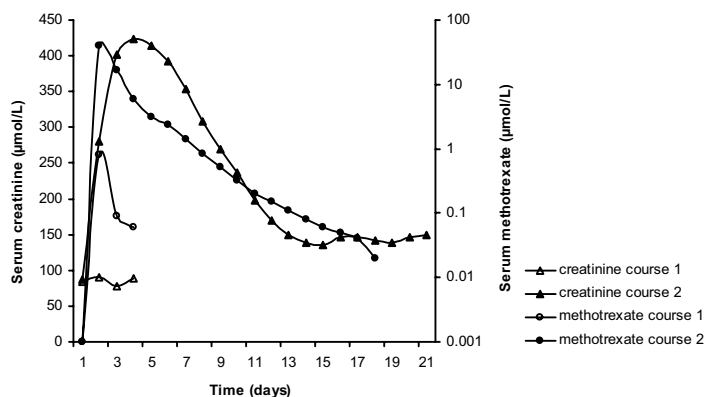
administration and a continuous infused thymidine rescue therapy (8 g/m^2 per 24 hours) was started in addition. On day 5 the serum methotrexate levels remained around 2.40 µmol/L. Leucovorin eye drops (0.03%, three drops every 6 hours) and leucovorin mouth washes with swallowing (30 mg every 6 hours) were started to prevent conjunctivitis and mucositis.

The serum level was 0.150 µmol/L at 11 days after methotrexate administration. The leucovorin dosage was then reduced to 600 mg every 24 hours, and the thymidine dosage to 5 g/m^2 every 24 hours. On day 13 the serum drug level was 0.080 µmol/L, so the leucovorin dosage was further reduced to 300 mg every 24 hours and thymidine to 2.5 g/m^2 every 24 hours, and the alkalisation frequency was decreased (200 ml sodium bicarbonate 8.4 % iv every 24 hours). The patient developed grade 3 anaemia (nadir day 12 after methotrexate infusion; probably due to the first course) which was treated with red blood cell transfusion. In comparison with course one, the methotrexate half-life was increased from 13 hours (days 0-3) to 32 hours (days 0-13). Serum methotrexate and creatinine concentrations were decreased to <0.020 µmol/L and 147 µmol/L, respectively, at 17 days after administration. On day 19 serum hepatic enzymes levels were normal and alkalisation of urine, and leucovorin and thymidine rescues were stopped. The patient was discharged 21 days after iv high-dose methotrexate administration. According to the treatment protocol whole brain radiation therapy (17 x 1.8 Gy) was given 1 month after the second course of chemotherapy with a surdosage (8 x 1.8 Gy). Complete remission of lymphoma was achieved that persisted for three years. Unfortunately, the patient suffered from impairment of cognitive functioning which seriously affected the quality of life.

Methods

Leucovorin (HPS, Zaandam, The Netherlands) 1.2 g was added with aseptic filtration to 500 ml of saline for iv infusion. Fifteen g of thymidine (Sigma Chemical Co., St. Louis, Mo.)

was added with aseptic filtration to 1000 ml saline for iv infusion. Quality control of both agents was performed by standard laboratory procedures in the laboratory of the hospital pharmacy.

A medline literature search was performed to find other cases using the following search items: high-dose methotrexate, toxicity, pharmacokinetics, leucovorin, thymidine, carboxypeptidase G_2, hemodialysis, hemoperfusion, hemodiafiltration, and plasma perfusion.

Results and discussion

Treatment with high-dose methotrexate may result in unpredictable acute toxicity despite hydration, alkalisation of urine, and rescue therapy. Patients who are not sufficiently hydrated and/or have a urinary pH < 7.0 are at increased risk for development of renal dysfunction. Decreased renal excretion may then lead to more severe toxicity. Intensified hydration and alkalisation of urine may decrease the risk of methotrexate toxicity in these patients. Each patient's creatinine clearance, hydration status and urinary pH has to be known prior to drug administration. Furthermore, serum methotrexate levels have to be carefully monitored and standard leucovorin rescue therapy has to be initiated within 24 hours after the methotrexate infusion. In general, in patients with serum methotrexate levels exceeding 0.1 µmol/L 48 hours after drug administration and/or acute drug-induced toxicity the rescue therapy needs to be intensified. Leucovorin rescue therapy alone may not prevent acute methotrexate toxicity in serum concentrations exceeding 10 µmol/L.[20,22] Our literature search yields a large number of reports on pharmacological research and clinical aspects of methotrexate administration and its rescue therapy.[4,5,7-9,11,13-21,23] In our patient leucovorin rescue therapy was intensified by continuous iv administration in combination with leucovorin mouth washes and eye drops. On day 3, the intracellular rescue was intensified by continuous thymidine infusion since the serum methotrexate concentration persisted at a toxic level (6.0 µmol/L) together with a high serum creatinine level (423 µmol/L). Alternative rescue therapy including CPDG and extrarenal procedures, e.g. haemodialysis were not used because these methods only lower the extracellular methotrexate concentration. Moreover, extrarenal methods result in transient decreases in extracellular methotrexate concentration which necessitates repeated and/or combined use of haemodialysis, haemoperfusion and haemodiafiltration to efficiently lower methotrexate concentration.[12,14,17,24] In our patient acute renal failure occurred unexpectedly after administration of the second cycle of high-dose methotrexate. This might be attributable to the urinary pH of 6.5 at a certain time which decreases the solubilities of methotrexate and in particular 7-hydroxy-methotrexate and can result in tubular epithelial damage. Interaction of methotrexate with diphantoin and antibiotics may have decreased the plasma protein binding of methotrexate. All these factors may have contributed to higher free methotrexate levels and renal toxicity. Furthermore,

the presence of a third compartment (pleural effusion) may have contributed to the long-term high serum methotrexate concentrations due to the retarded distribution in and from extravascular fluid accumulations.[1,2]

In conclusion, high dose methotrexate-induced acute severe renal failure was followed by high serum methotrexate levels during a long period of 12 days. Intensification of the leukovorin rescue therapy, administration of thymidine, increased frequency of alkalisation, and cessation of diphantoin therapy was sufficient to prevent further toxicity. Renal clearance improved and serum methotrexate levels decreased to nontoxic levels, and no additional extracellular rescue therapy was needed to prevent further short-term toxicity. It should be noted that the observed loss of the cognitive function in our patient may be related to the prolonged high serum methotrexate concentration in combination with whole-brain radiotherapy. Nevertheless, there is as yet no defined schedule and optimal dosage of rescue therapy in patients with high methotrexate serum concentrations. We would recommend intensification of leucovorin rescue therapy by continuous infusion, eye drops and mouth washes in combination with continuous administration of thymidine to prevent methotrexate toxicity in these patients.

References

1. Crom W. Methotrexate and other antifolates. In: Grochow LB, Ames MM, editors. A clinician's guide to chemotherapy pharmacokinetics and pharmacodynamics. Baltimore: Williams and Wilkins Baltimore 1998.
2. Schornagel JH, McVie JG. The clinical pharmacology of methotrexate. Cancer Treat Rev 1983;10: 53-75.
3. Powis G. Effect of human renal and hepatic disease on the pharmacokinetics of anticancer drugs. Cancer Treat Rev 1982;9:85-124.
4. Decker DA, Edmonson JH, Gilchrist GS, et al. High-dose methotrexate with a safe rescue program. Oncology 1981;38:262-264.
5. Flombaum CD, Meyers PA. High-dose leucovorin as sole therapy for methotrexate toxicity. J Clin Oncol 1999;17:1589-1594.
6. Wolfrom C, Hepp R, Hartmann R, et al. Pharmacokinetic study of methotrexate, folinic acid and their serum metabolites in children treated with high-dose methotrexate and leucovorin rescue. Eur J Clin Pharmacol 1990;39:377-383.
7. Abelson HT, Fosburg MT, Beardsley PG, et al. Methotrexate-induced renal impairment: clinical studies and rescue from systemic toxicity with high-dose leucovorin and thymidine. J Clin Oncol 1983;1:208-216.
8. Grem JL, King SA, Sorensen JM, et al. Clinical use of thymidine as a rescue agent from methotrexate toxicity. Invest New Drugs 1991;9:281-290.
9. Howell SB, Ensminger WD, Krishan A, et al. Thymidine rescue of high-dose methotrexate in humans. Cancer Res 1978;38:325-330.
10. Howell SB, Krishan A, Frei E. Cytokinetic comparison of thymidine and leucovorin rescue of marrow in humans after exposure to high-dose methotrexate. Cancer Res 1979;39:1315-1320.
11. DeAngelis LM, Tong WP, Lin S, et al. Carboxypeptidase G_2 rescue after high-dose methotrexate. J Clin Oncol 1996;14:2145-2149.
12. Grimes DJ, Bowles MR, Buttsworth JA, et al. Survival after unexpected high serum methotrexate concentrations in a patient with osteogenic sarcoma. Drug Safety 1990;5:447-454.
13. Hum M, Kamen BA. Successful carboxypeptidase G_2 rescue in delayed methotrexate-elimination due to renal failure. Pediatr Hematol Oncol 1995;12:521-524.
14. Jambou P, Levraut J, Favier C, et al. Removal of methotrexate by continuous venovenous hemodiafiltration. Contrib Nephrol 1995;116:48-52.
15. Kepka L, De Lassence A, Ribrag V, et al. Successful rescue in a patient with high dose methotrexate-induced nephrotoxicity and acute renal failure. Leuk Lymphoma 1998;29:205-209.
16. Molina R, Fabian C, Cowley B. Use of charcoal hemoperfusion with sequential hemodialysis to reduce serum methotrexate levels in a patient with acute renal insufficiency. Am J Med 1987;82: 350-352.
17. Relling MV, Stapleton BF, Ochs J, et al. Removal of methotrexate, leucovorin, and their metabolites by combined hemodialysis and hemoperfusion. Cancer 1988;62:884-888.
18. Wall SM, Johansen MJ, Molony DA, et al. Effective clearance of methotrexate using high-flux hemodialysis membranes. Am J Kidney Dis 1996;28:846-854.
19. Widemann BC, Hetherington ML, Murphy RF, et al. Carboxypeptidase-G_2 rescue in a patient with high-dose methotrexate-induced nephrotoxicity. Cancer 1995;76:521-526.
20. Widemann BC, Balis FM, Murphy RF, et al. Carboxypeptidase-G_2, thymidine, and leucovorin rescue in cancer patients with methotrexate-induced renal dysfunction. J Clin Oncol 1997;15: 2125-2134.
21. Zoubek A, Zaunschirm HA, Lion T, et al. Successful carboxypeptidase G_2 rescue in delayed methotrexate elimination due to renal failure. Pediatr Hematol Oncol 1995;12:471-477.
22. Relling MV, Fairclough D, Ayers D, et al. Patient characteristics associated with high-risk methotrexate concentrations and toxicity. J Clin Oncol 1994;12:1667-1672.
23. Bertino JR. "Rescue" techniques in cancer chemotherapy: use of leucovorin and other rescue agents after methotrexate treatment. Semin Oncol 1977;4:203-216.
24. Howell SB, Blair HE, Uren J, et al. Hemodialysis and enzymatic cleavage of methotrexate in man. Eur J Cancer 1978;14:787-792.

Chapter 3.2

Population pharmacokinetics of methotrexate and its major metabolite 7-hydroxy-methotrexate in cancer patients treated with high-dose methotrexate

HJG Desirée van den Bongard, Alwin DR Huitema, Olaf van Tellingen, Paul Baas, Jan H Schornagel, Jan HM Schellens and Jos H Beijnen

Summary

An integrated population pharmacokinetic model for methotrexate and 7-hydroxy-methotrexate was developed to study the influence of demographic factors, biochemical parameters and use of concomitant medication, on the pharmacokinetic parameters of both compounds. Serum concentration-time data of methotrexate and its 7-hydroxy metabolite from 76 patients (308 courses) treated with high-dose methotrexate (400 mg-12,000 mg/m²) were simultaneously fitted to selected pharmacokinetic models using non-linear mixed-effect modelling (NONMEM). The influence of several covariates on the pharmacokinetics of both compounds was investigated. Furthermore, the pharmacokinetics of methotrexate and 7-hydroxy-methotrexate in 4 patients (7 courses) with pleural effusion and a pleural drain were studied.

The data were best described using an integrated 3-compartment model for methotrexate and a 2-compartment model for 7-hydroxy-methotrexate with first-order elimination from the central compartment and the central metabolite compartment, respectively. The investigated covariates had no significant influence on the pharmacokinetics of both compounds.

The maximal concentration of 7-hydroxy-methotrexate was lower compared to that of methotrexate, and the elimination of the metabolite was slower than that of the parent compound. The methotrexate fraction that diffused to pleural effusion ranged from 0.00019% to 0.13% of the administered dose. In conclusion, the integrated population model could accurately describe the pharmacokinetic parameters of methotrexate and 7-hydroxy-methotrexate. This population model may aid further research to elucidate the relationship between the pharmacokinetics of both compounds and their induced toxicity and drug-drug interactions.

Introduction

High-dose methotrexate is used in combination chemotherapy schemes in the treatment of osteosarcoma, certain non-Hodgkin lymphomas (NHL), acute lymphocytic leukaemia (ALL) and malignant mesothelioma.[1-4] Its elimination occurs by renal excretion consisting of glomerular filtration and concentration dependent tubular reabsorption and secretion.[1,2] Methotrexate is primarily converted to 7-hydroxy-methotrexate by the hepatic enzyme aldehyde oxidase. The conversion shows interpatient variability due to variations in the amount of aldehyde oxidase present.[2,5] Both compounds show first-order kinetics.[1,2,6-12] The elimination of 7-hydroxy-methotrexate, however, is slower than that of the parent compound resulting in higher 7-hydroxy-methotrexate concentrations than methotrexate at later time-points after drug infusion.[6,7]

The pharmacokinetics of methotrexate and 7-hydroxy-methotrexate vary considerably among patients.[2,6,7] The elimination of methotrexate is prolonged in patients with renal dysfunction or third space collections of fluid, i.e. pleural effusion or ascites, due to the delayed distribution in and from these extravascular fluid accumulations.[1-3] The methotrexate concentrations are routinely monitored clinically, to identify patients at high risk for developing significant toxicity after intravenous high-dose methotrexate administration. Several normograms based on the elimination of methotrexate from serum are clinically used to identify the patients at high risk for toxicity. These normograms vary in the serum concentrations and time-points that are used to determine when to intensify the rescue therapy to prevent or minimise toxicity.[3,13]

Methotrexate and 7-hydroxy-methotrexate can both cause renal and hepatic toxicity.[14-16] Precipitation of 7-hydroxy-methotrexate in renal tubuli at low urinary pH values is thought to be the mechanism responsible for the nephrotoxicity of high-dose methotrexate.[6,7,16] The hydroxylated metabolite can reduce the cellular uptake of methotrexate by interference with membrane transport but it can also increase the efflux of methotrexate from cells.[17,18] Several drug-dug interactions have been reported for methotrexate. Drugs including non-steroidal anti-inflammatory drugs (NSAIDs), salicylates, sulphonamides, penicillin, gastric hydrogen pump inhibitors and probenecid can increase the exposure to methotrexate.[19-26] Moreover, naproxen and pantoprazole may inhibit the 7-hydroxy-methotrexate clearance.[27-29]

The aim of this study was to develop an integrated population pharmacokinetic model of 7-hydroxy-methotrexate and methotrexate and to study the influence of demographic factors, biochemical parameters and use of concomitant medication, on the pharmacokinetic parameters of both compounds. In addition, the pharmacokinetic behaviour of both compounds was studied in pleural effusion in patients with a pleural drain, after the administration of high-dose methotrexate. The presented model may aid further optimisation of methotrexate therapy to increase the drug's efficacy and to minimise its toxicity.

Materials and methods

Patient population and data collection

Data were obtained from cancer patients treated with methotrexate as single agent or in combination chemotherapy in various treatment schedules between November 1994 until October 2001. In all these courses methotrexate was administered intravenously. A part of the patient population consisted of patients with malignant mesothelioma who were included in a phase II study that consisted of treatment with methotrexate (fixed dose of 3000 mg 3-hour iv inf) as single agent or in combination with doxorubicin (fixed dose 40 mg iv bolus inf every 2 weeks). All patients gave informed consent and the study protocol was approved by the Medical Ethics Committee of the Institute. The toxicity and efficacy results of this treatment schedule in malignant mesothelioma patients will be published elsewhere. The other part of the patients was treated with methotrexate as implemented in regular treatment schedules, e.g. for NHL, ALL and osteosarcoma.

Each course consisted of prehydration and urine alkalisation with sodium bicarbonate 1.4% administered orally and iv. Methotrexate administration was not started until the urinary pH of the patient was higher than 7. If the urinary pH remained $\leq$ 7, prehydration had to be continued with 500 ml sodium bicarbonate 1.4% (administered iv in 1 hour). Methotrexate was dissolved in 1000 ml sodium chloride 0.9%, followed by a continuous iv infusion of sodium chloride 0.45%/glucose 2.5% during 22 hours. Hydration and alkalisation were continued for 3 days with 4 x daily 1 gram of sodium bicarbonate in capsules. Briefly, inclusion criteria included sufficient blood cell counts (leukocytes $\geq 4.0 * 10^6$/L, granulocytes $\geq 2.0 * 10^6$/L, platelets $\geq 100 * 10^6$/L) and normal renal (serum creatinine < 120 µmol/L) and liver function/enzymes (serum bilirubin < 25 µmol/L), performance status according to the World Health Organisation (PS) $\leq$ 2.

Twenty-four hours after the start of the methotrexate infusion leucovorin rescue therapy was started (15 mg every 6 hours po). In each patient, routine 24- and 48-hour blood samples were collected after the start of the methotrexate infusion. If the serum drug concentration was < 0.04 µmol/L, the leucovorin therapy was discontinued, if the serum drug concentration was > 0.04 µmol/L and < 0.1 µmol/L, the leucovorin therapy was continued for another 24 hours (15 mg every 6 hours po). If the serum drug concentration was $\geq$ 0.1 µmol/L at 48 hours, the blood sampling was continued in combination with intensification of the rescue therapy until the serum drug concentration was below 0.1 µmol/L. Additional blood samples were obtained at the following time-points: before the start of the methotrexate infusion, at the end of the methotrexate infusion, 2 and 4 hours after the end of the infusion. Each blood sample was collected in serum tubes (5 ml). Blood was allowed to clot at room temperature (20 min) and then centrifuged at 1600 *g* for 5 minutes. Serum was stored at –20°C until analysis.

In patients with pleural effusion and a pleural drain, pleural effusion samples were obtained before the start of the methotrexate infusion, at 3 hours after the end of the methotrexate

infusion, and at 24 and 48 hours after the end of the infusion. Pleural effusion sampling was continued every 24 hours until hospital discharge. The fraction of the administered methotrexate dose that diffused into pleural volume was calculated by multiplying the methotrexate and 7-hydroxy-methotrexate concentrations with the collected pleural volume between each concentration-time point.

Methotrexate and 7-hydroxy-methotrexate concentrations were measured in serum and pleural effusion using a validated reverse-phase high-pressure liquid chromatography (HPLC) method as published elsewhere.[30] The pre-treatment procedure of the serum samples consists of a deproteinisation method. The lower detection limit of the HPLC assay is 0.04 µmol/L for both methotrexate and 7-hydroxy-methotrexate and the between-day precision was ≤ 7.0%.[30]

Population pharmacokinetic analysis

The program NONMEM (non-linear mixed-effect modelling, version V level 1.1, double precision) using the NMTRAN pre-processor and the PREDPP package (ADVAN5), operating on an MS-DOS computer, was used for the analysis.[31] The concentration-time data of both compounds were logarithmically transformed and were simultaneously described by the pharmacokinetic models. The first order method was used in all of the analysis processes. The model building procedure consisted of a three-step approach.

Figure 1. Graphical representation of the pharmacokinetic model of methotrexate and 7- hydroxy-methotrexate. V1, V2 and V3 indicate the apparent volume of the central compartment, the first peripheral compartment and the second peripheral compartment. V4 and V5 indicate the apparent volume of the first metabolite compartment and second metabolite compartment, respectively. CLMTX and CL7-OH-MTX indicate the clearance of methotrexate and 7-hydroxy-methotrexate, respectively. k12, k21, k13, k31, k14, k45 and k54 indicate the intercompartmental rate constants
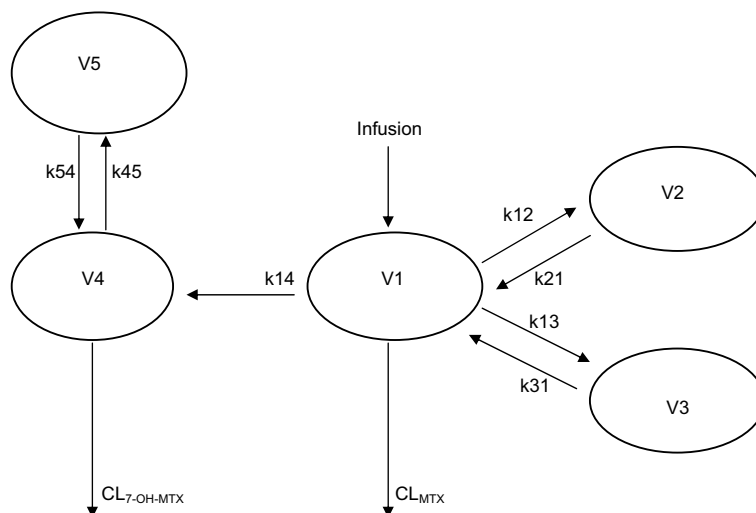
Basic population pharmacokinetic model

The first step consisted of the development of a basic population pharmacokinetic model. The methotrexate concentration-time data were best described by a linear 3-compartment model with first-order elimination from the central compartment using ADVAN 5. The 7-hydroxy-methotrexate concentration-time data were best described by a linear 2-compartment model with first-order elimination of the metabolite from this central compartment (Figure 1). The following pharmacokinetic parameters were estimated: volume of the central compartment ($V1_{MTX}$ in L), volume of the first peripheral compartment ($V2_{MTX}$ in L), volume of the second peripheral compartment ($V3_{MTX}$ in L), apparent volume of the first metabolite compartment ($V1_{7\text{-}OH\text{-}MTX}$ in L), apparent volume of the second metabolite compartment ($V2_{7\text{-}OH\text{-}MTX}$ in L), intercompartmental clearance between the central compartment and the peripheral compartments of methotrexate ($Q1_{MTX}$ and $Q2_{MTX}$ in L/h), apparent intercompartmental clearance between the first and second metabolite compartment ($Q_{7\text{-}OH\text{-}MTX}$ in L/h), clearance from the central compartment (CL_{MTX} in ml/h) and apparent clearance from the metabolite compartment ($CL_{7\text{-}OH\text{-}MTX}$ in ml/h).

Standard errors for all parameters were calculated using the COVARIANCE option in the NONMEM program. Interindividual variability in $V2_{MTX}$, CL_{MTX}, $CL_{7\text{-}OH\text{-}MTX}$, $Q2_{MTX}$ and $Q_{7\text{-}OH\text{-}MTX}$ and interoccasion variability in CL_{MTX} and $CL_{7\text{-}OH\text{-}MTX}$ were estimated using a proportional error model.

For instance, interindividual and interoccasion variability in $CL_{7\text{-}OH\text{-}MTX}$ were defined as in equation 1:

$$CL_{7\text{-}OH\text{-}MTX\ i} = CL_{7\text{-}OH\text{-}MTX,\ pop} *(1+ \eta_i^{CL7\text{-}OH\text{-}MTX} + \kappa_i^{CL7\text{-}OH\text{-}MTX}) \qquad \text{equation 1}$$

where $CL_{7\text{-}OH\text{-}MTX\ i}$ represents the $CL_{7\text{-}OH\text{-}MTX}$ of the ith individual, $CL_{7\text{-}OH\text{-}MTX,\ pop}$ is the typical population value of $CL_{7\text{-}OH\text{-}MTX}$, $\eta_i^{CL7\text{-}OH\text{-}MTX}$ is the interindividual random effect that is normally distributed with mean zero and variance ω^2, and $\kappa_i^{CL7\text{-}OH\text{-}MTX}$ is the interoccasion random effect that is normally distributed with mean zero and variance π^2.

The residual variability, i.e. the difference between the logarithmically transformed measured concentration in an individual and its respective prediction was modelled using a combined additive and proportional model.

Selection of basic models was based on the minimum value of the objective function (OFV) that is equal to minus twice the log likelihood of the data, reliability of parameter estimates (according to the standard error values of the parameters estimates), and the fit of the model to the data (goodness of fit plots). The difference in the OFV of hierarchical models, that is equal to minus twice the log likelihood of the data, approximates to a chi-squared-distribution with 1 degree of freedom. The significance level was set at $p < 0.001$, which is associated with an OFV decrease of 10.8. Furthermore, the goodness of fit plots were examined in the program Xpose (Xpose, version 2.0, Uppsala University, Sweden)

as implemented in the S-PLUS statistical package (version 2000, Mathsoft, Cambridge, Mass.).[32]

Intermediate model

The second step consisted of the individual Bayesian regression analysis. For each subject, individual pharmacokinetic parameters were calculated using the individual methotrexate and 7-hydroxy-methotrexate serum concentration-time data and the population pharmacokinetic parameter estimates obtained in the first step. The individual Bayesian estimates were plotted against the demographic factors, blood chemistry parameters and use of concomitant medication that might cause a drug-drug interaction with methotrexate (=covariates). Relevant covariates were investigated for their correlation with the pharmacokinetic parameters of both compounds (age, gender, body surface area (BSA), PS, serum creatinine, serum alanine-aminotransferase (ALT), serum aspartate-aminotransferase (AST), serum alkaline phosphatase, serum albumin, serum bilirubin and serum lactate dehydrogenase (LDH), concomitant use of medication that can interact with methotrexate and/or 7-hydroxymethotrexate, and presence of pleural effusion or ascites. The relations between the covariates and the Bayesian parameter estimates of each individual patient were investigated graphically.

The selected covariates that showed a graphical relation with a pharmacokinetic parameter were tested by univariate analysis. These covariates were entered individually into the basic population pharmacokinetic model by forward inclusion. Continuous covariates, e.g. BSA, were centred to their median values. For instance, the relationship between CL_{MTX} and BSA was described as in equation 2:

$$CL_{MTX} = \theta_2 * (1 + \theta_3 * (BSA - 1.94)) \hspace{3cm} \text{equation 2}$$

where CL_{MTX} represents the value of CL_{MTX} in L/h, θ_2 the CL_{MTX} value of a (median) patient with a BSA of 1.94 m^2, and θ_3 is the increase or decrease in CL_{MTX} per m^2 BSA difference.

Dichotomous covariates were modelled as described in equation 3:

$$V2_{MTX} = \theta_1 * \theta_2{}^{FLAG1} \hspace{4cm} \text{equation 3}$$

where $V2_{MTX}$ represents the value of $V2_{MTX}$ in L, θ_1 the $V2_{MTX}$ value in females (FLAG1 =0), and θ_2 the change in $V2_{MTX}$ in males (FLAG1=1).

The difference in the OFV was evaluated after the introduction of a covariate in the model. During the forward inclusion of the covariates in the basic model, the significance level was

set at p < 0.005 that is associated with an OFV decrease of > 7.83. All significant covariates were incorporated into an intermediate multivariate model.

Final population pharmacokinetic model

The development of the intermediate model was followed by multivariate analysis that consisted of a stepwise backward elimination procedure. Covariates retained in the model when elimination of the covariate caused an OFV increase of > 10.8 that is associated with a significance level of p < 0.001.

The validity of the interindividual variability model was checked by evaluating correlations between the individual random effects (η) of the pharmacokinetic parameters that were included in the model.

Results

Patient population and dataset

In total, concentration-time data were obtained from 76 patients (308 courses). The administered dose ranged from 400 mg to 12000 mg/m^2 and the duration of infusion ranged from a 1-hour iv infusion to a 24-hour iv infusion. The patient characteristics are summarised in Table 1. Patients with various malignancies and treatment schedules were included in the dataset: 29 patients with malignant mesothelioma, 10 of these patients were treated with methotrexate (3000 mg 3-hour iv inf) as single agent, and 19 patients were treated with methotrexate (3000 mg 3-hour iv inf) in combination with doxorubicin. Furthermore, 20 patients with esophageal/gastric carcinoma were treated with methotrexate (1500 mg/m^2 2-hour iv inf) in combination with doxorubicin and fluorouracil. Ten patients with head and neck carcinoma were treated with methotrexate as single agent (400 mg 24-hour iv inf). Patients with NHL (n=12) were treated with methotrexate (1-3 g/m^2 1 to 24-hour iv inf) in combination chemotherapy with lomustine, procarbazine and intrathecal administration of cytosine arabinoside and methotrexate. One patient with ALL was treated with methotrexate (2150 mg/m^2 24-hour iv inf), teniposide, mercaptopurine and cytosine arabinoside. One osteosarcoma patient was treated with methotrexate (12 g/m^2 6-hour iv inf) in combination with ifosfamide and etoposide. One patient with a trophoblastic tumour was treated with methotrexate (1000 mg/m^2 12-hour iv inf) in combination with etoposide, actinomycin, cyclofosfamide and vincristin. Two patients with choriocarcinoma were treated with methotrexate (300 mg/m^2 12-hour iv inf) in combination with cisplatin, etoposide, cyclofosfamide and actinomycin.

In 21 of these patients additional blood samples were taken. This part of the patient population consisted of 3 patients (malignant mesothelioma) treated with methotrexate as single agent (fixed dose of 3000 mg, 3-hour iv infusion), 16 patients (malignant mesothelioma) treated with methotrexate (fixed dose of 3000 mg) in combination with

**Table 1.** Patient characteristics and baseline values of the covariates

	Number	Median value	Range
Patient characteristics			
Male	62		
Female	14		
Age (years)		51	17-77
WHO Performance status			
0	10		
1	58		
2	8		
Body surface area (m^2)	1.94		1.56-2.45
Tumour type			
Malignant mesothelioma	29		
Esophageal/Gastric cancer	20		
Head and neck cancer	10		
Non-Hodgkin lymphoma	12		
Choriocarcinoma	2		
Acute lymphocytic leukaemia	1		
Osteosarcoma	1		
Trophoblastic tumour	1		
Pre-treatment			
None	36		
Prior chemotherapy	15		
Local radiotherapy	19		
Surgical therapy	16		
Photo-dynamic therapy	1		
Dose			400 mg-12000 mg/m^2
Biochemical parameters			
Creatinine (µmol/L)		72	32-120
Blood urea nitrogen (mmol/L)		4.0	3.0-8.0
Total bilirubin (mmol/L)		7.0	2.0-6.0
AST (U/L)		15	4-139
ALT (U/L)		19	5.0-368
Alkaline Phosphatase (U/L)		107	10-519
GGT (U/L)		56	7.0-675
Albumin (g/L)		40	22-128
LDH (U/L)		269	134-2786
Third compartment			
Pleural effusion (present/not present)[a]	12/64		
Ascites (present/not present)	3/73		

[a] Four of these patients had a pleural drain during the methotrexate infusion until hospital discharge.

doxorubicin, 1 patient (NHL) was treated with methotrexate (1000 mg/m², 3-hour iv infusion) in combination with lomustin and cytosine arabinoside, and 1 patient (gastric carcinoma) was treated with methotrexate (1500 mg/m²-hour iv infusion) in combination with fluorouracil and doxorubicin.

In total, 984 serum methotrexate and 994 serum 7-hydroxy-methotrexate concentration-time points were obtained during 308 courses. From these data, complete concentration-time curves of methotrexate and 7-hydroxy-methotrexate (206 and 204 concentration-time points, respectively) were obtained during 33 courses of intensive sampling in 21 patients. In Figure 2, these data are detailed including an additional curve that represents concentration-time data as obtained in 1 patients at 24 hour after the start of the infusion (△). The 2 upper curves (△,○) are obtained in 2 patients who died due to methotrexate (and 7-hydroxy-methotrexate) induced toxicity (stomatitis, nephrotoxicity, rash). Both patients had

Figure 2. Concentration-time curves of patients in the intensively sampled group (n=21, 33 courses) (■ and ○) for methotrexate (A) and 7-hydroxy-methotrexate (B). One of these patients showed prolonged elimination of both compounds (○). A concentration-time curve (samples are obtained from 24 hours after the methotrexate infusion) of 1 patient who showed prolonged elimination is depicted (△). All concentration-time points, as obtained after the administration of methotrexate, are depicted with the start of the administration at time zero

A.

B.
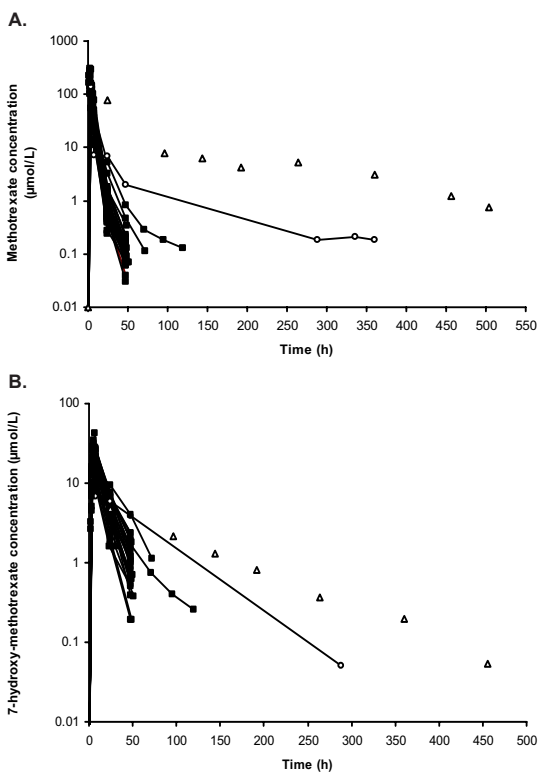
malignant mesothelioma and were treated with a fixed dose of 3000 mg of methotrexate in combination with a fixed dose of adriamycin (40 mg). One of these patients (○) developed pleural effusion after the methotrexate infusion. The other patient (△) developed ascitic fluid after the administration. In the latter patient a pneumectomy was performed in the past. Consequently, the additional lung cavity might have contributed to the development of third space fluids.

Pleural effusion samples were obtained in 4 patients (during 7 courses) with a pleural drain (in total, 36 samples). The total production of pleural volume ranged from 36 ml to 1960 ml. The methotrexate and 7-hydroxy-methotrexate concentrations in pleural effusion is depicted in Figure 3. The maximal concentration (Cmax) of 7-hydroxy-metabolite was lower than the Cmax of methotrexate (1/10 of the Cmax of methotrexate) in pleural effusion. The fraction of the administered methotrexate dose that diffused into pleural effusion

Figure 3. Methotrexate (A) and 7-hydroxy-methotrexate concentration (B) in pleural effusion in 4 patients (during 7 courses) after the administration of a fixed dose of 3000 mg. The course number of each patient is depicted between parentheses
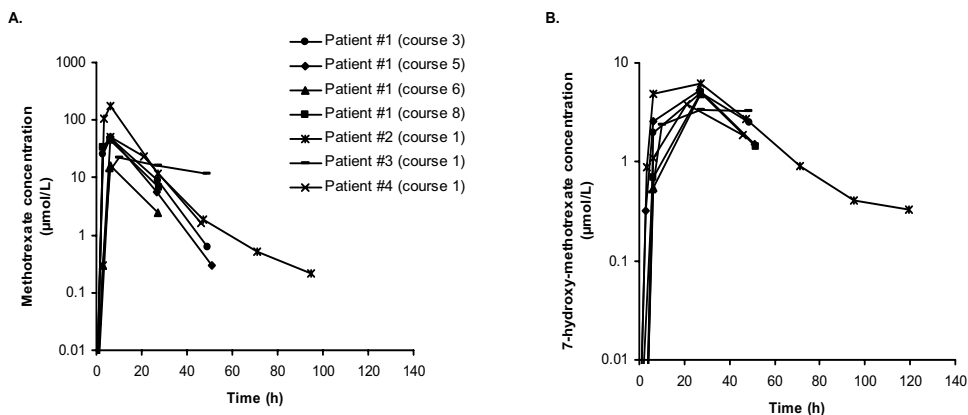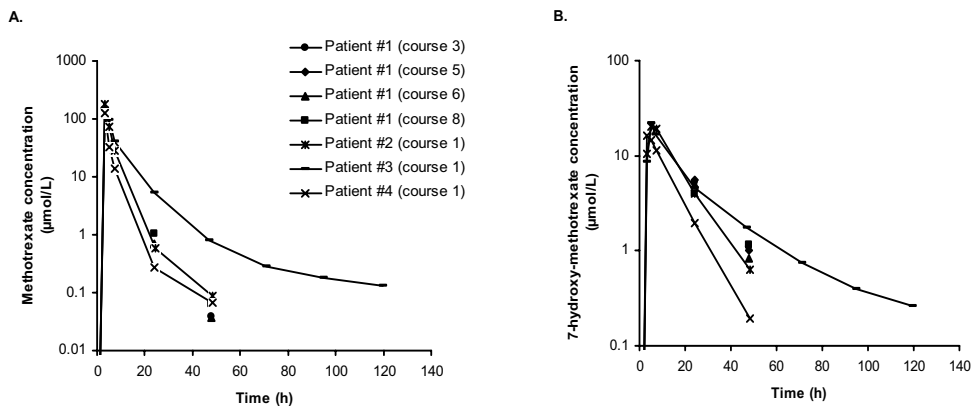

Figure 4. Methotrexate (A) and 7-hydroxy-methotrexate (B) concentrations in serum in 4 patients (during 7 courses) with pleural effusion after the administration of a fixed dose of 3000 mg

ranged from 0.00019% to 0.13 %. The serum concentrations of the 2 compounds in these patients during the same courses are depicted in Figure 4. The 7-hydroxy metabolite is rapidly formed with maximal concentrations being approximately 1/10 of the methotrexate concentrations in serum. The elimination of 7-hydroxy-methotrexate is slower than that of methotrexate in both serum and pleural effusion. The variability in serum concentrations of both compounds, however, is small compared to the high variability of pleural effusion values. In total, pleural effusion was present in 12 patients during 35 courses (Table 1). In patients (8 patients) without a pleural drain, the pleural effusion was evacuated prior to the

methotrexate administration. Ascitic fluid was present in 3 patients during 3 courses and was also evacuated prior to the methotrexate administration.

The use of concomitant medication during the methotrexate administration was as follows: 13 patients used gastric hydrogen pump inhibitors during 35 courses (dose of omeprazole ranged from 1*20 to 2*40 mg/day po and lansoprazole 60 mg/day po), 3 patients used salicylates during 7 courses (ascal 80-100 mg day po), 3 patients used NSAIDs during 6 courses (diclofenac 75-100 mg/day po), 2 patients used penicillin derivates (penicillin $6*10^6$ E/day and amoxicillin 3*625 mg/day iv), 1 patient used co-trimoxazole (2*960 mg/day po), 1 patient used phenytoin (3*150 mg/day po), 1 patient used triamterene (1*25 mg/day po). The gastric hydrogen pump inhibitors, salicylates and the NSAIDs were studied in the population analysis for their possible influence on the pharmacokinetic parameters of methotrexate and 7-hydroxy-methotrexate.

Population pharmacokinetic analysis

Basic population pharmacokinetic model

Several pharmacokinetic models were applied to the data. The first model tested consisted of 2 compartments for methotrexate and 1 compartment for 7-hydroxy-methotrexate (OFV = 987). The same model with an additional compartment for patients with pleural effusion or ascites showed a marked decrease in the OFV (ΔOFV = -16.0, p < 0.001) but the model predicted concentrations for both compounds were underestimated. Therefore, 1 compartment was added for 7-hydroxy-methotrexate which resulted again in a statistically significant decrease in OFV (ΔOFV = -39.3, p < 0.001) but the model predicted concentrations were still underestimated at high concentrations of both compounds. The model was further optimised by the addition of a third compartment for methotrexate in all patients. This resulted in an additional statistically significant decrease in OFV (ΔOFV = -177, p < 0.001). The model predicted concentrations improved and were only slightly underestimated at the maximal concentrations of methotrexate and 7-hydroxy-methotrexate.

It was assumed that the underestimation could be caused by the relatively high number of concentration-time points obtained at 24 hours and later after the methotrexate administration (625 and 635 for methotrexate and 7-hydroxy-methotrexate, respectively). The dataset comprised only 46 concentration-time points obtained between the start of the administration and before 24 hours after the start of the methotrexate administration. A model was fitted to the same population model with different residual errors for the 2 subpopulations. This resulted in a non-significant difference in OFV (ΔOFV = 0.35, p > 0.25), therefore the linear 5-compartment model was considered as the final basic model (Figure 1).

The population pharmacokinetic parameter estimates including the standard errors, the interindividual variability and the residual errors are summarised in Table 2. The pharmacokinetic parameters were estimated accurately, except for $V_{7\text{-OH-MTX}}$. The relative

standard error of this parameter was 72%. Interindividual variability was determined for CL_{MTX} (39%), $V2_{MTX}$ (65%), $Q2_{MTX}$ (34%), $CL_{7\text{-}OH\text{-}MTX}$ (37%) and $QF_{7\text{-}OH\text{-}MTX}$ (9.3%). Interoccasion variability was determined for CL_{MTX} (18%) and $CL_{7\text{-}OH\text{-}MTX}$ (17%). For methotrexate, the residual variability of the logarithmically transformed concentrations consisted of an additional error of 0.0432 and a proportional error of 0.49. For 7-hydroxy-methotrexate, the residual variability of the logarithmically transformed concentrations consisted of an additional error of 0.0515 and a proportional error of 0.68. Inclusion of interindividual or interoccasion variability on the other pharmacokinetic parameters did not result in a significant decrease in OFV value. This should not be interpreted as an absence of interindividual variability in these pharmacokinetic parameters. It indicates that the data did not contain sufficient information to estimate the interindividual and interoccasion variability of these parameters.

Finally, the correlations between the interindividual variability of CL_{MTX}, $V2_{MTX}$, $Q2_{MTX}$, $CL_{7\text{-}OH\text{-}MTX}$ and $Q_{7\text{-}OHMTX}$ were graphically evaluated. The matrix plots showed a possible positive correlation between the $\eta V2_{MTX}$ and $\eta Q2_{MTX}$ and between ηCL_{MTX} en $\eta Q2_{MTX}$ (data not shown). The inclusion of these correlations in the population model did not result in an improved fit of the model according to the standard error values and the goodness of fit plots.

Table 2. Population pharmacokinetic parameters of the final population model of methotrexate and 7-hydroxy-methotrexate

	Estimate	RSE (%)	Interindividual variability (%)	Interoccasion variability (%)
Pharmacokinetic parameters				
$V1_{MTX}$ (L)	21.3	15		
CL_{MTX} (L/h)	9.08	13	39	18
$Q1_{MTX}$ (L/h)	1.39	45		
$V2_{MTX}$ (L)	9.03	44	65	
$Q2_{MTX}$ (L/h)	0.936	28	34	
$V3_{MTX}$ (L)	513	34		
$CL_{7\text{-}OH\text{-}MTX}$ (L/h)	21.4	9.2	37	17
$V1_{7\text{-}OH\text{-}MTX}$ (L)	197	8.2		
$Q_{7\text{-}OH\text{-}MTX}$ (L/h)	4.87	15	9.3	
$V2_{7\text{-}OH\text{-}MTX}$ (L)	180	72		
Residual variability				
Proportional error$_{MTX}$	0.493	27		
Additional error$_{MTX}$	0.0432	36		
Proportional error$_{7\text{-}OH\text{-}MTX}$	0.677	14		
Additional error$_{7\text{-}OH\text{-}MTX}$	0.0515	35		

$V1_{MTX}$ = Volume of the central compartment of methotrexate; CL_{MTX} = Clearance of methotrexate from the central compartment; $V2_{MTX}$ = Volume of the first peripheral compartment of methotrexate; $Q1_{MTX}$ = Clearance between the central and the first peripheral compartment of methotrexate; $V3_{MTX}$ = Volume of the second peripheral compartment; $Q2_{MTX}$ = Clearance between the central and the second peripheral compartment of methotrexate; $CL_{7\text{-}OH\text{-}MTX}$ = Clearance of 7-hydroxy-methotrexate from the first metabolite compartment; $V1_{7\text{-}OH\text{-}MTX}$ = Volume of the second metabolite compartment; $V2_{7\text{-}OH\text{-}MTX}$ = Volume of the second metabolite compartment; $Q_{7\text{-}OH\text{-}MTX}$ = Clearance between the first and the second metabolite compartment.

Intermediate model

The graphical analysis of the plots of covariates versus individual pharmacokinetic parameters indicated a possible relationship between concomitant use of gastric hydrogen pump inhibitors, serum total bilirubin (decreased clearance at higher total bilirubin levels), BSA (decreased clearance at higher BSA), pleural effusion/ascites and CL_{MTX}, between gastric hydrogen pump inhibitors and $CL_{7\text{-OH-MTX}}$ and between gender and $V2_{MTX}$. Forward inclusion (p < 0.005) of these covariates in the basic model, however, revealed that these covariates were not significantly correlated with the pharmacokinetic parameters of methotrexate and 7-hydroxy-methotrexate.

Final population pharmacokinetic model

Since no significant influence of covariates on the pharmacokinetic parameters could be detected, the final model was equal to the basic model.

In Figure 5, the model predicted concentrations (5A and 5C) and the Bayesian individual predicted concentrations (Figure 5B and 5D) are depicted for methotrexate and 7-hydroxy-methotrexate, respectively. Model (Figure 5A and 5C) and Bayesian (Figure 5B and 5D) predicted concentrations for methotrexate and 7-hydroxy-methotrexate were symmetrically distributed around the line of unity. The model predicted concentrations are based on the population pharmacokinetic parameter estimates, whereas the individual Bayesian predicted concentrations are based on the population pharmacokinetic parameter estimates and the individual observed concentrations.

Discussion

The pharmacokinetics of methotrexate and 7-hydroxy-methotrexate vary considerably among patients.[2,6,7] Since both compounds can cause life-threatening toxicity it is important to study which covariates can cause the variability in their pharmacokinetic behaviour. The aim of this study was to perform a simultaneous modelling of methotrexate and its primary metabolite 7-hydroxy-methotrexate to asses their pharmacokinetic parameters, the intra- and interindividual variability, and to determine the influence of covariates and concomitant use of medication on the pharmacokinetic parameters of both compounds. The dataset consisted of 2 subpopulations, 1 selected cohort with complete concentration-time curves (n=21, 33 courses) and 1 unselected cohort with routinely measured concentration-time data (n=55, 275 courses).

According to the OFV, the standard error values of the parameter estimates, and the goodness of fit plots, it appeared that the data were best fitted by an integrated 3-compartment model with linear elimination of methotrexate from the central compartment and a 2-compartment model with linear elimination of 7-hydroxy-methotrexate (Figure 1). All parameters were estimated accurately, except for $V_{7\text{-OH-MTX}}$ (relative standard error was

Figure 5. Goodness of fit plots of the observed concentrations versus the model and Bayesian predicted concentrations. Observed versus model predicted methotrexate concentrations (A), observed versus Bayesian predicted methotrexate concentrations (B), observed versus model predicted 7-hydroxy-methotrexate concentrations (C), observed versus Bayesian predicted 7-hydroxy-methotrexate concentrations (D). Solid line is the line of identity
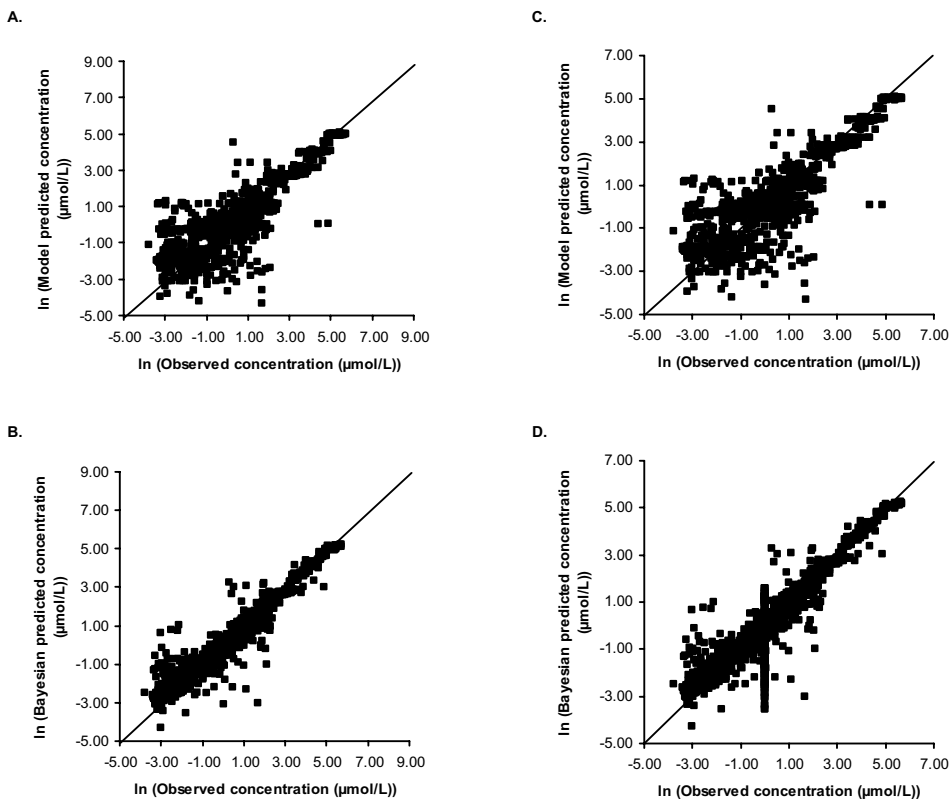
72%) and the residual error of the population model was relatively high. We assume that this can be attributed to the relative low number of concentration-time data obtained shortly after the infusion of methotrexate compared to the high number of routinely measured methotrexate concentrations (24- and 48-hour concentrations). In previous population pharmacokinetic models of methotrexate after high-dose administration intravenously, the drug was modelled to linear 2- or 3-compartment models.[8-11] The population values of the pharmacokinetic parameters in our study were in the same range. The total volume of distribution of methotrexate in our study (543 L) was substantially higher compared to the other population analyses. Since the volume of distribution of the central (21.3 L) and the first peripheral compartment (9.03 L) of methotrexate is in accordance with previous reported values, we assume that the volume of the third compartment in our study is high due to the relative high number of patients with pleural effusion or ascites (20%) in

combination with the inclusions of time-points long after the administration in patients with pleural effusion or ascites.

In one previous reported population analysis the methotrexate and 7-hydroxy-methotrexate data were simultaneously modelled.[12] The pharmacokinetic parameter estimates were in the same range as in our study. However, this model was based on concentration-time data obtained in only 8 patients compared to 76 patients in our study. Furthermore, the influence of covariates on pharmacokinetic parameters was not studied. In our population analysis, some covariates, BSA, gender, concomitant use of proton pump inhibitors and salicylates, serum total bilirubin and presence of ascites and pleural effusion (with and without a pleural drain), showed an influence on the volume of distribution or clearance of methotrexate, or the 7-hydroxymethotrexate clearance. However, the intermediate analysis showed that these influences were not significant. In two population analyses (n=34 and n=23), significant relationships between patient weight and age, and the volume of distribution of methotrexate, methotrexate clearance and renal function as determined by the glomerular filtration rate, were observed.[8,9] Our patient population consisted of more patients (n=76) but no significant influence of covariates on the pharmacokinetic parameters could be detected. This may be attributed to the low percentage of full concentration-time data (11%) in the dataset. Moreover, no patients with abnormal renal function were included in the dataset (serum creatinine ≤ 129 μmol/L).

Concomitant use of drugs that can interact with methotrexate had no significant influence on the pharmacokinetic parameters of methotrexate and 7-hydroxy-methotrexate. It is well known that some of these covariates, e.g. concomitant use of NSAIDs and salicylates, ascites and pleural effusion, can cause delayed methotrexate elimination that can result in life-threatening toxicity.[3,12,19-26] We assume that the non-significant relationships are caused by the high diversity of our patient population and the small number of patients that used concomitantly other medication. Moreover, the non-significant influence of the presence of pleural effusion and ascites on the pharmacokinetic parameters demonstrates the correct clinical management of the pleural drain, and the ascitic fluid and pleural effusion drainage prior to methotrexate administration. The concentration-time data in pleural effusion as obtained in four patients with a pleural drain, showed that only a low fraction of the administered methotrexate dose diffused into pleural effusion (range: 0.00019% to 0.13%). Moreover, therapeutic serum drug levels were achieved in these patients despite the pleural drain. This is confirmed by the serum concentration-time curves obtained in 2 patients who developed pleural effusion and ascites after the methotrexate administration. The elimination of both methotrexate and 7-hydroxy-methotrexate is substantially prolonged in both patients (Figure 2).

After iv administration of methotrexate, drug- drug interactions have been reported to occur due to protein binding replacement and decreased renal clearance of the drug.[19-26] Since the plasma protein binding of methotrexate is about 50%, it seems unlikely that interactions

caused by displacement of methotrexate from binding sites can have clinical relevance.[29,33] Since 7-hydroxy-methotrexate is 91-93% protein-bound in plasma, this metabolite can contribute to drug-drug interactions with highly albumin-bound compounds.[29,33] Only a few drug-drug interactions have been reported for 7-hydroxy-methotrexate.[27-29] Naproxen can increase the unbound fraction of 7-hydroxy-methotrexate.[28,29] Pantoprazole has been reported to inhibit the metabolite elimination of the hydroxylated metabolite in 1 patient.[27] Future studies should focus on the relationship between 7-hydroxy-methotrexate, concomitant medication and observed toxicity after the administration of high-dose methotrexate.

In conclusion, we showed that the pharmacokinetics of methotrexate and 7-hydroxy-methotrexate can be best described by an integrated linear 3- and 2- compartment model. This population model can be used to explore the relationships between the 7-hydroxy metabolite and its toxicity. Moreover, this population model may aid further research to elucidate the relationship between the pharmacokinetics of methotrexate, 7-hydroxy-methotrexate, and toxicity and possible drug-drug interactions.

Acknowledgements

References

1. Jolivet J, Cowan KH, Curt GA, et al. The pharmacology and clinical use of methotrexate. N Engl J Med 1983;18:1094-1104.
2. Schornagel JH, McVie JG. The clinical pharmacology of methotrexate. Cancer Treat Rev 1983;10: 53-75.
3. Treon SP, Chabner BA. Concepts in use of high-dose methotrexate therapy. Clin Chemistry 1996;42:1322-1329.
4. Fizazi K, John WJ, Vogelzang NJ. The emerging role of antifolates in the treatment of malignant pleural mesothelioma. Sem Oncol 2002;29:77-81.
5. Kitamura S, Sugihara K, Nakatani K, et al. Variation of hepatic methotrexate 7-hydroxylase activity in animals and humans. Life 1999;48:607-611.
6. Stewart AJ, Margison JM, Wilkinson PM, et al. The pharmacokinetics of 7-hydroxy-methotrexate following medium-dose methotrexate therapy. Cancer Chemother Pharmacol 1985;14:165-167.
7. Erttmann R, Bielack S, Landbeck G. Kinetics of 7-hydroxy-methotrexate after high-dose methotrexate therapy. Cancer Chemother Pharmacol 1985;15:101-104.
8. Odoul F, Le Guellec C, Lamagnère J-P, et al. Prediction of methotrexate elimination after high dose infusion in children with acute lymphoblastic leukaemia using a population pharmacokinetic approach. Fundam Clin Pharmacol 1999;13:595-604.
9. Batey MA, Wright JG, Azzabi A, et al. Population pharmacokinetics of adjuvant cyclophosphamide, methotrexate and 5-fluorouracil (CMF). Eur J Cancer 2002;38:1081-1089.
10. Sabor C, Debord J, Roullet B, et al. Comparison of 2- and 3-compartment models for the Bayesian estimation of methotrexate pharmacokinetics. Internat J Clin Pharmacol Therap 1995;32:164-169.
11. Bruno R, Iliadis A, Favre R, et al. Dosage predictions in high-dose methotrexate infusions. Part 2: Bayesian estimation of methotrexate clearance. Cancer Drug Deliv 1985;4:277-283.
12. Bore P, Bruno R, Lena N, et al. Methotrexate and 7-hydroxy-methotrexate pharmacokinetics following intravenous bolus administration and high-dose infusion of methotrexate. Eur J Cancer Clin Oncol 1987;23:1385-1390.
13. Favre R, Monjanel S, Alfonsi M, et al. High-dose methotrexate: a clinical and pharmacokinetic evaluation. Cancer Chemother Pharmacol 1982;9:156-160.
14. Bore P, Iliadis A, Catalin J, et al. Pharmacokinetics of methotrexate and 7-hydroxy-methotrexate after methotrexate infusions. Cancer Drug Delivery 1987;4:177-183.
15. Smeland E, Fuskevåg OM, Nymann K, et al. High-dose 7-hydroxy-methotrexate: acute toxicity and lethality in a rat model. Cancer Chemother Pharmacol 1996;37:415-422.
16. Fuskevåg O, Kristiansen C, Lindal S, et al. Maximum tolerated doses of methotrexate and 7-hydroxy-methotrexate in a model of acute toxicity in rats. Cancer Chemother Pharmacol 2000;46:69-73.
17. Lankelma J, van der Klein E. The role of 7-hydroxy-methotrexate during methotrexate anti-cancer therapy. Cancer Letters 1980;9:133-142.
18. Gaukroger JM, Wilson L. Protection of cells from methotrexate toxicity by 7-hydroxy-methotrexate. Br J Cancer 1984;50:327-333.
19. Evans WE, Christensen ML. Drug interactions with methotrexate. J Rheumatol Suppl 1985;12: 15-20.
20. Thyss A, Kubar J. Clinical and pharmacokinetic evidence of a life-threatening interaction between methotrexate and ketoprofen. Lancet 1986;1:256-258.
21. Ferrazzini G, Klein J, Sulh H, et al. Interaction between trimethoprim-sulfamethoxazole and methotrexate in children with leukemia. J Pediatr 1990;117:823-826.
22. Thyss A, Milano G, Renée N. Severe interaction between methotrexate and a macrolide-like antibiotic. J Natl Cancer Inst 1993;85:582-583.
23. Ronchera CL, Hernández T, Peris JE, et al. Pharmacokinetic interaction between high-dose methotrexate and amoxycillin. Ther Drug Monitor 1993;15:375-379.
24. Karsh J. Adverse reactions and interactions with aspirin. Drug Safety 1990;5:317-327.
25. Reid T, Yuen A, Catolico M, Carlson RW. Impact of omeprazole on the plasma clearance of methotrexate. Cancer Chemother Pharmacol 1993;33:82-84.

26.   Titier K, Lagrange F, Péhourq F, et al. Pharmacokinetic interaction between high-dose methotrexate and oxacillin. Ther Drug Monitor 2002;24:570-572.

27.   Tröger U. Severe myalgia from an interaction between treatments with pantoprazole and methotrexate. Br Med J 2002;324:1497.

28.   Ekstrom PO, Giercksky KE, Anersen A, et al. Alterations in methotrexate pharmacokinetics by naproxen in the rat as measured by microdialysis. Life Sci 1997;60:359-364.

29.   Slørdal L, Sager G, Aarbakke J. Pharmacokinetic interactions with methotrexate: Is 7-hydroxy-methotrexate the culprit? Lancet 1988;1:591-592.

30.   Van Tellingen O, van der Woude HR, et al. Stable and sensitive method for the simultaneous determination of N^5-methyltetrahydrofolate, leucovorin, methotrexate and 7-hydroxy-methotrexate in biological fluids. J Chromatography 1989;488:379-388.

31.   Boeckmann AJ, Sheiner LB, Beal SL. NONMEM Users guide-part V introductory guide. NONMEM Project Group. University of California at San Francisco.

32.   Jonsson EN, Karlsson MO. Xpose – an S-PLUS based population pharmacokinetic/ pharmacodynamic model building aid for NONMEM. Comput Methods Programs Biomed 1999;58:51-64.

33.   Benet LZ, Hoener B. Changes in plasma protein binding have little clinical relevance. Clinical Pharmacol Ther 2002;71:115-121.

Paclitaxel

4

Chapter 4.1

A population analysis of the pharmacokinetics of Cremophor EL using nonlinear mixed-effect modelling

HJG Desirée van den Bongard, Ron AA Mathôt, Olaf van Tellingen, Jan HM Schellens and Jos H Beijnen

Summary

The purpose of this study was to develop a population pharmacokinetic model for Cremophor EL used as a formulation vehicle for paclitaxel. Plasma concentration-time data of 70 patients (85 courses, 3- and 96-hour iv infusions) treated with paclitaxel dissolved in Cremophor EL were used. The non-linear mixed effect modelling (NONMEM) program was used for the population pharmacokinetic analysis. The influence of patient characteristics and biochemical parameters on the pharmacokinetics of Cremophor EL was determined. The stability of the final model was evaluated using the bootstrap resampling method.

The data were most optimally described by a 3-compartment model with Michaelis-Menten elimination from the central compartment. The following pharmacokinetic parameters were estimated: volume of the central compartment ($V1=2.59$ L), volumes of two peripheral compartments ($V2=1.81$ L, $V3=1.61$ L), intercompartmental clearance between central and peripheral compartments ($Q12=1.44$ L/h, $Q13=0.155$ L/h), maximal elimination rate ($V_{max}=0.193$ ml/h), and concentration at half V_{max} ($K_m=0.122$ ml/L). Interindividual variability of the pharmacokinetic parameters was quantified for V1 (25%), V2 (36%), and V_{max} (31%). Residual variability consisted of a combined additional (0.095 ml/L) and proportional error (7%). Gender, body surface area and performance status according to the World Health Organisation were significantly correlated with V1, V2, V_{max}, respectively ($p < 0.0001$). The median parameter estimates of 1000 bootstrap samples were in accordance with those obtained with the original data set indicating the validity of the population model. In conclusion, the population model was able to adequately describe the pharmacokinetic parameters and influence of covariates on pharmacokinetics of Cremophor EL. This model can be used when studying the relationship between the pharmacokinetics and toxicity of Cremophor EL, and the drug's influence on the pharmacokinetics of paclitaxel.

Introduction

Cremophor EL is a polyethoxylated castor oil that is used for the formulation of vitamin preparations and a variety of poorly water-soluble drugs including teniposide, cyclosporin A, and paclitaxel.[1-3] Taxol® is the pharmaceutical product in which paclitaxel is dissolved (6 mg/mL) in a mixture of Cremophor EL and ethanol (1:1, v/v).[4]

Cremophor EL can cause hypersensitivity reactions by complement activation.[5-7] Cremophor EL can cause neurotoxicity probably caused by the ethoxylated derivatives of castor oil.[7] Despite the extensive use of Cremophor EL as a solubilising agent in clinical formulations and its reported toxicity, the pharmacokinetics in humans have not been extensively studied.[1,8-11] There is, however, substantial evidence that Cremophor EL can alter the pharmacokinetics of certain cytotoxic drugs with clinical implications, e.g. paclitaxel.[7,11-14] In several studies the pharmacokinetics of Cremophor EL in mice and cancer patients have been studied in relation to its use as pharmaceutical solubilizer of paclitaxel.[11-14] Dose increments of paclitaxel dissolved in Cremophor EL result in disproportional increases in the systemic exposure to paclitaxel, as represented by the area under the plasma concentration-time curve (AUC). In the absence of Cremophor EL, a linear pharmacokinetic behaviour of paclitaxel was observed.[12] Several mechanisms of the nonlinear pharmacokinetics of paclitaxel induced by Cremophor EL have been reported.[11,13-20] Cremophor EL might inhibit the elimination of paclitaxel by preventing access of the drug to the elimination sites.[15] Furthermore, it has been suggested that Cremophor EL induces a serum lipoprotein dissociation product with a high affinity for paclitaxel.[18,20]

More recently, it has been demonstrated that Cremophor EL can form micelles in blood in vitro, acting as a high-affinity drug-transporting site for paclitaxel that results in a decreased free paclitaxel fraction in plasma.[13,14,16,17,19] Cremophor EL can decrease the blood:plasma ratio of paclitaxel at higher dose-levels by reducing the uptake in red blood cells.[2]

The pharmacokinetic behaviour of paclitaxel can thus be influenced by the pharmacokinetics of Cremophor EL. Consequently, Cremophor EL can modify the toxicity profile of paclitaxel.[21] Assessment of the clinical pharmacokinetics of Cremophor EL during paclitaxel administration may be of major importance. The purpose of this study was to develop a population pharmacokinetic model of Cremophor EL when administered in combination with paclitaxel. In this population analysis, the pharmacokinetic parameters and the patient characteristics that correlate with the pharmacokinetics of Cremophor EL were determined.

Materials and Methods

Patient population

Plasma concentration-time data (85 courses) of Cremophor EL concentrations were collected during safety and pharmacokinetic multicentre studies of paclitaxel performed in 70 cancer patients (21 patients with hepatic dysfunction). The results of these studies have been

published recently.[22-25] In these studies paclitaxel was infused intravenously (iv) with or without co-infusion of carboplatin in patients with primarily metastatic breast-, ovarian- and non-small cell lung cancer. The patient characteristics are summarised in Table 1. Every course was included separately in the data set that resulted in 85 identification numbers (ID) in this population pharmacokinetic analysis. Paclitaxel (Taxol®, Bristol Myers Squibb, Syracuse, NY) was provided as a sterile 6 mg/ml solution and dissolved in Cremophor EL: Ethanol 1:1, v/v. Prior to administration this solution was diluted with 500-1000 ml 0.9%

Table 1. Patient characteristics (n=70) and serum parameter values during 85 courses

	Number	Median	Range
Patient characteristics			
Female	44		
Male	26		
Number of courses with pharmacokinetic data			
First course	70		
Second course	15		
Dose range Paclitaxel (in mg/m^2)			
3-hour infusion	78		100-250
24-hour infusion	3		135-175
96-hour infusion	4		105-135
Dose range Cremophor EL (in ml/m^2)			
3-hour infusion	78		8.3-20.8
24-hour infusion	3		11.2-14.5
96-hour infusion	4		8.7-11.6
Dose range Carboplatin (in mg/m^2)			
3- hour infusion	32		300-400
Age (in years)		52	24-75
Primary site of disease			
Lung	32		
Ovarian	17		
Breast	16		
Colon	1		
Pancreas	1		
Sarcoma	1		
Endometrium	1		
Granulosa theca cell	1		
WHO Performance status			
0	21		
1	48		
2	16		
BSA (in m^2)		1.82	1.50-2.30
Biochemical parameters			
Creatinine (in µmol/L)		78	37-120
AST (in U/L)		19	7-260
ALT (in U/L)		21	3-343
Alkaline Phosphatase (in U/L)		112	52-1269
GGT (in U/L)		116	7-1527
Albumin (in g/L)		36	23-52
Total bilirubin (in µmol/L)		7	3-50
LDH (in U/L)		306	190-5942

BSA = body surface area; AST = aspartate aminotransferase; ALT = alanine-amino transferase; GGT = gamma-glutamyl-transpeptidase; LDH = lactate dehydrogenase; WHO = World Health Organisation.

sodium chloride solution to a final paclitaxel concentration between 0.3 and 1.2 mg/ml. As Cremophor EL may leach plasticiser from the infusion lines, adapted PVC-free administration equipment was used. Paclitaxel was iv infused in 3-, 24-, and 96-hour infusions at doses ranging from 100 to 250 mg/m². The corresponding Cremophor EL doses ranged from 8.3-20.8 ml/m² in the 3-hour infusion schedule (78 courses), from 11.2 to 14.5 ml/m² in the 24-hour infusion schedule (3 courses), and from 8.7 to 11.6 ml/m² in the 96-hour infusion schedule (4 courses). Written informed consent was obtained from all patients. Standard premedication with dexamethasone (20 mg orally at 12 and 6 hours prior to paclitaxel administration), clemastine (2 mg iv. 30 minutes prior to paclitaxel administration) and cimetidine (300 mg iv. shortly prior to paclitaxel administration) was administered to prevent hypersensitivity reactions. If indicated, $5-HT_3$-receptor antagonists were administered iv as standard antiemetic agent. The Medical Ethics Committees of the participating hospitals approved the studies.

Pharmacokinetic sampling and bio-analysis

Plasma concentration-time data were obtained by pharmacokinetic sampling during the first course (n=70) and the second course (n=15). The samples for Cremophor EL analysis were collected into heparinised tubes prior to the start of the infusion, at 1 and 2 hours after the start, at the end of the infusion and at 5, 30, 60 minutes, and 1.5, 2, 4, 8, 10, 12, 30, and 48 hours after the end of the infusion in the 3-hour infusion schedules. In the 24-hour infusion schedules, blood samples were taken prior to the start of the infusion, at 3, 10 and 20 hours after the start of the infusion, at the end of the infusion, and at 5, 15, 30, and 60 minutes, and 2, 4, 8, 12, 24, 30 hours after the end of the infusion. In the 96-hour infusion schedule, blood samples were taken prior to the start of the infusion, at 8, 48 and 72 hours after the start of the infusion, at the end of the infusion, and at 4, 9 and 19 hours after the end of the infusion. Whole blood was centrifuged immediately after withdrawal for 5 min at 3000 rpm, and the plasma fraction was stored at –20°C until analysis. The Cremophor EL concentrations in plasma were determined by a validated reversed-phase high-performance liquid chromatographic method based on the determination of ricinoleic acid after saponification of Cremophor EL, followed by precolumn derivatization and reversed-phase high-performance liquid chromatography as has been described in detail elsewhere.[11,26]

Population pharmacokinetic analysis

The program NONMEM (non-linear mixed effect modelling (NONMEM, version V 1.1, double precision) and PREDPP package were used throughout the analysis.[27] Since the patients were sampled extensively, first-order conditional estimation was applied with interaction. The NONMEM analysis consisted of the following three-step approach.[28]

Basic population pharmacokinetic model

The first step consisted of the development of a basic population pharmacokinetic model. The data were described by a three-compartment model with Michaelis-Menten elimination (Figure 1). The following pharmacokinetic parameters were estimated: volume of the central compartment (V1 in L), volume of the first peripheral compartment (V2 in L), volume of the second peripheral compartment (V3 in L), intercompartmental clearance from the central compartment to the first peripheral compartment (Q12 in L/h), and to the second peripheral compartment (Q13 in L/h), maximal elimination rate (Vmax in ml/h), and the concentration at half of the Vmax (Km in ml/L). Standard errors for all parameters were calculated using the COVARIANCE option in the NONMEM program. Interindividual variability in V1, V2, and Vmax was estimated using a lognormal error model. For V1 the interindividual variability was defined as in equation 1:

$$V1_i = V1_{pop} * (1 + \eta_i^{V1}) \qquad\qquad \text{equation 1}$$

where $V1_i$ represents the V1 of the ith individual, and $V1_{pop}$ is the population value, and η_i^{V1} is the interindividual random effect that is normally distributed with mean zero and variance ω^2.

The residual variability was estimated using a combined additive and proportional model:

$$C_{obs,ij} = C_{pred,ij} (1+\varepsilon_2) + \varepsilon_1 \qquad\qquad \text{equation 2}$$

Figure 1. Schematic overview of the basic population pharmacokinetic model: a three-compartment model with Michaelis-Menten elimination from the central compartment (V1). V2 and V3 indicate the two peripheral compartments. k12, k21, k13 and k31 indicate the intercompartmental rate constants. Vmax is the maximal elimination rate, and Km is the plasma-concentration of Cremophor EL at half of the Vmax
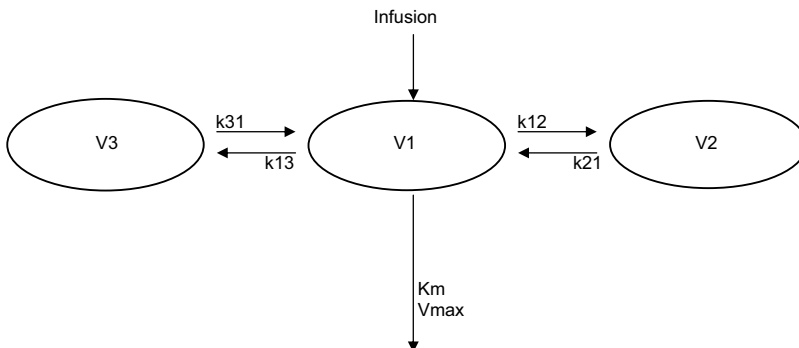
where $C_{obs,ij}$ is the jth observed concentration in the ith patient ($C_{obs,ij}$) and its respective prediction ($C_{pred,ij}$), and ε is an independent random variable with mean 0 and standard deviation σ that is assumed to be constant in this population analysis.

The stability of the basic pharmacokinetic model was evaluated by the bootstrap resampling technique as implemented in the program Wings for NONMEM (WFN version 3).

designed by Dr. N.H. Holford and available via the internet (http://wfn.sourceforge.net).[29] The median parameter estimates obtained from the 1000 bootstrap replications were compared with those obtained from the original data set.

Intermediate model

The second step consisted of the individual Bayesian regression analysis. For each subject, individual pharmacokinetic parameters were calculated using the individual Cremophor EL plasma concentration-time data and the population pharmacokinetic parameter estimates obtained in the first step. The individual Bayesian estimates were plotted against the demographic factors and blood chemistry parameters (as covariates). The relations between the covariates and the Bayesian parameter estimates of each individual patient were investigated graphically in the program Xpose (Xpose, version 2.0, Uppsala University, Sweden) as implemented in the S-PLUS statistical package (version 2000, Mathsoft, Cambridge, Mass.).[30] The following 13 covariates were investigated for their correlation with the pharmacokinetics of Cremophor EL: age, gender, weight, body surface area (BSA), performance status according to the World Health Organisation (PS), serum creatinine, serum alanine-aminotransferase (ALT), serum aspartate-aminotransferase (AST), serum alkaline phosphatase, serum gamma-glutamyl-transpeptidase (GGT), serum albumin, serum bilirubin and serum lactate dehydrogenase (LDH). The selected covariates that showed a graphical relationship with a pharmacokinetic parameter were tested by univariate analysis. These covariates were entered individually into the basic population pharmacokinetic model by forward inclusion. Continuous covariates, e.g. BSA, were centred to their median values.[31] For instance, the relationship between V2 and BSA was described as in equation 3:

$$V2 = \theta_3 * (1 + \theta_4 * (BSA - 1.82)) \hspace{4cm} \text{equation 3}$$

where V2 represents the value of V2 in L, θ_3 the V2 value of a (median) patient with a BSA of 1.82 m^2, and θ_4 is the increase or decrease in V2 per m^2 BSA difference.

Dichotomous covariates were modelled as described in equation 4:

$$V1 = \theta_1 * \theta_{10}^{FLAG1} \hspace{5cm} \text{equation 4}$$

where V1 represents the value of V1 in L, θ_1 the V1 value in females (FLAG1 =0), and θ_{10} the change in V1 in males (FLAG1=1).

Several criteria were taken into account when comparing the models. The difference in the NONMEM objective function value that is equal to minus twice the log likelihood of the data, after the introduction of a covariate in the model, approximates to a chi-squared-distribution with one degree of freedom. During the forward inclusion of the covariates in the basic model, the significance level was set at $p < 0.005$ that is associated with a decrease in the NONMEM objective function value of > 7.88. All significant covariates were incorporated into an intermediate multivariate model.

Final population pharmacokinetic model

The development of the intermediate model was followed by multivariate analysis that consisted of a stepwise backward elimination procedure. Covariates retained in the intermediate model when elimination of the covariate caused an increase in the NONMEM objective function value of > 10.83 that is associated with a significance level of $p < 0.001$. The stability and performance of the final model was evaluated using the bootstrap method by fitting the final model to 1000 bootstrap samples. The parameter estimates and the 95% confidence intervals obtained from the original data set were compared with the median parameters estimates including the 2.5%-97.5% percentile range obtained from the 1000 bootstrap replicates.

Figure 2. Plasma concentration versus time curves of Cremophor EL in three representative patients treated with a 3-hour (●), 24-hour (▲) and a 96-hour (■) iv infusion of paclitaxel, dissolved in Cremophor EL, at doses of 30, 24.6, and 19.4 ml, respectively (corresponding paclitaxel doses of 360, 295, and 235 mg, respectively)
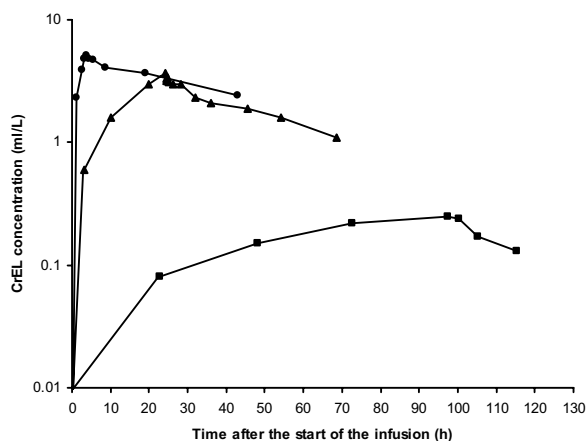
Results

The plasma concentrations *versus* time curves of Cremophor EL after the start of the infusion were analysed. Individual plots of plasma concentration *versus* time curves after a 3-, 24- and 96-hour iv infusion are shown in Figure 2.

Population pharmacokinetic analysis

Basic population pharmacokinetic model

Two- and three-compartment models with first order elimination and Michaelis-Menten elimination, and with linear distribution and saturable distribution were fitted to the Cremophor EL concentration-time data. According to the objective function values (OFV), the standard error values, and the goodness of fit plots, it appeared that the data were best described by a three-compartment model with Michaelis-Menten elimination (Figure 1). The population pharmacokinetic parameters (without taking covariates into account) including the standard errors, the interindividual variability and the residual errors are summarised in Table 2. All pharmacokinetic parameters were estimated accurately, except for the Km. The relative standard error of this parameter was 71%. Interindividual variability was determined for V1, V2, and Vmax. Inclusion of interindividual variability for V3, Q12, Q13 and Km did not improve the fit. This should not be interpreted as an absence of interindividual variability in these pharmacokinetic parameters. It indicates that the data did not contain sufficient information to estimate the interindividual variability of these parameters. The residual variability consisted of an additional error of 0.099 ml/L, and a proportional error of 6.8%.

The stability of the basic pharmacokinetic model was tested by the bootstrap method. From the original concentration-time data, 1000 bootstrap resamples were generated. The median values of the parameter estimates obtained by 1000 bootstrap resamples were in accordance with the parameters of the model (data not shown). Parameter estimates of the basic model were all within 5.6% of the median bootstrap value. We concluded that the stability of the basic population pharmacokinetic model was adequate. The basic model was used in the development of the final population pharmacokinetic model.

Intermediate model

The graphical analysis of the plots of the covariates *versus* individual pharmacokinetic parameters indicated a possible relationship between BSA, age, weight, gender, PS, bilirubin, AST, ALT and V1, between BSA, age, weight, gender, PS, creatinine, alkaline phosphatase, GGT, AST, ALT and V2, and between BSA, creatinine, age, weight, gender, PS, creatinine, AST, ALT and Vmax. Forward inclusion (p < 0.005) of these covariates in the basic model resulted in an intermediate multivariate model with the following significant covariates: V1: gender, weight, PS, BSA, V2: gender, BSA, weight, and Vmax: PS, BSA, weight.

Table 2. Population parameters of the basic and final population pharmacokinetic model of Cremophor EL and the corresponding parameter estimates obtained by 1000 bootstrap resamplings

PK parameter	Basic population PK model		Final population PK model		1000 bootstrap replicates	
	Estimate	RSE (%)	Estimate	RSE (%)	Median	2.5-97.5 percentiles
PK parameter						
V1 (L)	2.86	7	2.59	7	2.59	2.16-2.92
Influence of gender $(\theta_{10})^{a}$			1.30	7	1.31	1.13-1.51
Q12 (L/h)	1.42	28	1.44	24	1.42	0.925-2.46
V2 (L)	1.75	9	1.81	9	1.81	1.49-2.13
Influence of BSA $(\theta_{11})^{b}$			1.13	18	1.13	0.67-1.51
Q13 (L/h)	0.154	25	0.155	22	0.155	0.099-0.239
V3 (L)	1.60	8	1.61	7	1.61	1.36-1.97
Km (ml/L)	0.197	71	0.122	61	0.124	0.026-0.870
Vmax (ml/h)	0.214	11	0.193	9	0.196	0.151-0.265
Influence of PS 2 $(\theta_{12})^{c}$			1.48	10	1.48	1.22-1.88
Inter-individual variability						
V1 (%)	30.8	20	24.7	22	24.2	19.8-30.5
V2 (%)	41.5	27	36.5	28	35.5	26.7-47.0
Vmax (%)	33.9	27	30.7	24	30.4	23.6-39.4
Residual error						
Additional (ml/L)	0.0985	32	0.0951	34	0.0943	0.0512-0.190
Proportional (%)	6.83	8	6.94	8	6.78	5.30-7.77

[a] V1 = $\theta_1 * \theta_{10}^{FLAG1}$, where V1 is expressed in L, θ_1 represents the V1 value in females (FLAG1 =0), and θ_{10} is the change in V1 value in males (FLAG1=1).

[b] V2 = $\theta_3 * (1 + \theta_{11} * (BSA - 1.82))$.

[c] Vmax = $\theta_7 * \theta_{12}^{FLAG2}$, where Vmax is expressed in L/h, θ_7 represents the Vmax value in patients with a PS of 0 or 1 (FLAG2=0) and θ_{12} is the change in Vmax in patients with a PS of 2 (FLAG2=1).

BSA = body surface area; Km = the plasma concentration at half of the Vmax; PS = performance status according to the World Health Organisation; Q12 = intercompartmental clearance from the central to the first peripheral compartment; Q13 = intercompartmental clearance from the central to the second peripheral compartment; RSE = relative standard error; V1 = volume of the central compartment; V2 = volume of the first peripheral compartment; V3 = volume of the second peripheral compartment; Vmax = maximal elimination rate.

Table 3. Differences in the objective function value between the final population pharmacokinetic model and the final model with one significant covariate eliminated

NONMEM Objective function value:			
Basic population PK model -857.9			
Final population PK model -909.5			
Eliminated covariate	**Objective function**	**Difference in objective function**	**p value**
Gender on V1	-891.7	17.7	< 0.0001
BSA on V2	-894.0	15.4	< 0.0001
PS 2 on Vmax	-893.9	15.6	< 0.0001

BSA = body surface area; PS = performance status according to the World Health Organisation; V1 = volume of the central compartment; V2 = volume of the first peripheral compartment; V3 = volume of the second peripheral compartment; Vmax = maximal elimination rate.

Figure 3. Significant relationships between individual pharmacokinetic parameters (Bayesian estimates) and covariates (p < 0.0001); between V1 and gender (A), between V2 and BSA (B), and between Vmax and PS (C)
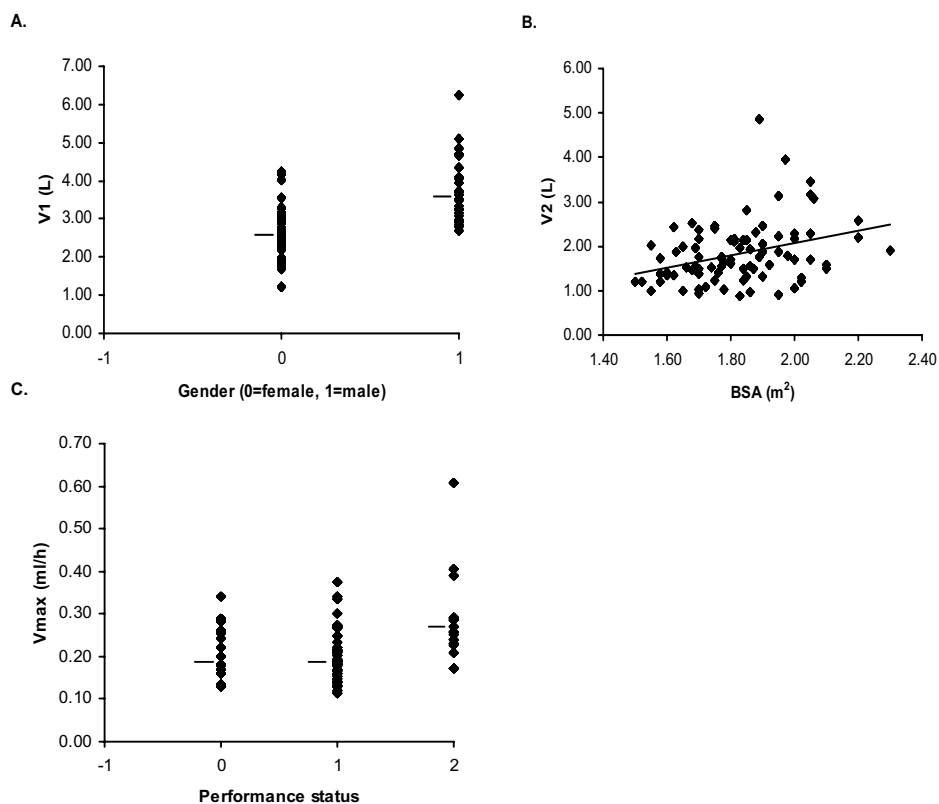
Final population pharmacokinetic model

Stepwise backward elimination (p < 0.001) was used to obtain the final population pharmacokinetic model. Gender was significantly correlated with V1, BSA with V2, and a PS of 2 with Vmax. Figure 3 shows the relationships between the Bayesian estimates of V1, V2 and Vmax, and gender, BSA and PS calculated from the final model. Inclusion of these three covariates in the final population pharmacokinetic model resulted in a decrease in the objective function value of 51.6 when compared to the value of the basic model (Table 3). The final population pharmacokinetic model of Cremophor EL is defined in the equations 5-7:

$$V1 = (2.59 * (1.30^{FLAG1}))$$ equation 5

where FLAG1 = 1 in males, FLAG1 = 0 in females

$$V2 = 1.81 - (1 + 1.13 * (BSA - 1.82))$$ equation 6

$$Vmax = (0.193 * (1.48^{FLAG2}))$$ equation 7

where FLAG2 = 1 when PS = 2, FLAG2 = 0 when PS = 0 or 1.

In the final model, V1 was 30% higher in males, Vmax was 48% higher in patients with a PS of 2 compared to patients with a PS of 0 or 1, and V2 was higher in patients with a higher BSA.

The correlation between the interindividual variability of V1, V2 and Vmax was evaluated. The matrix plots showed no correlation between η_i^{V1}, η_i^{V2}, and η_i^{Vmax} (plots not shown). The inclusion of the covariance between interindividual variability of V1 and V2, V2 and Vmax, V1 and Vmax (ΔOFV = -4.7) produced no significant decrease in the objective function in NONMEM. We concluded that there was no significant correlation, and therefore, it was not included in the final model. The population pharmacokinetic parameters of the final model including the standard errors, interindividual variability, and the residual errors are summarised in Table 2. The interindividual variabilities decreased to 24.7% (V1), 36.5% (V2), and 30.7% (Vmax). The residual error was almost unchanged (additional error 0.095 ml/L, proportional error 6.94%). The relative standard error of the Km was decreased to 61% in the final model compared to 71% in the basic model.

The Cremophor EL concentrations obtained after the 3- or 24- h infusions were higher than the Km value during the whole observation period, whereas the concentrations obtained after the 96-hour infusion were in the Km range. In order to explore the impact of the four patients receiving 96-hour infusion on the Km value, we repeated the final analysis with these four patients excluded. This resulted in an increase of the Km value to 1.15 ml/L with

a relative standard error of 71%. Consequently, the concentration-time data of the 96-hour infusions substantially influence the estimation of the Km value.

Plots indicating the goodness of fit of the final model are depicted in Figure 4. Model- and Bayesian-predicted concentrations were symmetrically distributed around the line of unity (Figures 4A and 4B). No trend was seen in the plot of individual weighted residuals (i.e. the weighted difference between the observed and the individually predicted concentrations) *versus* individually predicted concentrations (Figure 4C). Moreover, no time-dependent trend was observed in the plot of the weighted residuals (the weighted difference between

Figure 4. Goodness of fit plots of the observed concentrations versus the model predicted concentrations (A) and Bayesian predicted concentrations (B) as estimated by the final population pharmacokinetic model. Figure 4C is a plot of the individual weighted residuals (i.e. the weighted difference between the observated and the Bayesian predicted concentrations) versus the Bayesian predicted concentrations. Figure 4D is a plot of the weighted residuals (i.e. the weighted difference between observed and model predicted concentrations) versus time. In Figures 4A and 4B the solid line is the line of identity
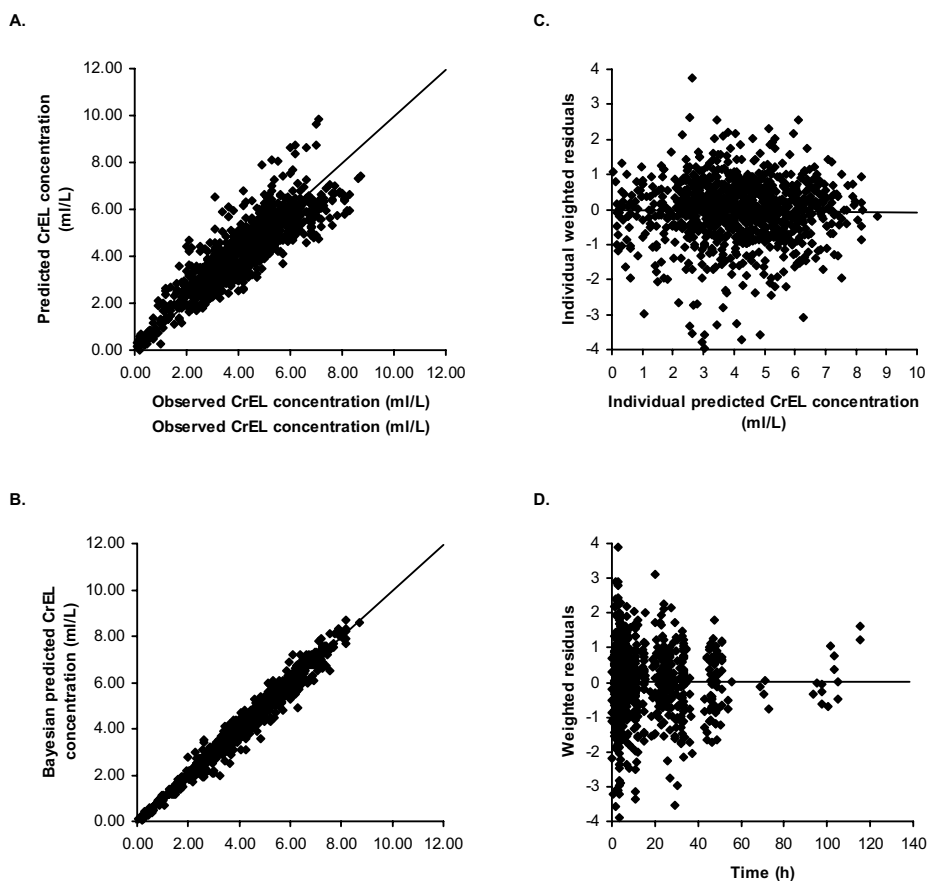
the observed and the predicted concentrations based on the parameter estimates for the typical individual *versus* time (Figure 4D).

The final model was fitted to the 1000 bootstrapped samples to evaluate its stability and performance. The values of all parameter estimates obtained by bootstrapping are summarised in Table 2. The median parameter estimates were all within 2.7% of the parameter estimates of the final model, indicating that the performance and stability of the final population pharmacokinetic model of Cremophor EL was adequate. However, the 97.5% percentile of the Km value (0.87) produced by the bootstrap procedure was considerably higher than the boundary of the 95% confidence interval produced by the final model (0.27). This difference was probably caused by bootstrap datasets that did not contain patients receiving the 96-hour infusions resulting in higher estimated Km values.

Discussion

Despite the extensive clinical use of Cremophor EL as a formulation vehicle for various hydrophobic drugs, reports of its pharmacokinetics are sparse.[1,8-11] It has recently been reported that Cremophor EL can influence the pharmacokinetic and toxicity profile of the drugs dissolved in it, e.g. paclitaxel.[7,11-14] The amount of Cremophor EL used in the formulation of hydrophobic drug varies from 5.5 ml/m² (propofol, diazepam, and aplidine) to 12 ml/m² (paclitaxel).[7]

The purpose of this study was to develop a population pharmacokinetic model of Cremophor EL, as the solvent for paclitaxel, and to elucidate relationships between the pharmacokinetic parameters and patient characteristics, i.e. demographic factors and blood chemical variables.

Previous reports with respect to the pharmacokinetics of Cremophor EL are conflicting. Noncompartmental pharmacokinetic analyses have shown that the elimination of Cremophor EL can be linear as well as non-linear with a disproportional increase of the exposure at higher Cremophor EL doses.[1,8,10,11] In these studies various assays for the determination of Cremophor EL in plasma were used that could have contributed to the differences in Cremophor EL concentrations. In one study the bioassay was based on the determination of the modulation of the multidrug resistance (mdr) *in vitro* by inhibition of P-glycoprotein inhibition.[1] In this study, the Cremophor EL concentrations in plasma were lower compared to the plasma concentrations determined by two other assays that are based on the measurement of ricinoleic acid and the binding of Cremophor EL to Coomassie brilliant blue G-250.[1,2,4,26] Moreover, the bio-assay based on mdr modulation has some disadvantages including the relatively large sample volume and its relatively poor sensitivity and precision.[26]

Our final population pharmacokinetic model revealed that the plasma concentration-time data of Cremophor EL could be best described by a three-compartment model with

Michaelis-Menten elimination after iv infusion as a solvent of paclitaxel in cancer patients. The saturated elimination could be due to capacity-limited Cremophor EL metabolism of the carboxylesterases within the systemic circulation.[7,9] The estimated population value of the total volume of distribution (=V1+V2+V3) was low (6.0 L) implying that the volume of distribution in humans is not much larger than the volume of the central blood compartment. This is in accordance with the low volume of distribution found in studies in which a noncompartmental pharmacokinetic analysis of Cremophor EL was performed.[8,10] This also implies that the distribution of Cremophor EL is limited to the peripheral tissues. Moreover, it can be hypothesised that V1 refers to the plasma compartment, and that V2 and V3 refer to the blood cells and micelles, respectively.

In our final population model, the interindividual variability in V1, V2 and Vmax could partially be explained by gender, BSA and PS, respectively. The volume of the central compartment was 31% higher in males than in females. The volume of the first peripheral compartment increased with BSA, and the Vmax was 48% higher in patients with a PS of 2 compared to patients with a PS of 0 or 1. The renal and hepatic elimination of Cremophor EL has been demonstrated to be very low. In one patient, 0.08% of the administered dose was excreted in urine after a 3-hour iv infusion.[32] It has been reported that Cremophor EL is eliminated by serum carboxylesterases as ricinoleic acid.[7,33] In a study of 27 patients performed at our institute, a higher Cremophor EL clearance was observed in patients with hepatic dysfunction than in patients with normal hepatic function after noncompartmental pharmacokinetic analysis.[9] In this population analysis, 21 of these patients were included. The relationships between the biochemical parameters, that indicate hepatic dysfunction, and the Vmax were not significant. We hypothesized that the higher Vmax in patients with a PS of 2 in our population analysis could be attributable to a higher serum esterase concentration in these patients. Higher serum esterase levels can be caused by hepatic dysfunction that results from liver metastasis that is more often present in patients with a PS of 2 compared to patients with a PS of 0 or 1.

The bootstrapping resampling method, that is considered to be a powerful internal validation technique, showed that the final population pharmacokinetic model was stable.[34] The median values of the parameter estimates obtained by bootstrapping were in accordance with the parameter estimates of the final model. The distribution of all parameter estimates showed a narrow range (Table 2) except for the Km. This observation is in accordance with the high relative standard error (61%) of the Km value in the final population pharmacokinetic model implying that the population parameter estimate is not very accurate.

The 95% confidence interval of Km obtained by the bootstrap resampling was large compared to the confidence interval obtained with the final model. As indicated before this may result from the small number of patients receiving Cremophor EL in the 96-hour infusion. This indicates that bootstrapping is of limited use when a small subset of patients has a large impact on the estimation of a pharmacokinetic parameter.

It is known that the pharmacokinetic behaviour of Cremophor EL can influence the pharmacokinetic and toxicity profile of paclitaxel and other dissolved drugs.[11-14] Several suggested mechanisms for the non-linear pharmacokinetics of paclitaxel have been rejected by van Zuylen et al.[14] They reported that the observed decrease in hepatobiliary elimination of paclitaxel in the presence of Cremophor EL in rats is not caused by alterations in paclitaxel elimination by Cremophor EL but by micelle formation in plasma. Consequently, paclitaxel cannot reach the elimination sites.[14] They also excluded altered protein binding due to the formation of high-density lipoproteins induced by Cremophor EL because an *in vitro* study showed that the paclitaxel accumulation in erythrocytes induced by Cremophor EL is also observed in the absence of any plasma proteins.[13] It has been reported that the micellar formation of Cremophor EL most likely affects the paclitaxel pharmacokinetics in plasma.[11,13,14,17,19] Consequently, the free paclitaxel fractions in plasma are lower at higher Cremophor EL concentrations in plasma.[11,13,14,17,19]

In conclusion, we have showed that the non-linear pharmacokinetics of Cremophor EL after iv infusion can accurately be described by the developed population pharmacokinetic model. This population model of Cremophor EL could be used in the development of a pharmacokinetic/pharmacodynamic population model to further explore the relationships between the pharmacokinetics of Cremophor EL and its toxicity. Moreover, this population pharmacokinetic model could be used to further develop a detailed population pharmacokinetic model of paclitaxel after iv administration when it is dissolved in Cremophor EL.

References

1. Rischin D, Webster LK, Millward MJ, Linahan BM, et al. Cremophor pharmacokinetics in patients receiving 3-, 6-, and 24-hour infusions of paclitaxel. J Natl Cancer Instit 1996;88:1297-1301.

2. Webster L, Linsenmeyer M, Millward M, et al. Measurement of cremophor EL following taxol: plasma levels sufficient to reverse drug exclusion mediated by the multidrug-resistant phenotype. J Natl Cancer Instit 1993;85:1685-1690.

3. Woodcock DM, Jefferson S, Linsenmeyer ME, et al. Reversal of the multidrug resistance phenotype with cremophor EL, a common vehicle for water-insoluble vitamins and drugs. Cancer Res 1990;50:4199-4203.

4. Sparreboom A, Loos WJ, Verweij J, et al. Quantitation of cremophor EL in human plasma samples using a colorimetric dye-binding microassay. Anal Biochem 1998;255:171-175.

5. Dorr RT. Pharmacology and toxiciology of Cremophor EL diluent. Ann Pharmacother 1994;28: S11-14.

6. Nannan Panday VR, Huizing MT, ten Bokkel Huinink WW, et al. Hypersensitivity reactions to the taxanes paclitaxel and docetaxel. Clin Drug Invest 1997;14:418-427.

7. van Zuylen L, Verweij J, Sparreboom A, et al. Role of formulation vehicles in taxane pharmacology. Invest New Drugs 2001;19:125-141.

8. Meerum Terwogt JM, van Tellingen O, Nannan Panday VR, et al. Cremophor EL pharmacokinetics in a phase I study of paclitaxel (Taxol®) and carboplatin in non-small cell lung cancer patients. Anticancer Drugs 2000;11:687-694.

9. Nannan Panday VR, Huizing, MT, van Tellingen O, et al. Pharmacologic study of cremophor EL in cancer patients with impaired hepatic function receiving taxol®. J Oncol Pharm Practice 1999;5:83.

10. Sparreboom A, Verweij J, van der Burg MEL, et al. Disposition of cremophor EL in humans limits the potential for modulation of the multidrug resistance phenotype in vivo. Clin Cancer Res 1998;4:1937-1942.

11. van Tellingen O, Huizing MT, Nannan Panday VR, et al. Cremophor EL causes (pseudo-) non-linear pharmacokinetics of paclitaxel in patients. Br J Cancer 1999;81:330-335.

12. Sparreboom A, van Tellingen O, Nooijen WJ, et al. Nonlinear pharmacokinetics of paclitaxel in mice results from the pharmaceutical vehicle cremophor EL. Cancer Res 1996;56:2112-2115.

13. Sparreboom A, van Zuylen L, Brouwer E, et al. Cremophor EL-mediated alteration of paclitaxel distribution in human blood: Clinical pharmacokinetic implications. Cancer Res 1999;59:1454-1457.

14. van Zuylen L, Karlsson MO, Verweij J, et al. Pharmacokinetic modelling of paclitaxel encapsulation in cremophor EL micelles. Cancer Chemother Pharmacol 2001;47:309-318.

15. Ellis AG, Webster LK. Inhibition of paclitaxel elimination in the isolated perfused rat liver by cremophor EL. Cancer Chemother Pharmacol 1999;43:13-18.

16. Kessel D. Properties of cremophor EL micelles probed by fluorescence. Photochem and Photobiol 1992;56:447-451.

17. Knemeyer I, Wientjes MG, Au JL. Cremophor reduces paclitaxel penetration into bladder wall during intravesical treatment. Cancer Chemother Pharmacol 1999;44:241-248.

18. Sykes E, Woodburn K, Decker D, et al. Effects of cremophor EL on distribution of Taxel to serum lipoproteins. Br J Cancer 1994;70:401-404.

19. van Zuylen L, Gianni L, Verweij J, et al. Inter-relationships of paclitaxel disposition, infusion duration and cremophor EL kinetics in cancer patients. Anti Cancer Drugs 2000;11:331-337.

20. Woodburn K, Kessel D. The alteration of plasma lipoproteins by cremophor EL. J. Photochem Photobiol B Biol 1994;22:197-201.

21. Gelderblom H, Verweij J, Nooter K, et al. Cremophor EL: the drawbacks and advantages of vehicle selection for drug formulation. Eur J Cancer 2001;37:1590-1598.

22. Eisenhauer EA, ten Bokkel Huinink WW, Swenerton KD, et al. European-Canadian randomized trial of taxol in relapsed ovarian cancer: high vs low dose and long vs short infusion. J Clin Oncol 1994;12:2654-2666.

23. Huizing MT, Keung ACF, Rosing H, et al. Pharmacokinetics of paclitaxel and metabolites in a randomized comparative study in platinum-pretreated ovarian cancer patients. J Clin Oncol 1993;11:2127-2135.

24. Huizing MT, Giaccone G, van Warmerdam LJC, et al. Pharmacokinetics of paclitaxel and carboplatin in a dose-escalating and dose-sequencing study in patients with non-small-cell lung cancer. J Clin Oncol 1997;15:317-329.

25. Nannan Panday VR, ten Bokkel Huinink WW, et al. Pharmacokinetics of paclitaxel administered as a 3-hour or 96-hour infusion. Pharmacol Res 1999;40:67-74.

26. Sparreboom A, van Tellingen O, Huizing MT, et al. Determination of polyoxyethyleneglycerol triricinoleate 35 (Cremophor EL) in plasma by pre-column derivatization and reversed-phase high-performance liquid chromatography. J Chrom B 1996;681:355-362.

27. Boeckmann AJ, Sheiner LB, Beal SL. NONMEM Users Guide - Part V Introductory Guide. NONMEM Project Group. University of California at San Francisco 1994.

28. Maitre PO, Bührer M, Thomson D, Stanski DR. A three-step approach combining bayesian regression and nonmem population analysis application to midazolam. J Pharmacokin Biopharm 1991;19:377-384.

29. Ette EI. Stability and performance of a population pharmacokinetic model. J Clin Pharmacol 1997;37:486-495.

30. Jonsson EN, Karlsson MO. Xpose – an S-PLUS based population pharmacokinetic/pharmacodynamic model building aid for NONMEM. Comput Methods Programs Biomed 1999;58:51-64.

31. Jonsson EN, Karlsson MO. Automated covariate model building within NONMEM. Pharmac Res 1998;15:1463-1468.

32. Gelderblom H, Verweij J, Brouwer E, et al. Disposition of [G-3H]paclitaxel and cremophor EL in a patient with severely impaired renal function. Drug Metab Dispos 1999;27:1300-1305.

33. van Tellingen O, Beijnen JH, Verweij J, et al. Rapid esterase-sensitive breakdown of polysorbate 80 and its impact on the plasma pharmacokinetics of docetaxel and metabolites in mice. Clin Cancer Res 1999;5:2918-2924.

34. U.S. Department of Health and Human Services, Food and Drug Administration Guidance for industry: Population Pharmacokinetics. Rockville MF, USA 1999.

Chapter 4.2.1

Development and validation of a population pharmacokinetic model of paclitaxel in cancer patients

HJG Desirée van den Bongard, Ron AA Mathôt, Jan HM Schellens and Jos H Beijnen

Summary

Paclitaxel is an anticancer agent with non-linear pharmacokinetic behaviour. The purpose of this study was to develop and to validate a population pharmacokinetic model for paclitaxel in cancer patients. A population pharmacokinetic model was developed using 100 total plasma concentration-time profiles of paclitaxel after 3- and 24-hour intravenous infusion in 61 patients (dose range 100-250 mg/m²). Population pharmacokinetic parameters were estimated by non-linear mixed effects modelling (NONMEM). The relationships between 13 covariates and the pharmacokinetic parameters of paclitaxel were tested. The validity of the final model was evaluated by the bootstrap resampling method of the data and performing a predictive check.

The data were best described by a 3-compartment model with saturable transport to one peripheral compartment and Michaelis-Menten elimination from the central compartment. The following population pharmacokinetic parameter estimates were obtained: volume of the central compartment (V=12.1 L), maximal transport rate from the central compartment to peripheral compartment 1 (Tmax=216 µmol/h), plasma concentration at half Tmax (Tm=2.59 µmol/L), intercompartmental rate constants (k_{21}=0.916 h^{-1}, k_{13}=1.63 h^{-1}, k_{31}=0.0722 h^{-1}), maximal elimination rate (Vmax=47.0 µmol/h), and plasma concentration at half Vmax (Km=0.656 µmol/L). Inter-individual variability for V, Tmax and Vmax was 20%, 26% and 22%, respectively. Inter-occasion variability could be quantified for k_{21} (15%), k_{13} (26%), k_{31} (39%), and Vmax (18%). Body surface area (BSA) was significantly correlated with V and Tmax ($p < 0.005$). The fits of 1000 bootstrap replicates to the data and the predictive check confirmed the robustness of the model.

This developed population model adequately describes the pharmacokinetic parameters of paclitaxel in cancer patients. Furthermore, it has been demonstrated that BSA guided dosing for paclitaxel is important. This population model forms the basis of future studies with pharmacokinetically guided dosing of paclitaxel.

Introduction

Paclitaxel (Taxol®) is a taxane derivative that acts on microtubular structures by binding directly to tubulin, causing microtubuli stabilisation that arrests cell division in the G2/M phase of the cell cycle. The drug has a profound antitumour activity against a variety of solid tumours, especially against lung, breast, ovarian, and head and neck tumours.[1,2]

For paclitaxel, non-linear pharmacokinetics in plasma have been described in several studies.[3-10] In recently published reports the non-linearity has been attributed to its formulation vehicle Cremophor EL that forms micelles in plasma in which paclitaxel is entrapped.[11-15] Relationships between plasma pharmacokinetics and pharmacodynamics of paclitaxel were reported in ovarian cancer patients. Myelotoxicity was related to the duration of the paclitaxel concentration in plasma above the threshold levels of 0.05 or 0.1 µmol/L.[3,4] Furthermore, paclitaxel doses higher than 175 mg/m² have been reported to result in higher response rates and more neutropenia in patients with non-small cell lung cancer (NSCLC).[16,17] In a retrospective analysis of a phase I study of paclitaxel plus carboplatin in 55 NSCLC patients, a longer survival was observed in patients with a plasma paclitaxel concentration above 0.1 µmol/L equal to or longer than 15 hours compared to the survival in patients with a duration time above the threshold concentration shorter than 15 hours.[5] Based on these established pharmacokinetic-pharmacodynamic relationships, pharmacokinetically guided dosing may be used to attain paclitaxel plasma concentrations above 0.1 µmol/L during 15 hours or longer. In the present study, a population pharmacokinetic model was developed based on concentration-time data of patients treated at various paclitaxel doses. A covariate analysis was performed and the final population model was validated, in contrast to other pharmacokinetic studies of paclitaxel. The population model was developed in order to evaluate the feasibility of pharmacokineticcally guided dosing of paclitaxel in a future study.

Methods

Patient population

Plasma concentration-time data (100 courses) of paclitaxel were collected during safety and pharmacokinetic studies of paclitaxel that were performed in 61 cancer patients in multi-center studies. The results of these studies have been published in detail elsewhere.[5,18] In these studies paclitaxel was infused intravenously with co-infusion of carboplatin in chemonaive patients with NSCLC IIIB and IV (n=55, 3-h iv infusion), and paclitaxel as a single agent in with platinum pre-treated advanced ovarian cancer patients (n=6, 24-h iv infusion). Patient characteristics are summarised in Table 1.

Paclitaxel (Taxol®, Bristol Myers Squibb, Syracuse, NY) was provided as a sterile 6 mg/ml solution and dissolved in Cremophor EL:Ethanol 1:1, v/v. Prior to administration this solution was diluted with 500-1000 ml 0.9% sodium chloride solution to a final paclitaxel concentration between 0.3 and 1.2 mg/ml. As Cremophor EL may leach plasticiser from the

infusion lines, an adapted PVC-free administration equipment was used. Written informed consent was obtained from all patients. Standard pre-medication with dexamethasone (20 mg orally at 12 and 6 hours prior to paclitaxel administration), clemastine (2 mg iv 30 minutes prior to paclitaxel administration) and cimetidine (300 mg iv shortly prior to paclitaxel administration) was administered to prevent hypersensitivity reactions. If indicated, 5-HT_3-receptor antagonists were administered intravenously as standard anti-emetic agent. The studies were approved by the Medical Ethics Committees of the participating hospitals.

Pharmacokinetic sampling and bio-analysis

Plasma concentration-time data were obtained by pharmacokinetic sampling during the first (n=59) and the second course (n=41). The samples for paclitaxel analysis were collected in heparinised tubes. In the 3-hour infusion schedules, blood samples were taken prior to the start of the infusion, at 1 and 2 hours after the start, at the end of the infusion, at 5, 10, 15, 30, 45, and 60 minutes, and at 1.5, 2, 3, 4, 6, 8, 10, 12, 24, 30, and 48 hours after the end of the infusion. In the 24-hour infusion schedules, blood samples were taken prior to the start of

Table 1. Patient characteristics (n=61) and serum parameter values

	Number	Median	Range
Patient characteristics			
Female	20		
Male	41		
Number of courses with pharmacokinetic data			
First course	59		
Second course	41		
Dose range paclitaxel (in mg/m^2)			
3-hour infusion	55		100-250
24-hour infusion	6		135-175
Dose range carboplatin (in mg/m^2)			
3- hour infusion	55		300-400
Primary site of disease			
Lung	55		
Ovarian	6		
Age (in years)		55	38-75
WHO Performance status			
0	18		
1	29		
2	14		
BSA (in m^2)		1.81	1.50-2.22
Biochemical parameters			
Creatinine (in μmol/L)		77	37-144
AST (in U/L)		13	3-62
ALT (in U/L)		13	1-150
Alkaline Phosphatase (in U/L)		82	50-539
GGT (in U/L)		34	10-384
Albumin (in g/L)		35	18-52
Total bilirubin (in μmol/L)		6	3-14

BSA = Body surface area; AST = aspartate aminotransferase; ALT = alanine-amino transferase; GGT = gamma-glutamyl-transpeptidase; LDH = lactate dehydrogenase; WHO = World Health Organisation.

the infusion, at 3, 10, 20 hours after the start of the infusion, at the end of the infusion, 5, 15, 30, and 60 minutes, and 2, 4, 8, 12, 24, 30 hours after the end of the infusion. Whole blood was centrifuged immediately after withdrawal during 5 minutes at 3000 rpm, and the plasma fraction was stored at −20°C until analysis. The paclitaxel concentrations in plasma were determined by a validated isocratic high-performance liquid chromatographic (HPLC) method with solid-phase extraction as the sample pre-treatment procedure, as has been described in detail elsewhere.[19,20] The quantitaion range of the HPLC method was 10-10,000 ng/ml.

Population pharmacokinetic analysis

The program NONMEM (nonlinear mixed effect modelling (NONMEM, version V 1.1, double precision) using the NMTRAN pre-processor and the PREDPP package (ADVAN 6), operating on an MS-DOS computer.[21] The POSTHOC option in NONMEM was used to obtain Bayesian estimates of the pharmacokinetic parameters. All concentration-time data were logarithmically transformed, and the first order method was used in all of the analysis processes. The first order conditional estimate method was not used in this population analysis due to its high computational intensity. The model building procedure consisted of the following three-step approach.[22]

Basic population pharmacokinetic model

The first step consisted of the development of a basic population pharmacokinetic model. The data were best described by a 3-compartment model with Michaelis-Menten elimination from the central compartment, saturable transport to the first peripheral compartment and linear distribution to the second peripheral compartment (Figure 1). The following

Figure 1. Three-compartment model with Michaelis-Menten elimination from the central compartment V. Tmax is the maximal transport rate to the first peripheral compartment, and Tm is the plasma concentration of paclitaxel at half Tmax. k21, k13 and k31 indicate the intercompartmental rate constants. Vmax is the maximal elimination rate, and Km is the plasma concentration of paclitaxel at half of the Vmax
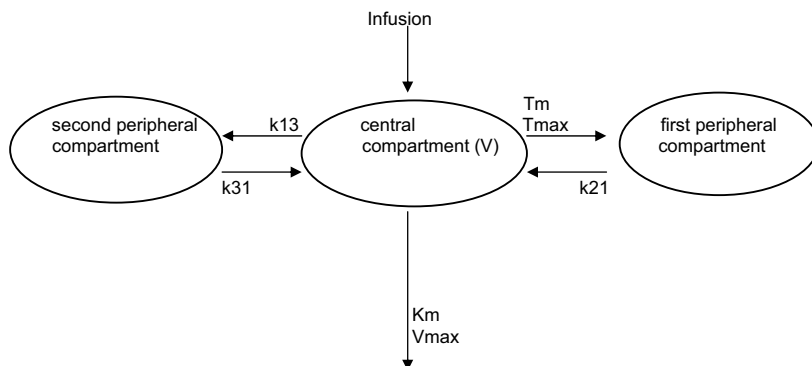
pharmacokinetic parameters were estimated: volume of the central compartment (V in L), the maximal transport rate to the first peripheral compartment (Tmax in μmol/h), the total plasma concentration of paclitaxel at half of the Tmax (Tm in μmol/L), intercompartmental rate constants from the peripheral compartments to the central compartment (k21 and k31 in h^{-1}) and from the central compartment to the second peripheral compartment (k13 in h^{-1}), the maximal elimination rate (Vmax in μmol/h), and the plasma concentration of paclitaxel at half of the Vmax (Km in μmol/L). Standard errors for all parameters were calculated using the COVARIANCE option in the NONMEM program. Inter-individual variability in V and Tmax was estimated using a proportional error model. For V the inter-individual variability was defined as in equation 1:

$$V_i = V_{pop} * (1 + \eta_i^V) \qquad\qquad \text{equation 1}$$

where V_i represents the V of the ith individual in L, V_{pop} is the typical population value, and η_i^V is the inter-individual random effect that is normally distributed with mean 0 and variance ω^2.

Variability in the individual pharmacokinetics between the first and second course (inter-occasion variability) was estimated using a proportional model. For instance, inter-occasion variability in Vmax was defined as in equation 2:

$$Vmax_i = Vmax_{pop} * (1 + \kappa_i^{Vmax}) \qquad\qquad \text{equation 2}$$

where $Vmax_j$ represents the Vmax of the ith individual in μmol/h, $Vmax_{pop}$ is the typical population value of Vmax and κ_i^{Vmax} is the inter-occasion random effect that is normally distributed with mean 0 and variance π^2.

Residual variance was modelled using an additive error model:

$$\ln (C_{obs,ij}) = \ln (C_{pred,ij}) + \varepsilon \qquad\qquad \text{equation 3}$$

where $C_{obs,ij}$ is the observed concentration and $C_{pred,ij}$ is its respective prediction. ε is a random variable with mean 0 and variance σ^2.

The inter-individual variability in residual variance was accounted for by the assumption that the population was a mixture of 2 subpopulations (subpopulations 1 and 2) differing in σ^2. Several criteria were taken into account when comparing the basic models. The value of the objective function (OFV), that is equal to minus twice the log likelihood of the data, the reliability of parameters estimates (according to the standard error values of the parameter

estimates), and the fit of the model to the data (goodness of fit plots). The difference in the OFV of models approximates to a chi-squared-distribution with 1 degree of freedom. The significance level was set at p < 0.001, which is associated with an OFV decrease of 10.8. The goodness of fit plots were studied in the program Xpose (Xpose, Version 2.0, Uppsala University, Sweden) as implemented in the S-Plus statistical package (version 2000, Mathsoft, Cambridge, Mass.).[23]

Intermediate model

For each subject, individual pharmacokinetic parameters were calculated using the individual paclitaxel plasma concentration-time data and the population pharmacokinetic parameter estimates obtained in the first step. The individual Bayesian estimates were plotted against the demographic factors and blood chemistry parameters (=covariates). The relations between the covariates and the Bayesian parameter estimates of each individual patient were investigated graphically in the program Xpose. Thirteen covariates were investigated for their influence on the pharmacokinetics of paclitaxel (age, gender, weight, body surface area (BSA), performance status according to the World Health Organisation (PS), serum creatinine, serum alanine-aminotransferase (ALT), serum aspartate-aminotransferase (AST), serum alkaline phosphatase, serum gamma-glutamyl-transpeptidase (GGT), serum bilirubin, serum lactate dehydrogenase (LDH), and serum albumin). Since the number of patients treated with paclitaxel as a single agent was low (n=6) compared to the number of patients treated with paclitaxel in combination with carboplatin (n=55), we have not studied the influence of carboplatin on the pharmacokinetic behaviour of paclitaxel.

The selected covariates that showed a graphical relation with a pharmacokinetic parameter were tested by univariate analysis. These covariates were entered individually into the basic population pharmacokinetic model by forward inclusion. Continuous covariates, e.g. BSA, were centred to their median values.[24] For instance, the relationship between V and BSA was described as in equation 4:

$$V = \theta_1 * (BSA / 1.81)^{\theta_{12}} \qquad\qquad \text{equation 4}$$

where V is expressed in L, θ_1 represents the population value of V of a (median) patient with a BSA of 1.81 m², and θ_{12} is an exponential factor.

Relationships with dichotomous covariates were investigated as described in equation 5:

$$Vmax = \theta_8 * \theta_{14}^{FLAG} \qquad\qquad \text{equation 5}$$

where Vmax is expressed in µmol/h, θ_8 the Vmax value in patients with PS 0 or 1 (FLAG = 0), and θ_{14} the change in Vmax in patients with PS 2 (FLAG = 1).

During the forward inclusion of the covariates in the basic model, the significance level was set at $p < 0.01$ that is associated with a decrease in the NONMEM objective function value of > 6.7. All significant covariates were incorporated into an intermediate multivariate model.

Final population pharmacokinetic model

The development of the intermediate model was followed by multivariate analysis that consisted of a stepwise backward elimination procedure. Covariates were retained in the intermediate model when elimination of the covariate caused an increase in the NONMEM objective function value of > 7.9 that is associated with a significance level of $p < 0.005$.

The validity of the interindividual variability model was checked by evaluating correlations between the individual random effects (η) of the pharmacokinetic parameters that were included in the model.

The stability and performance of the final model was evaluated by the bootstrap resampling technique as implemented in the computer program Wings for NONMEM (WFN version 3) designed by Dr. N.H. Holford and available via the internet (http://wfn.sourceforge.net).[25] The median parameter estimates and 95% confidence intervals obtained from 1000 bootstrap replications were compared with those obtained from the original data set.

A predictive check was performed for the final population pharmacokinetic model.[26,27] One thousand data sets were simulated from the original concentration-time data of each administered dose (100, 125, 150, 175, 200, 225 and 250 mg/m^2 in a 3-h iv infusion, 135 and 175 mg/m^2 in a 24-h iv infusion). For each dose-level the mean and corresponding 95% confidence interval of the time above the plasma concentration 0.1 µmol/L of the simulated concentration-time data was calculated. The corresponding observed means of each dose-level were compared with the 95% predicted intervals of the simulated means.

Results

Population pharmacokinetic analysis

Basic population pharmacokinetic model

Two- and three-compartment models with linear and saturable distribution, first order elimination and Michaelis-Menten elimination were fitted to the plasma concentrations versus time curves of paclitaxel. According to the objective function values (OFV), the standard error values, and the goodness of fit plots, it appeared that the data were best described by a 3-compartment model with Michaelis-Menten elimination and saturable distribution to peripheral compartment 1 (Figure 1). All pharmacokinetic parameters were estimated accurately according to the relative standard error ≤ 29%. The patient population was divided in 2 subpopulations, the fraction of the patients belonging to subpopulation 1 was 16.5%. Inter-individual variability was determined for V (23%) and Tmax (27%).

Inter-occasion variability was determined for V (12%), k21 (17%), k13 (22%), k31 (42%), and Vmax (26%). Inclusion of inter-individual variability for the other pharmacokinetic parameters did not improve the fit. This should not be interpreted as an absence of inter-individual variability in these parameters. It indicates that the data do not contain sufficient information to estimate the inter-individual and inter-occasion variability of these parameters. The residual variabilities of subpopulations 1 and 2 consisted of an additional error of 0.316 and 0.123, respectively.

Intermediate model

In the second step, the individual Bayesian estimates of the pharmacokinetic parameters were calculated using the individual paclitaxel plasma concentration-time data and the population pharmacokinetic parameter estimates obtained in the basic population model. The graphical analysis of the plots of covariates versus individual pharmacokinetic parameters indicated a possible relationship between BSA, weight, gender and V; between age, gender, BSA and Tmax; and between BSA, PS and Vmax. Forward inclusion (p < 0.01) of these covariates in the basic model resulted in an intermediate multivariate model with the following significant relations between pharmacokinetic parameters and covariates: BSA and V, BSA and Tmax, BSA and Vmax, and PS and Vmax.

Final population pharmacokinetic model

The development of the intermediate model was followed by stepwise backward elimination (p < 0.005) of these covariates in the basic population pharmacokinetic model. BSA appeared to be significantly related to V and Tmax, and PS with Vmax. Inclusion of these covariates resulted in a decrease in the objective function value of 65.1 compared to the basic population model. However, validation of the obtained population model with the bootstrap resampling method resulted in a non-significant relation between PS of 2 and Vmax due to the inclusion of 1 in the 2.5%-97.5% percentile range (0.88-1.65) of θ_{14} (equation 5). Consequently, the correlation between PS and Vmax was deleted from the model. The objective function value of the obtained final model was 122.6 points lower than the objective function of the basic model. The significant relationship between the covariates and the pharmacokinetic parameters are given in equations 6 and 7:

$$V = 12.1 * (BSA/1.81)^{1.16} \qquad\qquad \text{equation 6}$$

$$Tmax = 216 * (BSA/1.81)^{1.05} \qquad\qquad \text{equation 7}$$

where V is expressed in L, BSA in m^2 and Tmax in µmol/h.

Both equations indicate that V and Tmax increase with increasing BSA.

Table 2. Population parameters of the final population pharmacokinetic model of paclitaxel and corresponding parameter estimates obtained by 1000 bootstrap resamplings

	Final population model		1000 bootstrap replicates	
	Estimate	RSE (in %)	Median	2.5-97.5%
Pharmacokinetic parameter				
V (L)	12.1	5.4	12.0	10.7-13.8
Influence of BSA (θ_{12})[a]	1.16	33	1.12	0.231-1.86
Tmax (µmol/h)	216	5.6	219	194-248
Influence of BSA (θ_{13})[b]	1.05	49	0.999	0.224-2.271
Tm (µmol/L)	2.59	10	2.66	2.18-3.40
k21 (h^{-1})	0.916	7.0	0.914	0.779-1.080
k13 (h^{-1})	1.63	8.7	1.61	1.32-1.95
k31 (h^{-1})	0.0722	7.9	0.0713	0.061-0.0836
Km (µmol/L)	0.656	15	0.684	0.460-0.905
Vmax (µmol/h)	47.0	10	48.2	36.5-58.1
Population 1-2	0.380	27	0.366	0.119-0.574
Inter-individual variability				
IIV-V (%)	20	31	20	13-26
IIV-Tmax (%)	26	27	25	17-33
IIV-Vmax (%)	22	33	21	0-29
Inter-occasion variability				
IOV- k21 (%)	15	48	16	7-23
IOV- k13 (%)	26	25	25	18-31
IOV-k31 (%)	39	30	39	29-53
IOV-Vmax (%)	18	32	19	13-29
Residual error				
Additional error 1	0.202	11.0	0.203	0.167-0.301
Additional error 2	0.105	7.6	0.103	0.0919-0.129

[a] $V = \theta_1 * (BSA /1.81)^{\theta 12}$
[b] $Tmax = \theta_2 * (BSA /1.81)^{\theta 13}$
where BSA is expressed in m^2, θ_1 and θ_2 represent the population value of V and Tmax, respectively, of a patient with a (median) BSA of 1.81 m^2, θ_{12} and θ_{13} are exponential factors.
Additional error = 1 residual variability of subpopulation 1; Additional error 2 = residual variability of subpopulation 2; BSA = body surface area; IIV = inter-individual variability; IOV = inter-occasion variability; k21 = rate constant from the first peripheral compartment to the central compartment; k13 = rate constant from the central to the second peripheral compartment; k31 = rate constant from the second peripheral to the central compartment; Km = plasma concentration at half Vmax; Population 1-2 = fraction of the patient population (n = 61) belonging to subpopulation 1; RSE = Relative standard error; Tmax = maximal transport rate from the central to the first peripheral compartment; Tm = plasma concentration at half Tmax; V = volume of the central compartment; Vmax = maximal elimination rate.

The correlation between the inter-individual variability and the inter-occasion variability of the pharmacokinetic parameters was evaluated. The matrix plots showed no correlation (data not shown) and were not included in the final model. The population pharmacokinetic parameters of the final model including the standard errors, inter-individual variability, and the residual errors are summarised in Table 2. In the final model, the inter-individual variability of V, Tmax and Vmax was 20%, 26% and 22% (versus an inter-individual variability of V and Tmax of 23% and 27% in the basic model, respectively. The goodness of fit plots of the observed concentrations versus the predicted concentrations of the final model are depicted in Figure 2A. In Figure 2B the observed concentrations versus the

Figure 2. Goodness of fit plots for the final population pharmacokinetic model. Plot of the observed logarithmically transformed concentrations *versus* the model predictions of the paclitaxel concentrations (A). Plot of logarithmically transformed observed concentrations *versus* the individual Bayesian predictions of the paclitaxel concentrations (B). The solid line is the line of identity
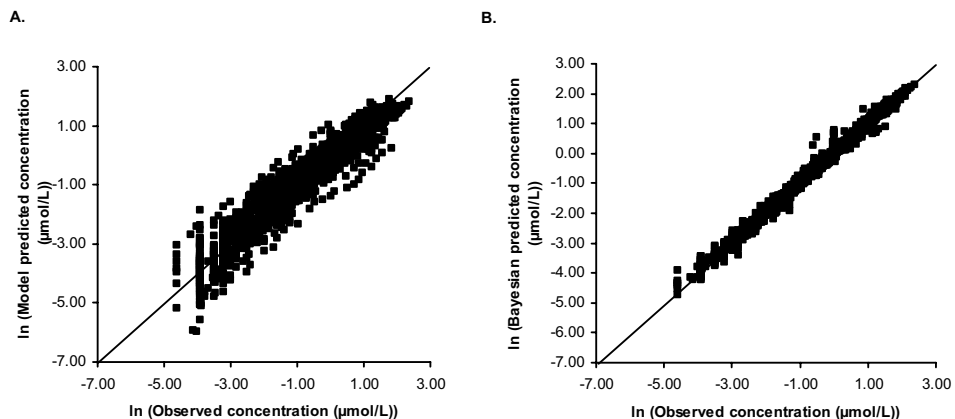
Table 3A. Results of the predictive check performed for all dose-levels. After the intravenous infusion of paclitaxel in 3 hours

Dose-level (mg/m^2)	Observed mean duration of time concentration > 0.1 µmol/L (h)	95% prediction interval (h)
100 (n=6)	6.7	6.0-10.7
125 (n=7)	8.8	7.4-13.4
150 (n=6)	9.9	8.1-16.2
175 (n=7)	17.1	11.5-22.7
200 (n=8)	17.1	12.5-23.2
225 (n=18)	20.9	17.5-25.7
250 (n=3)	21.6	14.4-34.2

Table 3B. Results of the predictive check performed for all dose-levels. After the intravenous infusion of paclitaxel in 24 hours

Dose-level (mg/m^2)	Observed mean duration of time concentration > 0.1 µmol/L (h)	95% predicted CI (h)
135 (n=2)	26.7	ND
175 (n=4)	28.0	22.5-28.9

ND = not determined.

individual predicted concentrations based on the individual concentrations and the Bayesian parameter estimates are depicted.

The final model was fitted to 1000 bootstrapped samples of the data in order to evaluate its stability and performance. The values of the parameter estimates obtained by 1000 bootstrap replicates are included in Table 2. Median values of the parameter estimates of

the final model were within 6.7% of the parameter value calculated in NONMEM. The 95% confidence interval of the parameter estimates of the final model calculated in NONMEM was in accordance with the 2.5-97.5 percentile range of the parameter obtained by 1000 bootstrap replicates of the final model. This indicates that the robustness of the final model of paclitaxel was adequate.

The results of the predictive check for all dose levels and infusion schedules are summarised in Table 3A and 3B. The observed mean durations of time that the total paclitaxel concentration in plasma was above 0.1 µmol/L were compared with values obtained after simulation of 1000 paclitaxel concentration-time curves. All observed means were in the 95% predicted intervals of the simulated means at all dose-levels. Moreover, the simulation revealed that after the first intravenous infusion of the standard dose of 175 mg/m^2 in 3 hours, the duration of time that the concentration was higher than 0.1 µmol/L during 15 hours or longer in 52% of the patients.

Discussion

The purpose of this study was to develop a population pharmacokinetic model of paclitaxel in cancer patients. The pharmacokinetic behaviour of paclitaxel has been described based on 2- or 3-compartment models in combination with saturable distribution and Michaelis-Menten elimination.[4,9,10] In our study, the plasma concentration versus time data were best described by a three-compartment model with saturable transport to one peripheral compartment and Michaelis-Menten elimination from the central compartment after intravenous infusion in cancer patients. Inter-individual variability was determined for V, Tmax and Vmax, and inter-occasion variability for k21, k13, k31 and Vmax. Further inclusion of inter-individual or inter-occasion variability did not improve the fit. BSA could partially explain the inter-individual variability in the volume of the central compartment and the maximal transport rate to one peripheral compartment; the two pharmacokinetic parameters increased with increasing BSA.

The non-linear pharmacokinetic behaviour of paclitaxel has also been described in various pharmacokinetic models as both saturable elimination and/or saturable distribution.[4,9,10] These pharmacokinetic models include a two-compartment model with saturable tissue distribution and saturable elimination based on total plasma concentration-time data of 30 children with solid tumours, a four-compartment model with saturable distribution and saturable elimination based on total paclitaxel and 6α-hydroxypaclitaxel concentrations in 30 patients after intravenous infusion, and a three-compartment model with saturable transport based on total plasma concentration-time data of 21 patients.[4,9,10] Our pharmacokinetic population model is also a pharmacokinetic 3-compartment model with saturable transport based on total plasma concentration-time data of 61 cancer patients. The parameter estimates do not have the same values in both population models except for the value of

the apparent volume of distribution. In addition, we performed a covariate analysis, and the stability of our final model was demonstrated by the bootstrap resampling method, which is considered to be a powerful internal validation technique.[28] Furthermore, the validity was confirmed by the predictive check. Predictions of time that the paclitaxel > 0.1 µmol/L were similar to the observed values for all studied dose-levels (Table 3).[28]

Several investigators have studied the pharmacokinetic/pharmacodynamic relation of paclitaxel with the emphasis on myelotoxicity. Most studies revealed a threshold model in which the myelotoxicity is related to the duration of exposure above a certain threshold value (0.05 or 0.1 µmol/L).[3;4] Furthermore, an improved survival in non-small cell lung cancer patients (stage IIIB and IV) with a plasma concentration above 0.1 µmol/L during a period longer than 15 hours was observed compared to patients in which this threshold value was shorter than 15 hours above 0.1 µmol/L.[5] Therefore, we initiated a study to investigate whether it is feasible to attain a duration of 15 hours or longer above the threshold value in all patients by pharmacokinetically guided dosing. For this dose-individualisation study we developed and validated this population model of paclitaxel. The population model is an empirical model since it is well known that the non-linear behaviour of paclitaxel is caused by the formulation vehicle Cremophor EL due to the formation of micelles in blood *in vitro*.[11-14] These micelles act as high-affinity drug-transporting sites for paclitaxel that result in a decreased free paclitaxel fraction in plasma and a reduced uptake of paclitaxel in red blood cells.[11-15] The first peripheral compartment in our population model might represent the Cremophor EL micelles in plasma according to the saturated transport to this compartment. The second peripheral compartment may be represented by the peripheral tissues.

Recently, a mechanism-based population model was developed based on free and total paclitaxel concentrations in plasma, total blood concentrations, and Cremophor EL concentrations obtained in 26 patients.[29] Nevertheless, although this is a more physiologic model, it has not been validated. Since no free plasma and total blood concentrations were present in our data-set, and our empirical model has been proven to be stable and has a good performance, it will be used for a future dose-adaptation study in NSCLC patients treated with paclitaxel and carboplatin. The results of the predictive check showed that in 52% of the patients that received 175 mg/m² of paclitaxel, the plasma concentration was higher than 0.1 µmol/L longer than 15 hours. According to these results, a dose adaptation should be performed in 48% of the patients after the infusion of the first course of paclitaxel.

In conclusion, we have shown that the non-linear pharmacokinetics of paclitaxel after a 3- and 24-hour intravenous infusion can accurately be described by the validated final population pharmacokinetic model. This robust population model can be used in pharmacokinetically guided dosing of paclitaxel.

References

1. Whizzing MT, Sewberath Misser VH, Pieters RC, et al. Taxanes: a new class of antitumor agents. Cancer Invest 1995;13:381-404.

2. Kearns CM. Pharmacokinetics of the taxanes. Pharmacotherapy 1997;17:105S-109S.

3. Huizing MT, Keung ACF, Rosing H, et al. Pharmacokinetics of paclitaxel and metabolites in a randomized comparative study in platinum-pre-treated ovarian cancer patients. J Clin Oncol 1995;11:2127-35.

4. Gianni L, Kearns CM, Gianni A, et al. Nonlinear pharmacokinetics and metabolism of paclitaxel and its pharmacokinetic/pharmacodynamic relationships in humans. J Clin Oncol 1995;13:180-90.

5. Huizing MT, Giaccone G, Van Warmerdam LJC, et al. Pharmacokinetics of paclitaxel and carboplatin in a dose-escalating and sequencing study in patients with non-small-cell lung cancer. J Clin Oncol 1997;15:317-29.

6. Mross K, Holländer N, Hauns B, et al. The pharmacokinetics of a 1-h paclitaxel infusion. Cancer Chemother Pharmacol 2000;45:463-470.

7. Ohtsu T, Sasaki Y, Tamura T, et al. Clinical pharmacokinetics and pharmacodynamics of paclitaxel: a 3-hour infusion versus a 24-hour infusion. Clin Cancer Res 1995;1:599-606.

8. Nannan Panday VR, Ten Bokkel Huinink WW, Vermorken JB, et al. Pharmacokinetics of paclitaxel administered as a 3-hour or 96-hour infusion. Pharmacol Res 1999;40:67-74.

9. Sonnichsen DS, Hurwitz CA, Pratt CB, et al. Saturable pharmacokinetics and paclitaxel pharmacodynamics in children with solid tumors. J Clin Oncol 1994;12:532-538.

10. Karlsson MO, Molnar V, Freijs A, et al. Pharmacokinetic models for the saturable distribution of paclitaxel. Drug Metab Dispos 1999;27:1220-1223.

11. Van Tellingen O, Huizing MT, Nannan Panday VR, et al. Cremophor EL causes (pseudo-) non-linear pharmacokinetics of paclitaxel in patients. Br J Cancer 1999;81:330-335.

12. Sparreboom A, van Tellingen O, Nooijen WJ, et al. Nonlinear pharmacokinetics of paclitaxel in mice results from the pharmaceutical vehicle cremophor EL. Cancer Res 1996;56:2112-2115.

13. Sparreboom A, van Zuylen L, Brouwer E, et al. Cremophor EL-mediated alteration of paclitaxel distribution in human blood: Clinical pharmacokinetic implications. Cancer Res 1999;59:1454-1457.

14. Van Zuylen L, Karlsson, MO, Verweij, J, et al. Pharmacokinetic modeling of paclitaxel encapsulation in cremophor EL micelles. Cancer Chemother Pharmacol 2001;47:309-318.

15. van Zuylen L, Gianni L, Verweij J, et al. Inter-relationships of paclitaxel disposition, infusion duration and cremophor EL kinetics in cancer patients. Anti-Cancer Drugs 2000;11:331-337.

16. Kosmidis P, Mylonakis N, Skarlos D, et al. Paclitaxel (175 mg/m²) plus carboplatin (6 AUC) versus paclitaxel (225 mg/m²) plus carboplatin (6AUC) in advanced non-small-cell lung cancer (NSCLC): A multicenter randomized trial. Ann Oncol 2000;11:799-805.

17. Giaccone G, Huizing M, Postmus PE, et al. Dose-finding and sequencing study of paclitaxel and carboplatin in non-small cell lung cancer. Sem Oncol 1995;22 (suppl 9):78-82.

18. Eisenhauer EA, ten Bokkel Huinink WW, Swenerton KD, et al. European-Canadian randomized trial of taxol in relapsed ovarian cancer: high vs low dose and long vs short infusion. J Clin Oncol 1994;12:2654-66.

19. Willey TA, Bekos EJ, Gaver RC, et al. A high performance liquid chromatographic procedure for the quantitative determination of paclitaxel in human plasma. J Chromatogr 1993;621:231-236.

20. Huizing MT, Sparreboom A, Rosing H, et al. Quantification of paclitaxel metabolites in human plasma. J Chromatogr 1995;674:261-268.

21. Boeckmann AJ, Sheiner LB, Beal SL. NONMEM Users Guide - Part V Introductory Guide. NONMEM Project Group. University of California at San Francisco, 1994.

22. Maitre PO, Bührer M, Thomson D, et al. A three-step approach combining bayesian regression and nonmem population analysis application to midazolam. J Pharmacokin Biopharm 1991;19: 377-384.

23. Jonsson EN, Karlsson MO. Xpose – an S-PLUS based population pharmacokinetic/ pharmacodynamic model building aid for NONMEM. Comput Methods Programs Biomed 1999;58:51-64.

24. Jonsson EN, Karlsson MO. Automated covariate model building within NONMEM. Pharm Res 1998;15:1463-1468.
25. Ette EI. Stability and performance of a population pharmacokinetic model. J Clin Pharmacol 1997;37:486-495.
26. Yano Y, Beal SL, Sheiner LB. Evaluating pharmacokinetic/pharmacodynamic models using the posterior predictive check. J Pharmacokin Pharmacodyn 2001;28:171-192.
27. Friberg LE, Freijs A, Sandström M, et al. Semiphysiological model for the time course of leukocytes after varying schedules of 5-fluorouracil in rats. J Pharmacol Exp Ther 2000;295:734-740.
28. U.S. Department of Health and Human Services, Food and Drug Administration. Guidance for industry: Population Pharmacokinetics. Rockville MF, USA, 1999.
29. Henningsson A, Karlsson MO, Viganò L, et al. Mechanism-based pharmacokinetic model for paclitaxel. J Clin Oncol 2001;19:4065-4073.

Chapter 4.2.2

A feasibility study of Bayesian pharmacokinetically guided dosing of paclitaxel in patients with non-small cell lung cancer

HJG Desirée van den Bongard, Ron AA Mathôt, Alwin DR Huitema, Hilde Rosing, Ciska Koopman-Kroon, Paul Baas, Nico van Zandwijk, Marianne Keessen, Jos H Beijnen and Jan HM Schellens

Summary

Relationships between the time above a threshold concentration of paclitaxel in plasma and the drug's efficacy and toxicity were previously reported in cancer patients. The purpose of this study was to evaluate the feasibility of Bayesian dose individualisation to attain paclitaxel plasma concentrations above 0.1 µmol/L during 15 hours or longer. Patients with non-small cell lung cancer were treated with paclitaxel and carboplatin. During the first course, the standard dose (175 mg/m²) of paclitaxel was administered intravenously (iv) in 3 hours. Carboplatin was administered iv in a dose calculated according to the Calvert formula with a target area under the concentration-time curve of 6 mg/ml*min. The paclitaxel dose was individualised in subsequent courses based on a previously developed population pharmacokinetic model of paclitaxel and on the observed paclitaxel concentrations in plasma during the previous course(s). The paclitaxel dosage was individualised to achieve a plasma concentration of 0.1 µmol/L during 15 hours or longer in the subsequent course.

At interim analysis, 11 patients had been included who received 44 evaluable courses. Eleven of these courses (first course) consisted of standard dosing (175 mg/m²), and 33 were individualised courses (175 mg/m² or higher). During the first course, the time above the threshold concentration ranged from 11.6 to 31.6 hours; for 7 patients (64%) the duration of time above the threshold concentration was longer than 15 hours (range 15.4-31.6 hours). During the second course, the time above the threshold concentration was longer than 15 hours in 9 of the 11 patients (82%) ranging from 17.6-25.3 hours. During the third course and subsequent courses, the drug threshold concentration was longer than 15 hours in 15 of the 22 courses (68%). Dose increments, ranging from 180 to 295 mg/m², were performed in 14 of the 33 individualised courses (4 in the second course).

Toxicity consisted mainly of haematologic toxicity (granulocytopenia grade 3/4 in 82% of the patients). In conclusion, the preliminary results indicate that pharmacokinetically guided dosing of paclitaxel in the second course resulted in a higher percentage of patients with a duration of time that the paclitaxel concentration of 0.1 µmol/L was achieved during 15 hours or longer compared to the first course that consisted of standard dosing of paclitaxel. More patients will be included to demonstrate the feasibility of individualised dosing in subsequent courses.

Introduction

Paclitaxel (Taxol®) is a taxane derivative that acts on microtubular structures by binding directly to tubulin, causing microtubular stabilisation that arrests cell division in the G2/M phase of the cell cycle. The drug has a profound antitumour activity against a variety of solid tumours, especially against lung, breast, ovarian, and head and neck tumours.[1,2] The combination of paclitaxel with a platinum compound is one of the combination chemotherapy schedules used in the treatment of patients with advanced non-small cell lung cancer (NSCLC).[3] To offset cisplatin-related toxicity, cisplatin has been substituted by carboplatin. In a randomised study of paclitaxel in combination with cisplatin or carboplatin, the latter combination revealed no significant difference in survival and response rates.[3,4]

Relationships between plasma pharmacokinetics and pharmacodynamics of paclitaxel have been reported in ovarian cancer patients whereby myelotoxicity was related to the time period in which paclitaxel concentrations in plasma were above 0.05 or 0.1 µmol/L.[5,6] In a retrospective analysis of a phase I study of 55 NSCLC patients, a longer survival was observed in patients with a time above a threshold paclitaxel concentration of 0.1 µmol/L longer than 15 hours, compared to the survival in patients in which the time above the threshold concentration was shorter than 15 hours.[7] The purpose of this study was to evaluate whether pharmacokinetically guided dosing is feasible to attain paclitaxel concentrations above 0.1 µmol/L during 15 hours or longer and to document preliminary activity and toxicity of this approach in first line of treatment with chemotherapy for advanced NSCLC.

Materials and methods

Patients

Chemonaive patients with histologically proven NSCLC stage IIIB or stage IV were included in the study. Eligibility criteria included: a performance status ≤ 2 on the World Health Organisation (WHO) scale, life expectancy of ≥ 3 months to allow adequate follow-up of toxicity, adequate haematopoietic (absolute neutrophil count $\geq 1.5*10^9$/L, platelet count $\geq 100*10^9$/L), hepatic (total bilirubin ≤ 25 µmol/L), aspartate aminotransferase (AST), and alanine aminotransferase (ALT) ≤ 2.5 times the normal upper limit (in case of liver metastasis AST/ALT ≤ 5 times the normal upper limit) and renal function (serum creatinine ≤ 140 µmol/L and creatinine clearance ≥ 50 ml/min). Exclusion criteria consisted of active bacterial infections, clinical signs of active brain tumour involvement or leptomeningeal disease, known alcoholism, drug addiction and/or psychotic disorders leading to inadequate follow-up, pregnancy or breast-feeding. Written informed consent was obtained from all patients. The study was approved by the Medical Ethics Committee of the Institute.

Trial treatment

All courses consisted of carboplatin infusion in 30 minutes followed by paclitaxel in a 3-hour infusion. Paclitaxel (Taxol®, Bristol Myers Squibb, Syracuse, NY) was provided as a sterile 6 mg/ml solution and dissolved in a mixture of Cremophor EL and dehydrated alcohol (1:1, v/v). Prior to administration, this solution was diluted with 500-1000 ml 0.9% sodium chloride solution to a final paclitaxel concentration between 0.3 and 1.2 mg/ml. As Cremophor EL may leach plasticizer from the infusion lines, a PVC-free administration equipment was used. Carboplatin (Paraplatin®, Bristol-Myers Squibb, Syracuse, NY) was supplied as a lyophilised product in a vial containing 150 mg carboplatin and 150 mg mannitol as bulking agent. Immediately before use the content of each vial was reconstituted with 15 ml of water for injection, and the total dose was added to 5% dextrose for intravenous infusion. The reconstituted and diluted product was protected from light and administered as soon as possible after reconstitution.

In each course, the carboplatin dosage was calculated according to the Calvert formula with a target area under the concentration-time curve (AUC) of 6 mg/ml*min and GFR is the glomerular filtration rate based on the ^{51}CrEDTA-clearance determination:[8]

$$\text{Dose} = \text{target AUC}_{\text{free}} \cdot (\text{GFR} + 25) \qquad\qquad \text{equation 1}$$

where dose is expressed in mg, AUC in mg/ml*min and GFR is expressed in ml/min.

The GFR is approximated by the creatinine clearance (CL), which in turn was estimated by the Cockcroft-Gault formula (CL_{CR-CG}):[9]

$$CL_{CR-CG} = \frac{1.23 \cdot (140 - \text{age}) \cdot \text{bodyweight}}{S_{CR}} (\cdot\, 0.85 \text{ if female}) \qquad\qquad \text{equation 2}$$

where CL_{CR-CG} is expressed in ml/min, age in years, S_{CR} in µmol/L and weight in kg.

A previous study revealed that replacement of the GFR by the creatinine clearance as determined by CL_{CR-CG} resulted in an overestimation of the AUC with 10.9% compared to the observed AUC based on the concentration-time data.[10] Therefore, the Calvert formula was modified by multiplying the CL_{CR-CG} with 1.1 ((CL_{CR-CG} +25)*1.1).

Standard premedication with dexamethasone (20 mg orally at 12 and 6 hours prior to paclitaxel administration), clemastine (2 mg iv 30 minutes prior to paclitaxel administration) and cimetidine (300 mg iv at 30 minutes prior to paclitaxel administration) was administered to prevent potential hypersensitivity reactions. Furthermore, a 5-HT$_3$-receptor antagonist (1 mg granisetron) was iv infused as standard anti-emetic agent. Treatment was discontinued in case of patient's refusal, non-compliance of the patient with the protocol, and progressive disease.

Pharmacokinetics and bio-analysis

Pharmacokinetic sampling was performed during all courses. During the first course, whole blood samples were collected in heparinised tubes prior to start of the carboplatin infusion, at the end of the carboplatin infusion (=prior to start of the paclitaxel infusion), 1.5 hours after the start of the paclitaxel infusion, at the end of the paclitaxel infusion, 30 and 60 minutes after the end of the paclitaxel infusion, 2, 4, 6, 9, and 19 hours after the end of the paclitaxel infusion. Plasma was obtained by centrifugation at 3000 rpm for 5 minutes. Plasma was transferred to polypropylene tubes and stored at approximately –20°C until analysis.

During subsequent courses of paclitaxel, whole blood samples were obtained prior to the start of the paclitaxel infusion, at the end of the paclitaxel infusion, 9 and 19 hours after the end of the paclitaxel infusion. Plasma was obtained by centrifugation at 3000 rpm for 5 minutes, and transferred to polypropylene tubes and stored at approximately –20°C until analysis of the paclitaxel concentrations.

Paclitaxel was determined in plasma using a validated isocratic high-performance liquid chromatographic method with solid phase extraction as sample pre-treatment as previously described.[5,7,11] The quantitation range of the method was 10-10,000 ng/ml.

Pharmacokinetically guided dosing

In the first course, the paclitaxel treatment consisted of the standard dose of 175 mg/m^2 (3-hour iv infusion). In the second course and subsequent courses the paclitaxel dosage was individualised to achieve a plasma concentration of 0.1 µmol/L during 15 hours or longer after the start of the infusion. The dosage adaptation was performed with a validated population pharmacokinetic model of paclitaxel that will be published elsewhere. Briefly, this population model was developed based on 100 concentration-time curves from 61 chemonaive NSCLC stage IIIB and IV patients (n=55) treated with paclitaxel (3-hour iv infusion) in combination with carboplatin and from advanced ovarian cancer patients (n=6), pre-treated with platinum, treated with paclitaxel (24-hour iv infusion) as single agent. The population pharmacokinetic parameter estimates are summarised in Table 1. This population model consists of a 3-compartment model with saturable distribution to one peripheral compartment and Michaelis-Menten elimination from the central compartment using non-linear mixed effect modelling (NONMEM, version V 1.1, double precision) (Figure 1).[12] The concentration-time data were logarithmically transformed. Inter-individual variability (IIV) and inter-occasion variability (IOV) were estimated using a proportional error model. IIV was quantified for the volume of the central compartment (V), maximal transport rate from the central compartment to peripheral compartment 1 (Tmax) and the maximal elimination rate (Vmax). IOV was quantified for the intercompartmental rate constants (k21, k13, k31) and Vmax. The residual variance was modelled using an additive error model with the assumption that the population was a mixture of two subpopulations (subpopulations 1 and 2) with a different variance. Body surface area (BSA) was significantly correlated with V and Tmax (p < 0.005).

Table 1. Population pharmacokinetic parameter estimates used for the Bayesian predictions

	Estimate	RSE (in %)
Pharmacokinetic parameter		
V (L)	12.1	5.4
Influence of BSA $(\theta_{12})^a$	1.16	33
Tmax (µmol/h)	216	5.6
Influence of BSA $(\theta_{13})^b$	1.05	49
Tm (µmol/L)	2.59	10
k21 (h^{-1})	0.916	7.0
k13 (h^{-1})	1.63	8.7
k31 (h^{-1})	0.0722	7.9
Km (µmol/L)	0.656	15
Vmax (µmol/h)	47.0	10
Population 1-2	0.380	27
Inter-individual variability		
IIV-V (%)	20	31
IIV-Tmax (%)	26	27
IIV-Vmax (%)	22	33
Inter-occasion variability		
IOV- k21 (%)	15	48
IOV- k13 (%)	26	25
IOV-k31 (%)	39	30
IOV-Vmax (%)	18	32
Residual error		
Additional error 1	0.202	11.0
Additional error 2	0.105	7.6

^{a} V = θ_1 * (BSA /1.81)$^{\theta 12}$
^{b} Tmax = θ_2 * (BSA /1.81)$^{\theta 13}$
where BSA is expressed in m^2, θ_1 and θ_2 represent the population value of V and Tmax respectively, of a patient with a (median) BSA of 1.81 m^2, θ_{12} and θ_{13} are exponential factors.
Additional error 1 = residual variability of subpopulation 1; Additional error 2 = residual variability of subpopulation 2; BSA = body surface area; IIV = inter-individual variability; IOV = inter-occasion variability; k21 = rate constant from the first peripheral compartment to the central compartment; k13 = rate constant from the central to the second peripheral compartment; k31 = rate constant from the second peripheral to the central compartment; Km = plasma concentration at half Vmax; Population 1-2 = fraction of the patient population (n = 61) belonging to subpopulation 1; RSE = Relative standard error, Tmax = maximal transport rate from the central to the first peripheral compartment; Tm = plasma concentration at half Tmax; V = volume of the central compartment; Vmax = maximal elimination rate.

Figure 1. Three-compartment model with Michaelis-Menten elimination from the central compartment. Tmax is the maximal transport rate to the first peripheral compartment, and Tm is the plasma concentration of paclitaxel at half Tmax. k21, k13 and k31 indicate the intercompartmental rate constants. Vmax is the maximal elimination rate, and Km is the plasma concentration of paclitaxel at half of the Vmax
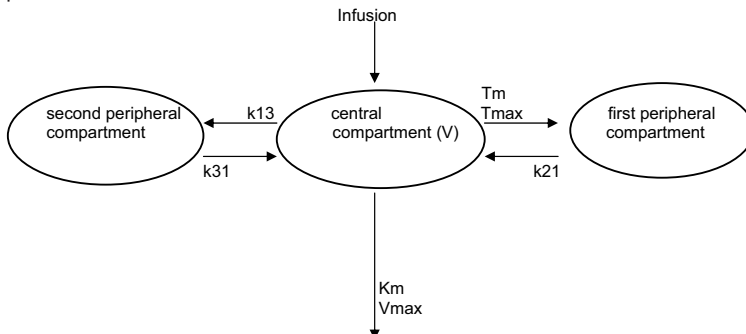
Bayesian estimates of the pharmacokinetic parameters were obtained using the POSTHOC option based on the population pharmacokinetic parameter values and the individual paclitaxel concentration-time data in the previous course(s). The obtained individual pharmacokinetic parameter estimates were used to predict the concentration-time data during the subsequent course after the administration of 175 mg/m². The duration of time that the paclitaxel concentration > 0.1 µmol/L was derived from these predicted concentration-time data. If the predicted duration of time of the paclitaxel plasma concentration above 0.1 µmol/L would be shorter than 15 hours in the subsequent course, the paclitaxel dosage was increased (in 5 mg steps) until the predicted duration of time was 15 hours or longer. The fit of the population model to the observed individual concentration-time data in this feasibility study, was evaluated by goodness of fit plots. The goodness of fit plots were examined in the program Xpose (Xpose, version 2.0, Uppsala University, Sweden) as implemented in the S-PLUS statistical package (version 2000, Mathsoft, Cambridge, Mass.).[13]

In addition, the theoretical values of the duration of time above the threshold concentration after the administration of 175 mg/m², were simulated based on the calculated pharmacokinetic parameter estimates in each individual during courses with dose increment. The theoretical value was compared to the observed duration of time.

Patient evaluation

Pre-treatment evaluation included a complete medical history and complete physical examination (including neurologic examination). Before each course, an interim history including concomitant medications was taken, toxicities and performance status were recorded and a physical examination was performed. Haematology was checked weekly during all courses. Blood chemistry including liver and renal function, liver enzymes, serum electrolytes, total protein, albumin and glucose levels were checked weekly during the first course. During subsequent courses blood chemistry was checked prior to each course. The observed toxicity was graded according to the National Cancer Institute Common Toxicity Criteria (NCI CTC).[14] Tumour measurement were performed every other cycle. Responses were evaluated according to the WHO criteria.[15] Standard tumour measurement procedures included CT scan, MRI, ultra sound imaging and/or histopathology.

Results

Patients

At interim analysis, 11 patients with NSCLC stage IIIB or IV were entered in this dose individualisation study. Patient characteristics and serum parameter values before the administration of the first course are summarised in Table 2. Patients included 3 females and 8 males and had a median age of 59 years (range 43 to 73). One patient was pre-treated with

Table 2. Pre-treatment characteristics of the patients (n=11)

	Number	Median value	Range
Patient characteristics			
Female	3		
Male	8		
Age		59	43-73
WHO Performance status			
0	3		
1	6		
2	2		
Tumour stage			
IIIB	2		
IV	9		
Histologic type			
Squamous cell carcinoma	4		
Adenocarcinoma	3		
Large cell carcinoma	4		
Pre-treatment			
None	8		
Prior chemotherapy	0		
Radiotherapy	3[a]		
Surgical therapy	1[b]		
Intertreatment interval			
<3 months	2		
3-6 months	1		
>6 months	0		
Biochemical parameters			
BSA (m^2)		1.90	1.63-2.06
Creatinine (µmol/L)		74	63-115
Total bilirubin (µmol/L)		6	3-15
Albumin (g/L)		39[d]	36-44
Alkaline Phosphatase (U/L)		111[c]	60-305
AST (U/L)		18	12-34
ALT (U/L)		20	7.8-44
GGT (U/L)		45	12-224
LDH (U/L)		379	243-776

[a] Local radiotherapy in 1 patient, radiotherapy on the skull and right humerus in 2 other patients.
[b] Surgical extirpation of a cerebral tumour (metastasis).
[c] n=10.
AST = aspartate aminotransferase; ALT = alanine-amino transferase; BSA = Body surface area; BUN = blood urea nitrogen; GGT = gamma-glutamyl-transpeptidase; LDH = lactate dehydrogenase; WHO = World Health Organisation.

surgery, and 3 patients with radiotherapy. A total of 46 courses of paclitaxel and carboplatin was administered.

Pharmacokinetics and bio-analysis

In total, 247 paclitaxel concentration-time points were obtained. The paclitaxel concentrations in plasma as obtained during the first course are presented in Figure 2 (n=11). The duration of time that the paclitaxel concentration was > 0.1 µmol/L was not evaluable during 2 of the 46 courses (courses 3 and 4) in 1 patient due to dose reductions of 25% and 50% after granulocytopenia grade 4 complicated with fever during the second (175 mg/m²) and third course (130 mg/m²), respectively. Paclitaxel pharmacokinetics were studied during the first

Figure 2. Paclitaxel concentrations in plasma after the iv infusion of 175 mg/m² during the first course (n=11). The dashed lines represent the plasma concentration in plasma > 0.1 µmol/L and the time point at 15 hours after the start of the paclitaxel infusion
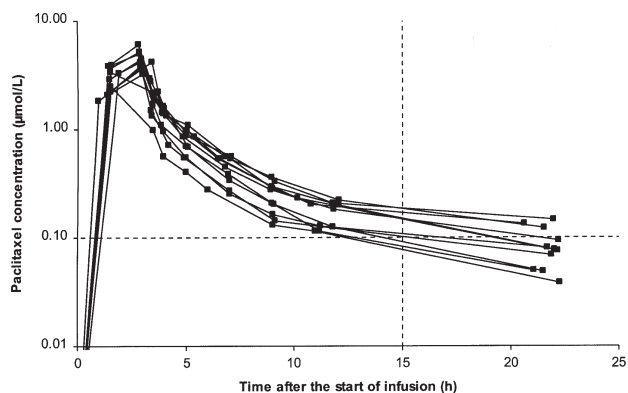
cycle (n=11), second cycle (n=11), third cycle (n=6), fourth cycle (n=6), fifth cycle (n=5), and sixth cycle (n=5).

Pharmacokinetically guided dosing

Drug monitoring was performed during all courses (44 evaluable courses). In the second course and subsequent courses (33 courses), the paclitaxel dosage was individualised based on the observed concentrations in the previous course(s). Bayesian predicted concentrations were obtained based on the population pharmacokinetic parameters and the individual observed concentrations. Subsequently, the predicted time above the paclitaxel concentration of 0.1 µmol/L was derived from these Bayesian predicted concentrations.

The goodness of fit plots of the observed concentrations versus the model predicted concentrations and the Bayesian predicted concentrations during all courses are depicted in Figure 3. The Bayesian predicted concentrations were symmetrically distributed around the line of unity (Figure 3B). The model predictions were lower than the observed concentrations especially at higher concentrations (Figure 3A).

The dose individualisation resulted in the administration of a standard dose (175 mg/m²) or an increased dose, to achieve a plasma concentration of 0.1 µmol/L during 15 hours or longer after the start of the infusion. Dose increments ranging from 180 to 205 mg/m² were performed in 14 of the 33 courses (in 7 patients). The duration of time that the paclitaxel concentration in plasma > 0.1 µmol/L for each course is summarised in Table 3.

During the first course (standard dose of 175 mg/m²), the drug threshold time > 0.1 µmol/L ranged from 11.6 to 31.6 hours. In 7 of these patients (64%), the duration of time was longer than 15 hours ranging from 15.4 to 31.6 hours. During the second course (individualised dose of 175 to 205 mg/m²), the paclitaxel concentration was above threshold during 15 hours or longer in 9 of the 11 patients (82%) ranging from 17.6 to 25.3 hours (Figure 4). In

Figure 3. Goodness of fit plots for the observed paclitaxel concentrations versus the model predictions of the paclitaxel concentrations (A) and the individual Bayesian predictions of the paclitaxel concentrations (B) (n=11). The solid line represents the line of identity
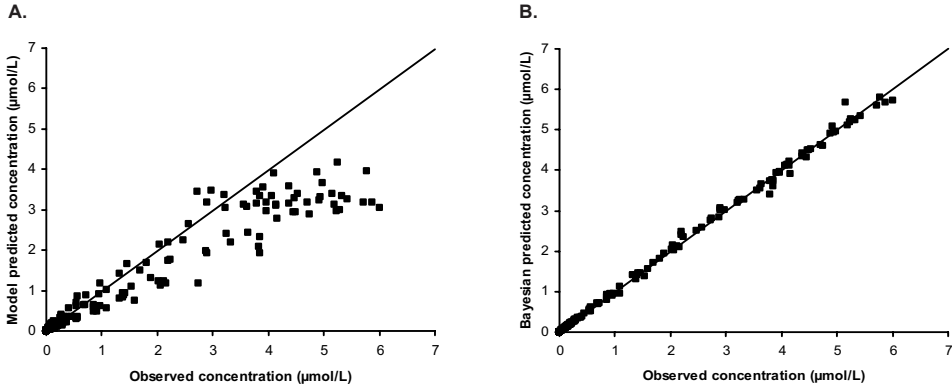
Table 3. Median duration of time that paclitaxel concentration in plasma was above 0.1 μmol/L in each course

Course number	Number of patients	Number of individualised doses (dose in mg/m^2)	Median duration of time (h) (range)
1	11	0 (175)	17.5 (11.6-31.6)
2	11	7 (175)	18.8 (14.3-25.3)
		2 (180)	
		1 (200)	
		1 (205)	
3	6	3 (175)	15.5 (11.5-26.3)
		2 (180)	
		1 (200)	
4	6	3 (175)	15.8 (12.4-17.5)
		2 (180)	
		1 (190)	
5	5	4 (175)	15.2 (12.2-18.3)
		1 (195)	
6	5	2 (175)	17.7 (10.9-19.6)
		2 (180)	
		1 (195)	

the other 2 patients the observed time above the threshold concentration was 14.3 and 14.7 hours. In 3 of the 4 patients in whom the duration of time above the threshold concentration was shorter than 15 hours during the first course, it was accomplished to obtain a duration of time longer than 15 hours during the second course. Dose individualisation in the second course resulted in a higher median duration of time above the threshold concentration of 0.1 μmol/L. Moreover, the lower limit of the duration that the threshold concentration was achieved, was higher in the second course compared to the first course. During the third course and subsequent courses, the observed time above the threshold concentration was achieved in 15 of the 22 courses (68%) ranging from 15.1 to 26.3 hours. In the other 7

Figure 4. The duration of time that the paclitaxel in plasma was higher than 0.1 µmol/L in patients during course 1 after the administration of the standard dose (175 mg/m^2) and after the administration of the individualised doses (175 mg/m^2 or higher) during subsequent courses (A). The time above the threshold concentration in the first 11 patients during the first and the second course (B)

A.
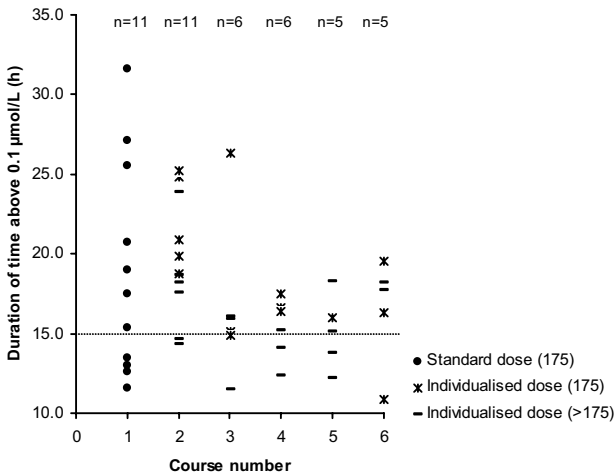
B.
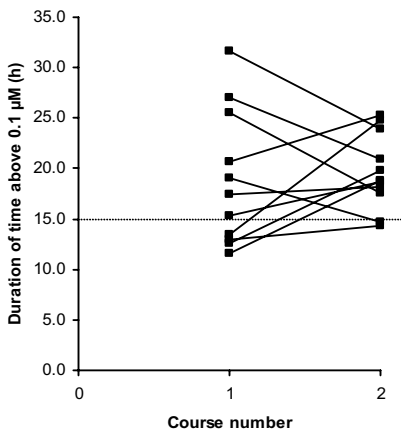
courses the duration of time ranged from 10.9 to 14.9 hours. The low duration of 10.9 hours was observed in 1 patient during the sixth course despite the dose individualisation (180 mg/m^2). In this patient no dose increment was indicated during courses 2 to 5 according to the Bayesian predictions of the paclitaxel concentrations in plasma. However, the duration of time that the paclitaxel concentration was higher than 0.1 µmol/L was below 15 hours in each course (course 2: 14.3 h, course 3: 11.5 h, course 4: 12.4 h, course 5: 12.2 h).

Figure 5. The simulated time above the threshold concentration after the administration of 175 mg/m² compared to the observed time after dose increment
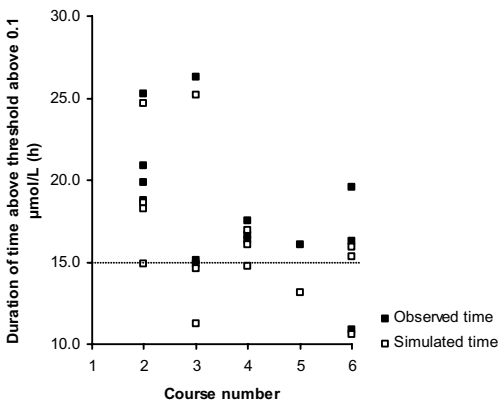
The duration of time that the paclitaxel concentration was above 0.1 µmol/L after the administration of the standard dose (175 mg/m²), was simulated in 6 patients who received individualised doses higher than 175 mg/m² (during 14 courses). In Figure 5, the simulated values of the duration of time in patients treated with the standard dose of 175 mg/m² are compared to the duration of time after the administration of the increased dose (180-205 mg/m²). After standard dosing (175 mg/m²) the simulated duration of time above the threshold concentration was shorter than 15 hours during 6 courses. In contrast, the observed duration of time above the threshold was shorter than 15 hours in only 2 courses. However, these results also show that in 8 of the 14 courses no dose individualisation was needed.

Patient evaluation

Toxicity

In the first 11 patients, haematologic toxicity consisted mainly of granulocytopenia (range CTC grade 1 to 4). Both leukocytopenia and thrombocytopenia ranged from CTC grade 1 to 3 (Table 4). Neutropenic fever was observed in 1 patient with granulocytopenia grade 4 during the third course (175 mg/m²), necessitating hospitalisation and iv antibiotics. The baseline levels of white blood cells (WBC) and granulocytes (ANC) decreased during later courses resulting in more pronounced leukocytopenia and neutropenia during later courses (data not shown). A positive correlation between the haematologic toxicity and the duration of time that the paclitaxel concentration in plasma is higher than 0.1 µmol/L cannot be observed yet. This will be evaluated after all patients (n=25) have been included in the study.

Non-haematologic toxicity consisted of alopecia CTC grade 1 and 2 after the first course, neurotoxicity CTC grade 1 and 2 after the first and sixth course, respectively, skin erythema CTC grade 1 after the first course, and cystitis CTC grade 1 after the third course. Furthermore,

Table 4. Haematologic toxicity during all courses (n=45)

Toxicity	Course #1 (n=11)	Course #2 (n=10)[a]	Course #3 (n=7)	Course #4 (n=7)	Course #5 (n=5)	Course #6 (n=5)
Leukocytes						
Grade 1	3	3	1	0	0	1
Grade 2	2	1	4	4	3	2
Grade 3	2	3	2	3	2	2
Grade 4	0	0	0	0	0	0
Granulocytes						
Grade 1	2	0	0	0	1	0
Grade 2	1	0	1	1	0	2
Grade 3	3	4	3	4	0	1
Grade 4	1	2	3	2	4	2
Platelets						
Grade 1	2	2	3	4	1	2
Grade 2	0	0	0	1	1	3
Grade 3	0	1	0	0	1	0
Grade 4	0	0	0	0	0	0

[a] Toxicity was evaluable in 10 patients during the second course since one patient died at two days after the administration of the second course.

gastro-intestinal complaints CTC grade 1 to 3 were observed. Toxicity was not more severe in courses with dose increment compared to courses without dose increment.

Response

The observed tumour responses in 11 patients were: a confirmed partial response in 1 patient, stable disease in 5 patients and progressive disease in 5 patients. Two patients with NSCLC stage IV died after the second administration (2 and 18 days after the administration) due to progressive disease. The other 9 patients are still alive (at 3 to 8 months after the start of the first course).

Discussion

The main purpose of this study was to demonstrate the feasibility of Bayesian pharmacokinetically guided dosing strategy of paclitaxel to achieve a drug concentration in plasma above 0.1 µmol/L during 15 hours or longer. A previously validated population pharmacokinetic model of paclitaxel generated by applying data of two other studies, was used to generate Bayesian predictions of the paclitaxel concentrations in plasma. Subsequently, the duration of time that the paclitaxel concentration in plasma > 0.1 µmol/L was derived from these individual Bayesian predicted concentrations. In this study we used this population model to predict the individual paclitaxel concentrations in subsequent courses based on the individual observed concentrations in previous courses. During each course, we were able to determine the paclitaxel concentration in plasma and determine the dose individualisation before the start of the subsequent course.

In Figure 4, the preliminary results of the first 11 patients show that the Bayesian estimated concentrations are well predicted but the model predictions show some bias at higher concentrations. This may be attributed to differences in demographic characteristics and blood chemistry parameters of the two populations, i.e. the population to develop the model and the current population, and the relatively small number of patients that has been evaluated in the feasibility study until now. Since the Bayesian predictions are used for the dose adjustment, the dose individualisation results are not influenced by the bias of the model predictions.

The preliminary results of this feasibility study show that dose individualisation during the second course results in a higher median duration of time that the paclitaxel concentration is above 0.1 µmol/L in plasma compared to the first dose without dose individualisation (Table 3 and Figure 4). The duration of time above the threshold concentration was attained in 9 of 11 patients in the second course compared to 7 of 11 patients in the first course. Until now, no increase in the duration of the threshold concentration can be observed in the third and subsequent courses compared to the duration of time after the first course. This is probably due to small patient cohorts (n=6 and n=5).

In 9 of the 33 individualised courses (27%) the dose individualisation did not result in a time above threshold longer than 15 hours. This can be attributed to the relatively high interoccasion variability of the pharmacokinetic parameters (15%-39%) resulting in a relatively high variation in the pharmacokinetic parameters of individuals between the courses. Therefore, dose individualisation can not result in a duration time above the threshold concentration longer 15 hours since the interoccasion variability can result in an increase or a decrease in the pharmacokinetic parameter estimates in the subsequent course. However, more patients and courses are needed to decide whether it is feasible to achieve the threshold concentration during the defined threshold time by dose individualisation. Moreover, in one patient with the relatively high BSA (2.1 m^2) dose individualisation did not result in a time above the threshold concentration of 15 hours. This may be attributed to the BSA since only a few patients with BSA value higher than 2 m^2 were included in the original patient population that was used for the development of the population pharmacokinetic model of paclitaxel.

The severity of the bone marrow toxicity, especially granulocytopenia, increased during subsequent courses, but no relationship between the dose increments and severity of toxicity could be reported (data not shown). The primary toxicity was granulocytopenia that was more pronounced during later courses. This cumulative effect has already been observed in an earlier study with NSCLC patients treated with the combination chemotherapy paclitaxel and carboplatin.[7] Thrombocytopenia was mild (grade 0 to 2). Several other investigators reported a reduced platelet toxicity for the paclitaxel-carboplatin combination that can be attributed to the reduced uptake of platinum agents in cells due to the formulation vehicle of paclitaxel, Cremophor EL.[16,17]

The pharmacokinetics of paclitaxel are non-linear caused by Cremophor EL due to its formation of micelles in plasma. Paclitaxel is entrapped in these micelles and this results in a decreased free paclitaxel concentration in plasma and a reduced uptake of paclitaxel in red blood cells.[18-22] Several studies showed that the exposure-efficacy relationship for paclitaxel can be best described by a threshold model.[5,7,23] But the relationship between the unbound drug concentration and toxicity or response have not been elucidated yet.

In conclusion, the preliminary results of this study show that Bayesian pharmacokinetically guided dosing of paclitaxel is feasible. In the second course, in 82% of the patients the drug threshold time above 0.1 µmol/L during 15 hours or longer compared to only 64% the first course. In the third course and subsequent courses this was accomplished in 68% of the patients. In total, in 27% of the individualised doses the target drug threshold time was not achieved. Another 14 patients will be included in this study to investigate whether dose individualisation to attain the threshold concentration during 15 hours or longer can be feasible. Future directions should also focus on the pharmacokinetic-pharmacodynamic relationships of the unbound paclitaxel concentration.

Acknowledgements

References

1. Huizing MT, Sewberath Misser VH, Pieters RC, et al. Taxanes: a new class of antitumor agents. Cancer Invest 1995;13:381-404.
2. Rowinsky EK, Donehower RC. Taxanes. N Engl J Med1995;332:1004-1014.
3. Novello S, Le Chevalier T. European perspectives on paclitaxel/platinum-based therapy for advanced non-small cell lung cancer. Sem Oncol 2001;28:3-9.
4. Schiller JH, Harrington D, Belani CP, et al. Comparison of four chemotherapy regimens for advanced non-small-cell lung cancer. N Engl J Med 2002;346:92-98.
5. Huizing MT, Keung ACF, Rosing H, et al. Pharmacokinetics of paclitaxel and metabolites in a randomised comparative study in platinum-pre-treated ovarian cancer patients. J Clin Oncol 1995;11:2127-2135.
6. Gianni L, Kearns CM, Gianni A, et al. Nonlinear pharmacokinetics and metabolism of paclitaxel and its pharmacokinetic/pharmacodynamic relationships in humans. J Clin Oncol 1995;13:180-190.
7. Huizing MT, Giaccone G, Van Warmerdam LJC, et al. Pharmacokinetics of paclitaxel and carboplatin in a dose-escalating and sequencing study in patients with non-small-cell lung cancer. J Clin Oncol 1997;15:317-329.
8. Calvert AH, Newell DR, Gumbrell LA, et al. Carboplatin dosage: prospective evaluation of a simple formula based on renal function. J Clin Oncol 1989;7:1748-1756.
9. Cockcroft DW, Gault MH. Prediction of creatinine clearance from serum creatinine. Nephron 1976;16:31-41.
10. Van Warmerdam LJC, Rodenhuis S, Ten Bokkel Huinink WW, et al. Evaluation of formulas using the serum creatinine level to calculate the optimal dosage of carboplatin. Cancer Chemother Parmacol 1996;37:266-270.
11. Willey TA, Bekos EJ, Gaver RC, et al. A high performance liquid chromatographic procedure for the quantitative determination of paclitaxel in human plasma. J Chromatogr 1993;621:231-36.
12. Boeckmann AJ, Sheiner LB, Beal SL. NONMEM Users Guide - Part V Introductory Guide. NONMEM Project Group. University of California at San Francisco, 1994.
13. Jonsson EN, Karlsson MO. Xpose – an S-PLUS based population pharmacokinetic/ pharmacodynamic model building aid for NONMEM. Comput Methods Programs Biomed 1999;58:51-64.
14. National Cancer Institute, Division of Cancer Treatment, Bethesda, MD. Guidelines for Reporting of Adverse Drug Reactions, 1988.
15. World Health Organisation, Geneva, Switzerland. WHO Handbook for reporting results of Cancer Treatment, 1979.
16. Kearns CM, Egorin MJ. Considerations regarding the less-than-expected thrombocytopenia encountered with combination paclitaxel/carboplatin chemotherapy. Sem Oncol 1997;24:91-96 (Suppl 2).
17. Van Zuylen L, Verweij J, Sparreboom A. Role of formulation vehicles in taxane pharmacology. Invest New Drugs 2001;19:125-141.
18. Van Tellingen O, Huizing MT, Nannan Panday VR, et al. Cremophor EL causes (pseudo) non-linear pharmacokinetics of paclitaxel in patients. Br J Cancer 1999;81:330-335.
19. Sparreboom A, van Tellingen O, Nooijen WJ, et al. Nonlinear pharmacokinetics of paclitaxel in mice results from the pharmaceutical vehicle cremophor EL. Cancer Res 1996;56: 2112-2115.
20. Sparreboom A, van Zuylen L, Brouwer E, et al. Cremophor EL-mediated alteration of paclitaxel distribution in human blood: Clinical pharmacokinetic implications. Cancer Res 1999;59: 1454-1457.
21. Van Zuylen L, Karlsson, M.O., Verweij, J, et al. Pharmacokinetic modeling of paclitaxel encapsulation in cremophor EL micelles. Cancer Chemother Pharmacol 2001;47: 309-318.
22. van Zuylen L, Gianni L, Verweij J, et al. Inter-relationships of paclitaxel disposition, infusion duration and cremophor EL kinetics in cancer patients. Anti-Cancer Drugs 2000;11: 331-337.
23. Henningsson A, Karlsson MO, Viganò L, et al. Mechanism-based pharmacokinetic model for paclitaxel. J Clin Oncol 2001;19:4065-4073.

Chapter 4.3

Development and validation of a method to determine the unbound paclitaxel fraction in human plasma

HJG Desirée van den Bongard, E Marleen Kemper, Olaf van Tellingen, Hilde Rosing, Ron AA Mathôt, Jan HM Schellens and Jos H Beijnen

Summary

Paclitaxel is pharmaceutically formulated in a mixture of Cremophor EL and ethanol (1: 1, v/v). The unbound fraction of the anticancer drug paclitaxel in plasma is dependent on both plasma protein binding as well as by entrapment in Cremophor EL micelles. We have developed a simple and reproducible method for the quantification of the unbound paclitaxel fraction in human plasma. After the addition of ^{3}H-paclitaxel and ^{14}C-glucose (unbound reference), human plasma was spiked with paclitaxel and Cremophor EL and incubated at 37°C for 30 minutes. Plasma ultrafiltrate was obtained by a micro partition system (MPS-1). A small amount of plasma (100 μl) in the collection cup prevented loss of paclitaxel due to adsorption. The radionuclides were separated after combustion of the biological samples using a sample oxidiser and the radioactivity was determined by liquid scintillation counting. The unbound fraction of paclitaxel was calculated by dividing the ratios of ^{3}H and ^{14}C in plasma ultrafiltrate and in plasma. The method was precise, with a within-day precision ranging from 3.9% to 11.0%. The between-day precision ranged from 5.8% to 13.1% at pharmacologically relevant Cremophor EL and paclitaxel concentrations (ranging from 0.25% to 2.0% (v/v) and 10 to 1000 ng/ml, respectively). In patient plasma (spiked with 100 ng/ml paclitaxel) with low serum albumin values containing 1% of Cremophor EL, the unbound fraction appeared to be significantly higher than in plasma with normal albumin values. The determination of the unbound fraction of paclitaxel proved to be stable during a 10-week storage at –20°C. Furthermore, the assay was applicable in patient samples.

This assay can satisfactorily be used to determine the unbound fraction of paclitaxel in plasma and its design can also be used to determine the unbound concentrations of other hydrophobic drugs.

Introduction

Paclitaxel is a taxane derivative that acts on microtubular structures, causing microtubular stabilisation that arrests the tumor cells in the G_2/M phase of the cell cycle. Paclitaxel has shown profound antitumour activity against a variety of solid tumours, especially against lung, breast, ovarian, and head and neck tumours.[1,2] Due to the formulation vehicle Cremophor EL, the pharmacokinetics of paclitaxel are non-linear, as manifested by disproportional increases in both the maximal plasma concentration (C_{max}) and the area under the plasma concentration-time curve (AUC) at higher doses.[3-7] It has been demonstrated that Cremophor EL can form micelles in blood in vitro, acting as a high-affinity drug-carrier site of paclitaxel. Consequently, the unbound paclitaxel concentration in plasma is lower at higher Cremophor EL concentrations in plasma.[4-6,8] Since the unbound drug concentration in blood can be the active fraction, measurement of total paclitaxel levels can result in inaccurate assessment of pharmacokinetic-pharmacodynamic relationships of paclitaxel. Therefore, it is important to measure the total paclitaxel concentration in plasma (= the sum of protein-bound, micellar encapsulated and unbound paclitaxel in plasma) in combination with the unbound fraction of paclitaxel.[9,10] In earlier studies, the unbound fraction of paclitaxel has been determined by equilibrium dialysis, however, the time to reach equilibrium ranged from 5 to over 64 hours.[4,5,11-13] The binding of paclitaxel to human plasma is approximately 95% at pharmacologically relevant concentrations, especially to human serum albumin and α-acid glycoprotein.[12] The purpose of this study was to develop an accurate and more rapid assay to determine the unbound fraction of paclitaxel in human plasma.

Materials and Methods

Chemicals and reagents

Paclitaxel reference standard was obtained from Bristol Myers Squibb (Syracuse, NY).

Determination of unbound fraction of paclitaxel

A stock solution of paclitaxel at a concentration of 1 mg/ml in methanol was used to spike control human plasma (Central Laboratory for the Blood Transfusion Services, Amsterdam, The Netherlands) to obtain a concentration of 10,000 ng/ml of the drug. This plasma sample was stored at –20°C. Cremophor EL was obtained from Sigma Chemical Co. (St. Louis, MO, USA). Tritiated paclitaxel (^{3}H-paclitaxel) was manufactured by Moravek Biochemicals Inc (Brea, CA, USA), and carbon-14 (^{14}C)-radiolabelled glucose was manufactured by Amersham International Ltd. of Little Chalfont (Buckinghamshire, United Kingdom). Before use, ^{3}H-paclitaxel was purified by an HPLC method. ^{3}H-paclitaxel (specific activities between 17.4 and 24.4 MBq/ml) was diluted in blank human plasma to a target concentration of 6670

Bq/ml. ^{14}C-glucose (specific activity of 9.25 MBq/ml) was diluted in blank human plasma to a target concentration of 333 Bq/ml. Both solutions were mixed in a ratio of 1:1, v/v. Scintillation fluids, for the determination of the radioactivity levels, consisted of Monophase S, Permafluor E+ and Carbo-Sorb (Packard Bioscience B.V., Groningen, The Netherlands). Cellulose was purchased from Sigma Chemical Co., St. Louis, MO, USA.

Determination of total paclitaxel concentration in plasma

Ethanol, ammonium acetate, glacial acetic acid, n-hexane and triethylamine were obtained from Merck (Darmstadt, Germany). Acetonitrile (HPCL gradient grade) was obtained from Biosolve Ltd. (Barneveld, The Netherlands), methanol (ChromAR®) was obtained from Promochem (Wesel, Germany).

Determination of unbound fraction of paclitaxel in plasma

Sample preparation

Blank human plasma was thawed and spiked with Cremophor EL to final concentrations of 0, 0.25, 0.5, 1.0 and 2.0% in triplicate (v/v). Aliquots of the 10,000 ng/ml paclitaxel plasma standard were added to obtain concentrations of 10, 100 and 1000 ng/ml. Subsequently, ^{3}H-paclitaxel and ^{14}C-glucose (solutions in blank human plasma) were both added (10 µl per ml spiked plasma). All plasma samples were then incubated in a water bath at 37°C for 30 minutes. Blank human plasma was incubated (in triplicate) to determine any background radiation in plasma and plasma ultrafiltrate in each run. After the incubations, 500 µl of each plasma sample was transferred to an ultrafiltration device, Amicon micropartition systems (Amicon Corporation, Danvers MA, USA) with membrane discs with a cut off level of 30,000 MW (Millipore Corporation, Amicon, Beverly MA, USA). Subsequently, the ultrafiltration devices were centrifuged at approximately 1500 *g* at 37ºC for 20 minutes yielding about 120 µl plasma ultrafiltrate.

Measurement of radioactivity levels

One hundred µl of each plasma and plasma ultrafiltrate sample was transferred to Combusto cones™ (Packard Bioscience B.V., Groningen, The Netherlands) filled with cellulose.
The radionuclide content in all plasma and plasma ultrafiltrate samples was separated in ^{3}H and ^{14}C by combustion of the samples in a sample oxidiser model 307 (Packard, Meriden, CT, USA). Scintillation fluid was added by the oxidizer in 2 glass vials: Monophase S in the ^{3}H-vial, Permafluor E+ and Carbo-Sorb in the ^{14}C-vial. After manual mixing for 20 seconds, the radioactivies in the vials were measured using a (Tri-carb 2300 TR) liquid scintillation counter (Packard, Meriden, CT, USA). The disintegrations per minute (dpm) levels in each sample were counted for 15 minutes with quench correction by external standardisation.

Calculation of the unbound fraction

The ^{3}H dpm levels in plasma (^{3}H plasma) and plasma ultrafiltrate (^{3}H plasma ultrafiltrate) were divided by the ^{14}C concentrations in these samples (^{14}C plasma and ^{14}C plasma ultrafiltrate, respectively). Subsequently, the unbound fraction of paclitaxel was calculated by the ratio between the ^{3}H/^{14}C ratio in plasma ultrafiltrate and ^{3}H/^{14}C ratio in plasma:

$$\text{Unbound fraction} = \frac{^{3}\text{H}/^{14}\text{C plasma ultrafiltrate}}{^{3}\text{H}/^{14}\text{C plasma}} \cdot 100 \qquad\qquad \text{equation 1}$$

where the unbound fraction is expressed in %.

All dpm levels were corrected for the measured background levels in the corresponding blanks.

Validation procedures

A three-run validation was completed for the determination of the unbound fraction of paclitaxel in plasma. The validation involved the following assay parameters: precision (reproducibility and repeatability) and stability. Furthermore, influence of paclitaxel and Cremophor EL concentrations on the unbound paclitaxel fraction in plasma, and the influence of the albumin and total bilirubin levels on the unbound fraction was determined.

Calibration standards were not required since the unbound fraction was calculated by using equation 1. According to this equation, the limit of detection (LOD) and the lower limit of quantification (LLQ) are related to the LLQ of the method to determine the total paclitaxel concentration in plasma. Since there are no standard samples for protein binding, it was not possible to test the accuracy of the assay.

To determine the influence of the Cremophor EL and paclitaxel concentrations on the unbound fraction of paclitaxel, 3.5 ml plasma was spiked with 1% Cremophor EL and 3.5 ml plasma without Cremophor EL as a control in polypropylene tubes (in triplicate) in three separate runs. Subsequently, all plasma was spiked with paclitaxel, ^{3}H-paclitaxel and ^{14}C-glucose as previously described. Plasma was incubated followed by ultrafiltration and determination of the radioactivity levels. After calculation of the unbound fractions in all samples, the influence of Cremophor EL on the unbound fraction of paclitaxel in plasma was determined by the student's t test with a significance level of 0.01. The influence of the paclitaxel concentrations of 10, 100 and 1000 ng/ml on the unbound fraction was determined by one-way analysis of variance (ANOVA).

To determine the precision, six replicates of plasma spiked with Cremophor EL to a final concentration of 0.25%, 1.0% and 2.0% were prepared with paclitaxel to a final concentration of 100 ng/ml. Samples were processed as previously described. All samples were analysed in 3 separate analytical runs. The between-day precision (reproducibility) and within-day

precision (repeatability) were calculated for each concentration by ANOVA using the following equations:[14]

$$\text{Within - Day Precision (WDP)} = \frac{(MS_{WG})^{1/2}}{\text{Overall mean}} \cdot 100 \qquad\qquad \text{equation 2}$$

where MS_{WG} = Mean Square Within Groups.

$$\text{Between - Day Precision (BDP)} = \frac{(MS_{BG} - MS_{WG}/n)^{1/2}}{\text{Overall mean}} \cdot 100 \qquad\qquad \text{equation 3}$$

where MS_{BG} = Mean Square Between Groups and n = number of replicates within each day.

Hence, the between-day precision was expressed as the variance additional to the within-day variance, resulting from analysing the samples in different runs.

The unbound fraction of paclitaxel was determined in plasma of cancer patients (who were not treated with paclitaxel) with low serum albumin and/or high serum total bilirubin levels. The unbound fraction values in plasma with abnormal albumin and/or total bilirubin levels were compared to the unbound fraction in blank plasma. Five of these patients had a low serum albumin level (range 22-29 g/L [normal values: 44-56 g/L]), 3 of these patients had a high serum total bilirubin level (range 21-129 µmol/L [normal values: <16 µmol/L]), and 4 of these patients had both high serum total bilirubin and low serum albumin levels (ranges 18-31 µmol/L and 16-24 g/L, respectively). Whole blood samples were centrifuged at 2000 *g* followed by transfer of plasma to Falcon tubes. Heparinised venous blood was obtained from 2 healthy volunteers. Blank plasma was obtained by centrifugation and was used as a reference. Patient and reference plasma was stored at -20°C until analysis. After thawing, half of the plasma samples were spiked with Cremophor EL to a final concentration of 1%, and half of the plasma samples was processed without Cremophor EL. All plasma samples were spiked with paclitaxel to a final concentration of 100 ng/ml. The samples were further processed as described in the 'Materials and methods' section. In total, 5 replicates of each sample were analysed in 2 separate runs. The unbound paclitaxel fraction in plasma as determined in patient plasma was compared with that in normal plasma by regression analysis with a significance value of 0.01.

Finally, stability was tested by the determination of the unbound fraction in plasma spiked with 100 ng/ml paclitaxel without and with Cremophor EL to a final concentration of 2%. Six replicates of each sample were prepared and analysed at time zero according to the procedure as described in the 'materials and methods' section. The rest of the spiked plasma was stored in polypropylene tubes during 10 weeks at -20°C. After storage, samples were pre-treated and analysed as described previously. The unbound fraction values as

determined at 10 weeks were compared with the values as determined at day 0, and was not allowed to deviate more than 15% from the baseline value.

Patient samples

The unbound fraction of paclitaxel in plasma was determined in plasma samples obtained from a 74-year-old male patient with non-small cell lung cancer stage IIIB. The treatment consisted of 336 mg (3–hour iv infusion of 175 mg/m²) paclitaxel (Taxol®, Bristol Myers Squibb) and 630 mg (30-min iv infusion with target AUC 6 mg/ml*min) carboplatin (Paraplatin®). The patient was not pre-treated with any chemotherapeutic agents.

Paclitaxel was provided as a sterile 6 mg/ml solution in a mixture of Cremophor EL and dehydrated alcohol (1:1, v/v). Prior to administration, this solution was diluted with 500 ml 0.9% sodium chloride solution. As Cremophor EL may leach plasticiser from the infusion lines, a PVC-free administration equipment was used. Standard pre-medication with dexamethasone (20 mg orally at 12 and 6 hours prior to paclitaxel administration), clemastine (2 mg iv 30 minutes prior to paclitaxel administration) and cimetidine (300 mg iv at 30 minutes prior to the paclitaxel administration) was administered to prevent potential hypersensitivity reactions caused by Cremophor EL. Furthermore, $5\text{-}HT_3$-receptor antagonists (1 mg granisetron) was iv infused as standard anti-emetic agent. Before treatment, the Eastern Co-operative Oncology Group performance status was 0 on the World Health Organisation scale, and the haematopoietic (white blood cells $6.6 \times 10^9/L$, platelets $280 \times 10^9/L$) renal (serum creatinine 79 µmol/L), hepatic function and hepatic enzymes (serum total bilirubin 6 µmol/L, alkaline phosphatase 58 U/L, aspartate aminotransferase (AST) 16 U/L, and alanine aminotransferase (ALT) 25 U/L) were normal. Written informed consent was obtained before start of the treatment.

Ten blood samples were collected by intravenous sampling from the arm opposite to the arm used for the infusion, just before the start of the infusion (blank), 1.5 hours after the start of the infusion, at the end of the infusion, and 30 minutes, 1, 2, 4, 6, 9 and 18 hours after the end of the infusion. Whole blood samples were centrifuged at 2000 g and plasma was transferred to polypropylene tubes, and stored at -20°C until analysis. ³H-paclitaxel and ¹⁴C-glucose was added to all samples followed by the determination of the unbound fraction as previously described. The total paclitaxel concentrations in plasma were determined by an HPLC assay as described below.

Determination of total paclitaxel concentrations in plasma

A validated isocratic high-performance liquid chromatographic method was used for the quantitative determination of paclitaxel that has been published elsewhere.[9,10] Briefly, aliquots of a paclitaxel stock solution (10 mg of paclitaxel reference material in 2.0 ml of ethanol) were added to blank human plasma to obtain plasma concentration standards with final concentrations ranging from 10 to 10,000 ng/ml. 2'-methyl paclitaxel was used as

internal standard and samples were extracted on Cyano Bond Elut columns (1.0 ml; 100 mg, Varian, Palo Alto, CA, USA). The columns were first conditioned with 2.0 ml of methanol and 0.01 M ammonium acetate buffer, pH 5.0. A volume of 1.0 ml of plasma diluted with 0.2 M ammonium acetate buffer pH 5.0 (1:1, v/v) was transferred to the column. The columns were washed consecutively with 2.0 ml of methanol-0.01 M ammonium acetate, pH 5.0 (2:8, v/v) and 1.0 ml of *n*-hexane. The columns were dried under maximum vacuum (15 mm Hg) for 1 minute. The analytes were eluted from the columns with 2.0 ml of a mixture of acetonitrile-triethylamine (1,000:1, v/v). The eluent was evaporated to dryness under a nitrogen stream at 40°C. Samples were reconstituted with in a mixture of acetonitrile, methanol and distilled water (4:5:1, v/v) by vortex mixing for 1 minute. Detection was performed by UV absorbance measurement at 227 nm. Runtimes were approximately 20 minutes. The calibration curves were calculated by weighted (1/x) linear regression analysis.

Calculations

The unbound paclitaxel concentration in plasma was calculated by multiplying the unbound fraction with the total paclitaxel concentration in plasma, as described in equation 4:

Unbound concentration = unbound fraction · total concentration   equation 4

where the unbound and total concentrations are expressed in ng/ml and the unbound fraction in %.

All statistical analyses were performed in the program Statistical Product and Service solutions (SPSS) for Windows, version 11.0 (SPSS, Chicago, IL, USA) with a significance level of 0.01.

Results and discussion

Determination of the unbound fraction of paclitaxel in plasma

The MPS-1 system is a generally accepted method to determine the protein binding of drugs such as platinum agents.[15] However, adsorption of paclitaxel occurred rapidly when this hydrophobic substance was present in a protein-free environment such as ultrafiltrate. To prevent adsorption of paclitaxel, the collection cups of the Amicon ultrafiltration device were filled with 100 µl of blank plasma before ultrafiltration. Since the yield of ultrafiltrate varied from sample to sample it was essential to include an unbound reference compound. The recovery of ^{14}C-glucose in plasma ultrafiltrate after ultrafiltration ranged from 95% to 101% as determined (in triplicate) in plasma spiked with paclitaxel (10-1000 ng/ml). Consequently, all ^{14}C-glucose passed the filtration membrane and could be used as unbound reference in

Figure 1. Unbound fraction values in plasma spiked with 100 ng/ml paclitaxel containing 0.25% to 2.0% Cremophor EL, and in spiked plasma without Cremophor EL (in triplicate, mean ± SD)
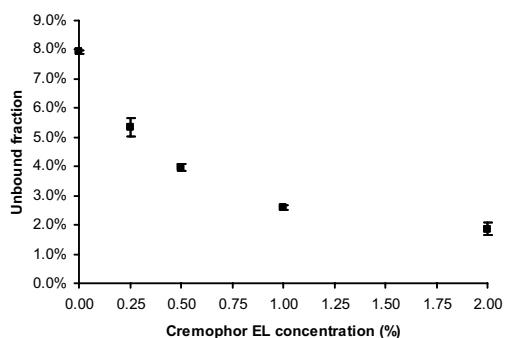
this ultrafiltration method. We have previously shown that Cremophor EL in plasma does not pass the ultrafiltration membrane, in spite of the fact that the molecular weight of 3000 is far less than the membrane cut off value of 30 kD.[5] In the first instance, the radioactivity concentrations were determined by direct liquid scintillation counting using 2 channels for ^{3}H and ^{14}C. However, the substantial overlap in the energy spectra of these radionuclides reduced the precision of the method. Complete separation of the ^{3}H- and ^{14}C-radionuclides was achieved after combustion of the samples in the sample oxidiser.

We tested the applicability of the method using blank human plasma spiked with known amounts of Cremophor EL and paclitaxel. The values of the unbound fractions as determined (0 to 2% Cremophor EL and 100 ng/ml paclitaxel) are depicted in Figure 1 and are in agreement with previous results.[4,5,13] It was observed that the unbound fraction decreased at higher Cremophor EL in plasma.

Validation procedure

The results of the influence of Cremophor EL and paclitaxel concentrations on the unbound fraction in plasma, are summarised in Table 1. The unbound fraction was significantly higher (p < 0.0001) in all plasma samples without Cremophor EL (mean value 9.0%) compared to plasma with a Cremophor EL concentration of 1% (mean value 3.0%). The unbound fraction was not significantly influenced by the paclitaxel concentration in plasma (p > 0.01). The results of the test for precision are summarised in Table 2. The within-day precision and the between-day precision for all samples were less than 13.1%. Consequently, the method has a sufficient repeatability and reproducibility for clinical studies. The mean values of the unbound fraction were 5.9%, 2.8% and 2.0% for plasma containing 0.25%, 1% and 2% Cremophor EL, respectively.

In Table 3, the influences of low albumin and/or high total bilirubin levels on the unbound fraction are summarised. For plasma containing 1% of Cremophor EL, a low serum albumin level (with and without elevated serum total bilirubin levels) significantly increased the

Table 1. Unbound fraction (mean% ± SD%) in plasma with 1% Cremophor EL and without Cremophor EL at various paclitaxel concentrations (as determined in triplicate at 3 different days)

Paclitaxel concentration (ng/ml)	Cremophor EL 0%	p value[a]	n	Cremophor EL 1%	p value[a]	n
10	8.8 ± 0.4	0.44	9	3.0 ± 0.3	0.782	8
100	8.9 ± 0.9	0.729	9	2.9 ± 0.3	0.393	8
1000	9.7 ± 0.5	0.928	8	3.1 ± 0.3	0.430	8

[a] ANOVA.

Table 2. Within-day precision (WDP) and Between-day precision (BDP) for plasma with various Cremophor EL concentration and 100 ng/ml paclitaxel as determined on 3 different days in 6-fold

Cremophor EL concentration (%)	Unbound fraction (%) Mean ± SD	WDP (%)	BDP (%)	n
0.25	5.9 ± 0.35	3.9	13.1	17
1.0	2.8 ± 0.32	5.9	8.2	16
2.0	2.0 ± 0.22	11.0	5.8	18

Table 3. Unbound paclitaxel fraction (mean ± SD) in plasma (spiked with 100 ng/ml of paclitaxel) containing 1% Cremophor EL and no Cremophor EL in patients with low serum albumin and/or high serum total bilirubin levels and in normal plasma (in 5-fold)

Abnormal laboratory parameter (normal range)	Cremophor EL 1%	n	Cremophor EL 0%	n
Albumin↓ (22-29 g/L)[a]	3.82% ± 0.24%	6	11.0% ± 1.5%	6
Total bilirubin↑ (21-129 µmol/L)[b]	3.46% ± 0.20%	6	11.1% ± 0.30%	6
Albumin↓(16-24 g/L) and total bilirubin↑ (18-31 µmol/L)	3.72% ± 0.054%	5	9.56% ± 0.69%	6
Normal levels	3.27% ± 0.065%	6	11.5% ± 0.43%	6

[a] Normal serum albumin values: 44-56 g/L.
[b] Normal serum total bilirubin value < 16 µmol/L.

unbound fraction in plasma (p = 0.005). Interestingly, however, for plasma containing no Cremophor EL the low serum albumin level had no significant effect on the unbound fraction (p = 0.840). Elevated serum bilirubin level had no influence on the unbound fraction of paclitaxel either with or without Cremophor EL in plasma.

Finally, the stability test showed that the mean values of the unbound fraction at 10 weeks after the preparation of the spiked samples were still 97.2% and 98.5% (for the Cremophor EL concentrations 0% and 2%, respectively) of the values as determined at the day of preparation.

Patient samples

To show the applicability of the method we have determined the unbound fraction in plasma samples obtained from a cancer patient receiving an iv infusion of paclitaxel (175 mg/m^2). The unbound fraction ranged between 3.4% and 4.8% (Table 4). As expected, the

Table 4. Unbound paclitaxel fraction in plasma of a patient treated with a 3-hour intravenous infusion of 175 mg/m^2 paclitaxel

Time after start of the infusion (h)	Unbound fraction (%)
0	0
1.53	4.7
3.42	3.4
3.72	3.7
4.03	3.5
5.12	3.6
7.02	3.4
8.98	3.9
11.20	4.2
21.05	4.8

Figure 2. Total (□) and unbound (■) paclitaxel concentrations in plasma of a patient treated with a 3-hour intravenous infusion of paclitaxel (175 mg/m^2)
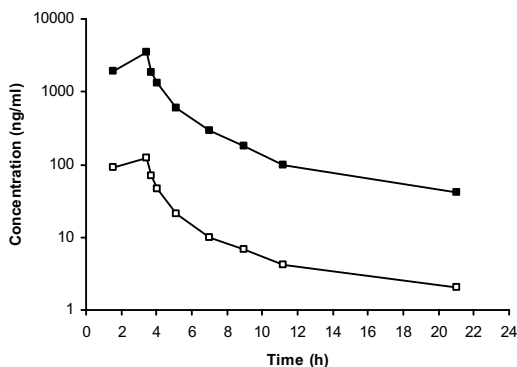
unbound fraction in plasma was lowest at the end of the infusion and shortly after infusion due to the relatively high Cremophor EL concentration in plasma at these time points. The total paclitaxel concentrations ranged from 42.1 ng/ml and 3554 ng/ml, whereas the unbound paclitaxel concentrations ranged from 2.0 ng/ml to 121 ng/ml (Figure 2).

Conclusions

The presented method to determine the unbound fraction of paclitaxel in plasma proved to be a precise method at pharmacologically relevant paclitaxel and Cremophor EL concentrations. In agreement with the equilibrium dialysis method, the unbound fraction decreased at higher Cremophor EL concentrations in plasma.[4,5,11] Furthermore, it was shown that the unbound fraction was significantly increased at lower plasma albumin levels, but only when the sample contained Cremophor EL. The method proved to be applicable for patient samples.

If suitable radiolabelled tracers are available, the design of this method may also be applicable to determine unbound levels of other hydrophobic substances.

References

1.   Huizing MT, Sewberath Misser VH, Pieters RC, et al. Taxanes: a new class of antitumor agents. Cancer Invest 1995;13:381-404.
2.   Kearns CM. Pharmacokinetics of the taxanes. Pharmacotherapy 1997:17:105S-109S.
3.   Sparreboom A, van Tellingen O, Nooijen WJ, et al. Nonlinear pharmacokinetics of paclitaxel in mice results from the pharmaceutical vehicle Cremophor EL. Cancer Res 1996;56:2112-2115.
4.   Sparreboom A, van Zuylen L, Brouwer E, et al. Cremophor EL-mediated alteration of paclitaxel distribution in human blood: Clinical pharmacokinetic implications. Cancer Res 1999;59:1454-1457.
5.   Van Tellingen O, Huizing MT, Nannan Panday VR, et al. Cremophor EL causes (pseudo-) non-linear pharmacokinetics of paclitaxel in patients. Br J Cancer 1999;891:330-335.
6.   Van Zuylen L, Karlsson MO, Verweij J, et al. Pharmacokinetic modelling of paclitaxel encapsulation in Cremophor EL micelles. Cancer Chemother Pharmacol 2001;47:309-318.
7.   Van Zuylen L, Verweij J, Sparreboom A. Role of formulation vehicles in taxane pharmacology. Invest New Drugs 2001;19:125-141.
8.   Van Zuylen L, Gianni L, Verweij J, et al. Inter-relationships of paclitaxel disposition, infusion duration and Cremophor EL kinetics in cancer patients. Anti-Cancer Drugs 2000;11:331-337.
9.   Huizing MT, Sparreboom A, Rosing H, et al. Quantification of paclitaxel metabolites in human plasma by high performance liquid chromatography. J Chromatogr B 1995;674:261-268.
10. Willey TA, Bekos EJ, Gaver RC, et al. A high performance liquid chromatographic procedure for the quantitative determination of paclitaxel (Taxol®) in human plasma. J Chromatogr 1993;621: 231-36.
11. Henningsson A, Karlsson MO, Viganò L, et al. Mechanism-based pharmacokinetic model for paclitaxel. J Clin Oncol 2001;19:4065-4073.
12. Kumar GN, Walle K, Bhalla KN, et al. Binding of taxol to human plasma, albumin and α1-acid glycoprotein. Res Comm Pathol Pharmacol 1993;80:337-344.
13. Brouwer E, Verweij J, De Bruijn P, et al. Measurement of fraction unbound paclitaxel in human plasma. Drug Metab Dispos 2000;28:1141-1145.
14. Rosing H, Man WY, Doyle E, et al. J Liq Chrom and Rel Technol 2000;23:329-354.
15. van Warmerdam LJC, van Tellingen O, Maes RAA, et al. Validated method for the determination of carboplatin in biological fluids by Zeeman atomic absorption spectrometry. Fres J Anal Chem 1995;351:1820-24.

Summary and Conclusions

Chemotherapy represents one of the main treatment modalities of advanced cancer. Despite significant improvement in the treatment of advanced cancer over the past decades, tumour response rates and survival still need to be improved in patients with advanced cancer. Therefore, it is important to find new anticancer agents with a novel mechanism of action and to further optimise existing treatment.

Introduction

Anticancer agents have a narrow therapeutic window, which limits optimal dosing. Moreover, the interpatient pharmacokinetic variability is generally high because of variable drug absorption, distribution and elimination processes. In cancer treatment, most anticancer agents are administered at the maximum dose tolerated by the patient with a dose calculation based on body surface area (BSA) of the patient. Therapeutic drug monitoring (TDM) and the assessment of pharmacokinetic parameters allow the characterisation of relationships between pharmacokinetic parameters of anticancer agents and pharmacodynamics (therapeutic efficacy and toxicity). Due to the narrow therapeutic window of anticancer agents and the high interpatient pharmacokinetic variability, pharmacokinetically guided administration of anticancer agents has been studied. In Chapter 1, the current insights into pharmacokinetically guided administration of anticancer agents are reviewed. Pharmacokinetically guided administration, using pharmacokinetic parameters including area under the plasma concentration-time curve (AUC), steady-state plasma drug concentration (C_{ss}), maximal plasma drug concentration (C_{max}) and drug exposure time above a threshold plasma concentration, has been studied for many anticancer agents. Lower interpatient variation in pharmacokinetic parameters has been reported by applying pharmacokinetically guided administration of anticancer agents. In particular, the AUC-guided administration of carboplatin has been extensively studied. The drug's total body clearance is predominantly determined by glomerular filtration. Consequently, the AUC of carboplatin is better correlated with creatinine clearance than the BSA with creatinine clearance. Several formulae, limited sampling models and Bayesian analyses have been derived to predict the AUC of carboplatin. The application of these formulae results in less variability in AUC of carboplatin than administration per unit of BSA. The relationship between AUC and pharmacodynamics has also been studied for other anticancer agents, e.g. for cyclophosphamide, etoposide, fluorouracil, topotecan. However, AUC-guided administration has only found wide clinical application for carboplatin. In current practice, the Calvert and Cockcroft-Gault formulae are widely used to calculate the carboplatin dose (based on a target AUC) and the glomerular filtration rate, respectively.

Relationships between pharmacodynamics and other pharmacokinetic parameters than AUC (C_{ss}, C_{max} and drug exposure time above a defined threshold concentration) have been reported as well for anticancer agents, for example cisplatin, doxorubicin, methotrexate and paclitaxel. TDM is routinely used in the clinic only for methotrexate, to guide supportive measures in patients at high risk for developing significant toxicity after the administration of intermediate and high-doses of methotrexate.

The relationships between the pharmacokinetic parameters and the therapeutic efficacy and toxicity need to be investigated in prospective randomised studies to validate pharmacokinetic-pharmacodynamic relationships before implementation of adaptive control algorithms in clinical practice.

E7070

The second chapter describes pharmacokinetic studies of E7070, a novel sulphonamide anticancer agent that arrests tumour cells in the G_1-S phase of the cell cycle. Pharmacokinetic studies during phase I trials of E7070 revealed non-linear pharmacokinetics of the drug, as manifested by disproportional increase in systemic exposure to the drug at higher dose levels. A mass balance study was conducted to evaluate the excretion and pharmacokinetics of E7070 and its metabolite 1,4 benzene-sulphonamide (M1) in cancer patients after intravenous infusion of E7070 (Chapter 2.1.1). One thousand mg of E7070 was radiolabelled by carbon-14 (^{14}C) in the benzenedisulphonamide moiety, or in the indole moiety. E7070 exposure was significantly higher than M1, consequently, M1 is only a minor metabolite in humans. The excretion of the benzene-sulphonamide and the indole moieties of E7070 followed the same pattern with a higher renal than gastro-intestinal excretion. A high proportion of the radioactivity in human plasma, urine and faeces was represented by compounds other than E7070 and M1. Consequently, E7070 is extensively converted into currently unidentified metabolites. Glucuronidation is a major metabolic pathway.

A population analysis of the plasma concentration-time data as obtained in phase I studies, revealed that a three compartment model with non-linear distribution was best fitted to the data. Therefore, we studied the *in vitro* distribution of E7070 in whole blood at pharmacologically relevant concentrations (Chapter 2.1.2). This study indicated that E7070 is preferentially bound to red blood cells, after incubation of the drug in whole blood. This binding was a saturable process at higher concentrations in whole blood. The plasma protein binding of E7070 was high (98-99%) without any evidence of saturation of protein binding with E7070 at the concentrations tested. Moreover, an *in vitro* and *in vivo* pharmacokinetic study of E7070 and acenocoumarol was performed since three patients treated with prophylactic daily oral maintenance therapy with acenocoumarol developed a haemorrhagic tendency and/or a prolonged prothrombin time following the intravenous administration of E7070. The study revealed that E7070 can interact with acenocoumarol

by reducing its metabolic clearance, and to a minor extent, by reducing the plasma protein binding of acenocoumarol (Chapter 2.2). The pharmacological research of E7070 will be continued. The knowledge about the elimination pathways of E7070 in humans is pivotal for the further development of the drug. Currently, metabolism studies and phase II trials are ongoing to identify the chemical structures of the metabolites, and to evaluate the antitumour activity in patients with solid tumours, respectively.

Methotrexate

High-dose methotrexate is used in combination chemotherapy schemes in the treatment of osteosarcoma, certain non-Hodgkin lymphomas and acute lymphocytic leukaemia. Methotrexate, an antimetabolite, is primarily converted to 7-hydroxy-methotrexate. The pharmacokinetics of methotrexate and 7-hydroxy-methotrexate vary considerably among patients. Both compounds can cause renal and hepatic toxicity. Serum methotrexate levels above 0.1 µmol/L at 48 hours after iv drug administration are considered to be toxic and require intensification of the rescue therapy. In Chapter 3.1, we presented a patient with methotrexate-induced renal failure. The methotrexate levels in serum were higher than 0.1 µmol/L during a long period of 12 days (Chapter 3.1). Intensification of the leucovorin rescue therapy and the initiation of thymidine rescue therapy proved to be successful, and further toxicity was prevented. An integrated population pharmacokinetic model of methotrexate and 7-hydroxy-methotrexate was developed to study the pharmacokinetics of both compounds (Chapter 3.2). An integrated three-compartment model for methotrexate and a two-compartment model for 7-hydroxy-methotrexate was applied with first-order elimination of methotrexate from the central compartment and first-order elimination of 7-hydroxy-methotrexate from the central metabolite compartment. The influence of covariates (age, gender, BSA, performance status according to the World Health Organisation (PS), serum creatinine, serum alanine-aminotransferase (ALT), serum aspartate-aminotransferase (AST), serum alkaline phophatase, serum albumin, serum bilirubin and serum lactate dehydrogenase (LDH), concomitant use of gastric hydrogen pump inhibitors, salicylates and non-steroidal anti-inflammatory drugs (NSAIDs), and presence of pleural effusion or ascites) on the pharmacokinetic parameters was tested using univariate and multivariate analyses. Although several covariates, e.g. the presence of pleural effusion or ascites, concomitant use of gastric hydrogen pump inhibitors and NSAIDs, are known to influence the pharmacokinetics of methotrexate, no significant influence of any covariate on the pharmacokinetic parameters could be identified. Furthermore, the methotrexate and 7-hydroxy-methotrexate concentrations were determined in pleural effusion as obtained in patients with a pleural drain. The methotrexate fraction that diffused to the pleural effusion appeared to be very low.

This population model may aid further research to elucidate the relationship between the pharmacokinetics of both compounds and pharmacodynamics (therapeutic efficacy and toxicity) and possible drug-drug interactions.

Paclitaxel

Paclitaxel is a taxane derivative that acts on microtubular structures by binding directly to tubulin, causing microtubuli stabilisation that arrests tumour cells in the G_2-M phase of the cell cycle. Taxol® is the pharmaceutical product in which paclitaxel is dissolved in a mixture of Cremophor EL and ethanol (1:1, v/v). The pharmacokinetics of paclitaxel are non-linear, as manifested by a disproportional increase in both the maximal plasma concentration and the area under the plasma concentration-time curve at higher doses. *In vitro* studies have demonstrated that Cremophor EL can form micelles in plasma, acting as a high-affinity drug-transporting site for paclitaxel. Consequently, Cremophor EL causes a decreased unbound paclitaxel fraction in plasma and a reduced uptake of paclitaxel in red blood cells. A population pharmacokinetic model of Cremophor EL, was developed to study the pharmacokinetics of Cremophor EL in patients treated with paclitaxel dissolved in Cremophor EL (Chapter 4.1). The Cremophor EL plasma concentration-time data were most optimally described by a three-compartment model with linear distribution and Michaelis-Menten elimination from the central compartment. The influence of the covariates (age, gender, weight, BSA, PS, serum creatinine, ALT, AST, AF, serum gamma-glutamyltransferase (GGT), serum albumin, serum bilirubin and LDH) on the pharmacokinetic parameters was studied using univariate and multivariate analyses. Gender, BSA and PS were significantly correlated with the volume of the central compartment, the first peripheral compartment and the maximal elimination rate of Cremophor EL, respectively. The stability of the final population model was demonstrated using a bootstrap procedure. The developed population model of Cremophor EL can be used to further explore the relationships between the pharmacokinetics of Cremophor EL and its toxicity.

A method for the quantification of the unbound paclitaxel fraction in human plasma was developed and validated using pharmacologically relevant Cremophor EL and paclitaxel concentrations (Chapter 4.3). The method was precise: the within-day precision ranged from 3.9% to 11%, the between-day precision ranged from 5.8% to 13%. The unbound fraction appeared to be significantly higher in plasma with low serum albumin values compared to plasma with normal serum albumin values (containing 1% of Cremophor EL). The determination of the unbound fraction proved to be stable during a 10-week storage at –20°C. The assay was found applicable to determine the unbound concentration of paclitaxel in samples of a cancer patient treated with paclitaxel. The design of this assay can also be used to determine the unbound concentrations of other hydrophobic drugs.

A population pharmacokinetic model for paclitaxel was developed to describe the pharmacokinetics in patients with advanced non-small cell lung cancer and ovarian cancer (Chapter 4.2.1). The plasma concentration-time data were best described by a three-compartment model with saturable transport to one peripheral compartment and Michaelis-Menten elimination from the central compartment. The relationships between covariates (age, gender, weight, BSA, PS, serum creatinine, ALT, AST, serum alkaline phosphatase, GGT, serum bilirubin, LDH and serum albumin) and the pharmacokinetic parameters of paclitaxel were tested using univariate and multivariate analyses. BSA of the patient was significantly correlated with the volume of the central compartment and the maximal transport rate from the central compartment to the first peripheral compartment. The robustness of the final population model was demonstrated using a bootstrap procedure. This population model of paclitaxel was used to evaluate the feasibility of Bayesian dose individualisation to attain paclitaxel plasma concentrations above 0.1 µmol/L during 15 hours or longer in each course (Chapter 4.2.2). The first course consisted of standard dosing of paclitaxel (175 mg/m², 3-hour iv inf). The paclitaxel dosage was individualised in subsequent courses based on a previously developed population pharmacokinetic model of paclitaxel and on the observed paclitaxel concentrations in plasma during the previous course(s). The preliminary results of the first eleven patients indicate that pharmacokinetically guided dosing of paclitaxel results in a higher percentage of patients in whom the duration of exposure above the threshold concentration is 15 hours or longer in the second course (individualised dose), as compared to the first course (standard dose). However, more patients will be included to demonstrate the feasibility of individualised dosing in the third course and subsequent courses.

Final remarks

The analyses described in this thesis have provided detailed insight into the pharmacokinetics of the novel anticancer agent E7070 and the widely applied cytotoxic agents paclitaxel and methotrexate. The results may turn out to be of great help to optimise the clinical application of these anticancer agents.

Samenvatting en conclusies

Cytostatica (antikanker middelen) zijn één van de belangrijkste behandelingsmethoden van kanker. Ondanks een aanzienlijke verbetering in de behandeling van gemetastaseerde (uitgezaaide) kanker in de afgelopen decennia, kunnen het tumorrespons percentage en de overleving nog steeds worden verbeterd in deze patiënten. Daarom is het belangrijk om cytostatica te ontdekken met een nieuw werkingsmechanisme en het gebruik van de bestaande cytostatica te optimaliseren.

Introductie

Cytostatica hebben een smalle therapeutische breedte, met andere woorden de optimale dosering wordt beperkt door het optreden van bijwerkingen. De farmacokinetiek kan grote variabiliteit vertonen tussen patiënten, dat wil zeggen dat de concentraties van het geneesmiddel (bijvoorbeeld de bloedspiegels van het geneesmiddel) uitgezet tegen de tijd, sterk kunnen verschillen door de onderlinge variatie in opname, distributie (verdeling) over het lichaam en eliminatie (uitscheiding en omzetting) van de middelen. De meeste cytostatica worden gedoseerd aan de hand van de maximaal getolereerde dosis door de patiënt, waarbij de dosisberekening plaatsvindt aan de hand van het lichaamsoppervlakte van de patiënt. Het bepalen van de plasma- of serumconcentraties na toediening van cytostatica en de berekening van de farmacokinetische parameters van cytostatica, maken het mogelijk om de relaties tussen de farmacokinetiek en de farmacodynamiek (therapeutisch effect en bijwerkingen) te onderzoeken. Vanwege de smalle therapeutische breedte van cytostatica en de hoge variabiliteit in farmacokinetiek tussen patiënten, is doseren op geleide van de farmacokinetiek onderzocht. In Hoofdstuk 1 wordt een overzicht gegeven van de huidige inzichten met betrekking tot doseren op geleide van de farmacokinetiek. Bij deze manier van doseren kan gebruik worden gemaakt van farmacokinetische parameters als oppervlakte onder de plasma concentratie-tijd curve (AUC), stabiele plasma concentratie (C_{ss}), maximale plasma concentratie (C_{max}) en de duur van de blootstelling boven een bepaalde plasma concentratie van het cytostaticum. Deze parameters zijn bestudeerd voor vele cytostatica. Door het doseren op geleide van de farmacokinetiek wordt de variabiliteit in farmacokinetische parameters tussen patiënten kleiner. De dosering op geleide van het oppervlakte onder de plasma concentratie-tijd curve van carboplatine is uitgebreid onderzocht. De klaring van carboplatine wordt met name bepaald door de glomerulusfiltratie in de nieren. Hierdoor is het oppervlakte onder de plasma concentratie-tijd curve van carboplatine beter gecorreleerd met de creatinineklaring dan met de dosis per eenheid lichaamsoppervlakte. Verscheidene formules, methoden waarbij slechts enkele bloedmonsters hoeven worden afgenomen ('limited sampling' technieken) en Bayesian analyses zijn ontwikkeld om de AUC van carboplatine te voorspellen. De toepassing van

deze formules resulteert in minder variabiliteit in de AUC van carboplatine in vergelijking met toediening per eenheid lichaamsoppervlakte. De relatie tussen de AUC en farmacodynamiek is ook onderzocht voor andere cytostatica, bijvoorbeeld voor cyclofosfamide, etoposide, fluorouracil en topotecan, maar AUC-geleide dosering wordt tot nu toe in de kliniek alleen voor carboplatine gebruikt. In de huidige praktijk worden de Calvert en Cockcroft-Gault formules gebruikt om de carboplatine dosering (gebaseerd op een van tevoren vastgestelde AUC) respectievelijk de glomerulusfiltratiesnelheid te berekenen. Relaties tussen de farmacodynamiek en andere farmacokinetische parameters dan AUC (C_{ss}, C_{max} en de duur van de blootstelling boven een bepaalde plasma concentratie) zijn gebruikt voor cytostatica, bijvoorbeeld cisplatine, doxorubicine, methotrexaat en paclitaxel. Het bepalen van de cytostatica concentraties in serum wordt echter alleen toegepast na het toedienen van methotrexaat (intermediaire en hoge doseringen). De relaties tussen de farmacokinetische parameters en het therapeutisch effect en toxiciteit zullen verder onderzocht moeten worden in prospectieve, gerandomiseerde studies om de farmacokinetiek-farmacodynamiek relaties te valideren, voordat de algoritmen voor een dosisaanpassing kunnen worden toegepast in de klinische praktijk.

E7070

Het tweede hoofdstuk beschrijft farmacokinetische studies van E7070, een nieuw cytostaticum waarvan de chemische structuur is gebaseerd op een sulfonamide. E7070 remt tumorcellen in de overgang van de G1- naar de S-fase van de celcyclus. Uit farmacokinetische studies, gedurende preklinische studies en fase I studies van E7070, bleek dat de farmacokinetiek niet-lineair is, gezien de meer dan evenredige verhoging van de systemische blootstelling bij hogere doseringen. Om de excretie (uitscheiding) en farmacokinetiek van E7070 en de metaboliet (omzetproduct) 1,4 benzeen-sulfonamide (M1) in kankerpatiënten te onderzoeken, werd een massabalans studie uitgevoerd na intraveneuze toediening van E7070 (Hoofdstuk 2.1.1). Duizend mg E7070 werd radioactief gelabeld met koolstof-14 (^{14}C) in de benzeendisulfonamide ring of in de indool ring. De systemische blootstelling aan E7070 was hoger dan die aan M1, dus E7070 wordt slechts in beperkte mate omgezet in M1. De excretiepatronen van de benzeen-sulfonamide ring en de indool ring van E7070 waren hetzelfde, namelijk een hogere excretie via de nier dan via de darmen. Een groot gedeelte van de radioactiviteit in plasma, urine en faeces werd niet verklaard door E7070 en M1. Hieruit volgt dat E7070 in hoge mate wordt omgezet in tot nu toe nog niet geïdentificeerde metabolieten van E7070. Voor deze metabolieten blijkt glucuronidatie een belangrijke route te zijn.

Uit een populatieanalyse van de plasma concentratie-tijd data, zoals verkregen in de Fase I studies, bleek dat de data het beste werden beschreven door een drie-compartimentenmodel met niet-lineaire distributie. Gezien de verzadigbare distributie van E7070, hebben we

de *in vitro* distrib'tie van E7070 in volbloed onderzocht bij farmacologisch relevante concentraties (Hoofdstuk 2.1.2). Uit deze studie bleek dat E7070, na incubatie in volbloed, met name wordt gebonden aan rode bloedcellen waarbij een verzadiging van de rode bloedcellen optrad bij hoger incubatieconcentraties. De plasma-eiwitbinding van E7070 was hoog (98-99%) en lineair bij verschillende incubatieconcentraties. Tevens hebben we *in vitro* en *in vivo* farmacokinetische studies van E7070 en acenocoumarol uitgevoerd, omdat drie patiënten die dagelijks werden behandeld met acenocoumarol, een verhoogde bloedingsneiging vertoonden en/of een verlengde protrombinetijd (tijd die nodig is om bloed te laten stollen) hadden nadat E7070 was toegediend. Uit deze studie bleek dat E7070 een geneesmiddeleninteractie kan vertonen met acenocoumarol door het verminderen van de metabole klaring van acenocoumarol en in mindere mate, door het verminderen van de plasma-eiwitbinding van acenocoumarol (Hoofdstuk 2.2).

Het farmacologisch onderzoek van E7070 zal worden voortgezet. De kennis omtrent de eliminatieroutes van E7070 na toediening aan mensen, is belangrijk voor de verdere ontwikkeling van het cytostaticum. Er worden nu studies uitgevoerd waarbij het metabolisme verder wordt opgehelderd en waarin de antitumor werking van E7070 in patiënten wordt onderzocht (fase II studies).

Methotrexaat

Toediening van hoge dosis methotrexaat, in combinatie met andere cytostatica, wordt gebruikt bij de behandeling van patiënten met onder andere osteosarcoom, non-Hodgkin lymfomen en acute lymfatische leukemie. Methotrexaat is een antimetaboliet en wordt met name omgezet in 7-hydroxy-methotrexaat. De farmacokinetiek van methotrexaat en 7-hydroxy-methotrexaat varieert in sterke mate tussen patiënten. Beide stoffen kunnen toxiciteit aan de nieren en aan de lever veroorzaken. Methotrexaat concentraties in serum die hoger zijn dan 0,1 µmol/L 48 uur na de toediening van methotrexaat worden als toxisch beschouwd en hierbij wordt de anti-toxiciteitsbehandeling geïntensifeerd. In Hoofdstuk 3.1 is een patiënt met nierschade beschreven, hetgeen werd veroorzaakt door methotrexaat. De methotrexaat concentraties in serum waren hoger dan 0,1 µmol/L gedurende 12 dagen. Verhoging van de leukovorin behandeling en start van de thymidine behandeling bleek succesvol te zijn waardoor verdere toxiciteit werd voorkomen. Een geïntegreerd populatiemodel van methotrexaat en 7-hydroxy-methotrexaat werd ontwikkeld om de farmacokinetiek van beide stoffen te onderzoeken (Hoofdstuk 3.2). De serum concentratie-tijd data van beide stoffen werden het beste beschreven door een geïntegreerd drie-compartimentenmodel voor methotrexaat en een twee-compartimentenmodel voor 7-hydroxy-methotrexaat met eerste orde eliminatie van methotrexaat vanuit het centrale compartiment en eerste orde eliminatie van 7-hydroxy-methotrexaat vanuit het centrale metaboliet compartiment. De invloed van co-variabelen (leeftijd, geslacht, lichaamsoppervlakte, performance status volgens de

Wereld Gezondheids Organisatie (PS), serum creatinine, serum alanine-aminotransferase (ALAT), serum aspartaat-aminotransferase (ASAT), serum alkalische fosfatase (AF), serum albumine, serum bilirubine en serum lactaat dehydrogenase (LDH), gelijktijdig gebruik van protonpompremmers, salicylaten en NSAID's en de aanwezigheid van pleuravocht of ascites) op de farmacokinetiek werd bestudeerd met behulp van univariaat en multivariaat analyses. Alhoewel van verscheidene co-variabelen, bijvoorbeeld de aanwezigheid van pleuravocht of ascites, gelijktijdig gebruik van protonpompremmers en NSAID's, bekend is dat ze de farmacokinetiek van methotrexaat kunnen beïnvloeden, werd er geen significante invloed van de co-variabelen op de farmacokinetische parameters van methotrexaat en 7-hydroxy-methotrexaat gevonden. Tevens werden de concentraties van methotrexaat- en 7-hydroxy-methotrexaat bepaald in pleuravocht van patiënten met een pleuradrain. De fractie methotrexaat die naar pleuravocht diffundeerde bleek erg laag te zijn.

Dit populatiemodel kan gebruikt worden om de relaties tussen de farmacokinetiek van methotrexaat en 7-hydroxy-methotrexaat en farmacodynamiek en mogelijke geneesmiddel eninteracties verder op te helderen.

Paclitaxel

Paclitaxel behoort tot de groep taxanen. Taxol® is het farmaceutisch product waarin paclitaxel is opgelost in een mengsel van Cremophor EL en ethanol (1:1, v/v). De farmacokinetiek van paclitaxel is niet-lineair, hetgeen blijkt uit een meer dan evenredige verhoging van zowel de C_{max} als de AUC bij hogere doseringen. *In vitro* studies hebben laten zien dat Cremophor EL micellen kan vormen in plasma, waaraan paclitaxel kan binden. Dit heeft tot gevolg dat Cremophor EL een verlaagde ongebonden paclitaxel fractie in plasma veroorzaakt en een verlaagde opname van paclitaxel in rode bloedcellen. Een populatie farmacokinetisch model van Cremophor EL werd ontwikkeld om de farmacokinetiek van Cremophor EL te bestuderen in patiënten die werden behandeld met Taxol® (Hoofdstuk 4.1). De Cremophor EL concentraties in plasma zoals gemeten voor, tijdens en na toediening van Taxol®, werden het beste beschreven door een drie-compartimentenmodel met lineaire distributie en Michaelis Menten eliminatie vanuit het centrale compartiment. De invloed van de co-variabelen (leeftijd, geslacht, gewicht, lichaamsoppervlakte, PS, serum creatinine, ALAT, ASAT, AF, gamma-glutamyltransferase (γ-GT), serum albumine, serum bilirubine en LDH) op de farmacokinetische parameters was onderzocht met behulp van univariaat en multivariaat analyses. Geslacht was significant gecorreleerd aan het volume van het centrale compartiment, lichaamsoppervlakte aan het volume van eerste perifere compartiment en PS aan de maximale eliminatiesnelheid van Cremophor EL. De stabiliteit van het finale populatiemodel werd bewezen met behulp van een 'bootstrap' procedure. Dit populatiemodel van Cremophor EL kan worden gebruikte om de relaties tussen de farmacokinetiek en toxiciteit verder te onderzoeken.

Een methode om de ongebonden fractie paclitaxel in humaan plasma te bepalen, werd ontwikkeld en gevalideerd met farmacologisch relevante Cremophor EL en paclitaxel concentraties (Hoofdstuk 4.3). De intra- en inter-dag precisie was kleiner dan 11% respectievelijk 13%. De ongebonden fractie bleek significant hoger te zijn in plasma verkregen in patiënten met lage serum albumine waarden (waaraan 1% Cremophor EL was toegevoegd) in vergelijking met plasma met normale serum albumine waarden. De bepaling van de ongebonden fractie was stabiel gedurende 10 weken opslag bij -20°C. De methode kon worden toegepast om de ongebonden paclitaxel fractie te bepalen in plasmamonsters verkregen in een patiënt die werd behandeld met paclitaxel. De opzet van deze methode kan ook worden gebruikt bij het bepalen van de ongebonden fractie van andere hydrofobe middelen.

Een populatie farmacokinetisch model voor paclitaxel werd ontwikkeld om de farmacokinetiek in patiënten met gemetastaseerde longkanker en eierstokkanker te beschrijven (Hoofdstuk 4.2.1). De plasma concentratie-tijd data werden het beste beschreven met een drie-compartimentenmodel met verzadigbaar transport naar één van de perifere compartimenten en Michaelis-Menten eliminatie naar het centrale compartiment. De relaties tussen de co-variabelen (leeftijd, geslacht, gewicht, lichaamsoppervlakte, PS, serum creatinine, ALAT, ASAT, AF, γ-GT, serum bilirubine, LDH en serum albumine) en de farmacokinetische parameters van paclitaxel werden getest met behulp van univariaat en multivariaat analyses. Het lichaamsoppervlakte was significant gecorreleerd met het volume van het centrale compartiment en de maximale transportsnelheid van het centrale compartiment naar het eerste perifere compartiment. De stabiliteit van het finale populatiemodel werd bewezen met een 'bootstrap' procedure. Dit populatiemodel van paclitaxel werd vervolgens gebruikt om de haalbaarheid van een dosisindividualisatie-studie te testen. In deze studie werd de dosis geïndividualiseerd om in elke kuur een paclitaxel concentratie in plasma boven 0,1 µmol/L gedurende 15 uur of langer te kunnen bereiken (Hoofdstuk 4.2.2). De eerste kuur bestond uit een standaarddosis van paclitaxel (175 mg/m², 3-uurs infuus). De paclitaxeldosering werd aangepast in volgende kuren op basis van het ontwikkelde populatiemodel van paclitaxel en op basis van de geobserveerde paclitaxelconcentraties in plasma gedurende de vorige ku(u)r(en). De voorlopige resultaten van de eerste 11 patiënten laten zien dat doseren op geleide van farmacokinetiek resulteert in een hoger percentage patiënten met een duur waarin de beoogde concentratie wordt bereikt gedurende 15 uur of langer, in vergelijking met patiënten gedurende de eerste kuur. Meer patiënten zullen geïncludeerd worden, om de haalbaarheid van de studie gedurende alle kuren te evalueren.

Slotopmerkingen

De analyses die in dit proefschrift zijn beschreven, laten een gedetailleerd overzicht zien van de farmacokinetiek van het nieuwe cytostaticum E7070 en de veelgebruikte cytostatica paclitaxel en methotrexaat. De resultaten die zijn beschreven in dit proefschrift kunnen hopelijk gebruikt worden bij het verder optimaliseren van de klinische toepassing van deze cytostatica.

Curriculum Vitae

Desirée van den Bongard werd geboren op 12 juli 1972 te Sittard. In 1990 behaalde zij het Atheneum B diploma aan de Scholengemeenschap Serviam te Sittard. In datzelfde jaar werd gestart met de studie Geneeskunde aan de Universiteit Maastricht. De doctoraalfase werd afgerond met een wetenschapsstage bij de vakgroepen 'Neonatal-Perinatal Medicine' en 'Physiology' aan het Southwestern Medical Center te Dallas, onder begeleiding van Professor dr. C.R. Rosenfeld, Dr. K.E. Kamm en drs. Y. Arens. In april 1996 werd het doctoraaldiploma behaald gevolgd door het artsdiploma in augustus 1998. Vanaf oktober 1998 is zij gedurende een half jaar werkzaam geweest als arts-assistent op één van de medisch oncologische afdelingen in het Antoni van Leeuwenhoek ziekenhuis te Amsterdam. In april 1999 werd ze aangesteld als onderzoeker in opleiding bij de afdeling Medische Oncologie in het Antoni van Leeuwenhoek ziekenhuis en de Apotheek van het Slotervaartziekenhuis (promotores Prof. dr. J.H.M. Schellens en Prof. dr. J.H. Beijnen). Gedurende deze periode werd het in dit proefschrift beschreven onderzoek uitgevoerd.

List of publications

van den Bongard HJGD, RAA, Beijnen JH, Schellens JHM. Pharmacokinetically guided administration of chemotherapeutic agents. Clin Pharmacokinet 2000;39:345-367.

van den Bongard HJGD, Mathôt RAA, Boogerd W, Schornagel JH, Soesan M, Schellens JHM, Beijnen JH. Successful rescue with leucovorin en thymidine in a patient with high-dose methotrexate induced acute renal failure. Cancer Chemother Pharmacol 2001;47: 537-540.

Crul M, van den Bongard HJGD, Tibben MM, van Tellingen O, Sava G, Schellens JHM, Beijnen JH. Validated method for the determination of the novel organo-ruthenium anticancer drug NAMI-A in human biological fluids by Zeeman atomic absorption spectrometry. Fres J Anal Chem 2001;369:442-445.

van den Bongard HJGD, Mathôt RAA, van Tellingen O, Schellens JHM, Beijnen JH. A population analysis of the pharmacokinetics of Cremophor EL using nonlinear mixed-effect modelling. Cancer Chemother Pharmacol 2002;50:16-24.

van den Bongard HJGD, Boot H, Baas P, Taal BG. The role of parallel stent insertion in patients with esophagorespiratory fistulas. Gastro-Intest Endosc 2002;55:110-115.

van den Bongard HJGD, Pluim D, Rosing H, Nan-Offeringa L, Schot M, Ravic M, Schellens JHM, Beijnen JH. An excretion balance and pharmacokinetic study of the novel anticancer agent E7070 in cancer patients. Anti-Cancer Drugs 2002;13:807-814.

van den Bongard HJGD, Mathôt RAA, Schellens JHM, Beijnen JH. Population pharmacokinetic analysis of paclitaxel in cancer patients. *Submitted for publication*

van den Bongard HJGD, Pluim D, van Waardenburg RCAM, Ravic M, Beijnen JH, Schellens JHM. An *in vitro* pharmacokinetic study of the novel anticancer agent E7070: red blood cell and plasma protein binding in human blood. *Submitted for publication*

van den Bongard HJGD, Sparidans RW, Critchley DJP, Beijnen JH, Schellens JHM. Pharmacokinetic drug-drug interaction of the novel anticancer agent E7070 and acenocoumarol. *Submitted for publication*

van den Bongard HJGD, Kemper EM, van Tellingen O, Rosing H, Mathôt RAA, Schellens JHM, Beijnen JH. Development and validation of a method to determine the unbound paclitaxel fraction in human plasma. *Submitted for publication*

Dankwoord

Mijn vrienden wil ik bedanken voor hun interesse, vertrouwen, begrip en veel gezelligheid hetgeen we hopelijk nog lang en iets intensiever dan de afgelopen tijd kunnen voortzetten! Hierbij wil ik de huidige Maastrichtse groep apart noemen; ik ben jullie zeer dankbaar voor jullie gastvrijheid, steun en afleiding die ik hard nodig had tijdens de ziekenhuisopname van mijn vader.

Jeroen, ik ben blij dat we, ondanks alles wat er is gebeurd, elkaar respecteren en contact met elkaar kunnen hebben.

Mijn twee paranimfen, Katinka en Marjan wil ik bedanken voor hun toezegging om mij bij te willen staan op 14 november. Katinka, ik waardeer onze vriendschap enorm; je onvoorwaardelijke steun, je begrip en je voordeur die altijd voor me openstaat! Hopelijk wordt dit voor jou een goede generale. Marjan, een bijzondere collega, momenteel bijna ex-huisgenoot, bedankt voor de gezelligheid en veel succes in het Noorden.

Mijn familie wil ik bedanken voor hun interesse en steun. Lieve papa, bedankt voor het onvoorwaardelijke vertrouwen in mij. Wat moed, doorzettingsvermogen en levensinstelling betreft kan ik mij geen duidelijker voorbeeld wensen. Ik ben jullie zeer dankbaar voor het feit dat jullie mij veel vrijheid hebben gegeven wat de invulling van mijn leven en het vorm geven van mijn toekomst betreft. Pascal en Marianne, bedankt voor jullie morele steun en vertrouwen.

Desirée,
september 2002.